An investigation into the causal relationship between sensory attenuation and motor initiation: a novel hypothesis for motor control & movement disorders

Clare E Palmer

PhD

2018

DECLARATION OF AUTHORSHIP

*I **Clare E Palmer** confirm that the work presented in this thesis is my own. Where information has been derived from other sources, I confirm that this has been indicated in the thesis.*

ABSTRACT

Prior to and during movement afferent input to the cortex is reduced (Cohen and Starr, 1987; Hughes et al., 2013; Hughes and Waszak, 2011; Starr and Cohen, 1985). This robust phenomenon of sensory attenuation has been proposed to distinguish between biologically salient external sensations and our highly predictable self-generated sensory input. However, a recent theoretical framework, active inference, posits that this sensory gating may actually represent a necessary mechanism for movement initiation. Brown et al (2013) hypothesise that sensory attenuation "is a necessary consequence of reducing the precision of sensory evidence during movement to allow the expression of proprioceptive predictions that incite movement" (Brown et al., 2013; K. Friston et al., 2011; Friston et al., 2010). This theory predicts that estimates of the gain, or precision (inverse uncertainty), surrounding the ascending afferent input to sensorimotor cortex must be reduced in order to allow movements to be initiated (Brown et al., 2013). The mechanism underlying this theory comes from applying the ideas of predictive coding and Bayesian inference, that have been readily used to describe perception in multiple sensory modalities, to the sensorimotor system. However, this theory is grounded in computational and theoretical work, which is lacking empirical evidence. In this PhD, I conducted a series of experiments using behavioural tasks and electroencephalography (EEG) in humans to test specific predictions from this overarching hypothesis. More specifically, I aimed to better characterise somatosensory attenuation, determine the neurophysiological correlate of sensory precision in the cortex and determine the consequences of modulating sensory precision on behaviour and cortical oscillatory activity. As well as offering new insights into how we control movements, this PhD offers novel avenues for understanding movement disorders, in particular Parkinson's disease (PD), and generates a number of testable hypotheses for future clinical work.

ACKNOWLEDGEMENTS

This PhD is the culmination of 4 years of stubborn MATLAB code, broken EEG electrodes and a seesaw of emotions, teamed with hours of philosophical ponderings, wondrous Eureka moments and some great lab socials. None of this would have been possible without the wisdom, guidance and support of some very special people.

I would like to thank Antonella for her collaboration on study two (chapter four) and my brilliant student Kemi for collecting data for study three (chapter five). I'm extremely grateful to Sasha and especially Ryszard in helping with the computational work in study four (chapter six). I would also like to thank Marco for lending me his robots and expertise for study one (chapter three) and study three (chapter five).

The Kilner lab members and all the wonderful people on the 3rd floor have provided the perfect balance of scientific discussion and Prosecco required for a successful PhD, so to them I am extremely grateful. A special mention must go to Eleanor for putting up with my messy desk and copious amounts of carrier bags for 3 years.

My family and friends have been an incredible support to me throughout this PhD. They've been there to celebrate the successes and kept me distracted and motivated following the set-backs. Special thanks must go to the most wonderful and supportive parents any one could wish for. From buying the perfect stationary to continuously supplying cuddles, I couldn't have done it without you!

Ricci needs his own mention (mainly because he requested it). Thank you for the tea and pancakes, the late night discussions about the meaning of science and for being my shoulder to cry on. Even when I've been at my grumpiest, you haven't stopped smiling. You constantly encourage me and motivate me to be the best person I can be. I'm not sure I'd still be standing today without your support.

Finally, James: needless to say there would be no PhD without your supervision. You have taught me more than how to develop scientific ideas and analyse data. You have helped me realise that everyone makes mistakes, academia is not about being perfect and that life is for living, not fretting. Thank you. I hope we get to work with each other again in the future.

TABLE OF CONTENTS

TABLE OF FIGURES

CHAPTER 1

INTRODUCTION

When a rabbit hears a rustle of leaves in the woods, she must immediately determine the cause of the sound: was it the familiar scurrying of the critters in the forest; was it the patter of her feet on the forest floor; or the sound of a fox lurking nearby?

Much like the rabbit, we constantly receive a barrage of ambiguous sensory information that we must process and understand in order to respond appropriately. The attribution of sensory information to familiar or expected causes allows the brain to process only salient and unexpected stimuli. In this way the rabbit can ignore the familiar rustle of leaves caused by her own movements or the smaller creatures in the forest and react quickly to the unexpected noise from a large predator. Sensory attenuation describes the filtering or dampening of irrelevant sensory information and offers a mechanism by which self-generated sensations can be distinguished from more salient external stimuli. Indeed, afferent input is attenuated prior to and during movement (Cohen and Starr, 1987; Desantis et al., 2012; Hughes et al., 2013; Hughes and Waszak, 2011; Starr and Cohen, 1985; Weiss et al., 2011) and self-generated sensations are perceived as less intense than externally generated sensations (Bays et al., 2006, 2005; Blakemore et al., 2000; Shergill et al., 2003).

However, active inference, a recent theoretical framework, hypothesises that sensory attenuation is not a purely perceptual phenomenon, but in fact plays a necessary role in movement initiation. Brown et al., (2013) posit that sensory attenuation "is a necessary consequence of reducing the precision of sensory evidence during movement to allow the expression of proprioceptive predictions that incite movement" (Brown et al., 2013; K. Friston et al., 2011; Friston et al., 2010). This theory predicts that we must divert our attention away from ascending afferent input (i.e. reduce sensory precision or gain) in order to allow movements to be initiated. An inability to accurately attenuate sensory information over sensorimotor cortex has been associated with akinetic symptoms (Brown et al., 2013; A Macerollo et al., 2015; Macerollo et al., 2016).

However, this theory is grounded in computational and theoretical work, which is lacking empirical evidence. In this PhD, I have conducted a series of experiments using behavioural tasks and electroencephalography (EEG) in humans to test specific

predictions from this overarching hypothesis. More specifically, I aimed to better characterise somatosensory attenuation, determine the neurophysiological correlate of sensory precision over sensorimotor cortex and determine the consequences of modulating sensory precision in the proprioceptive and visual domains on behaviour and cortical oscillatory activity.

1.1. The importance of Bayesian predictive coding

The active inference theory provides a unifying account to describe how we perceive and act in the world. It generalises the ideas of predictive coding, which have traditionally been applied to sensory systems, to the motor system. In order to understand how active inference can be used to explain motor control, it is important to first visit the underlying principles of predictive coding and Bayesian inference.

1.1.1. Predictive coding and Bayesian inference

It has long been proposed that we do not perceive exactly what we see, but our brains infer what we expect to see based on prior experience (Helmholtz and König, 1896). Visual illusions provide a perfect example of this: the ability to see a 3D face or a hollow mask by simply manipulating the light and shade on a 2D image is due to a prior conception that light sources generally come from above (Gregory, 1980). When interacting in the world we receive a constant stream of sensory information; however, for any given sensory input there are multiple causes, therefore it is difficult to determine the true cause of the sensory data. In order to solve this inverse problem and understand the world around us, it has been proposed that the brain acts as an inference machine (Dayan et al., 1995; Helmholtz and König, 1896; Rao and Ballard, 1999). Within such frameworks a generative model is employed, which incorporates our prior beliefs about how different causes interact, to produce an estimate of what the sensory input should look like if these causes were correct. This can then be inverted to identify the true cause of a given sensation (Friston, 2008, 2005). This Bayesian approach is thought to underlie how the brain enables us to understand the world around us and has been proposed to form the basis of predictive coding frameworks (Dayan et al., 1995; Doya, 2007; Friston and Kiebel, 2009; Knill and Pouget, 2004; Körding and Wolpert, 2006).

There are a number of studies that have shown the brain uses Bayesian statistics for perceptual inference across different sensory modalities (Ernst and Banks, 2002; Ernst and Bülthoff, 2004; Kersten et al., 2004; Knill, 1998; Körding and Wolpert, 2004; van Beers et al., 1999; Wolpert et al., 1995). A central component of these studies is how the brain

represents uncertainty and how optimal inferences are made in a world rife with ambiguity. There are multiple sources of uncertainty in the world: the sensory input we receive will be more uncertain when driving on a foggy day compared to a clear day; there may be uncertainty in our model of the world and thus our prior beliefs if we enter a novel environment, such as an astronaut entering anti-gravity for the first time; and unpredictable changes to the environment create volatility uncertainty emerging from the stability of the world. The brain needs to be able to understand and characterise different forms of uncertainty at these different hierarchical levels in order to achieve optimal perceptual and motor performance.

Bayesian statistics allows us to formally quantify this uncertainty and use it to make optimal inferences. Prior beliefs about the probability of a given state or variable are combined with estimates of the likelihood of sensory input given possible states of the world. This produces an optimal estimation of the state given the sensory input received ('posterior'; Figure 1.1). These sources of information ('prior' and 'likelihood') are represented as probability distributions such that the variance of these distributions gives an estimate of the uncertainty surrounding their mean values. This is important for determining the degree to which prior beliefs are updated given a particular sensory input. The posterior distribution represents the optimal estimate of hidden states of the world. The relative variance of the prior and likelihood estimates determines which estimate the posterior distribution will more readily reflect (Figure 1.1). Importantly, the posterior distribution produced using Bayes theorem has much lower uncertainty than if sensory information alone were used; therefore Bayesian inference provides an optimal method to reduce uncertainty when trying to understand the causes of the sensations we receive. However, the brain cannot produce priors *de novo*, therefore empirical Bayes is employed whereby prior beliefs are based on sensory data and passed down from the hierarchical level above. For example, the posterior distribution from one level will form an empirical prior for the level below. Empirical priors act to reduce the many-to-one problem facing the inversion of the generative model and provide a better estimate of the true cause of the sensory input. The Bayesian model evidence (or prediction error) is a probability distribution, which represents how accurately the generative model was able to predict the true sensory input.

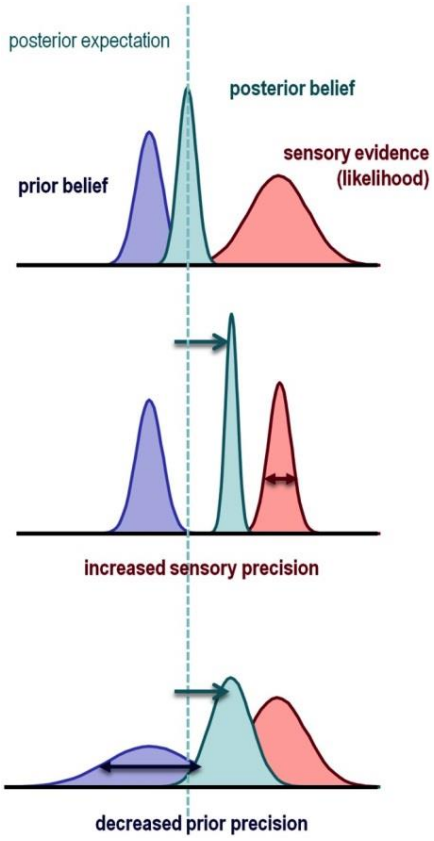

Figure 1.1 Schematic illustrating the importance of precision when forming posterior beliefs and expectations*. Prior beliefs, posterior beliefs and the likelihood of sensory evidence are represented here as Gaussian probability distributions. The dotted line corresponds to the posterior expectation, while the width of the distributions corresponds to their variance. Precision is the inverse of this variance and is used to weight the effect the prior and likelihood functions have on the posterior belief. As can be seen from the graphs the posterior distribution will be biased towards the more precise belief, therefore modulating the precision of the sensory evidence can manipulate the posterior distribution. Sensory attenuation is thought to reflect a decrease in the precision of this likelihood function. Figure taken from Adams et al (2013).*

Within predictive coding frameworks, backward projections pass predictions (based on empirical priors) down the cortical hierarchy and compares these with the afferent input at each level. If these predictions are incorrect the difference between these values produces a prediction error, which is then passed back up the hierarchy via reciprocal forward connections (Bastos et al., 2012; Rao and Ballard, 1999). This continues until the prediction error is minimized producing a Bayes-optimal estimate of the causes of the sensory input. Importantly, the influence of bottom-up prediction errors on higher levels of processing is adjusted by modulating the 'volume' or gain of prediction errors, which is termed *precision.* As indicated above, this is how uncertainty is represented in this framework and has a large influence over how meaningful the prediction error produced is. This is analogous to a paired sample t-test: the mean difference between the two samples (the predicted and actual sensory input) represents the prediction error; the standard error pooled across both samples represents the precision; and the t-statistic represents the precision-weighted prediction error. In this way, the variance of each sample is essential in determining if the mean difference is significant and thus the precision-weighting determines how readily the prediction error will update the model (Adams et al., 2013a; C. Palmer et al., 2016; Palmer and Macerollo, 2015). The Bayesian model evidence reflects this precision-weighted prediction error.

1.1.2. Active Inference and the Free Energy Principle

As highlighted, Bayesian inference and predictive coding play a fundamental role in explaining perception across a number of sensory modalities; however, these principles had not been used to explain sensorimotor control. Active inference applies the ideas of predictive coding to the sensorimotor system and provides a unifying theory to explain both perception and action in a single framework. This theory is embedded within a wider principle: the free energy principle. The free energy principle, generated from information theory, posits that biological agents resist a tendency to disorder; therefore they aim to minimize the entropy (surprise/uncertainty) in their sensory states. As entropy cannot be directly measured "free energy" is defined as the upper bound on the long term average of surprise or the lower bound on the negative log of the Bayesian model evidence(Friston and Kiebel, 2009; Friston et al., 2010). The Bayesian model evidence simply describes how well the generative model has accurately explained the sensory data, therefore, in simpler terms free energy can be likened to prediction error. Minimising free energy, or prediction error, therefore provides the motivation for how we perceive and behave. We can minimize prediction error by either: 1) changing our predictions to match our sensory input (perception); or, 2) changing our sensory input to match our predictions (action; Adams et al., (2013); Friston et al., (2011)). The former refers to perceptual inference described above and the latter to active inference. This framework posits that the ideas used to explain perception in exteroceptive sensory domains can also be applied to proprioception with the specific hypothesis that Bayesian inference in this domain can directly result in movement.

One key component of this theory is that the motor cortex does not produce motor commands; the descending input from the motor cortex to the spinal cord transmits a proprioceptive prediction about the sensory consequences of the movement, which is produced by a hierarchical generative model in the motor cortex. This prediction is then compared with proprioceptive input from muscle afferents in the spinal cord and any difference between the expected and actual proprioceptive signal produces a proprioceptive prediction error. This activates the classical motor reflex arc in the spinal cord, which resolves the prediction error by fulfilling the proprioceptive prediction. The neurophysiological mechanism by which this occurs is reflective of the equilibrium point hypothesis (EPH; Feldman, 1986).

The EPH states that the descending signals to the alpha and gamma motor neurons in the spinal cord specifies a threshold for the tonic stretch reflex, which determines the relationship between muscle force and muscle length. When the muscle is lengthened

more than expected above this threshold, the increased firing from the 1a afferents activates alpha motor neurons and causes the muscle to contract (e.g. the knee jerk reflex). The level of activation of the alpha motor neurons increases with the difference between the actual muscle length and the threshold. For voluntary movement to occur, descending signals change the equilibrium point, which therefore requires a change in muscle length and force to reach the equilibrium. Active inference applies predictive coding ideas and Bayesian inference to this theory in order to explain how movements occur as a result of a proprioceptive prediction error in the spinal cord. Descending proprioceptive predictions are compared with the afferent input at the level of the spinal cord and, via the same mechanism as highlighted in the EPH, muscles are activated in relation to the difference between these inputs.

Importantly, active inference highlights that prediction errors can also be produced at other levels of the anatomical pathway in the sensorimotor system, at any point where descending predictions and ascending afferent input can converge, for example the spinal cord, the ventral posterior nucleus of the thalamus or the sensorimotor cortex. Applying predictive coding ideas to the sensorimotor system generates specific predictions about the anatomical and physiological connections that need to be present. Adams et al., (2013a) review this literature and argue that it is neurobiologically plausible for the sensorimotor system to function according to the principles of the predictive coding framework, namely that the descending inputs from the motor cortex have the neurophysiological hallmarks of backward connections thought to represent predictions. This thesis will focus on testing the mechanisms involved in active inference in the sensorimotor cortex.

Active inference highlights how the mechanisms involved in perceptual inference can influence motor output (Brown et al., 2013). Descending predictions from the motor cortex to the spinal cord describe the proprioceptive consequences of the intended movement trajectory; these, plus other somatosensory consequences, such as predicted cutaneous reafference, are also transmitted to the somatosensory cortex. In this way, the motor cortex can be described as a multimodal sensory area, which predicts both proprioceptive and exteroceptive consequences of movement rather than a purely motor area (Hatsopoulos and Suminski, 2011). At this level of the hierarchy prediction errors can be produced from the comparison of somatosensory predictions from primary motor cortex (M1) and somatosensory reafferance from the periphery, which allows for perceptual inference in the somatosensory domain in relation to movement. Indeed, area 3a is anatomically positioned to receive descending input from M1 (Witham et al., 2010) and ascending proprioceptive information from the motor nuclei of the thalamus

(Huffman and Krubitzer, 2001). According to active inference, prediction errors at this level must also be resolved in one of two ways: 1) by updating the predictions in M1 (perception); or, 2) by generating movement through descending projections to the spinal cord (action). The precision-weighting of prediction errors in somatosensory cortex is therefore essential in determining whether movement occurs.

In addition, the active inference framework posits that sensory attenuation occurs across all sensory modalities with self-generated movement (Brown et al., 2013). There is experimental evidence to demonstrate that the perceived intensity of visual (Cardoso-Leite et al., 2010; Hughes and Waszak, 2011) and auditory (Desantis et al., 2012; Hughes et al., 2013; Martikainen et al., 2005; Weiss et al., 2011) sensations is reduced during movement, which supports this statement. However, it is not clear how sensory attenuation in other modalities directly modulates movement. Brown et al (2013) specifically address how a down-weighting of somatosensory input (proprioceptive and cutaneous) is essential for movement initiation; although similar mechanisms could be applied to other sensory modalities.

1.1.3. The role of modulating precision in movement initiation according to active inference

One specific hypothesis of the active inference framework is that sensory precision must be down-weighted in order to initiate movements: this is the central prediction tested in this PhD. Descending predictions and ascending afferent input are thought to converge on superficial pyramidal cells in the cortex, which are therefore described as prediction error units. Precision is modulated by altering the post-synaptic gain on these units such that prediction errors weighted by this precision are transmitted up the cortical hierarchy (Friston, 2005; K. Friston et al., 2011; Friston and Kiebel, 2009). This synaptic gain can be altered in two ways: 1) by modulating the uncertainty of the sensory input, for example by adding noise to the afferent signal; or, 2) through a top-down attentional mechanism. Prediction errors produced in the sensorimotor cortex following the production of a proprioceptive prediction to move must be resolved and the mechanism by which this occurs is determined by the relative precision-weighting of top-down predictions and bottom-up prediction errors. Active inference posits that in order to fulfil a future state, and thus reduce prediction error, an individual can either move, employing descending proprioceptive predictions, or the sensory environment can change and update the future state via an ascending sensory prediction error (Adams et al., 2013a). However, for top-down predictions that incite movement to be preferentially selected, the sensory gain of bottom-up prediction errors must be down-weighted. This is explained schematically in

Figure 1.2. When planning a movement there is a prediction error between the current proprioceptive state and the future proprioceptive state. In order to minimise this prediction error, somatosensory precision must be decreased in order to favour top-down proprioceptive predictions that incite classical motor reflex arcs. This modulation in synaptic gain is thought to underlie the sensory attenuation seen prior to and during movement in somatosensory cortex (Brown et al., 2013). It is unclear how sensory attenuation in other modalities can directly affect motor initiation, but it is likely to do with the integration of exteroceptive input in the motor cortex needed to produce accurate proprioceptive predictions; decreasing the precision of exteroceptive inputs to the motor cortex may increase the relative precision of proprioceptive predictions to move.

By building a generative model that determines the causes of externally and internally generated sensations, Brown et al (2013) have demonstrated this permissive role of somatosensory attenuation in motor initiation. The generative model was based on three main assumptions: 1) the free energy principle, which states that the brain aims to minimise the free energy of sensory inputs defined by the generative model; 2) the generative model used by the brain is hierarchical, nonlinear and dynamic; 3) the most likely state of the world (under this model) is encoded by neuronal firing rates. For this simulation the agent was given a prior belief about the hidden cause of an internally generated movement under a model with high sensory attenuation. The prior belief, with high precision, generated a posterior belief about the magnitude of an internally generated force. This caused an increase in the conditional expectation of an internal force. Sensory precision in this model was linked to the magnitude of this conditional expectation; therefore the attenuation of this precision was shown by an increase in the confidence intervals surrounding this hidden state (internal force). This resulted in movement as the proprioceptive prediction was fulfilled using the classical motor reflex arc (Figure 1.3A). In a second simulation, the magnitude of sensory attenuation was reduced such that the sensory precision remained higher than the precision of the prior beliefs about the internal hidden causes. This resulted in a predominance of bottom-up sensory prediction errors over top-down proprioceptive predictions and therefore the posterior belief did not represent an increase in the conditional expectation of the hidden internal force to reflect the hidden cause. Perceptual inference rather than active inference occurred. This led to a lack of proprioceptive predictions about the sensory consequences of movement and thus a failure to move (Figure 1.3B). This has been used to explain hypokinetic symptoms seen in patients with Parkinson's Disease (PD).

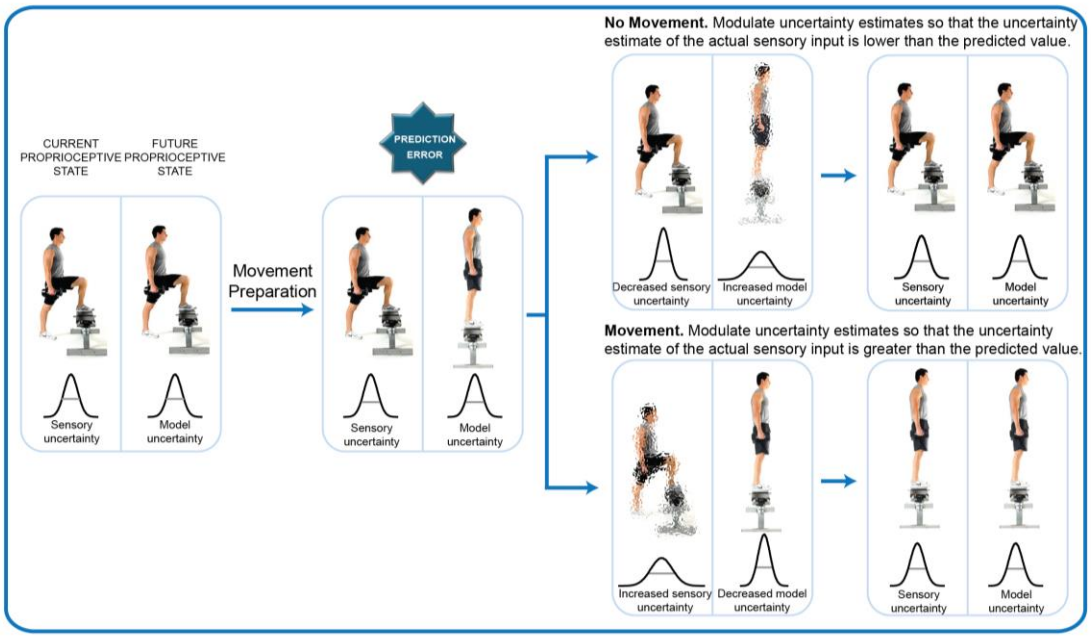

Figure 1.2. Schematic Illustrating Movement Initiation within the Active Inference Framework. *In the schematic, each panel depicts both the actual and the predicted sensory inputs. The character shows the action that is currently being performed (left) alongside the predicted action (right). The width of the distributions below and the clarity of the figure illustrate the uncertainty in these values. Before we start to plan a new movement, our prediction of our sensory input and the actual sensory input are equivalent (left panel). According to the active inference framework, when we start to prepare a movement, we generate a prediction of what the sensory input of this movement will be and this creates a prediction error between the current and the predicted sensory states (second panel). To minimize this error, an individual can: (i) stay still and update their prior beliefs (within the forward model) so that the predicted sensory input matches the actual sensory input (top row); or (ii) move, so that the actual sensory input matches the predicted sensory input (bottom row). Modulating the relative uncertainty in these sensory states will determine which option is selected. For example, to initiate movement [option (ii)], the uncertainty in the current sensory state is increased such that the individual will shift to the predicted sensory state with the lowest uncertainty. Figure taken from Palmer et al (2016).*

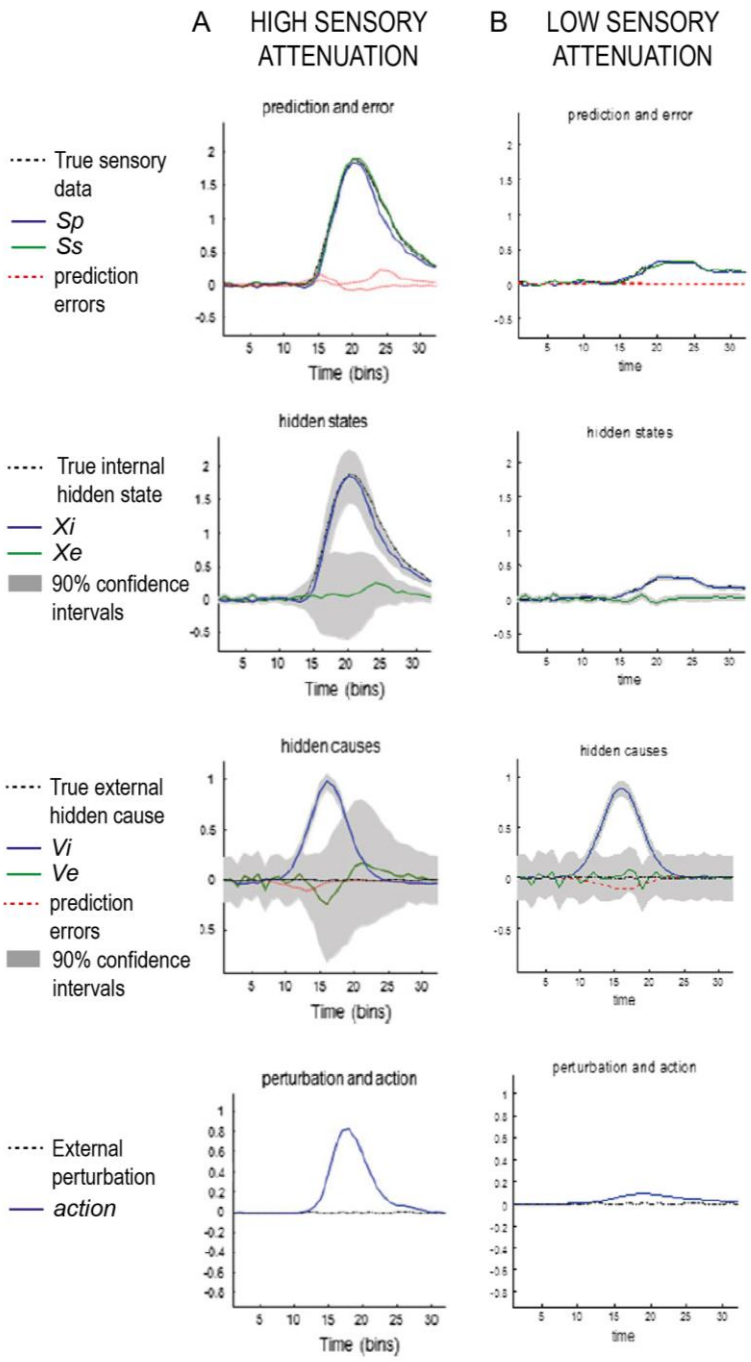

Figure 1.3. Simulations from a generative model demonstrating the permissive role of sensory attenuation in action. *In column A the model was set to have high sensory attenuation emulating a healthy, human agent. A prior belief was given to the model about an internally generated movement (Vi). This generated a posterior belief about the magnitude of forces generated internally (Xi) and externally (Xe) and the somatosensory (Ss) and proprioceptive consequences of the movement (Sp). The conditional expectation about an internally generated force increased following the hidden cause. Sensory precision decreased with an increase in the internally generated force shown by an increase in the confidence intervals surrounding the conditional expectation. Action was then enslaved to fulfil the prediction errors. In the second simulation, in column B, sensory attenuation was reduced such that sensory precision remained higher than the precision surrounding the hidden cause of the internally generated movement. As per perceptual inference, the posterior belief following the generation of this hidden cause did not reflect an increase in the conditional expectation of the internal force. With no proprioceptive prediction and therefore no prediction error between the current and predicted proprioceptive state, there was no movement. This demonstrates that akinesia can occur if sensory attenuation is reduced. Figure adapted from Brown et al (2013).*

It has been posited that precision is modulated by attentional mechanisms under the control of neuromodulators (Feldman and Friston, 2010). Previous evidence suggests that increased attention towards sensory information (increased sensory precision) during particular motor tasks can lead to impairments in movement. This supports the simulations demonstrating that increased sensory precision can cause akinetic symptoms. For example, sportspeople have been known to "choke" under pressure if they place too much attention on over-learned movements making them unable to perform properly (Beilock and Carr, 2001). Experimentally when healthy participants are asked to attend to the production of an overlearned sequence of key presses performance is impaired. This is associated with increased activation of prefrontal and anterior cingulate cortex during the attended vs unattended sequence production (Jueptner et al., 1997).

As previously highlighted active inference is employed as a hierarchical model in which prediction errors update predictions at each level of the cortical hierarchy; therefore, modulating sensory precision at different levels in this hierarchy will have different behavioural consequences. Simulations using a cortical model with nodes throughout the visual and motor systems demonstrate this using a cued reaching task (K. J. Friston et al., 2011). A sequence of lights cued an agent on where to reach. The generative model (similar to above) predicted when each light would come on and generated a series of predictions in a hierarchy, for example, indicating the properties of the cue and the proprioceptive consequences of moving the agent's finger. The agent then moved to the cue in order to minimise the prediction errors generated. When the sequence was reversed, the predictions of the model were then incorrect and prediction errors were used to update expectations to produce correct movements over a series of trials. Crucially, Friston et al then perturbed the model and simulated the resultant behaviour. Removing the modulation of precision (by removing dopaminergic modulatory connections) in the superior colliculus, which encodes the salience of cues, generated perseverate behaviour similar to that seen in PD. Prediction errors were constantly down-weighted such that they had a minimal effect on updating prior expectations causing a failure to recognise that the sequence had changed and a greater number of movement errors. In contrast, removing precision at both high and low levels of the hierarchy resulted in a lack of confidence in how to respond to the cues resulting in slower reaction times (RTs) and unsure movements. This study highlights the complexity of the sensorimotor system and the importance of precision at different points of the cortical hierarchy. Decreasing precision at the lowest level of this hierarchy increased RTs, however the active inference framework posits that a reduction in precision at this level should decrease RTs. Importantly, this study involves a model, which integrates visual

and proprioceptive information to generate movements; whereas the predictions regarding movement initiation focus on the somatosensory domain. In this thesis I will modulate precision within the visual and somatosensory domains to measure the consequence of this on motor control and oscillatory activity in sensorimotor cortex.

From these computational studies there is a clear hypothesis that the modulation of sensory precision is important in motor control. Modelling studies aiming to understand how active inference could be implemented in the brain demonstrate the different outcomes of modulating precision in different sensory domains at different levels of the cortical hierarchy. However, there is a lack of direct empirical evidence to support that behaviour and neural activity is modulated in accordance with this framework. This thesis tests a series of hypotheses that emerge from this framework regarding the role of modulating sensory precision in motor control.

1.2. What is the role of sensory attenuation in perception and action?

There is a plethora of work showing that afferent input to the cortex across sensory modalities is suppressed prior to and during a movement (Cohen and Starr, 1987; Hughes et al., 2013; Hughes and Waszak, 2011; Starr and Cohen, 1985). Active inference suggests that this sensory attenuation is a necessary step in order to allow movements to occur. However, there appears to be a dissociation in the literature between those who study sensory attenuation as a perceptual phenomenon and those who study this as a physiological phenomenon. This has important implications for defining the function of sensory attenuation in perception and action and also for determining the neurophysiological mechanism by which afferent input is attenuated. Here I review the previous literature measuring the functional role of somatosensory attenuation and motivate the main aim of the experimental work in study one (chapter three), which was to dissociate these forms of somatosensory attenuation in a single paradigm. This was essential foundation work for later determining the necessity of this phenomenon for movement initiation.

1.2.1. What is sensory attenuation?

Noise within the afferent sensory signal, variability in actions produced and a constant changing environment generate a sensory input full of uncertainty. Ambiguities in sensory processing and unpredictability of the environment fuel the need for a system which is

able to filter out irrelevant information and select the most salient information to aid action selection (Bays and Wolpert, 2007). Sensorimotor integration is therefore essential in fine-tuning this process and, as previously suggested, it is has been proposed that Bayesian inference underlies this. The specific role of somatosensory attenuation within this framework remains controversial. This is partly driven by the methods used to measure somatosensory attenuation. There are two fields within the literature that remain very isolated. One field characterises perceptual somatosensory attenuation using behavioural paradigms and fMRI, which quantifies how our somatosensory percept appears less intense when the somatosensory consequences of a given action are more predictable; for example, when we attempt to tickle ourselves we appear far less ticklish then when someone else tickles us. In contrast, there are a number of studies describing somatosensory attenuation as a physiological phenomenon that occurs prior to and during movement. This is defined as a decrease in the amplitude of the primary and secondary components of the somatosensory evoked potential (SEP) generated by peripheral nerve stimulation. It has been hypothesised that this physiological phenomenon may represent the mechanism underlying perceptual somatosensory gating, however these two forms of attenuation have never been measured within a single paradigm, therefore it is unknown whether they have distinct functional roles. Indeed, there are competing theories describing the functional role of somatosensory attenuation, which may be reconciled if these two forms of somatosensory attenuation are shown to be distinct.

1.2.2. The central cancellation theory for perceptual somatosensory attenuation

It has been proposed that the primary purpose of perceptual somatosensory attenuation is to make externally produced sensations more salient, which is why we appear more ticklish when someone else tickles us compared to when we try to tickle ourselves. The predictability of our own actions means they are less salient and therefore we readily attenuate the consequences of our own actions. A secondary related proposed function is to distinguish between self-generated and externally-generated actions for the correct perception of agency. This has been measured quantitatively in a force-matching paradigm. Participants were given a target force on their left hand and asked to match that force in two ways: 1) by pushing down on the same hand until they perceived the same force (self-condition); 2) by using an external joystick to control the force production on the hand that received the target force until they perceived the same force (external condition). This produces a highly replicable and robust result: participants consistently overestimate the matched force in the self-condition compared to the veridical target

force, yet accurately match the target force in the external condition. It is argued that this is because somatosensory attenuation occurs in the self-condition where the relationship between the force being produced and the force being perceived is well understood and predictable, but not the external condition where the relationship between the movement of the joystick and the robot producing the force is not known. Interestingly, schizophrenic patients match the force accurately in both conditions demonstrating that they have no somatosensory attenuation in the self-condition; this suggests the misattribution of agency which is typical in schizophrenia may be due to an inability to accurately predict the sensory consequences of one's own actions (Shergill et al., 2005). A relationship between scores of delusional ideation and the magnitude of somatosensory attenuation (difference between target force and matched force) has also been found in the general population (Teufel et al., 2010). This supports the role for perceptual somatosensory attenuation in distinguishing between sensations that are a result of our own actions and those that come from others.

A central cancellation theory has been proposed as a mechanism to achieve this function (Blakemore et al., 1998; Franklin and Wolpert, 2011) (Figure 1.4A). During a self-generated movement an efference copy of the motor command is produced, which is input into a forward model used to predict the consequences of that action. The predicted and actual sensory consequences are then compared. As there is no difference between the predicted and actual sensory feedback (no prediction error) in the self-condition, any reafferent input is cancelled out or attenuated leaving only externally produced afferent information; this allows an individual to distinguish externally produced sensations from their own. Similar mechanisms have been highlighted throughout the other sensory systems. Locating an object's position in space requires knowledge of the retinal location of the object as well as eye gaze direction; with no sensory receptors in the eye Helmholtz suggested an efference copy of the motor command used to control eye movement is required to predict the sensory consequences of eye movement (Helmholtz and König, 1896). (Blakemore et al., 1999) manipulated the predictability of a self-generated tactile stimulus to test this theory. Either a temporal delay was added between the self-generated movement and the subsequent tactile stimulation or an angular perturbation was added between the direction of the movement and the direction of the stimulus: participants rated the sensations as more intense or ticklish the greater the delay or perturbation, which suggested that the magnitude of somatosensory attenuation was directly linked to the magnitude of the prediction error. (Bays et al., 2005) further showed that increasing the delay between a tapping motion and the subsequent perception of a tap on the finger decreased somatosensory attenuation due to the decrease in

predictability of the somatosensory consequences. Attenuation occurred when the consequences of the tapping action were given up to 300ms before the action was completed suggesting somatosensory attenuation is a predictive mechanism that occurs before the sensory input is received (Figure 1.4B,C).

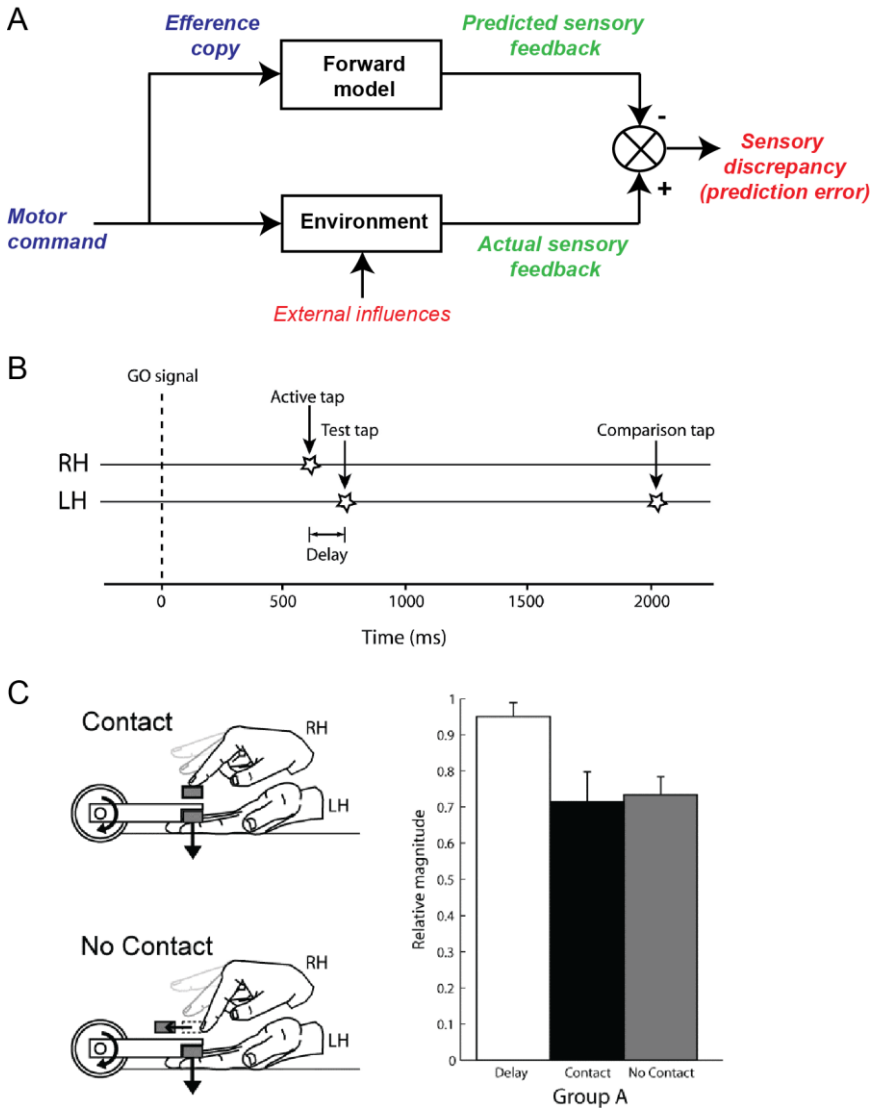

Figure 1.4. Central cancellation theory of sensory attenuation. *A) In this framework, when a motor command is produced an efference copy of that command is sent to a forward model. This model predicts the sensory consequences of the movement. The predicted and actual sensory input are compared and a sensory prediction error generated. In the case of a self-generated movement, the sensory consequences are highly predictable, therefore it is hypothesised that this reafferent information is attenuated. B) Bays et al (2005, 2006) tested how adjusting the predictability of the afferent feedback modulated sensory attenuation. Participants produced an active tap with their right hand (RH) on a force transducer, which generated a test tap on the participants left hand (LH) at different delays following the movement. Participants compared the magnitude of the test tap with a comparison tap. C) With no delay the mean perceived magnitude of the test tap compared to the comparison tap was reduced due to sensory attenuation (black bar); however, adding a delay and increasing the sensory prediction error reduced attenuation (white bar). When participants made a movement but it made no contact with the force transducer the perceived magnitude of the test tap was still reduced (grey bar), which suggests the mechanism involved in sensory attenuation is predictive. However, as sensory attenuation occurred when an implicit prediction error was present in this last condition, this has been used as evidence against the central cancellation theory. Figure adapted from Bays et al, 2005, 2006.*

Neuroimaging studies have been conducted to highlight where in the brain this attenuation occurs. The difference between externally and self-generated tactile stimulation correlated with a decrease in the BOLD signal over bilateral secondary somatosensory cortex (SII), the anterior lobe of the cerebellum and the anterior cingulate (Blakemore et al., 1998). The authors highlighted the potential role of the cerebellum as the comparator which receives the efference copy of the motor command and signals any prediction error to SII where activity is attenuated (Blakemore and Sirigu, 2003). Increasing the delay between a movement and a subsequent tap on the target hand increased the BOLD signal in SII (Shergill et al., 2013). This suggests that modulating the predictability of the tactile stimulus, reduced activity in SII. Other studies have highlighted SII as being important for distinguishing between expected and non-expected tactile stimuli given at various body locations (Drevets et al., 1995) and also between attended and unattended touch (Johansen-Berg et al., 2000), which emphasises that a change in neural activity in SII most likely underlies perceptual somatosensory attenuation.

However, there are clear differences between the central cancellation theory and active inference. Central cancellation suggests that the percept of intensity is encoded by prediction error, however within Bayesian predictive coding frameworks this is unlikely. Top-down predictions are compared with bottom-up sensory input to produce a prediction error, which is then fed forward to update current state estimations and future predictions; it is not the percept. The percept is thought to be a combination of prior beliefs and sensory input: the posterior (Friston and Kiebel, 2009). Moreover, movements that should result in a sensation but do not cause somatosensory attenuation despite the presence of an implicit prediction error (Bays et al., 2006); although this prediction error may be too small to see a perceivable difference in somatosensory attenuation. Somatosensory gating has also been found to occur up to 400ms before movement onset at which point predictions cannot have been made from the motor command, or efference copy (Bays et al., 2006, 2005; Voss et al., 2008), which weakens the foundations of the central cancellation theory. Finally, this theory is lacking as it does not explain physiological somatosensory attenuation, which occurs prior to and during movement regardless of the sensory consequences of that movement. This may not necessarily matter though if these phenomena are dissociable.

1.2.3. Active inference and somatosensory attenuation

Active inference has been used to describe both physiological and perceptual somatosensory attenuation within a single unifying framework. Physiological somatosensory attenuation, in contrast to perceptual somatosensory attenuation, is

defined by a decrease in the amplitude of the primary and secondary components of the SEP generated by giving peripheral nerve stimulation prior to and during movement (Cohen and Starr, 1987; Starr and Cohen, 1985). Neurophysiological recordings in macaque monkeys highlight this gating in both the spinal cord and cortex (Chapman et al., 1988; Seki and Fetz, 2012). Importantly, SEP gating in the primary somatosensory cortex also occurs in response to passive movement (Rushton et al., 1981): no predictions can be made about the consequences of passive movement, therefore the efference copy does not seem to play a fundamental role in SEP gating. This gating appears to occur centrally as direct intracortical microstimulation of M1 in the monkey causes an attenuation of the SEP in the absence of any EMG activity (Jiang et al., 1990). Repetitive stimulation of M1 reduces the magnitude of perceptual somatosensory attenuation in a force matching task (Voss et al., 2007), which suggests that perceptual somatosensory attenuation also occurs via a central mechanism.

As previously stated, active inference posits that somatosensory attenuation is the necessary consequence of reducing the precision of somatosensory evidence during movement to allow the expression of proprioceptive predictions that incite movement. The correlative evidence described above suggests that physiological somatosensory attenuation is associated with movement initiation (active movement) and also the modulation of proprioception (passive movement), which supports this theory. Moreover, patients with PD and functional movement disorders have impaired SEP attenuation, which improves with dopaminergic medication and improvement in motor symptoms (A Macerollo et al., 2015; Macerollo et al., 2016). There is evidence to suggest that attentional processes, which are thought to modulate sensory precision, can attenuate the amplitude of the SEP. SEP attenuation with passive movement is decreased if somatosensory information in the limb being used becomes important and relevant for an alternative task (Staines et al., 2002, 2000). In addition, when tactile information was used to guide a movement the primary components of the SEP were greater when that somatosensory information was unpredictable rather than predictable (Legon and Staines, 2006). In the unpredictable context, prediction errors are highly informative to guide movement, therefore predictive coding theories would predict that the precision-weighting of this signal would be increased. This supports that the attentional modulation of somatosensory precision may be reflected in the amplitude of components of the SEP. Interestingly, patients with prefrontal lesions have the inability gate irrelevant sensory inputs (Knight et al., 1999), which supports that this modulation is driven by top-down mechanisms.

The same framework has been used to describe perceptual somatosensory attenuation. According to this theory, during self-generated movement the predictability of the somatosensory reafferance means this input can be down-weighted by reducing the post-synaptic gain on pyramidal cells in the cortex that receive this input. This results in the requirement of an increased stimulus intensity for an equal neuronal response. When processing externally generated sensations, we have no prior information to aid the perception of this afferent input, therefore the precision of this signal is increased in the cortex. In this way the precision of ascending reafferance to the cortex selects the relative importance of top-down to bottom-up information. Indeed, during a mismatch negativity paradigm there is usually an enhanced ERP to a deviant "oddball" response, which can be explained due to an increase in sensory precision; however, this ERP is absent if the stimulus is self-generated because the precision of exogenous sensory evidence has been reduced (Curio et al., 2000).

Using the same generative model as described previously, (Brown et al., 2013) describe how perceptual somatosensory attenuation occurs in this framework. They demonstrate that the hidden state of an internally generated force has broader 90% confidence intervals than the hidden state of an externally generated force due to a reduction in somatosensory precision; therefore, if asked to report the somatosensory sensation at 90% confidence, the externally generated sensation would be more readily detected than the internally generated sensation. This suggests a modulation in d-prime, or sensitivity, caused by a modulation of sensory precision, which matches empirical psychophysical differences in detection rate when comparing internally and externally generated forces (Juravle and Spence, 2011; Van Hulle et al., 2013). The same model was also used to demonstrate how the results of the force matching illusion can be obtained by reducing somatosensory precision in the self-condition. As highlighted above, the posterior percept of the hidden state of the internally generated force had increased confidence intervals due to the decrease in somatosensory precision. In this simulation it was assumed that the subjective intensity of a stimulus would be at the lower bound of the 90% confidence interval surrounding this posterior percept. Therefore, due to the increased confidence intervals around the posterior, the perceived external force was always lower than the magnitude of the internally generated force and an increase in the internally generated force was needed for the magnitude of this perceived external force to equal the target force (prior belief) given. Giving prior beliefs at different target forces replicated the self-generated results recorded empirically by Shergill et al.,(2005, 2003).

Although this model explains how differences in somatosensory attenuation can generate behaviour in the self-condition of the force matching task, it does not describe the

veridical matching seen in the external condition of this task in healthy participants where participants match target forces using an external joystick. Furthermore, Brown et al fix the model to produce a particular outcome by yoking the perceived external force to the lower bound of the internally generated force thus ensuring the internally generated force would always be larger than that of the matched force replicating the force matching illusion. This model would be more convincing if the resultant matched force wasn't manipulated in this way.

There is clearly a lack of direct evidence to suggest that a modulation in synaptic gain, or sensory precision, underlies perceptual somatosensory attenuation. There is also a lack of experimental work in which these two types of somatosensory attenuation have been measured within a single paradigm to determine if they are functionally or mechanistically distinct. In this PhD, I aimed to determine the relationship between these two forms of somatosensory attenuation, which is vital in potentially dissociating their functional roles. This is also necessary in order to better understand the neurophysiological correlate of somatosensory attenuation.

1.3. Bayesian models, uncertainty and sensorimotor control

One fundamental assumption of the central hypothesis of this thesis is that the brain uses a hierarchical generative model to predict the sensory consequences of movements and updates this based on precision-weighted prediction errors. There is a plethora of evidence from the motor control literature to suggest that forward models are implemented in the sensorimotor system (Bastian, 2006; Blakemore and Sirigu, 2003; Miall et al., 1993; Paulin, 1993; Wolpert and Miall, 1996). For example, it has been shown that during a reaching movement, saccades move to a position in advance of the current hand position, which suggests that we predict the future sensory consequences of our motor commands (Ariff et al., 2002). Moreover, there is evidence demonstrating that the brain integrates estimates of uncertainty into these models in a Bayesian manner in the sensorimotor system. In one example participants were trained to reach towards a target shifted to the left of the true target location with no visual feedback. Giving visual feedback midway through the movement shifted the end point towards the real target location. Increasing the uncertainty (visual blur) in this feedback reduced the influence of the sensory data on the final reaching position. Increasing the uncertainty in the sensory evidence, increased participants' reliance on their prior estimation of where the target was in line with Bayesian statistics (Körding and Wolpert, 2004). There are multiple different frameworks of how Bayesian models control movement and how they may be

implemented in the brain. In particular, active inference offers an alternative approach to sensorimotor control then the current leading framework, Optimal Control Theory (OCT). There is a lack of empirical evidence to support the hypotheses produced by the active inference framework, however it offers an alternative outlook from which novel predictions and experimental paradigms can be tested.

1.3.1. Active inference vs Optimal Control

OCT is a popular theory describing how we control movements. This theory tries to address a key problem in motor control: how does the brain select the most optimal action out of several possible movement trajectories? (Franklin and Wolpert, 2011; Wolpert and Ghahramani, 2000). Within this Bayesian framework, a forward model estimates the current state of the body by combining predicted and current sensory input. This state estimation is then used to update optimal control functions, which rank possible actions based on cost functions aiming to minimise musculature noise whilst ensuring optimal achievement on the task at hand. Motor commands are generated via an inverse model, which reduces a future cost. An efference copy of these commands is sent to the forward model to predict changes in hidden states using sensory predictions. A number of studies have shown how that this model can accurately explain behaviour (Harris and Wolpert, 1998; Haruno and Wolpert, 2005; Todorov, 2004; Todorov and Jordan, 2002). However, this theory lacks a specific understanding of how each component could map onto neurophysiological connections in the brain; active inference tries to do this.

There are also some fundamental differences between OCT and active inference. Firstly, it has been argued that it is unlikely for movements to be specified with single learned cost functions (Friston, 2011); active inference replaces cost functions with prior beliefs that emerge naturally from perceptual inference. Secondly, OCT states that descending signals to the spinal cord transmit motor commands, whereas in active inference these descending signals are proprioceptive predictions about the proprioceptive consequences of the movement. This is an important difference as the type of connection described has implications for the neurobiology. In predictive coding frameworks, predictions are backward connections, whereas commands are driving, forward connections. Adams et al (2013) argue that the anatomical and physiological characteristics of the descending motor input to the spinal cord suggests that they are of the backward-type and more likely represent predictions rather than commands themselves. Finally, OCT places an inverse model within motor cortex, which generates motor commands, whereas in active inference predictions are generated by a hierarchical generative model and these are converted into motor commands within the spinal cord. Indeed, the EPH (described

earlier) shares many of these characteristics with active inference. The main advantage of active inference and the EPH is their solution to the redundancy problem of action selection: the correct motor command is automatically produced from the deviation of the descending control signal from the threshold point in the spinal cord, so there is no need for an inverse model in the cortex. Importantly, the active inference framework, unlike the EPH, can provide a unifying hypothesis of how predictive coding is implemented in the brain across a number of processes from perception and cognition to motor control. However, there is a lack of empirical evidence that movements are controlled according to the active inference framework. In particular, there is a lack of evidence demonstrating that neurophysiological correlates of the components important for predictive coding exist in the sensorimotor cortex.

1.3.2. Bayesian Models and sensorimotor learning

Sensorimotor adaptation paradigms offer a useful method to measure predictive coding within the sensorimotor system. Perturbations to movement trajectories generate prediction errors between the predicted and actual sensory consequences of the action and the neurophysiological correlate of these parameters can be measured. Bayesian models also provide a particularly useful account to explain sensorimotor learning in the presence of uncertainty. There are a number of different models which have been used to explain participant's behaviour on these types of tasks. Traditional reinforcement-learning models explain how an animal receives new information, which is then used to update its beliefs about the environment in proportion to prediction errors: the prediction error must be multiplied by a learning rate to determine the degree to which a given belief is updated (Rescorla and Wagner, 1972; Sutton and Barto, 1998). Models, such as the Rescorla-Wagner (RW) learning model, are simple, computationally efficient and used widely in cognitive neuroscience; however, do not incorporate estimates of uncertainty which are integral for optimal perception and action.

Bayesian accounts of learning formalise how beliefs are updated based on new data and suggest that learning rates are dependent on current levels of uncertainty of prior beliefs relative to sensory input. Indeed, using a visuomotor adaptation task, (Wei and Körding, 2010) demonstrated that increasing uncertainty in the visual feedback of a cursor end-point position reduced learning rates, such that participants did not adapt to a visuomotor rotation as quickly. Here the Kalman filter was used for Bayesian estimation of hand position and best explained the experimental data suggesting that we do adapt to visuomotor perturbations in a Bayesian manner and respond to visual noise as predicted. Importantly, uncertainty can arise from a number of sources, not solely surrounding the

sensory input. In particular, (Yu and Dayan, 2005) suggest that the volatility of the environment ("unexpected uncertainty") will dictate the learning rate: in a fast-changing, volatile environment where more recent experience is important, the learning rate will be large, such that prediction errors have a large influence on the update of prior beliefs; however, if historical information is more important, such as in a stable environment, the learning rate will be smaller and require a larger prediction error to update prior beliefs. There have been a number of studies using Bayesian learning models to understand how humans use Bayesian inference to track reward probabilities in a changing environment and actively adapt their learning rate to this (Behrens et al., 2008, 2007). However, the approach used in these studies is computationally expensive and the learning process is assumed to be identical across participants.

An alternative approach has recently been suggested which applies Bayesian updating in a computationally efficient manner using one-step update equations designed to minimise free energy in a biologically plausible way. The Hierarchical Gaussian Filter (HGF), designed based on probability theory, explains how a participant learns about their environment from the sensory information available given their own generative model. The internal generative model represents how the participant believes sensory information is generated in the world; an inversion of this model produces a posterior probability distribution, which represents this belief and predicts what sensory information is expected. The HGF consists of two models. The perceptual model describes how these beliefs update over time in order to explain how a participant learns about an unknown, continuous variable that modulates over time. The response model then describes how the participant should behave given those beliefs by mapping the beliefs onto actions. Here participant-specific parameters dictate individual learning rates that modulate over time based on the participant's trial-wise behaviour unlike traditional reinforcement learning models, which have a fixed learning rate across time. Importantly, the perceptual model of the HGF is hierarchical and each level is coupled to higher levels by the variance in the modulation of the underlying hidden state; therefore, the volatility of the hidden state at the second level is dictated by the variance at the first level. In this way different forms of uncertainty can be captured at different levels of the hierarchy. For example: the first level captures irreducible uncertainty unaffected by learning in which an unexpected stimulus requiring an unexpected response generates a sensory prediction error; the second level represents estimation uncertainty in the stimulus transition probabilities describing how likely it is that the stimulus presented will be different from expected and generates a contingency prediction error; and the third level describes the volatility uncertainty that arises from the stability of the environment and generates a

volatility prediction error. The HGF produces individual time series of how beliefs evolve over time at each level of the hierarchy, therefore offers the opportunity to separate prediction, prediction error and precision parameters at different hierarchical levels. This is important as the active inference framework makes specific predictions about the presence of these parameters of predictive coding within the sensorimotor system and their role in motor control.

In this PhD, I used the HGF to explain participant's behaviour on a visuomotor adaptation paradigm and recorded EEG to determine the presence of these predictive coding parameters in the sensorimotor system specifically using a model underpinned by the active inference framework. The visuomotor adaptation paradigm used offers a useful tool to measure and manipulate parameters of predictive coding and has previously been used to assess neurophysiological correlates of predictive coding in the sensorimotor cortex (Tan et al., 2014a, 2016). **The active inference framework aims to generalise ideas from predictive coding to the sensorimotor system, therefore this study will offer an important insight into the plausibility of this hypothesis.**

1.4. The neurophysiological correlate of sensory precision

The active inference framework posits that a down-weighting of sensory precision is necessary for motor initiation. One aim of this thesis was to determine the neurophysiological correlate of sensory precision within the sensorimotor system. I aimed to modulate uncertainty of visual and somatosensory inputs to sensorimotor cortex to determine the resultant effect on oscillatory activity and behaviour.

In the active inference framework, precision (inverse variance or uncertainty) is encoded by synaptic gain (post-synaptic responsiveness) of superficial pyramidal cells in the cortex, which are responsible for transmitting prediction errors up the hierarchy (Friston, 2005; Friston and Kiebel, 2009). It has been suggested that neuromodulatory networks may act to modulate this synaptic gain via top-down attentional processes (Friston, 2005; Schroeder et al., 2001). Within the sensorimotor system, dopamine has been highlighted as an important neuromodulator for sensorimotor control and appears to modulate the precision-weighting of prediction errors. Indeed, pharmacological D1 and D2 receptor blockade in healthy participants specifically impaired participants' ability to react to unexpected events that generated large sensory prediction errors by replacing a prepared action with another action (Bestmann et al., 2014). The authors suggest that dopamine depletion led to an overreliance on top-down predictions, therefore there was a

diminished response to low-level sensory prediction errors. This can be likened to a reduction in the precision-weighting of sensory prediction errors.

In addition, it has been suggested that fast, synchronous oscillatory activity recorded in local field potentials (LFPs) or at the scalp with M/EEG can modulate synaptic gain and the synaptic gain of coupled neuronal populations determines the frequency of their oscillatory behaviour (Chawla et al., 1999; Friston et al., 2015). This suggests that oscillatory activity can have a mechanistic impact on neuronal processing and may not simply be an epiphenomenon of population activity. The timing of neuromodulatory changes in the brain can be quite slow, therefore it is likely that rapid attentional mechanisms that appear to modulate responses under different levels of uncertainty most likely rely on an interaction between neuromodulatory and electrophysiological mechanisms. It has been suggested that directed oscillatory coupling between different cortical areas or between laminar layers within a cortical region establishes a functional hierarchy: within both the visual and auditory systems, dynamic causal modelling (DCM) has highlighted a dominance of theta and gamma oscillatory activity in signalling bottom-up prediction errors and beta oscillations as signalling top-down predictions (Arnal et al., 2011; Arnal and Giraud, 2012; Bastos et al., 2012). The post-synaptic gain, corresponding to the estimated precision, is thought to be essential for selecting the influence of ascending information over descending information within these canonical cortical microcircuits. (Bressler and Richter, 2015) found that beta oscillations from extrastriate cortex to primary visual cortex in the monkey predicted the strength of evoked potentials in V1 suggesting this oscillatory activity may represent a gain control mechanism. Alternatively, (Bauer et al., 2014) found that attention-dependent pre-stimulus alpha band oscillations tracked stimulus predictability in a simple attentional RT paradigm, whereas a proxy for surprise, or prediction error, was tracked by attention dependent gamma band oscillations. This provides empirical evidence for an attention-dependent gain control, which is represented or controlled by oscillatory activity. These studies suggest that high frequency gamma oscillatory activity may more readily modulate precision, however these studies were not directly testing hypotheses regarding the role of oscillatory activity in modulating precision in the sensorimotor system.

Within the sensorimotor system beta oscillations (~12-30Hz) are dominant and appear to have an important, yet contentious, role in sensorimotor control (Davis et al., 2012; Engel and Fries, 2010; Little and Brown, 2014). I hypothesise that this frequency of oscillatory activity could correlate and potentially modulate sensory precision. The motivation for this hypothesis comes from circumstantial evidence, which suggests that modulations in sensorimotor beta power with movement readily reflect the time course of SEP

attenuation with movement (Cohen and Starr, 1987; Pfurtscheller, 1981). The modulation of sensorimotor beta power with movement and afferent input correlates with predictions from the active inference framework regarding the modulation of sensory precision.

Moreover, PD patients with disrupted dopamine signalling (previously hypothesised as a modulator of sensory precision) show abnormal sensorimotor beta oscillatory activity and have impaired motor control. PD is a neurodegenerative disorder caused by degeneration of dopaminergic neurons in the substantia nigra pars compacta (SNc) of the basal ganglia (Ehringer and Hornykiewicz, 1960). The hypokinetic motor symptoms of PD include tremor, rigidity, akinesia (inability to initiate movements) and bradykinesia (slowness of movements). Electrophysiological recordings from electrodes in the STN and sensors over the scalp demonstrate that PD patients have increased beta power and increased beta coherence across the cortico-subcortical loop, which correlates with the motor symptoms of PD (Brown, 2007, 2003; DeLong and Wichmann, 2007; Little et al., 2012). High frequency deep brain stimulation (DBS) of the STN improves motor symptoms in PD and has a greater efficacy when paired with an adaptive algorithm in which the stimulation is triggered by peaks in beta power (Little et al., 2013). As DBS shows optimal efficacy when it directly modulates beta activity, this suggests beta oscillatory activity plays a causal role in the motor symptoms of PD. In addition, dopaminergic medication reduces beta power and improves the motor symptoms of PD, which suggests that dopamine may play an important role in the modulation of beta oscillations (George et al., 2013; Jenkinson and Brown, 2011). One hypothesis is that a maladaptive or abnormal change in the processing of somatosensory precision caused by changes in dopaminergic signalling could underlie the increase in beta power seen in PD. Alternatively, this increase in beta power could mechanistically affect synaptic gain of somatosensory prediction errors. These changes in oscillatory activity and somatosensory precision would be hypothesised to directly contribute to the motor symptoms of PD in line with predictions from the active inference framework.

1.4.1. Current theories regarding the functional role of sensorimotor beta oscillations

Here I outline current theories regarding the functional role of sensorimotor beta oscillations in motor control to determine whether the hypothesis that this activity could represent sensory uncertainty is plausible. It has been known for a long time that beta oscillations over sensorimotor cortex desynchronise prior to and during movement and resynchronise following a movement (Gastaut, 1952; Hari and Salmelin, 1997; Jasper and Penfield, 1949; Jasper and Andrews, 1936; Pfurtscheller, 1981). However, the functional

role of this activity remains controversial. Motor control theories suggest that this modulation of beta oscillatory activity actively controls movement rather than being an epiphenomenon of movement. Evidence for this comes from patients with PD outlined above. However, the beta event-related desynchronization (ERD) during movement is not modulated by different types of movement execution, such as the speed of movement (Stancák and Pfurtscheller, 1995), index vs fourth-finger flexion (Salmelin et al., 1995) or ballistic vs sustained wrist movements (Alegre et al., 2003) and there is no difference in the ERD depending on whether participants are focusing on speed rather than accuracy in a reaching task (Pastötter et al., 2012). Moreover, sensorimotor beta power can be decreased by motor imagery (McFarland et al., 2000; Nakagawa et al., 2011), the observation of movement (Babiloni et al., 2002; Koelewijn et al., 2008), passive movement (Keinrath et al., 2006) and tactile stimulation (Cheyne et al., 2003; Gaetz and Cheyne, 2006), which suggests that the beta ERD is not purely associated with motor execution. On the other hand, the pre-movement decrease in beta power does appear to be related to movement preparation (J. Kilner et al., 2005): predictive warning cues revealing which hand to respond within a RT task leads to a greater decrease in beta power suggesting a role for beta oscillations in response selection (Doyle et al., 2005; van Wijk et al., 2009). However, other studies suggest this beta decrease is modulated more readily by experimental conditions in a task rather than specific movement parameters (Alegre et al., 2003; Cassim et al., 2000; Sanes and Donoghue, 1993; Stancák and Pfurtscheller, 1995). The literature on modulations of this pre-movement beta decrease is inconsistent and variable; however the consensus is that beta oscillations are not solely involved in motor execution.

It has been suggested that beta oscillations over sensorimotor cortex act to maintain the status quo of the system (Engel and Fries, 2010). Following the termination of a movement there is an increase in beta power due to a post-movement beta synchronisation (PMBS). This is thought to recalibrate the motor system and prevent the generation of any new movements. This is supported by the finding that corticospinal excitability is reduced during this period (Chen et al., 1998) and GABA levels in the motor cortex correlate with the magnitude of the PMBS (Gaetz et al., 2011). Indeed, beta oscillations appear to have an active akinetic process as spontaneous increases in beta power have been shown to slow movements (Gilbertson et al., 2005) and cortical stimulation of sensorimotor cortex in the beta frequency band has been shown to reduce motor output (Joundi et al., 2012; Pogosyan et al., 2009). Further evidence that the PMBS may encode proprioceptive error feedback (Tan et al., 2014a, 2014b) supports the idea that beta oscillations monitor and maintain the status of the sensorimotor system. In

addition, beta power increases during static postural maintenance and motor unit activity in the periphery is phase-locked to sensorimotor beta oscillations during postural maintenance supporting the idea that beta oscillations aim to maintain the state of the sensorimotor system by encoding cortical reafferance (Baker et al., 1997). This theory closely resembles predictions about how modulations in sensory precision would affect motor output: the precision-weighting of prediction errors determines their effect on current processing in sensorimotor cortex and therefore this precision-weighting acts to maintain the status of the system. This supports that sensorimotor beta power may correlate with this uncertainty estimate.

One assumption of this hypothesis is that sensorimotor beta oscillations have one distinct role that can be generalised across all changes in beta power. However, there are multiple distinct beta components prior to, during and following a movement, which suggests this assumption may not be correct. In warned RT tasks, there is often an increase in beta power prior to the cue onset, which appears to be separate from the PMBS following the previous trial. (Saleh et al., 2010) show a modulation in this power between two tasks with differing complexity (colour association vs simpler spatial cueing task), but the same timing and movement requirements. This suggests that here beta oscillations may act as part of a large-scale visuomotor attentional network to upregulate sensorimotor processing beyond somatosensation. This could be a distinct role from the beta ERD during movement. In addition, several studies have highlighted a decrease in beta power after the onset of a warning cue that is distinct from the preparatory decrease in beta power prior to movement (Alegre et al., 2006; Tzagarakis et al., 2010; van Wijk et al., 2009). This has been shown to modulate with uncertainty in the direction of the upcoming movement, such that there is a greater decrease in beta power on trials with the least uncertainty (Tzagarakis et al., 2015, 2010) and this is also reflected in a subthalamic beta power decrease which is greater following predictive warning cues which are likely to have less uncertainty compared to non-predictive warning cues (Williams et al., 2003). There is no confirmed hypothesis for what this post-warning-cue beta decrease is functionally involved in, however I hypothesise that this may be involved in the attentional modulation of synaptic gain shown previously to encode uncertainty. It will be important to determine if beta power both prior to and after a movement correlates with changes in sensory precision as predicted by a single unifying hypothesis or if this hypothesis only holds true for certain beta components.

1.4.2. The role of beta oscillations in predictive coding

Recently, there has been an increase in evidence to suggest that sensorimotor beta oscillations, specifically the PMBS, may have an important role in predictive coding. In particular the PMBS occurs at the same point in which error feedback or Bayesian updating following the movement may occur (Alegre et al., 2008). Indeed increasing evidence suggests that suppression of the PMBS is associated with error feedback (Luft et al., 2014). (Tan et al., 2014a) demonstrated this using a visuomotor adaptation task. Participants were instructed to make goal-directed movements to a target and the sensory feedback was perturbed using a visuomotor angular rotation causing participants to make large initial angular errors, which reduced over time with adaptation. They found that the PMBS increased as the initial angular movement error decreased. They also found a significant interaction between presentation order and perturbation angle such that trials with the same angular perturbation had a greater PMBS if they were presented later during the experiment despite the initial angular error of the response being equal. This suggests that the PMBS was not only modulated by the size of the error but by the salience of error; the variance in the PMBS from trial-to-trial was best explained by a Bayesian model which incorporated a prediction error weighted by the past history of errors rather than the prediction error on the current trial alone. This suggests the PMBS was tracking the uncertainty surrounding the presence of a prediction error and could therefore mediate Bayesian inference in motor adaptation.

A follow up study by (Torrecillos et al., 2015) replicated Tan and colleagues finding regarding the PMBS, but in addition highlighted that during motor preparation on the subsequent trial a pre-movement beta enhancement was differentially modulated compared to the PMBS. This foreperiod beta enhancement correlated with the adjustment of the motor command necessary to produce a more accurate movement on the next trial. Therefore, it appears that modulations in beta oscillatory activity during movement preparation were directly related to the updating of the motor command or the prediction for the upcoming trial rather than the prediction error.

As previously addressed prediction errors, within the active inference framework, are transmitted as precision-weighted prediction errors dependent on the synaptic gain of the cells transmitting this information. In the above paradigms this precision-weighting could not be dissociated from the prediction error signal. We cannot conclude whether or not the PMBS represented this precision parameter or simply represented the magnitude of the prediction error or whether these parameters are even dissociable. To help address this, (Tan et al., 2016) modulated expected uncertainty (known variability in the

environment) and estimation uncertainty (uncertainty in feedforward estimations) within the same experimental paradigm in order to determine whether the PMBS more readily correlated with uncertainty estimates or angular error (Figure 1.5). In a random priming condition, where the visuomotor angular rotation changed randomly from trial-to-trial, both expected and estimation uncertainty were high such that any observation that deviated from expected would have a very low probability of updating the model parameters and no adaptation would occur; in contrast, for the constant prime condition the same visuomotor rotation was given on every trial, therefore estimation uncertainty was low and participants successfully adapted to the rotation. At the end of this priming block the PMBS on average was much larger for the constant condition compared to the random condition; however, here, uncertainty and error could not be dissociated. Crucially, when both conditions were then given a new constant visuomotor rotation, there was a large decrease in estimation uncertainty for the constant but not the random condition and this was reflected in a significant decrease in the amplitude of the PMBS across these early trials following the constant block, but not the random block. Importantly, the angular error between conditions was equal in these trials, therefore the only variable modulating the PMBS amplitude was the estimation uncertainty. The authors suggest that the PMBS indexes the confidence surrounding feedforward estimations, which can then allow for more flexibility and the revision of motor plans. This is potentially modulated by dopamine within the basal ganglia in line with the research described earlier.

However, this account for the role of the PMBS does not generalize easily to explain all known modulations in sensorimotor beta oscillations. For example, if this account was applied to the beta ERD prior to and during movement, then the conclusion would be that we have the highest uncertainty in our model while we move, which would seem unlikely. Although the literature suggests that different components of the sensorimotor beta modulations may have different functional roles, a unifying hypothesis able to explain all components would be more appealing and convincing. Importantly, uncertainty is not only estimated for parameters of the forward model; an estimate of uncertainty in the actual sensory input is also required for Bayesian inference. The resulting precision-weighting of prediction errors is a ratio between prior precision and sensory precision; importantly, active inference highlights that an increase in the estimate of the uncertainty of the actual sensory input is an essential step for being able to move. However, the neurophysiological correlates of this change in uncertainty are unknown. In this thesis I hypothesise that sensorimotor beta power might be either the neurophysiological correlate of this estimate of sensory uncertainty or causally modulating this uncertainty.

Indeed, there is compelling evidence to predict that sensorimotor beta power and estimates of sensory precision might be positively correlated.

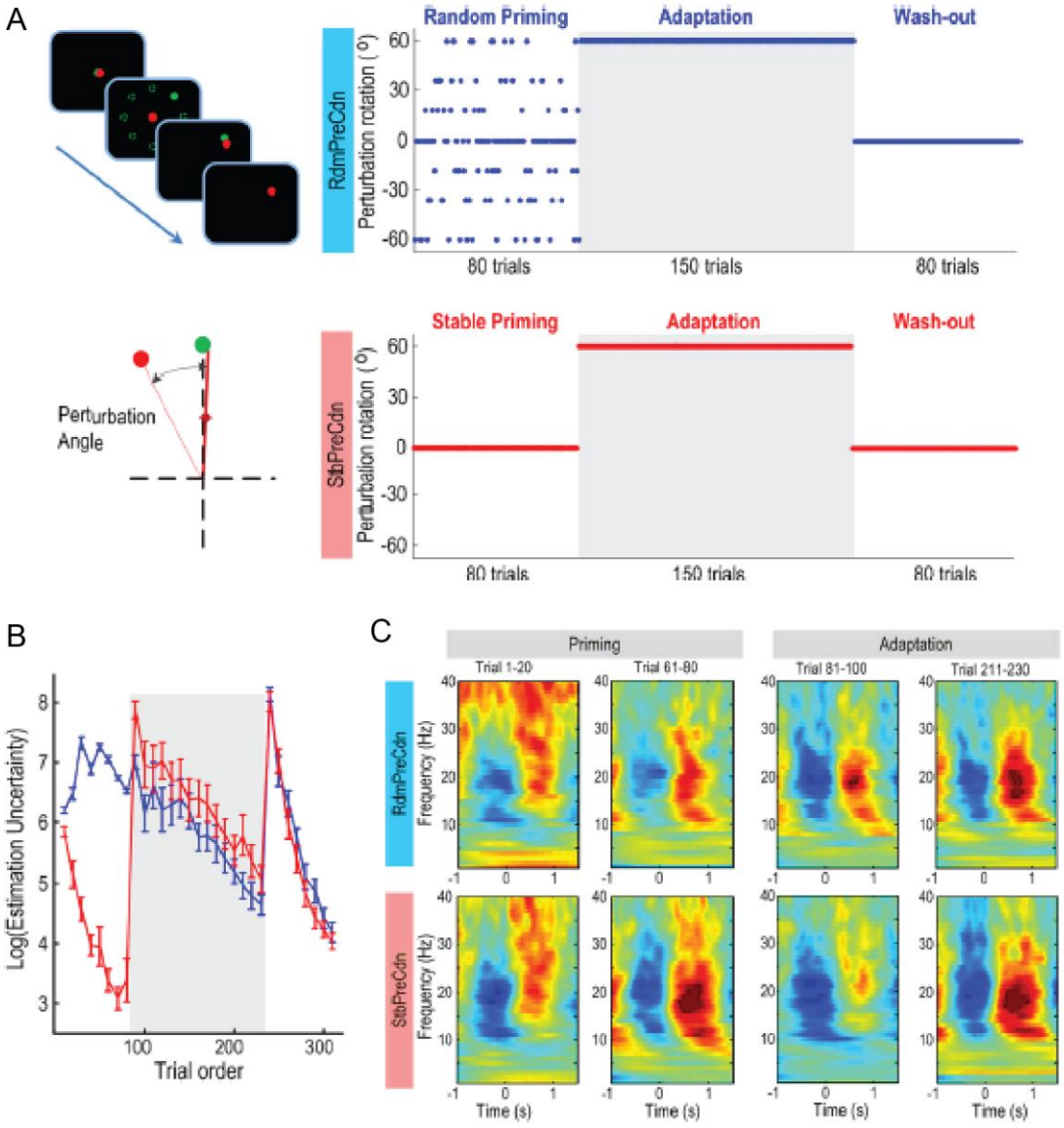

Figure 1.5. Experimental paradigm and results adapted from Tan et al (2016) showing the relationship between the PMBS and estimation uncertainty. *A) Participants were required to reach from a central start position to a target. An angular rotation was added between the actual joystick movement and the cursor on the screen. Participants completed the task under two conditions: a random priming condition where the angular rotation changed magnitude randomly across trials for the first block; and a stable priming condition where the angular rotation remained constant over the first block. The same 60° rotation was then applied to both conditions after 80 trials. B) A Bayesian learning model was used to dissociate the estimated mean, estimation uncertainty and expected uncertainty on each trial. For the stable priming condition (red) there was a large increase in estimation uncertainty following the first constant block, which was not seen in the random priming condition (blue). C) Changes in estimation uncertainty negatively correlated with the magnitude of the PMBS. In particular, over the first 20 trials of the adaptation block, there was a significant difference in the magnitude of the PMBS between conditions, which reflected this difference in estimation uncertainty. There was no significant difference in angular error at this time point, which could explain the modulation in the PMBS.*

1.4.3. Could beta oscillations originate in the somatosensory cortex and represent an afferent signal?

Importantly, if sensorimotor beta power correlates with somatosensory precision as hypothesised, then it would be expected that this oscillatory activity would be modulated by afferent input and would potentially be generated in somatosensory cortex. There is a plethora of correlative evidence to suggest that sensorimotor beta oscillations may represent a somatosensory signal. Firstly, the beta ERD over sensorimotor cortex occurs in response to peripheral tactile stimulation (Cheyne et al., 2003; Gaetz and Cheyne, 2006), passive movement (Parkkonen et al., 2015) and motor imagery (Kühn et al., 2006a; McFarland et al., 2000; Nakagawa et al., 2011), therefore an active motor command is not necessary to modulate sensorimotor beta power. Secondly, electrically stimulating the periphery causes a resynchronisation in the beta frequency over sensorimotor cortex (Hari et al., 1998; Müller et al., 2003; Pfurtscheller, 1981), which supports evidence that beta power signals cortical reafference. This rebound decreases with movement, the observation of movement (Hari et al., 1998) and the observation of sensory stimulation (Muthukumaraswamy and Johnson, 2004), which further suggests that sensorimotor beta oscillations are sensitive to somatosensory events. Finally, deafferented patients have decreased beta oscillatory activity within the motor system (Cassim et al., 2001).

Moreover, there is correlative evidence within the literature to suggest that modulations in sensorimotor beta oscillations may reflect changes in synaptic gain that could reflect somatosensory precision, as hypothesised in this thesis. Prior to and during movement the amplitude of SEPs recorded over sensorimotor cortex decreases (Cohen and Starr, 1987; Seki and Fetz, 2012) and this somatosensory attenuation is reminiscent of the modulation of sensorimotor beta oscillations with movement (Jasper and Penfield, 1949; Pfurtscheller, 1981). Passive movement also causes a reduction in SEP amplitude (Rushton et al., 1981; Seki and Fetz, 2012; Staines et al., 2000) and beta power (Keinrath et al., 2006; Müller et al., 2003). During periods of active holding, beta power increases (Baker et al., 1997) as does the amplitude of cutaneous SEPs over sensorimotor cortex (Rushton et al., 1981; Seki and Fetz, 2012); during this period sensorimotor beta oscillations are phase-locked to peripheral motor unit activity, which is important for postural maintenance and suggests the beta oscillations encode cortical reafference (Baker, 2007). Beta bursts have also been shown to enhance SEP amplitude following peripheral nerve stimulation (Lalo et al., 2007) and enhance transcortical stretch reflexes (Gilbertson et al., 2005). In addition, PD patients, who have abnormally high resting beta power, show a reduced modulation of sensorimotor beta oscillations with movement and

also have impaired SEP attenuation, both of which improve with dopaminergic medication (Macerollo et al., 2016).

Finally, the exact cortical origin of the beta ERD is still disputed with some studies reporting the source to be in the anterior bank of the central sulcus (Jasper and Penfield, 1949; Salmelin and Hari, 1994), others the postcentral bank (Jurkiewicz et al., 2006) and other studies have found both (Papakostopoulos, 1980; Sochůrková et al., 2006; Szurhaj et al., 2003). The PMBS has been localized to primary motor cortex and the supplementary motor area (Brovelli et al., 2002; Salmelin and Hämäläinen, 1995), however ECoG studies suggest the PMBS comes from a distributed cortical network including the whole sensorimotor and premotor area (Crone et al., 1998; Ohara et al., 2000; Pfurtscheller et al., 2003). It is difficult to conclude the origin of sensorimotor beta oscillations using source localisation methods as these methods are biased to the primary motor cortex due to the uniqueness of its cytoarchitecture. Betz cells in layer V of the primary motor cortex are giant pyramidal cells thought to be the largest cells in the cortex (Betz, 1874) and are most concentrated in area 4 on the crown of the precentral gyrus and reduce in number moving into the central sulcus towards areas 3a and 3b (Meyer, 1987). Due to this unique cellular physiology the same signal in M1 and S1 is likely to appear larger in M1 biasing source localisation methods.

Despite having a different cellular composition, both somatosensory and motor cortex have cellular physiology that promotes the generation of beta oscillations. In somatosensory cortex, layer V pyramidal neurons have gap junctional connections that allow for strong electrical coupling and can produce stable population oscillations (20-30Hz) even if synaptic potentials are pharmacologically blocked (Roopun et al., 2006). In primary motor cortex, intracellular recordings revealed a specific shape of the neuronal hyperpolarisation trajectory, which causes neurons to rhythmically fire within the beta frequency band; however, the specialised post-spike membrane potential changes seen in M1 neurons are not necessary to produce oscillatory activity in the beta band (Baker, 2007). Sensorimotor beta oscillations could therefore represent modulations in the precision-weighting of prediction errors in primary somatosensory cortex driven by the proprioceptive prediction to move. Indeed, corticomotor neurons, which are thought to carry predictions about the precision of proprioceptive input to gamma motor neurons in the spinal cord are present both in M1 and area 3a (Rathelot and Strick, 2009, 2006) where these signals can modulate the gain of the classical motor reflex arc in the spinal cord (Adams et al., 2013a). This provides a potential mechanism by which modulations of somatosensory precision in somatosensory cortex could modulate motor control and how this could be encoded by beta oscillatory activity.

1.5. A change in direction: does the sensory system drive the motor system?

The active inference theory predicts that a down-weighting of somatosensory information is required in order to initiate movements. Historically it has been argued that the role of the somatosensory system in motor control is to provide feedback to update and correct movements. However, increasing evidence suggests that the somatosensory system may play a more significant role in driving motor function. Beta power in LFPs of primates was shown to be stronger in S1 than M1 (Witham and Baker, 2007) and it has been found that neurons in somatosensory cortices fire coherently with M1 oscillations and a quarter of an oscillatory cycle before M1, which suggests that M1 oscillatory activity could be driven by the neuronal activity in S1 (Baker et al., 2003). A strong information drive from post-central to pre-central gyrus in the beta frequency band has also been found during isometric contraction in monkeys (Brovelli et al., 2004), which supports the hypothesis that sensorimotor beta oscillations represent a cortical reafferance or proprioceptive signal. However, these studies lack a measure of how this information drive then causally effects movement. For example, in mice, the primary somatosensory cortex directly drives the primary motor cortex for whisker retraction (Matyas et al., 2010).

Sensory processing deficits are prominent in PD but are disguised by severe motor symptoms. One hypothesis is that the motor impairments seen in PD are the result of an inability to correctly integrate proprioceptive and motor information (Konczak et al., 2009). Indeed, proprioception is impaired in PD causing patients to rely far more on visual cues to guide movement than healthy controls: when visual feedback is removed patients produce inaccurate movements and often undershoot targets (Klockgether et al., 1995). Numerous psychophysical studies suggest that kinesthesia (the conscious awareness of the position or movement of the limb) is altered in PD: patients with PD have a decreased sensitivity to detect small changes in limb position (Maschke et al., 2003), finger position (Putzki et al., 2006) and limb motion (Konczak et al., 2007) compared to healthy controls and this impairment has been shown to correlate with disease severity (Maschke et al., 2003). It has been suggested that these deficits in proprioception may play a more primary role in causing the motor symptoms in PD.

According to active inference, somatosensory attenuation is necessary to initiate movements. If decreases in beta power are correlated with this decrease in synaptic gain, and in turn a decrease in SEP amplitudes, then it may be theorised that the increased beta power in PD may reflect an inability to down-weight incoming sensory information. This

may be responsible for the akinetic symptoms and in turn should correlate with a lack of somatosensory attenuation. Indeed, SEP attenuation is reduced in PD patients and dopaminergic medication normalises SEP attenuation and improves motor symptoms (Macerollo et al., 2016). Similar results have been found in patients with functional movement disorders (A Macerollo et al., 2015). Moreover, PD patients have abnormal gating of 1a afferents in the spinal cord (Hiraoka et al., 2005; Morita et al., 2000): it is this circuitry that is hypothesised to play a central role in movement initiation in active inference and be mediated by modulations of precision in the cortex (Adams et al., 2013a). One way of testing the theory that sensory precision is related to motor initiation and modulations in sensorimotor beta power, would be to modulate the uncertainty of the afferent input in order to artificially change estimates of sensory precision and quantify the effect of this on movement parameters and oscillatory activity. One method of reducing sensory precision in this way would be to apply high frequency vibration to the periphery, which is assumed to modulate the proprioceptive signal and increase the uncertainty in sensory estimates of this input.

1.5.1. Using vibration to modulate sensory precision

Peripheral vibration has been used to investigate the role of muscle spindle activity in a variety of motor control tasks. Primary muscle spindle endings are readily activated by vibration of the muscle at the optimal vibration frequency of ~80Hz (Ribot-Ciscar et al., 1998; Roll et al., 1989). Vibration does not selectively activate Ia afferents, however secondary endings are activated much less readily at high vibration frequencies. Prolonged high amplitude vibration from 30-100Hz can produce an increase in muscle contraction referred to as the tonic vibration reflex (TVR). This reflects an increase in activity from afferent nerve fibers that activate monosynaptic and polysynaptic reflex arcs to cause the muscle to contract (Hagbarth and Eklund, 1966). Interestingly, when a TVR is produced there is a depression in the tendon jerk reflex and the H-reflex (De Gail et al., 1966; Delwaide, 1973). As there is concomitant muscle activity, this suggests that the vibration increases the tonic presynaptic inhibition of the afferent signal. Indeed, hindlimb vibration in the cat causes a depolarisation of primary afferents, which is reminscient of this presynaptic inhibition and the reflex depression seen in humans (Barnes and Pompeiano, 1970; Gillies et al., 1969). Therefore, peripheral vibration appears to modulate the gating of proprioceptive signals from the muscle spindles in the spinal cord. In addition, peripheral vibration at 60Hz causes an attenuation of early components of the cortical and cervical SEP (Abbruzzese et al., 1980; Cohen and Starr, 1985) further reflecting the role of vibration in modulating sensory gating. However, 50

Hz cutaneous vibration between the thumb and finger and 20 Hz vibration at the wrist does not produce significant SEP attenuation, which suggests that muscle spindle activation is necessary to evoke sensory attenuation (Kakigi and Jones, 1986; Legon and Staines, 2006).

It has previously been shown that high frequency vibration of forearm muscle tendons, which selectively activates muscle spindles (Brown et al., 1967; Burke et al., 1976; Roll et al., 1989), produces the illusion that the arm is moving or has been displaced (Craske, 1977; Goodwin et al., 1972; McCloskey, 1973). The central nervous system incorrectly interprets the increased firing rate of muscle spindles as if the affected muscle is lengthening, which generates uncertainty in estimates of the position of the limb. This has been demonstrated in a number of position-matching and pointing tasks all of which show increased error, or reduced accuracy, following high-frequency peripheral vibration (Capaday and Cooke, 1983; Cordo et al., 1995, 2005; Inglis and Frank, 1990; Tsay et al., 2016). The illusion of arm extension following muscle vibration is largest at a vibration frequency of 80-100Hz (McCloskey, 1973) reflecting the optimal frequency for activating the primary spindle endings, which supports the role of Ia afferents in producing this illusion. In PD patients, vibration-induced illusions appear no different between patients and healthy controls (Moore, 1987); however, when asked to make a voluntary movement to a target during vibration, PD patients undershoot the target less than healthy controls, which suggests the illusion is reduced in PD patients (Khudados et al., 1999; Rickards and Cody, 1997). There is no evidence for any abnormalities within the fusimotor system and the muscle spindles in PD, therefore it is likely that the reduced response to vibration in PD is due to a reduction in the central gating of the afferent signal in the spinal cord.

Peripheral vibration provides a non-invasive, easily available tool to activate muscle spindle discharge and potentially modulate the gating of afferent input. The proprioceptive illusions generated by peripheral vibration appear to increase uncertainty in the proprioceptive input to the cortex due to the mismatch between incorrect kinesthetic information and EMG activity supporting theoretical predictions that increasing sensory uncertainty modulates sensory gating. Evidence from neurophysiological studies suggests that vibration causes an increase in the presynaptic inhibition of afferent input in the spinal cord and attenuates cervical and cortical sensory signals. This may reflect a descending central mechanism designed to down-weight this uncertain proprioceptive information according to the active inference framework. Importantly, it has been posited that this sensory gating is necessary for movement to occur. Indeed, PD patients show reduced somatosensory gating in the spinal cord and the somatosensory cortex, which is correlated with impairments in motor control and an

increase in beta oscillations. Interestingly, peripheral vibration has been extensively studied as a treatment for PD, suggesting a link between the modulation of afferent input and motor initiation (Arias et al., 2009; Chouza et al., 2011; Ebersbach et al., 2008; Haas et al., 2006; Kapur et al., 2012; King et al., 2009); however, the results have been inconsistent due to differences in the vibration protocol used, the muscles targeted, the behaviours being measured and the patient groups studied. Recent work from this lab suggests that high frequency peripheral vibration decreases RTs and movement time in PD patients and healthy controls (under submission). With the assumption that vibration reduces somatosensory precision, I hypothesise that this gating places the motor system in a "ready-to-move" state and this may be associated with a decrease in sensorimotor beta oscillations.

1.6. Specific aims and hypotheses of this PhD

The active inference framework states that sensory attenuation, the gating or filtering of irrelevant sensory information, "is a necessary consequence of reducing the precision of sensory evidence during movement to allow the expression of proprioceptive predictions that incite movement" (Brown et al., 2013; K. Friston et al., 2011; Friston et al., 2010). From this prediction a number of specific testable hypotheses emerge regarding the functional role of sensory attenuation and the neurophysiological correlate of changes in sensory precision.

The first aim of this PhD (study one; chapter three) was to better characterise somatosensory attenuation. Somatosensory attenuation has been studied as a perceptual and physiological phenomenon in two isolated fields. The first study in this thesis tested the hypothesis that these two forms of somatosensory attenuation were functionally and neurophysiologically distinct by measuring perceptual and physiological somatosensory attenuation within a single paradigm. This is important foundation work needed to better characterise the specific definition of somatosensory attenuation that is integral to then understanding how this phenomenon could be involved in movement initiation as predicted by the active inference framework.

The second aim of this PhD (study two; chapter four; and study three; chapter five) was to modulate somatosensory precision and determine the effect of this on movement initiation and sensorimotor beta oscillatory activity. I aimed to decrease estimates of proprioceptive precision, by applying high frequency peripheral vibration to the wrist. This stimulus has been previously shown to activate muscle spindles causing unexpected firing of 1a afferents and kinaesthetic illusions of muscle lengthening, which create

uncertainty in the proprioceptive state (Cordo et al., 1995, 2005; Roll et al., 1989; Tsay et al., 2016). I tested the following hypotheses: 1) vibration would reduce proprioceptive accuracy in line with a decrease in proprioceptive precision; 2) vibration would decrease RTs in accordance with the active inference theory, which posits that a reduction in somatosensory precision is necessary for movement initiation; 3) vibration would decrease sensorimotor beta power under the assumption that this neural activity correlates with changes in somatosensory precision.

The final aim of this PhD (study four; chapter six) was to determine whether the neurophysiological correlate of parameters of predictive coding could be found within the sensorimotor system. The active inference framework provides a unifying hypothesis which generalises ideas from predictive coding to the sensorimotor system. I therefore used a visuomotor adaptation paradigm, from which estimates of parameters in predictive coding could be easily tracked, to test whether sensorimotor beta activity readily correlated with these parameters. Specifically, I hypothesised that sensorimotor beta power would correlate with modulations in sensory precision induced by adding noise into the visual feedback of participant's movements. According to active inference, sensory attenuation occurs across all sensory channels, therefore if sensorimotor beta power represents the downstream effect of this attenuation, which then modulates movement, I would expect the attenuation of visual input to also modulate beta oscillatory activity over sensorimotor cortex. The hypotheses of this PhD are summarised in Figure 1.6.

The experiments described in this thesis will have implications for our understanding of sensorimotor control and provide much needed empirical evidence to determine the veracity of the active inference framework. The findings will also have implications for understanding the sensorimotor symptoms in movement disorders, such as PD, which could be reframed within this model. This may open up new avenues for potential treatments.

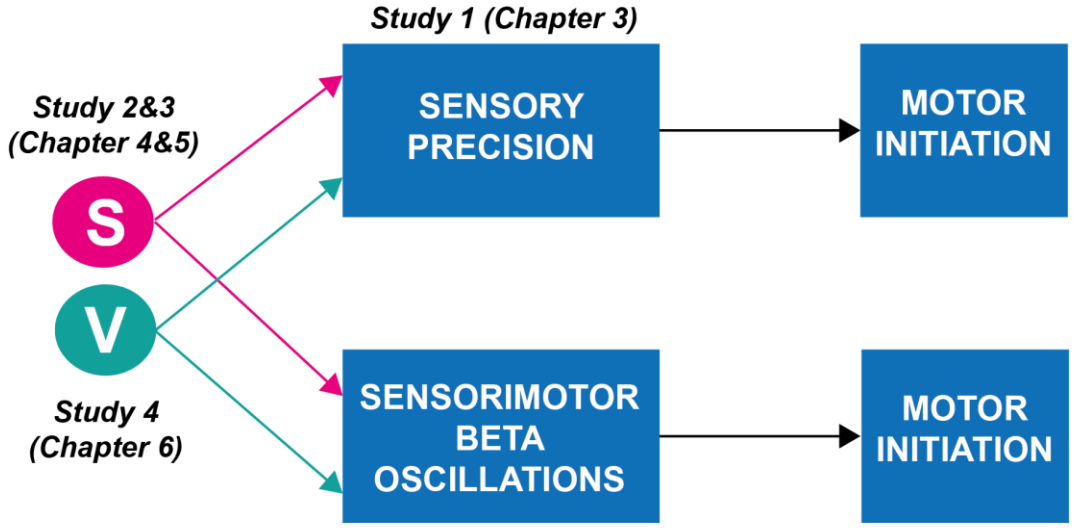

Figure 1.6. Schematic of the hypotheses tested in this PhD. *The active inference framework posits that a down-weighting of sensory precision is necessary in order to allow the proprioceptive predictions that incite movement to be fulfilled. Sensorimotor beta oscillations are thought to play an important role in executing movement and there are several correlative examples in the literature, which suggest that sensorimotor beta power could be the neurophysiological correlate of these modulations in sensory precision. For example, the time course of SEP attenuation with movement is very similar to the desynchronisation of beta oscillations with movement and there are many sensory inputs that modulate beta power. Study one (chapter three) of this thesis will aim to better characterise somatosensory attenuation, which has been described in both physiological and perceptual domains; this will aim to better determine whether these forms of sensory attenuation are neurophysiologically and likely functionally distinct. Studies two and three (chapters four and five) use peripheral vibration to modulate sensory precision in the proprioceptive domain in order to determine the relationship between sensory precision and movement initiation and sensorimotor beta power. Active inference provides a unifying account to explain perception and action in the brain and generalises the fundamentals of predictive coding to the sensorimotor system. In study four (chapter six) I used a hierarchical generative model to estimate parameters involved in active inference and determine the neurophysiological correlates of those hidden beliefs over sensorimotor cortex. Active inference posits that sensory attenuation occurs across all sensory channels during movement; therefore, in this experiment I modulated sensory precision in the visual domain to determine the effect of this on motor behaviour and sensorimotor beta power.*

CHAPTER 2

GENERAL METHODS

A range of behavioural, neurophysiological and computational modelling techniques were used throughout this PhD some of which are common to multiple results chapters. This chapter will give an overview of some common methods. The specific parameters for the implementation of each method will be given within each results chapter. For studies 1, 2 and 4 (chapters 3, 4 and 6) EEG was recorded during or alongside a behavioural task in order to answer questions regarding the functional role of sensorimotor beta oscillations. Below I outline the fundamentals of understanding the EEG signal and the background of different analysis methods used in this thesis.

2.1. What is EEG measuring?

When an action potential reaches a cortical pyramidal neuron the movement of ions into and out of the neuron generates a post-synaptic potential, which propagates along the pyramidal dendrites generating an intracellular current. This current flow produces an electric field surrounding the neuron and it is this extracellular volume current that is conducted through the cortical tissue, cerebrospinal fluid and skull and recorded by external electrodes on the scalp (Figure 2.1A). These electrodes record the electrical potential difference (voltage) across two electrodes by summing the charge produced by these extracellular currents at the scalp. The region of negative ions at one end of the neuron is referred to as the *sink* and the region of positive ions at the other end of the neuron is the *source*. Together this is referred to as a dipole. A positive or negative deflection on the scalp will reflect the sum of the charges closest to that electrode and will thus depend on the polarity of the dipole. An excitatory postsynaptic potential (EPSP) arriving at the apical dendrites will cause the extracellular fluid to become negative near the scalp and positive near the soma creating a negative deflection on the scalp; whereas an EPSP arriving near the cell soma will reverse this polarity (Figure 2.1B). The opposite will be true for IPSPs, therefore EEG cannot distinguish between the cellular mechanisms that may generate different charges at the scalp. Importantly, the orientation of the pyramidal neuron with respect to the cortical surface and the position of the electrodes will alter the deflections measured on the scalp. As electrodes measure the sum of charges in the vicinity, a potential difference will only be detected if the electrode is nearer one

end of the dipole (Figure 2.1C,D). EEG can detect both tangential and radial dipoles in the brain, therefore is sensitive to neuronal sources in both cortical gyri and sulci.

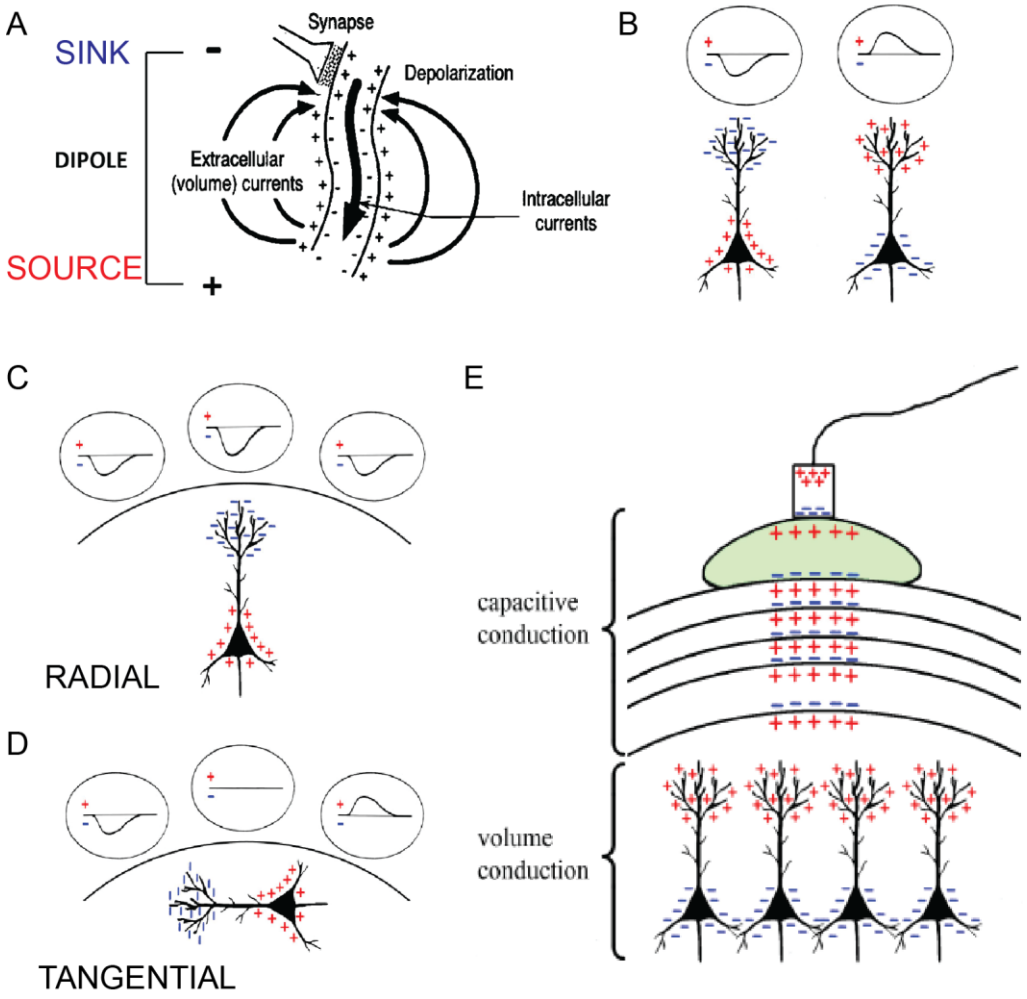

Figure 2.1. The neurophysiology underlying the EEG signal. *A) Post-synaptic potentials generate both intracellular and extracellular currents caused by the movement of ions into and out of the neuron. The distribution of ions creates a dipole characterised by a region of positive charge (source) in the extracellular space at one end and negative charge (sink) at the other end. B) Electrodes record the potential difference (voltage) across two electrodes by summing the charges produced by the extracellular currents nearest the scalp. The location of the sink or source nearest the scalp depends on the type of post-synaptic potential (EPSP or IPSP) and the location of the synapse which generated it (dendrites or cell soma); however, the EEG signal cannot determine between these options. C+D) Different signals are recorded dependent on the orientation of the neuron to the scalp and the position of the electrode. E) Volume conduction allows the signal to be transmitted through the brain to the dura. From this point a capacitance stack is created by the charges pushing against either side of the insulating layers to reach the electrode. In order for the charge to be large enough to be detected, pyramidal neurons must be synchronously active and arranged in parallel to ensure the charges sum and do not cancel out. Figure adapted from (Jackson and Bolger, 2014).*

The dipole produced from a single EPSP or IPSP is too small to be detected by electrodes at the scalp, therefore electrodes sum the charges from thousands of pyramidal cells. Pyramidal cells must be arranged in parallel in order for charges to be summed and not cancel out and neurons must be synchronously active to create a large enough signal. Importantly, the cortex is arranged in this way. Brain activity from deep structures such as the basal ganglia and hippocampus are difficult to measure with EEG because pyramidal cells are not always oriented parallel to the cortical surface and the electrical signal decays exponentially as it is conducted through other brain tissue to the scalp. Dipoles that are further away from the electrodes will produce potential differences of low amplitude with a broad distribution.

Volume conduction occurs by pools of ions of the same charge repelling pools of ions of the opposite charge repeatedly; however, this method cannot be used outside of the brain for the signal to reach the electrode and will stop as soon as the volume (cortical tissue) ends and an insulating layer is reached. Here insulating layers from the dura to the skull to the electrode gel create capacitors where ions of the same charge push against one side of the layer and attract ions of the opposite charge on the other side of the layer (Figure 2.1E). This creates a stack of capacitors that carry the signal to the electrode. Hair, air and skin cells are poor conductors, therefore electrode gel is necessary to create a path of good conductance from the skull to the electrode. It is important to note that as electrodes sum nearby charges at the scalp, the signal recorded will be influenced by a number of different sources of activity at different positions in the cortex, which is referred to as spatial smearing.

2.2. EEG Data collection

EEG data is recorded by placing electrodes over the scalp. All EEG data collected for this thesis was recorded using a BioSemi 128 active electrode system (Biosemi, Amsterdam, Netherlands) at a sampling frequency of 2048Hz. Two external reference electrodes were placed on the subjects' earlobes. The active electrodes used have an amplifier integrated into them to improve the signal-to-noise ratio (SNR) of the EEG signal (Rijn et al., 1990).

Maximising the SNR is an important issue with EEG as the signal from the brain is very small compared to the multiple sources of internal and external noise. Tools to distinguish between signal and noise are very important. The power supply in buildings serving electrical equipment is often the greatest source of noise for EEG. Active electrodes work by placing an amplifier next to the electrode on the scalp to minimise the impact of electrical noise that may be added to the signal as it passes along the wire to the computer

thus maintaining the SNR. The amplifier will have a high input impedence, which aims to maximise the voltage that is measured and transferred to the computer. Impedence can be discussed in a similar way to resistance. According to Ohm's law the voltage (V) recorded across two points is equal to the current (flow of charge between points; I) and resistance (R): V=IR. Importantly, voltage drops when measured across a resistor and the size of this drop refers to the proportion of the total resistance attributed to that resistor; the sum of voltage drops across resistors in a circuit equals the total voltage in the circuit. The amplifier inserts a very large resistor into the circuit, in the same way as a voltmeter, such that it represents almost all of the resistance in the circuit and so all of the voltage will drop across it. In this way the amplifier can maximise as much voltage measured as possible. Reducing the impedence between the scalp and the electrode using electrode gel acts to ensure as much signal as possible reaches the amplifier; here a large impedence is then used to measure the voltage. Internal noise from the participant's heartbeat, breathing or eyeblinks also reduces the SNR, but is difficult to reduce during data collection therefore must be removed offline during the preprocessing of the EEG data. The external reference electrodes can be used to deduct any physiological signals from the EEG data that are not deemed as brain activity.

2.3. EEG analysis techniques

EEG activity, measured as microvolts (μV), is recorded as the potential difference from one electrode relative to a reference electrode, therefore represents a relative value, which is difficult to interpret. Different analysis techniques, such as baseline subtraction, and the hardware used to record the signal can alter the absolute μV values and the μV is likely to be different between participants due to differences in skull shape and thickness for example. However, these are global factors that will affect all trials and conditions, therefore μV can be compared across conditions within participants, but not between participants or studies. The excitability of neuronal populations fluctuates over time and this oscillatory activity changes the polarity of the voltage measured. Rhythmic activity can therefore be seen within the raw, unfiltered EEG data; however time-frequency analyses are used to determine the specific effects of different aspects of this oscillatory activity. Before anything meaningful can be interpreted from the EEG data, a number of general pre-processing steps are required:

- *Filtering*. When the frequency of the signal of interest is known or hypothesised, filters can be applied to remove noise from the EEG data. High-pass filters attenuate signals of frequencies below a specified cut-off and low-pass filters

attenuate signals above a specified cut-off. Notch filters can be used to remove 50Hz noise from the electrical power supply.

- *Averaging*. When designing an EEG experiment it is important to have multiple trials in which a stimulus is presented and the resultant EEG signal is recorded. This is because the neural response to a single event is usually very small; therefore, by averaging over multiple trials the SNR is increased. However, it is important to note that averaging will have differential effects depending on whether the neural activity of interest is time-locked or phase-locked to the stimulus (see below).
- *Baseline correction*. Throughout EEG recording, the signal will slowly shift over time due to artefacts such as muscle tension and sweating, which means that the zero line between electrodes and trials may be different. It is therefore vital (particularly when doing evoked potential analyses) to subtract the mean signal over a baseline time window from the data of interest in order to correct for this. This baseline time window should precede the onset of the stimulus and be consist across trials and conditions. In this way any differences in the amplitude of the neural signal following the onset of the stimulus cannot be confounded by data not related to the stimulus.

After preprocessing, EEG data can then be analysed either in the time-domain by quantifying evoked potentials (ERPs) averaged over trials or in the time-frequency domain where the power or phase of oscillations at different frequencies are analysed over time. In most experimental studies, EEG data are analysed with respect to stimuli that are presented at specific times during a task in order to quantify task related changes in neural activity. EEG data are epoched into small time windows around these stimuli.

2.4. Evoked vs induced brain responses

When a stimulus is presented, EEG data can either be time-locked or phase-locked to the stimulus or neither. This has implications for the analysis method that can be employed to measure the EEG response (Figure 2.2). Phase-locked data refers to activity in which the phase of the signal is aligned to the onset of the stimulus and this phase alignment will be the same across all trials: this is referred to as an 'evoked' response. This data can be averaged across trials in the time and time-frequency domains to produce a measurable ERP and time-frequency power spectra. Non-phase locked activity, referred to as 'induced' activity, can only be averaged in the time-frequency domain, because in the time domain the peaks and troughs of the data will cancel out. Non-time locked activity occurs

at different time points following a stimulus and can be measured with time-frequency power, however the results will be smoothed and temporally less precise than time-locked analyses.

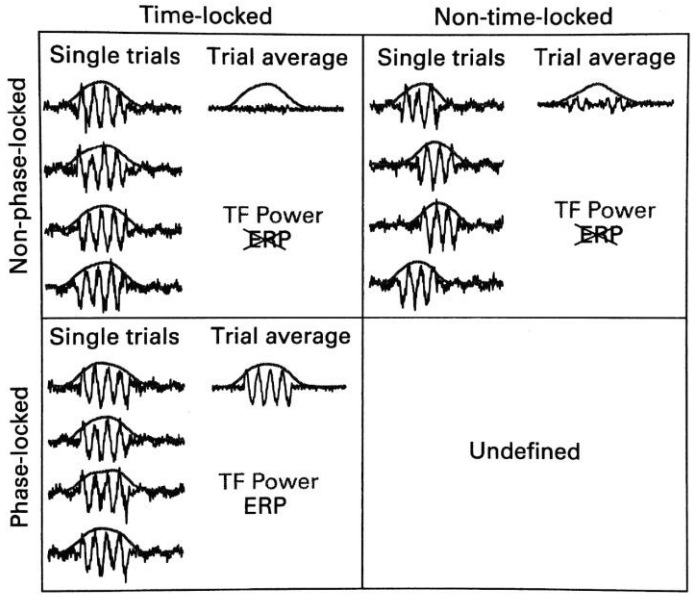

Figure 2.2. Trial averaging can have differing results dependent on whether the brain response measured is evoked or induced*. Evoked activity is phase-locked to the stimulus such that the phase of the signal is aligned across trials to the onset of the stimulus. Evoked potentials (ERPs) can only be analysed from averaging over multiple trials of phase-locked and time-locked EEG data, because if the peaks and troughs of the signal are not aligned over trials then they will cancel out. Induced activity is non-phase-locked and can only be averaged in the time-frequency domain. If the activity is also not time-locked i.e. it can occur at different time points following the stimulus across trials, then the results in the time-frequency domain will be smoothed and temporally less precise. Figure adapted from Cohen, (2014)*

2.4.1. ERP analysis

ERPs represent time-locked and phase-locked EEG signals that are optimally seen when several trials are averaged to improve the SNR. ERPs contain a series of peaks and troughs at particular time intervals, which may represent activity from different cortical areas associated with specific functions. The neurophysiological mechanisms underlying these waveforms are not well understood. An additive model suggests ERPs elicited by an external source represent a distinct internal event that is dissociable from the background EEG activity. In this model there is a distinction between the neurophysiological event that produces the ERP and that which produces oscillations (Mäkinen et al., 2005; Mazaheri and Jensen, 2006; Mazaheri and Picton, 2005; Shah et al., 2004). An alternative model is the phase reset model, which suggests that an ERP emerges from the sudden alignment of phases of ongoing oscillations caused by a perturbation to the ongoing activity by the stimulus. When these phase-locked trials are then averaged the result is a component of the ERP (Gruber and Müller, 2005; Klimesch et al., 2006; Makeig et al., 2002;

Penny et al., 2002). There is evidence for and against both of these theories; therefore the neural dynamics underlying ERPs are not well understood. However, recent evidence suggests that ERPs may represent a by-product of averaging travelling waves across multiple trials (Alexander et al., 2013). Travelling waves represent activations and deactivations that move through the brain. Current neuroimaging techniques often assume that the neural activity being measured is either stationary in space (analyse temporal data from a single electrode) or stationary in time (analyse topography of the neural signal across the brain at given time point). However, recent evidence suggests this may be incorrect and neuroimaging analysis methods need to be altered to truly understand brain dynamics and how changes in neural activity modulate voltage recorded at the scalp (Alexander et al., 2015).

In study one (chapter three) of this thesis the somatosensory evoked potential (SEP) was analysed over an ROI over sensorimotor cortex. This was generated by electrical stimulation of the median nerve at the wrist. SEPs were analysed by averaging over multiple trials. The difference between the amplitude of neighbouring peaks was used to quantify the magnitude of the primary, secondary and late components of the SEP. These values were then compared across conditions to determine if perceptual somatosensory attenuation modulated the amplitude of the SEP. In this study, I assume that the amplitude of the SEP relates to the synaptic gain of the pyramidal cells receiving the afferent input in the somatosensory cortices; an increased gain for the same afferent input (produced by the peripheral nerve stimulation) would result in a greater post-synaptic potential in pyramidal neurons and a greater response recorded at the scalp. This is thought to reflect changes in somatosensory precision. However, it must be noted that SEP amplitude can also be affected by increased synchronisation and neuronal recruitment, therefore this is not a pure measure of synaptic gain.

2.4.2. Time-frequency analysis

As previously stated, oscillatory activity of neuronal populations contributes to the EEG activity recorded. Oscillations can be described with three variables: frequency (measured in Hz) describes the speed with which the oscillation fluctuates; power reflects the amount of energy in a given frequency band; and, phase (measured in radians or degrees) is the position along the sine wave at any given point in time. Signal processing methods, such as a Fourier transformation, can be applied to EEG data to divide the activity into multiple frequency bands. In this way we can quantify how an experimental manipulation may specifically modulate certain frequencies of oscillatory activity. Traditionally brain rhythms are divided into the following frequency bands: delta (2-4Hz),

theta (4-8Hz), alpha (8-12Hz), beta (12-30Hz), lower gamma (30-80Hz) and upper gamma (80-150Hz). Power and phase can then be calculated for oscillations in the frequencies of interest. Power and phase are considered independent variables and reveal different characteristics about the underlying neural dynamics. In this thesis, I will only analyse the power of oscillatory activity. I hypothesise that changes in oscillatory activity, specifically within the beta frequency band, may represent modulations in synaptic gain; therefore, there is a clear prediction of how changes in synaptic gain could enhance the amplitude of the summed post-synaptic potential in a neuronal population, which could modulate oscillatory power calculated as the squared amplitude of the oscillation.

In this thesis, all data was time-locked to a specific event and epoched according to the experimental design of each study. Time-frequency analyses were conducted on EEG data between 1-99Hz in order to measure experimental effects in the entire spectrum; however, all hypotheses stated are with regard to the power of beta oscillations (~12-30Hz). Oscillatory phase was not analysed in this thesis. Time-frequency analyses represent the power of oscillatory activity at different frequency bands over time; data was averaged over selected electrodes of interest (specific to each study) in order to represent data in 2D time-frequency plots.

There are multiple different methods for time-frequency decomposition that have been taken from signal processing methods used in multiple areas of science and engineering and are used in this thesis.

Fourier Transform (FT). The Fourier transform (FT) represents the basic underlying principle used to extract frequency, power and phase information from a time series of data. The FT works by computing the dot product (the similarity between two vectors) between the time series, in this case the EEG signal, and sine waves of different frequencies. This produces the phase and power of the signal at each frequency specified (Figure 2.3). The Nyquist theorem states that at least two points per cycle are needed to measure a sine wave and therefore the fastest frequency that can be measured in any epoch of data is calculated by: number of data samples/2+1. This is important to ensure epoched data have enough samples to calculate the fastest specified frequency. However, the FT method lacks temporal localisation i.e. the FT does not show how frequency characteristics change over time, and therefore assumes stationarity of the data across the epoch, which is unlikely to be true for EEG data. Therefore, other time-frequency decomposition methods that are based on the same underlying principles of the FT, but take this into account may be more suited for analysing EEG data.

Short-time FT (SFT). The short time FT compensates for this lack of temporal localisation by computing the dot product between sine waves of different frequencies with short time segments of EEG data that overlap temporally. A taper (e.g. Hanning taper) should be applied to the EEG data to attenuate the amplitude of the EEG signal at the beginning and end of the time window in order to prevent edge artefacts. In this thesis I use a version of this method called Welch's method applied using the Matlab function 'pwelch'. This function returns the Power Spectral Density (PSD) estimate for discrete time segments using Welch's averaged, modified periodogram method. In each window a discrete FT produces a periodogram and the squared magnitude of this represents power. Using this method the temporal and frequency smoothing remain fixed, therefore wavelet convolution is potentially a better method where smoothing can be controlled.

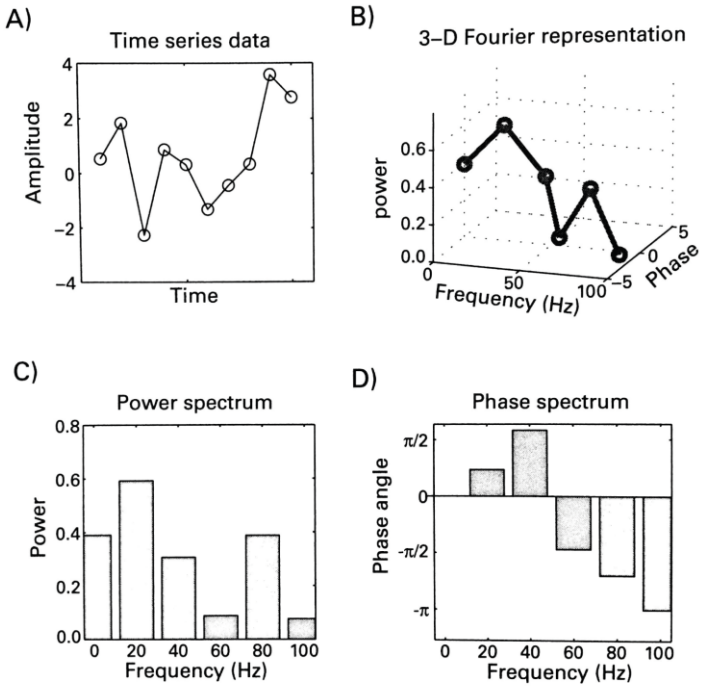

Figure 2.3. Demonstration of the variables that can be extracted from the Fourier Transform (FT). *A) Simulated time series data. B) A 3D representation of the results from the FT. The FT produces a value of the power (C) and phase (D) of the signal at each specified frequency collapsed over time. Figure adapted from Cohen, (2014).*

There are several options to calculate how power and phase change as a function of both frequency and time. These involve convolving a kernel with the EEG time series. This means sliding the kernel along the time series data, such that the dot product is calculated between the kernel and the corresponding segment of data for each time step. The corresponding dot product at each time point is placed at the centre of the kernel,

therefore zero padding needs to be added either side of time series data to ensure the two vectors compared are the same length (Figure 2.4). One optimal kernel for this convolution is the Morlet wavelet.

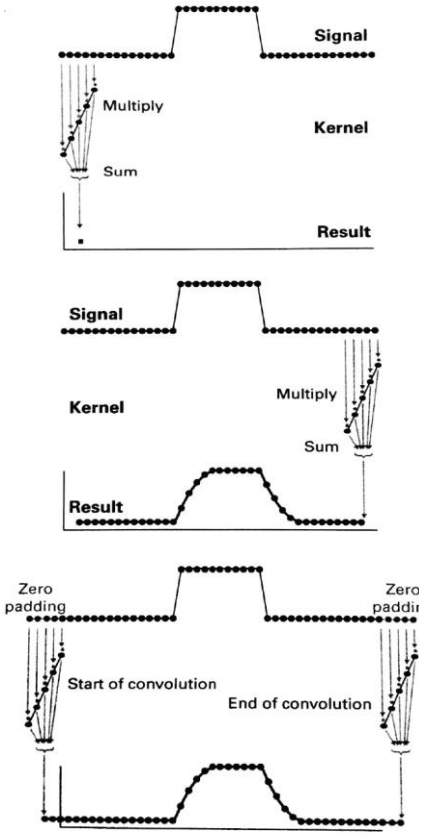

Figure 2.4. Overview of convolution. *The signal is weighted by the kernel by computing the dot product between the kernel and the signal. The dot product represents the similarity between two vectors and is calculated by multiplying the kernel and the corresponding window of time series data then summing the result. This produces a single data point. The kernel is then moved over one time-step and a second dot product is calculated. This continues for the whole time series. However, as the dot product at each point is placed at the central point of the kernel, the resultant weighted signal is shorter than the original. Zero-padding is therefore added on either side of the original time series in order to recreate a weighted signal that is the same length as the time series. Figure adapted from Cohen, (2014)*

Morlet wavelet analysis. Morlet wavelets are produced by placing a Gaussian window over a sine wave of a specified frequency and a specified number of cycles. The wavelet acts like a bandpass filter around the peak central frequency (Figure 2.5A); multiple wavelets with specified peak frequencies are used to extract data from the whole frequency spectrum. In order to extract power and phase information from this band-pass filtered signal, complex wavelets must be used. The convolution of a complex wavelet with the EEG signal produces a series of complex dot products that therefore have a real and imagined component. Power and phase are calculated based on the magnitude and angle of the complex dot product in polar space (Figure 2.5B). The number of cycles of the wavelet determines the trade-off between temporal and frequency smoothing. Figure 2.5C shows that for a low number of cycles, 3, the temporal precision is greater than for a higher number of cycles, 10; however, the frequency precision is greater for 10 cycles compared to 3. Therefore, the number of cycles can be adjusted depending on the requirement of the hypothesis to have high temporal or high frequency precision. In addition, if the number of cycles remains constant, the length of the time window will

decrease with increasing frequency such that temporal precision will increase and the frequency precision will decrease. To maintain a balance between temporal and frequency precision throughout the time-frequency decomposition then the number of cycles can be set to vary as a function of frequency.

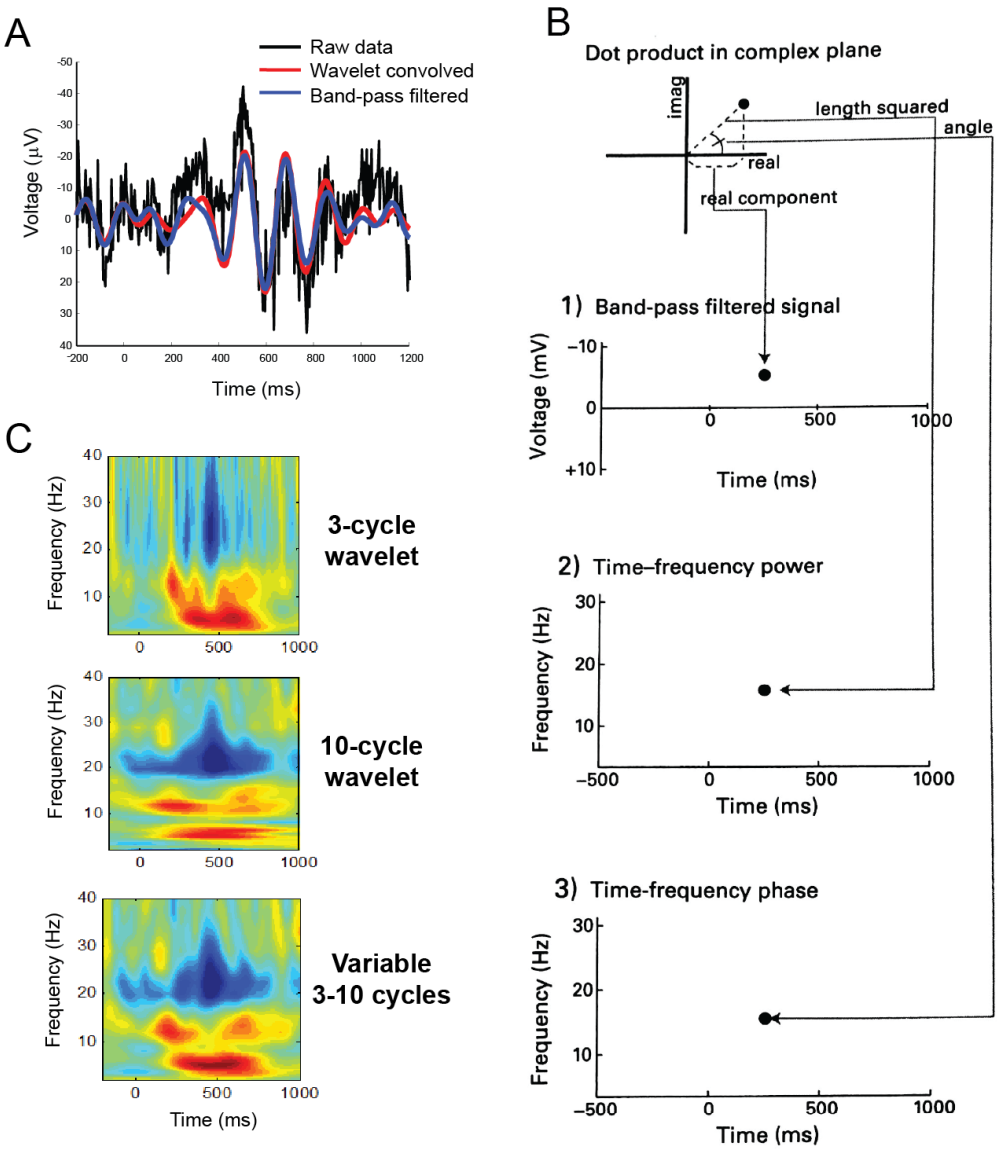

Figure 2.5. Overview of the Morlet Wavelet analysis method. *A) The Morlet wavelet acts as a band pass filter only extracting data from the peak central frequency of the wavelet. B) In order to extract phase and power from the band-pass filtered signal a complex wavelet must be used which has both real and imaginary parts. By imagining the dot product from the convolution of the wavelet and signal plotted in complex space, the calculation of phase and power can be understood. The squared length of the vector from the origin to the dot product is power and the angle of the vector with respect to the positive real axis is the phase. This is repeated with wavelets of different peak frequencies to complete the time-frequency plot. C) The number of cycles of the wavelet determines the trade-off between the temporal and frequency smoothing of the resultant time-frequency data. A low number of cycles will have better temporal precision (upper panel) and a high number of cycles will have better frequency precision (middle panel). By changing the number of cycles as a function of frequency, the balance between these precisions can be maintained (lower panel). Figure adapted from Cohen, (2014).*

Multitaper analysis. Multitapers offer another time-frequency decomposition method in which short time segments are multiplied by tapers with different spectral characteristics in a very similar way to the wavelet analysis (Figure 2.6). However, here the time window remains the same over all frequencies. The longer temporal support for higher frequencies means there is a better estimate of power, therefore this method is optimal for high frequency activity, however this occurs at the expense of temporal precision. Both time-frequency methods are correct, but simply differ in their trade-off between temporal and frequency smoothing.

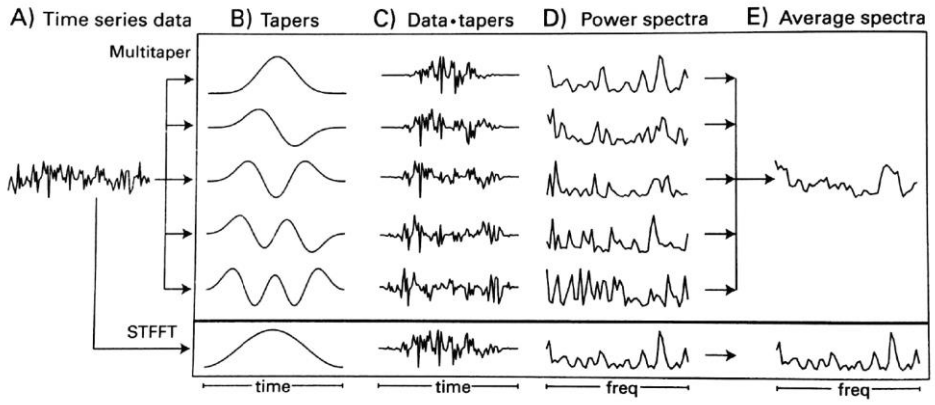

Figure 2.6. Overview of Multitaper analysis. *Tapers of different frequencies are convolved with the signal to produce power spectra at the specified frequencies. The multitaper method is an extension of the SFT method designed to increase the SNR. Overlapping segments of time in the SFT will still produce edge artefacts, therefore by using several tapers with different temporal characteristics this is reduced. The phase values refer to the phase of the sine wave collapsed over the tapered time window rather than representing a changing phase-angle with each time step. Figure adapted from Cohen, (2014)*

In this thesis both the Morlet wavelet analysis and the Multitaper analysis are used in different chapters using inbuilt SPM functions and custom written MATLAB code.

2.4.3. Baseline Normalisation

Importantly, raw power values produced by time-frequency decomposition are very difficult to interpret. The power law means power decreases with increasing frequency making it difficult to visualise power across a large range of frequency bands and difficult to make quantitative comparisons of power across frequency bands. Raw power is also modulated by individual differences in skull thickness and cortical anatomy and values are not normally distributed meaning parametric statistics cannot be applied directly to raw power values. However, these limitations can be overcome by normalising the data. This makes power easier to interpret by displaying power as a change from a specified baseline period, transforms all power values onto the same scale and ensures the data is normally

distributed. The specific method of baseline normalisation used for each analysis is specified in each chapter.

2.5. EEG Statistical Analyses

2.5.1. General Linear Model

To analyse the time-frequency data produced in this thesis I have used a General Linear Model (GLM) from within the SPM toolbox. The underlying principle of the GLM is linear regression: $Y=X*\beta1+\beta0+\varepsilon$. This equation describes the linear model which best explains the relationship between the variables Y and X. The intercept ($\beta0$) is a constant which describes the value of Y when X=0. The slope or gradient ($\beta1$) describes the predicted change in Y for every one unit change in X; this explains how these two variables are related. The residual error (ε) describes how far each data point sits from the estimated model; the linear model selected is the model that minimises the sum of squared errors (SSE). The GLM expands this simple situation so that each term includes a set of variables. This multiple regression therefore allows us to include a greater number of predictors that can be used to explain the observed data, which when used for neuroimaging is the neural activity. In this case, X represents a design matrix where each column represents a hypothesised regressor of interest and each data point or row is coded based on how that variable was modulated during the experimental task. For example (Figure 2.7), in a mismatch negativity task, all the trials in which a participant heard a standard tone would be coded 1 in column X1 whereas all the trials in which a participant heard a deviant tone would be coded 1 in column X2. For each column of the design matrix, Xi, the GLM estimates the relationship between the regressor and the observed neural activity, which produces the parameter βi. It is also important to include regressors of no interest, which may explain some of the variance in the observed data, but not be directly relevant to the task, for example eye movements or breathing rate. Including these in the model will decrease the residual errors and improve the model fit for each regressor of interest.

At the first level, the GLM is conducted for each voxel in the time-frequency image for each participant. In this thesis all analyses are conducted over a region of interest (ROI) over sensorimotor cortex. The estimated time-frequency images (βi) for each regressor of interest for each participant are then brought forward to the second level. At this level, in most cases in this thesis, a one sample t-test was used to determine if the relationship between the neural activity and the regressor of interest was consistent across participants. For example, if post-movement beta activity positively correlated with the

first regressor of interest in the majority of participants, then this activity would be significantly greater than 0 at the second level. A statistical parametric map (SPM) is then produced, which represents the t-statistic at each voxel in the time-frequency image.

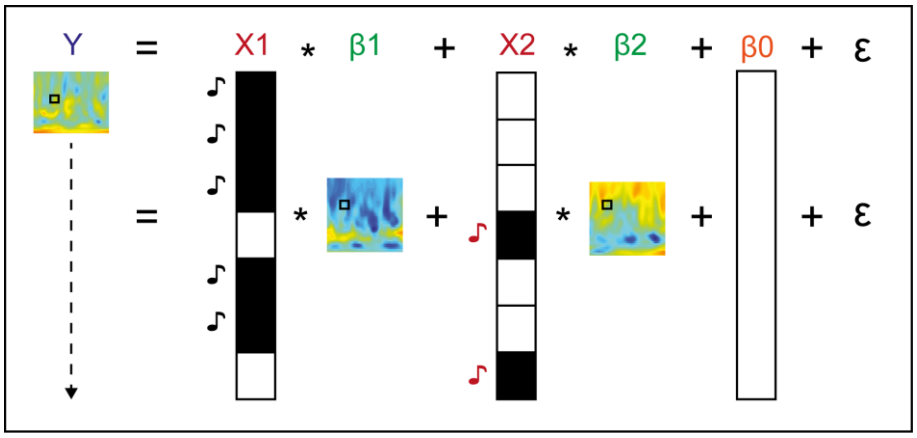

Figure 2.7. Overview of the General Linear Model (GLM) used in a first-level analysis. *Example mismatch negativity experiment to demonstrate the use of a GLM in determining whether any activity in the time-frequency data could be predicted by the deviant or standard tones presented. Y = observed data from one voxel of the time-frequency data for each trial. X1 = regressor of standard trials. X2 = regressor of deviant trials. β1 and β2 = gradient of the model which best explains the relationship between these regressors and Y. β0 = constant term. ε = residual error of the model. The GLM is repeated for every voxel in the time-frequency image, which produces a 2D plot for each estimated fit (β1 and β2). These β images can then be used in a second-level analysis to compared these model fits between subjects and determine if there were any consistent relationships between the time-frequency data and the experimental variables. Regressors of no interest can also be included to explain some of the variance in the EEG data, which will improve the model fits for the regressors of interest.*

2.5.2. Multiple comparisons problem

2.5.2.1. Random Field Theory for SPM

The multiple comparisons problem (MCP) must be addressed any time multiple t-tests are conducted on an experimental dataset as described above. The fundamental basis of this problem is that for any statistical test in which the alpha for rejecting the null hypothesis is 0.05, there is a 1 in 20 chance of reporting a false positive; as the number of tests increases, the probability of making a type 1 error increases. The Bonferroni method corrects for this by changing the alpha threshold for rejecting the null hypothesis to be higher: alpha/number of tests. However, for neuroimaging data this is far too conservative, because each voxel in a SPM is often highly correlated with neighbouring voxels (especially after spatial smoothing), therefore the data violate an underlying assumption of the Bonferroni method that the tests performed are independent. Random Field Theory (RFT) is an alternative method of correcting for multiple comparisons for neuroimaging (J. M. Kilner et al., 2005). The method calculates the expected Euler

characteristic (EC) for each t-threshold of an image, which states how many peaks are likely to appear above that threshold given the resolution of the image. From this we can determine the threshold at which the expected EC is 0.05; therefore, if any peaks remain after thresholding the image at this value, then the probability of those occurring by chance is less than 0.05. In this thesis, I have reported whether significant peaks of activation remained following correction by RFT.

2.5.2.2. Statistical Non-parametric Mapping (SnPM)

An alternative solution to the multiple comparisons problem for functional neuroimaging is to use non-parametric statistics. Statistical non-parametric mapping (SnPM) offers an alternative method for analysing neuroimaging data, which has been shown to be more robust and sensitive to identifying significant areas of activation in particular contexts (Holmes et al., 1996; Nichols and Holmes, 2002). SnPM analyses are based on the principles of permutation testing. For activation of a single voxel across multiple testing conditions, the null hypothesis of a permutation test states that the labels assigned to the different conditions being compared are arbitrary, therefore the activation in that voxel in each condition is the same. To test this a permutation distribution is generated by either randomly shuffling the condition labels, or randomly assigning the activation data to different conditions over a large number of different permutations. For each permutation a t-statistic is produced and the p-value is determined as the proportion of t-statistics in the distribution greater or equal to the t-statistic of the observed data. Therefore, at an α-level of 0.05, the null hypothesis is rejected if the observed t-statistic falls within the 95^{th} percentile of the permuted distribution and thus it is highly unlikely that the activation in that voxel occurred by chance. Using this non-parametric analysis, there are no assumptions regarding the distribution of the data, therefore this type of analysis is more robust if the observed data is not normally distributed, which is likely with neuroimaging data.

If the above analysis was repeated for all voxels in the brain or within an image of interest than the p-values produced would need to be corrected for multiple comparisons. To avoid the MCP the single voxel observed t-statistic can instead be compared to a maximum statistic generated across the whole image of interest. One method of generating this maximum statistic is to set a maximum suprathreshold cluster size (STCS), which acts as a critical threshold for detecting interconnected voxels of activity: clusters. Using the same logic as single voxel permutation tests, a permutation distribution can be generated from shuffling the labels of each voxel t-statistic within the image and determining the maximum STCS for each permutation. If the maximum STCS of the observed data is within

the 95th percentile of the permuted distribution than the observed cluster is unlikely to have occurred by chance. By comparing to this maximum statistic, the MCP is avoided.

This method is more sensitive than using RFT or the Bonferroni correction, therefore is less likely to produce Type II errors. By comparing these different methods the likelihood of a Type II error having occurred can be determined. For example, in chapter three of this thesis, a significant cluster of activity identified with SPM was no longer significant when corrected for using RFT; however, this was significant when the same analysis was repeated with SnPM, which suggests that using RFT may have been too conservative and produced a Type II error.

CHAPTER 3

Study One: Investigating the neurophysiological correlate of somatosensory attenuation using a force matching paradigm and median nerve stimulation

3.1. INTRODUCTION

Somatosensory attenuation, the top-down filtering or central gating of afferent information, has been extensively studied in two fields: physiologically and perceptually. Physiological somatosensory attenuation is represented as a decrease in the amplitude of the primary and secondary components of the somatosensory evoked potential (SEP), generated using median nerve stimulation, during and prior to movement of the stimulated limb (Rushton et al., 1981). Perceptual somatosensory attenuation is described using the analogy of a persons' inability to tickle oneself (Blakemore et al., 2000). This has been attributed to a central cancellation of the reafferent somatosensory signal by the efference copy of the motor command prior to making the tickling action. When someone else produces the tickling sensation, there is no efference copy to cancel out or reduce the incoming afferent signal, therefore the sensory information is not attenuated (Blakemore et al., 1999, 1998). It has been suggested that "movement-induced somatosensory gating may be the physiological correlate of the decreased sensation associated with self-produced tactile stimuli in humans" (Blakemore et al., 2000). However, the relationship between these two forms of somatosensory attenuation has never been formally tested. This was the aim of the study in this chapter.

Specific predictions about the neurophysiological correlates underlying the perceptual phenomenon have not been addressed. fMRI studies have attempted to localise the networks involved in somatosensory attenuation and suggest that perceptual attenuation may be driven by activity in the secondary somatosensory cortex (SII; Blakemore et al., 1998; Shergill et al., 2013). This is in contrast to SEP attenuation where it is has been shown that the early SEP components, which are attenuated during movement, originate from activity in the primary somatosensory cortex (SI; Jiang et al., 1990). Indeed, studies measuring neurophysiological attenuation to action-driven and externally-driven sensations in the auditory and visual domains have highlighted differences in the locus

and timing of attenuation dependent on the nature of the task (Bäss et al., 2008; Hughes et al., 2013; Roussel et al., 2014), therefore this may demonstrate a potential dissociation in mechanism depending on whether the task is low-level (e.g. active movement) vs high-level (e.g. force matching). Although it has been suggested that movement-induced SEP attenuation may underlie perceptual somatosensory attenuation, the relationship between the two may be more complex based on the structure of the cortical hierarchy.

This study aimed to measure perceptual and physiological somatosensory attenuation in a single paradigm to determine the relationship between these phenomena. The force matching task (Pareés et al., 2014; Shergill et al., 2005, 2003) was used to measure perceptual attenuation. Participants were asked to match target forces either by pressing on themselves (self-generated condition) or by using an external robot to manipulate the force applied (externally generated condition). Median nerve stimulation was given at specific time points throughout the behavioural task and EEG was recorded to quantify the relationship between SEP amplitude and perceptual sensory attenuation. Firstly, in line with the literature, I hypothesised that participants would overestimate the matched force in the self-condition compared to the external condition. Secondly, I hypothesised that SEPs evoked during force generation would be attenuated relative to SEPs evoked during a steady-state contraction once the matched force level was reached and being held. Finally, I hypothesised that if this physiological gating was the mechanism underlying perceptual somatosensory attenuation then the magnitude of SEP attenuation would be modulated by behavioural task condition; however, if these two forms of somatosensory attenuation were dissociable and potentially functionally distinct then SEP amplitudes would not be modulated by the behavioural task.

3.2. METHODS

3.2.1. Participants

18 healthy participants (male=9; female=9) aged 20-56 years old (mean ±SD: 28.24 ±8.53) took part in this study. Participants had no history of neurological or psychiatric illness. All participants were right handed and gave written informed consent prior to taking part. This study was approved by the UCL Research Ethics Committee and all testing took place at the UCL Institute of Neurology, Queen Square. 2 participants were excluded due to noisy EEG data.

3.2.2. Experimental setup

Participants sat at a desk with their left hand supernated and index finger extended under a force transducer. Two haptic robots were positioned in front of the participant (Figure 3.1A). One robot was stationed above the force transducer and directly produced forces on the left index finger. The second robot was positioned over a pliable object and controlled the force produced by the first robot in the "external" condition (see *Task Procedure: Force Matching Task*). The force transducer recorded all forces exerted on the left finger using Spike2 v6.17. The target forces applied were: 1N, 1.5N, 2N, 2.5N. A peripheral nerve stimulator was used to stimulate the median nerve at the left or right wrist at specific time points throughout the experiment. EEG data were recorded using a BioSemi 128 active electrode system at a sampling frequency of 2048Hz. Two external reference electrodes were placed on the participants' earlobes.

3.2.3. Task Procedure: Force Matching Task

To measure perceptual sensory attenuation a classic force-matching task was used (Pareés et al., 2014; Shergill et al., 2005). Participants received a force (produced by robot 1) on their left index finger for 3s. They were instructed to match the intensity of that force on the same finger by either pushing down on robot 1 to emulate the force produced ("self" condition) or by pushing down on robot 2 ("external" condition; see Figure 3.1A). Robot 2 was linearly connected to robot 1 such that a 1cm movement in robot 2 produced a 1.25N downward force on robot 1. Once the participants had produced the appropriate force they were instructed to hold the matched force until they heard the stop signal (4.5s). The inter-trial-interval (ITI) was 1s. Instructions for the behavioural task appeared on a computer screen in front of the participant throughout the experiment. Median nerve stimulation (MNS) was either given whilst holding the matched force only (x3 every 500ms from 3s after the GO signal; 32 trials per block; "Hold stimuli") or additionally during force production (x5 stimuli every 500ms from GO signal 12 trials per block; "Phasic stimuli"; see Figure 3.1B). Participants completed alternate blocks of each condition counterbalanced across participants. There were 44 trials in each block containing equal numbers (x11) of each target force (ratio of trials with and without phasic stimuli=3:8). There were 4 blocks of each condition in one session. Participants completed the same behavioural task in two sessions (mean (±SD) time between sessions: 2.8 days ±3.4). The stimulated wrist alternated between sessions and the order was counterbalanced across participants.

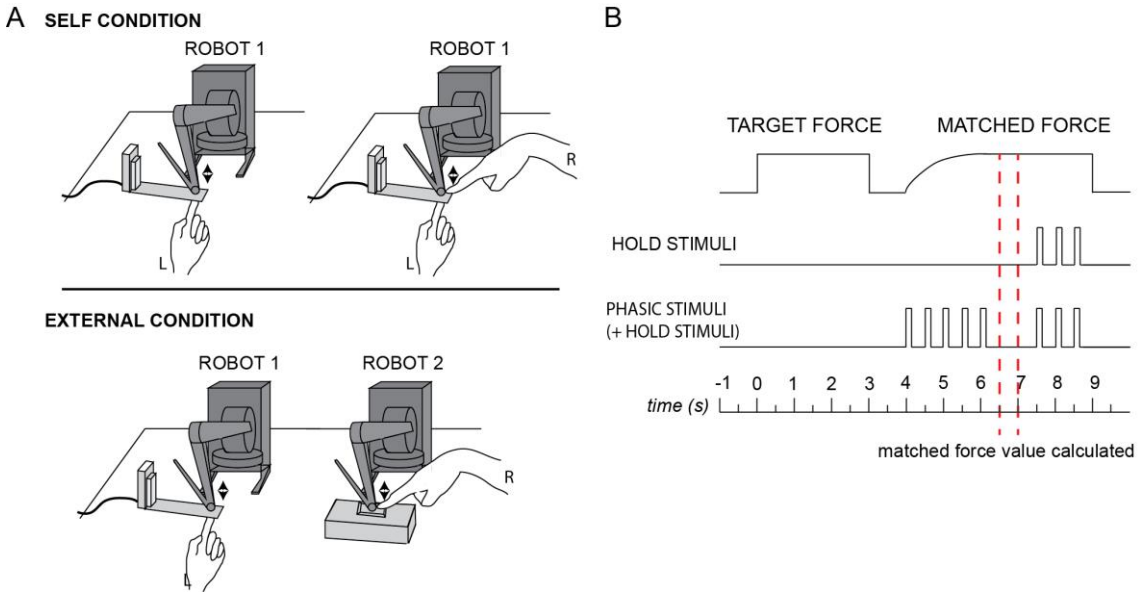

Figure 3.1. Experimental set up and task design for the force matching paradigm. *A) Self condition (upper panel): robot 1 was fixed onto a force transducer. Robot 1 produced a target force on the left index finger; this was matched by pushing down on robot 1 using the right index finger. External condition (bottom panel): robot 2 was linearly connected to robot 1 such that any force exerted on robot 2 was felt on the left index finger. The gain was altered so that more force was required in this condition to produce the same fore output across conditions. B) Schematic of the trial design for a single trial. The top line is the force output from the force transducer during the target and matched forces. The top middle line shows the timing of the hold stimuli relative to the force output; behavioural data were only used for these trials. The bottom middle line shows trials that additionally received phasic stimuli and the timing of these relative to the force output. The bottom line is a time axis in seconds aligned to the start of the target force at 0s. The red dotted lines mark the time period in which the magnitude of the matched force for each trial was calculated.*

3.2.4. Task Procedure: Movement Control

To record a measure of SEP attenuation during movement independent from the behavioural task, participants completed a movement control task in both sessions. The task consisted of alternating blocks of movement and rest. When participants saw the word "MOVE" presented on a computer screen accompanied by an auditory go signal, participants were instructed to make a rapid, large and frequent tapping motion of the index finger of the wrist being stimulated. When they saw the word "REST" participants were instructed to remain as still and relaxed as possible. During each block participants received 25 electrical pulses to the wrist at a frequency of 2Hz. There were 20 blocks in total in each session (10 rest, 10 movement) resulting in 250 SEPs per condition for each wrist.

3.2.5. Median Nerve Stimulation

Two electrodes were placed on the surface of the skin in the centre of the wrist above the median nerve with the cathode more distal just below the crease of the wrist. The intensity of the stimulation at threshold (slight thumb twitch) was identified and then

increased by 1mA to produce a definite thumb twitch. The intensity remained the same throughout the experiment with a pulse width of 0.2μm.

3.2.6. Behavioural Data Analysis

Force values were extracted from Spike into MATLAB. Trials in which median nerve stimulation was given during force production in the matching phase (phasic stimuli) were removed from the behavioural analysis. Mean force output per trial was calculated from a specific time window of 2.5-3s after the GO signal to start matching (Figure 3.1B). Median nerve stimuli were not given until 3s in these trials (no phasic stimuli given) and therefore would have had no interference with the behavioural data during this time window. The mean force output during the target force was also recorded in the same time window in order to determine the relationship between the voltage output of the force transducer and the force applied by the robot given in Newtons. A calibration procedure was then used to scale the force output (V) to determine the true magnitude difference in N from the given target force.

It has previously been shown that people with schizophrenia were impaired on the force matching task such that they did not overestimate force in the self condition (Shergill et al., 2005). In addition, the magnitude of perceptual sensory attenuation in a population of healthy controls negatively correlated with their scores of delusional ideation (a measure of schizotypy). To replicate previous findings we hypothesised that the magnitude of force matching would be negatively correlated with schizotypy scores. All participants completed the Peter's Delusion Inventory (PDI) prior to taking part in the experiment. An overcompensation score for the force matching task was calculated for each participant by finding the difference between the matched force and the target force in the self condition. Parametric and non-parametric correlation analyses measured the relationship between overcompensation scores and PDI scores (one-tailed) across participants.

3.2.7. EEG Data Analysis: Pre-processing

Data were pre-processed using SPM 12. EEG data were re-referenced, by deducting data from two external electrodes attached to the participants' earlobes. The data were then filtered using a highpass filter at 0.1Hz. For analysis of the time x frequency data only, a low pass filter at 100Hz was also used. A trigger was sent to the EEG system at the time of every median nerve stimulus. The data were epoched around the time of median nerve stimulation with a time window of -100ms to 250ms for the SEP data. For the time-frequency analysis epochs were generated from the first median nerve stimulus given

after force matching in trials with hold stimuli only with a time window of -7500ms to 0; in this way we could ensure that there were no stimulus artefacts in the window of interest. The different experimental blocks were merged into a single file. For the time-frequency analysis the power of the EEG signal at each frequency from 1 to 99Hz in steps of 2 was estimated using the Multitaper spectral estimation in SPM with a sliding time window of 400ms that moved in steps of 50ms. The data were transformed using the Log rescale function and baseline corrected using a 50ms window from the first 100ms of the epoched time window.

3.2.8. EEG Data Analysis: SEP analysis

The epoched EEG data were averaged over trials and the topography examined to determine a ROI over sensorimotor cortex. Individual ROIs over sensorimotor cortices were selected based on electrodes that showed a negative peak at ~20ms and a positive peak ~30-45ms after the stimulus. For each participant electrodes for analysis were selected from SEP data averaged over all conditions and the same ROI was used for all analyses for that participant. Epoched data were sub-divided dependent on whether the median nerve stimulation was given during the phasic part of the force matching or whilst holding the matched force. Five well characterised peaks of the SEP were identified and used for analysis: N20, P30, P45, N55 and P100. For each participant an average SEP across all conditions over the specified ROI was generated and from this the latency of each peak was identified; the same latencies were then used for all subsequent analyses. Mean latencies left hemisphere (ms): N20=20.4±1.2, P30=29.6±3.3, P45=45±3.7, N55=64±8.0, P100=95.1±10.7. Mean latencies right hemisphere (ms): N20=21.3±3.7, P30=31.4±6.2, P45=45.2±5.0, N55=61.8±8.9, P100=94.6±13.6. These latencies were used to calculate the amplitude of each peak in the SEP for each condition so there was no experimenter bias in determining peak amplitudes (Kilner, 2013). The amplitude difference between neighbouring peaks generated the dependent variable for each component of the SEP: primary complex = N20-P30; secondary complex = P45-N55; and the later component = N55-P100.

To replicate previous neurophysiological data showing SEP attenuation with movement, the mean amplitude difference of each SEP component was compared for MNS given during movement vs rest in the control task. To determine the effect of task condition on SEP attenuation the mean amplitude difference of each component was compared in a 2x2 repeated measures ANOVA with the following factors: self vs external task condition; and hold vs phasic stimuli. The contrast between hold vs phasic stimuli was included to provide a measure of physiological SEP attenuation (most commonly seen comparing

movement and rest) within the behavioural paradigm with the rationale that SEP components should show a greater decrease in amplitude during force generation (phasic stimuli) compared to those produced during an isometric contraction (hold stimuli). A significant interaction between task condition and MNS time point would therefore suggest greater physiological SEP attenuation in one task condition compared to the other.

To further substantiate the relationship between perceptual and physiological sensory attenuation, non-parametric and parametric correlations were also carried out between the magnitude of physiological sensory attenuation (difference between SEP amplitudes during the hold phase of force matching and the phasic phase) for each component of the SEP (N20-P30, P45-N55 and N55-P100) and PDI scores for both hemispheres.

3.2.9. EEG Data Analysis: Time-Frequency Analysis

A time-frequency analysis was conducted to investigate whether there was any aspect of the oscillatory neural signal that significantly correlated with the behavioural data. The time-frequency data files were converted into images for statistical analysis in SPM. Images were created of the average of all trials for each condition (SELF, EXTERNAL) and force level (1N, 1.5N, 2N, 2.5N) creating 8 images in total per participant. The time-frequency data were averaged over the ROI previously selected in the SEP analysis to remove the dimension of "scalp" for both hemispheres independently. The EEG data were then regressed against the behavioural outcomes of the task for each condition: 1) the magnitude of sensory attenuation (the target force – the matched force); 2) the target force given. The latter covariate was used to control for any changes in neural activity as a result of force applied to the left finger. A beta image was created for each participant and used in a one sample t test at the group level to determine in which voxels the regressions at the first level were either positively or negatively significantly different from 0. To test for any significant clusters in the time-frequency images we ran a permutation analysis using the SnPM toolbox within SPM with 500 permutations.

3.3. RESULTS

3.3.1. Behaviour: Participants overestimate force in the self condition compared to the external condition

As expected, there was significant perceptual sensory attenuation across participants in the force matching task replicating previous findings meaning that participants significantly overestimated the matched force in the self condition compared to the

external condition. A 2x4 repeated measures ANOVA comparing condition (self vs external) and force level (1N, 1.5N, 2N, 2.5N) for the matched force revealed a significant main effect of condition ($F(1,15)=19.43, p<0.001$), a significant main effect of force level ($F(3,45)=79.23, p<0.001$) and a significant interaction ($F(3,45)=3.10, p=0.036$). Overall participants produced significantly greater force output in the self condition (M±SD=2.34±0.41N) compared to the external condition (M±SD=1.80±0.79N; Figure 3.2A) demonstrating significant perceptual sensory attenuation. Pairwise comparisons between the two conditions at each force level showed that despite the significant interaction the matched force produced in the self condition was significantly larger than the external condition at each force level ($p<0.002$; corrected for multiple comparisons). Comparing the matched force and the target force against force level for each condition separately using two 2x4 rmANOVA revealed a significant difference between the matched force and the target force in the self condition ($F(1,15)=26.31, p<0.001$), but no significant difference between the matched force and the target force in the external condition ($p=0.168$). Both conditions showed a significant interaction between force level and the difference between the matched and the target force (self: $F(3,45)=25.19, p<0.001$; external: $F(3,45)=21.63, p<0.001$). As can be seen in Figure 3.2B, there was a greater difference between the matched force and the target force at lower force levels compared to higher force levels. Replicating previous findings by Teufel et al (2010), we found a significant negative correlation between the overall magnitude of perceptual sensory attenuation and scores of delusional ideation using the nonparametric Spearman's correlational analysis ($r_s=-0.56$, $p=0.012$; one-tailed; Figure 3.2C). Here we have shown that we were able to demonstrate significant behavioural sensory attenuation, replicating previous results, and critically, demonstrate that MNS given after matching did not abolish this effect.

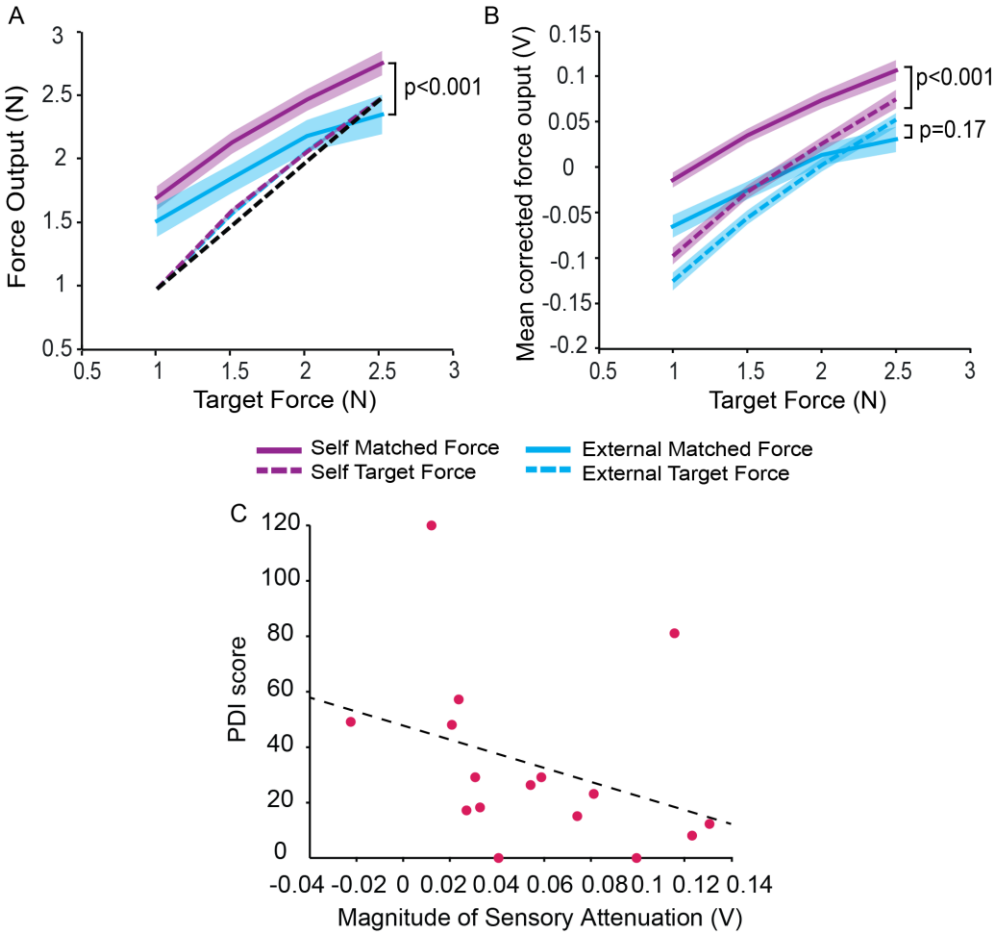

Figure 3.2. Behavioural data: greater overall force output in the self condition compared to the external condition. *A) Graph A plots the mean matched force for each target force level given (1N, 1.5N, 2N and 2.5N) for the self condition (purple, solid) and the external condition (blue, solid). The dotted black line represents the input target forces and the coloured dotted lines represent the mean force output calculated during the target force for each condition. The force output has been converted from voltage (V) to Newtons (N). B) Graph B plots the same data as graph A before it has been converted to N and having been mean corrected to demonstrate the statistical differences between the conditions. C) Correlation between the magnitude of perceptual sensory attenuation and scores of delusional ideation taken from the PDI replicating Teufel et al (2010)'s findings (parametric: r=-0.35, p=0.092; non-parametric: r=-0.56, p=0.012; both one tailed).*

3.3.2. Neurophysiology: Movement attenuates the primary and secondary complexes of the SEP

To ensure we could measure standard SEP attenuation previously recorded in response to movement, participants performed a simple control task in which we compared SEP amplitudes at rest and during movement. We were able to successfully replicate previous findings. SEPs recorded over sensorimotor cortex contralateral to the moving hand being stimulated were attenuated during movement compared to rest in a movement control task (Figure 3.3). The mean amplitude of the primary complex, N20-P30, from SEPs recorded over the hemisphere contralateral to movement, significantly decreased when the stimulated index finger was moving compared to rest; this was conducted separately

for right and left wrist MNS (left hemisphere: t(15)= -3.83,p=0.002; right hemisphere: t(15)=-5.68,p<0.001). The same result was found for the secondary component, P45-N55 (left hemisphere: t(15)= 2.70,p=0.017; right hemisphere: t(15) = 3.15,p=0.007). Individual ROIs were selected for each participant based on SEP data averaged across all conditions. Figure 3E shows the overlap of selected electrodes over each hemisphere.

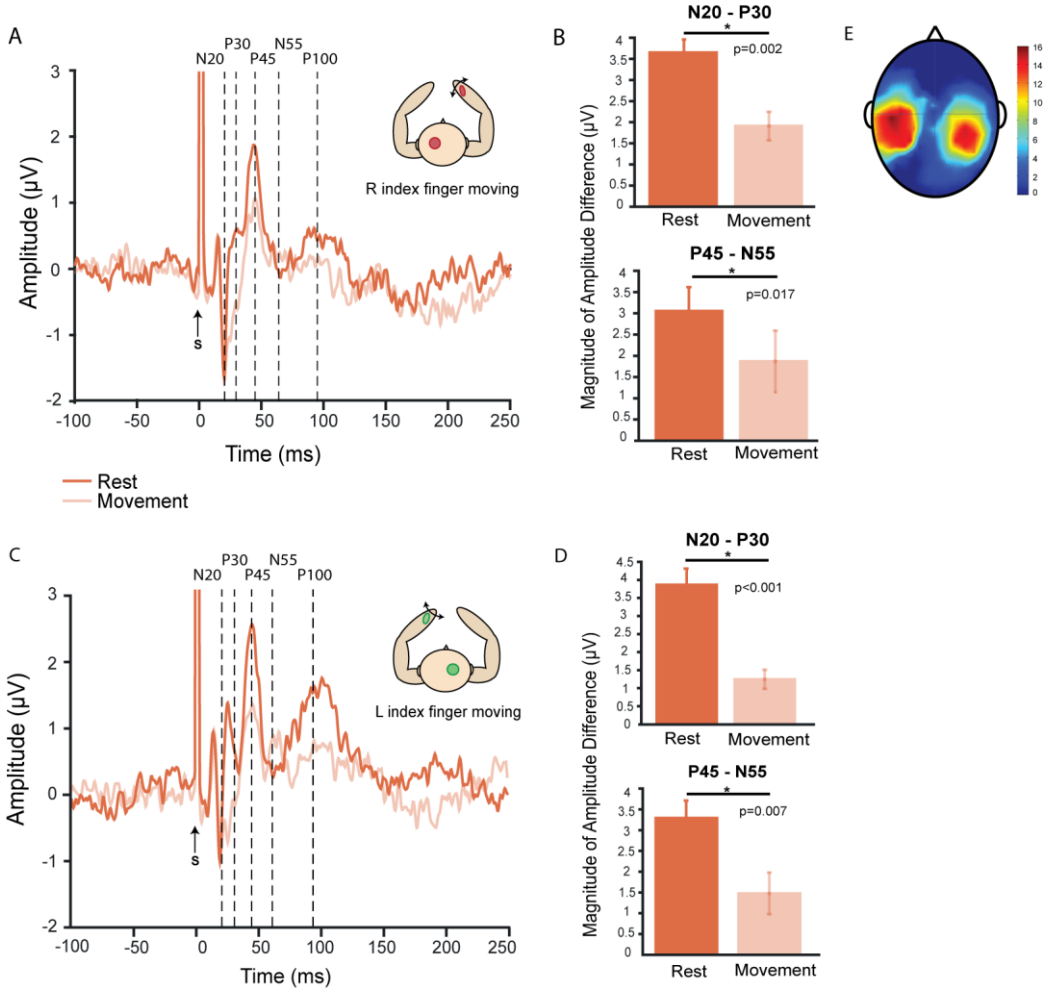

Figure 3.3. Movement decreases SEP amplitudes relative to baseline. *A+C) Average SEP traces in response to median nerve stimulation from a ROI over the right (A) and left (C) sensorimotor corticies for the rest (orange) and movement (pale orange) conditions of the movement control task. B+D) The magnitude of the mean SEP amplitude for N20 – P30 and P45 – N55 across all subjects is shown for the rest (orange) and movement (pale orange) conditions for the right (B) and left (D) sensorimotor cortices. E) Individual ROIs were selected for each subject based on SEP data averaged across all conditions, therefore the scalp map shows the overlap of selected electrodes over each hemisphere. The colour bar represents the number of participants for which that electrode (area) was selected for analysis. SEPs were baseline-corrected using the average amplitude in a 50ms pre-stimulus time window from -100ms. S = median nerve stimulus.*

3.3.3. Neurophysiology: SEP attenuation of the primary and secondary components was not modulated by behavioural task condition

MNS was given at two time points during the behavioural task: "phasic stimuli" were given directly after the GO cue to start matching during force generation; and "hold stimuli" were given during steady-state contraction when the target force was matched (see Figure 3.1B). We hypothesised that mean SEP amplitudes would be smaller for phasic SEPs compared to hold SEPs as it has been previously shown that there is greater physiological sensory attenuation during force generation compared to an isometric contraction. This contrast was used to demonstrate standard physiological SEP attenuation seen with movement during the behavioural task. We then compared mean SEP amplitudes at these time points and across conditions in the behavioural task using a 2x2 repeated measures ANOVA (condition: self vs external, x, stimulation time: phasic SEPs vs hold SEPs) with the hypothesis that a significant interaction between stimulation time and task condition would demonstrate a direct modulation of SEP attenuation with task condition.

Over left sensorimotor cortex, contralateral to the moving hand, there was a significant effect of stimulation time for both the primary (N20-P30: $F(1,15)=15.93, p=0.001$) and secondary (P45-N55: $F(1,15)=10.62$, $p=0.005$) components of the SEP. For both components the mean amplitude was greatest for the hold SEPs compared to the phasic SEPs demonstrating significant SEP attenuation during the behavioural task (Figure 3.4A,B,C). However, there was no significant effect of condition for either component (N20-P30: $p=0.183$, P45-N55: $p=0.516$) and no significant interaction (N20-P30: $p=0.430$, P45-N55: $p=0.893$) suggesting SEP attenuation of the primary and secondary components was not modulated by task condition.

Interestingly, similar results were found over right sensorimotor cortex, ipsilateral to the moving hand and contralateral to the finger receiving the matched force. There was no significant effect of stimulation time for the primary component (N20-P30: $p=0.902$); however, there was a significant effect of stimulation time for the secondary complex (P45-N55: $F(1,15)=11.94$, $p=0.004$). The mean amplitude for the hold SEPs was greater than the phasic SEPs (Figure 3.4E,F,G). Again there were no significant effects of condition (N20-P30: $p=0.157$, P45-N55: $p=0.565$) and no significant interactions (N20-P30: $p=0.724$, P45-N55: $p=0.389$). Attenuation of the primary and secondary components of the SEP was not significantly modulated by the behavioural task condition.

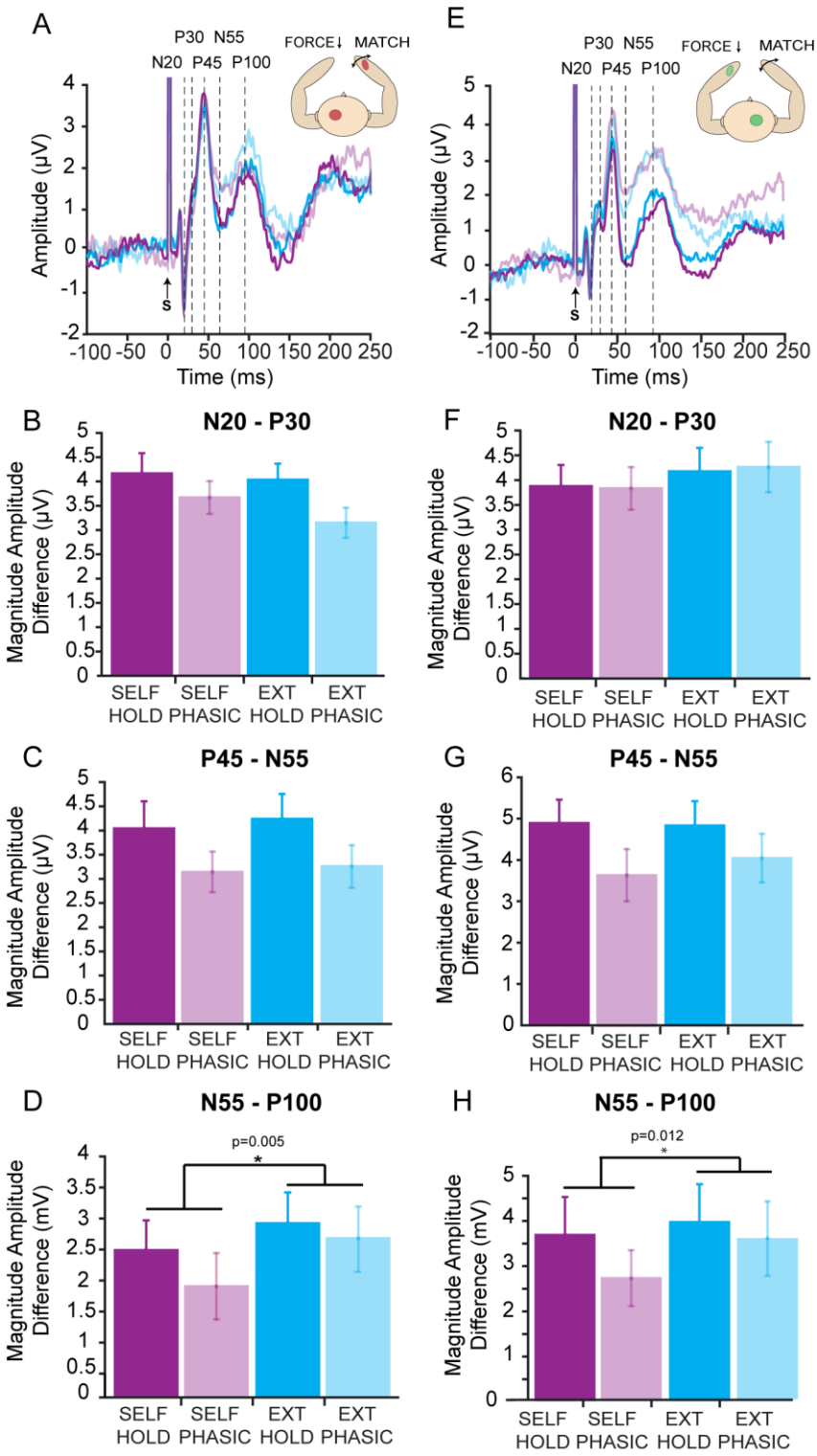

Figure 3.4. Attenuation of SEP amplitudes with stimulation time and behavioural task condition. *The left column (A-D) represent data taken from left sensorimotor cortex; the right column (E-H) represent data taken from right sensorimotor cortex. Graphs A+E show the average SEP traces across all subjects for the four experimental conditions: self hold stimuli (dark purple); self phasic stimuli (light purple); external hold stimuli (dark blue); and external phasic stimuli (light blue). The remaining graphs show the magnitude amplitude difference between adjacent SEP components for each condition for N20-P30 (B+F), P45-N55 (C+G) and N55-P100 (D+H). Graphs B,C+G show a significant effect of stimulation time representing significant attenuation but no significant effect of behavioural task condition. Graphs D+H show no significant effect of stimulation time but a significant effect of behavioural task condition. SEPs were baseline-corrected using the average amplitude in a 50ms pre-stimulus time window from -100ms.*

To ensure there were no specific modulations of SEP attenuation with force level, the same analysis used for the behavioural data was conducted. A 2x4 repeated measures ANOVA compared the magnitude of SEP attenuation (hold – phasic) at each force level for the self and external conditions. This was conducted separately for the primary and secondary SEP components and for both hemispheres. There were no significant main effects of condition (left hemisphere: N20-P30 p=0.238, P45-N55 p=0.766; right hemisphere: N20-P30 p=0.505, P45-N55 p=0.848), no significant main effects of force level (left hemisphere: N20-P30 p=0.404, P45-N55 p=0.401; right hemisphere: N20-P30 p=0.300, P45-N55 p=0.398) and no significant interactions between condition and force level (left hemisphere: N20-P30 p=0.233, P45-N55 p=0.923; right hemisphere: N20-P30 p=0.890, P45-N55 p=0.563).

To provide further support that SEP attenuation is not related to perceptual sensory attenuation, we found no significant correlations between attenuation of individual SEP components and scores of delusional ideation across either hemisphere, unlike with perceptual sensory attenuation, using non-parametric Spearman's analysis (left hemisphere: N20-P30 r=0.093, p=0.73, P45-N55 r=-0.040, p=0.88; right hemisphere: N20-P30 r=0.22, p=0.42, P45-N55 r=-0.17, p=0.52).

3.3.4. Neurophysiology: Attenuation of a later SEP component, N55-P100, was modulated by behavioural task condition

In contrast to the results regarding the primary and secondary SEP components, analysis of a later SEP component, N55-P100, using the same rmANOVA revealed a significant main effect of condition for both the left sensorimotor cortex, $F(1,15)=10.72$,$p=0.005$ (Figure 3.4D), and right sensorimotor cortex, $F(1,15)=8.25$, $p=0.012$ (Figure 3.4H). In both hemispheres the mean N55-P100 amplitude for the self condition (left hemisphere: M±SD = 2.02±1.93; right hemisphere: M±SD = 3.17±2.94) was significantly less than in the external condition (left hemisphere: M±SD = 2.53±1.86; right hemisphere: M±SD = 3.72±3.26). However, there was no significant interaction between the behavioural condition and the stimulation time for either hemisphere (left hemisphere: p=0.460; right hemisphere: p=0.216) and no significant main effect of stimulation time (left hemisphere: p=0.059; right hemisphere: p=0.123). Overall, the mean amplitude of the N55-P100 component was smaller over both hemispheres for the self-condition compared to the external condition suggesting that attenuation of this later SEP component correlated with perceptual sensory attenuation

To investigate whether attenuation of this later SEP component was modulated by force level, the same analysis used for the behavioural data and for the early SEP components was conducted. As the main ANOVA revealed a significant main effect of condition but no interaction or main effect of stimulation time, a 2x4 repeated measures ANOVA was conducted to compare the mean SEP amplitude across hold and phasic SEPs combined at each force level for the self and external conditions. For both hemispheres, there was a significant main effect of condition (left hemisphere: $F(1,15)=6.11$, $p<0.026$; right hemisphere: $F(1,15)=4.88$, $p=0.043$) with a lower SEP magnitude difference for the self-condition (left hemisphere: M±SD=2.01±2.22μV; right hemisphere: M±SD=3.03±3.05μV) compared to the external condition (left hemisphere: M±SD=2.55±2.12μV; right hemisphere: M±SD=3.54±3.59μV). However, there was no modulation of SEP amplitude with force level ($p=0.974$) and no significant interaction between condition and force level ($p=0.426$).

In addition, there was no significant correlation between attenuation of the N55-P100 SEP component and scores of delusional ideation across either hemisphere, unlike with perceptual sensory attenuation, using non-parametric Spearman's analysis (left hemisphere: N55-P100 $r=-0.25$, $p=0.34$; right hemisphere: N55-P100 $r=-0.15$, $p=0.59$).

3.3.5. Time-frequency Analysis: Negative correlation between gamma band activity and the magnitude of perceptual sensory attenuation

Having demonstrated no significant co-modulation of the SEP components with the behavioural data we next tested whether there were any modulations in the time-frequency domain that correlated with the behaviour. To this end a time-frequency analysis was carried out to identify whether any oscillatory activity over sensorimotor cortex correlated with the magnitude of perceptual sensory attenuation to provide a potential neurophysiological marker for this behavioural phenomenon. At the single participant level, the average magnitude of sensory attenuation (difference between the target force and the matched force) for each force level and each condition (2 x 4; average of all trials at each level of each factor; see methods for more details) was regressed against the EEG activity in the previously specified ROI across all frequencies and across the full time window of a single trial to determine if any neurophysiological activity correlated with the behavioural data. The target force averaged over the same trials was also included in the model to regress out the effect of target force. A one sample t-test at the second level revealed a significant cluster over the right sensorimotor cortex within

the gamma frequency band with a peak at 54Hz (cluster-level: p=0.004, corrected; peak-level: t=4.24,p<0.001,uncorrected). A non-parametric permutation analysis run with the SnPM toolbox confirmed this cluster to be significant at the corrected p<0.05 level. This activity was negatively correlated with the magnitude of perceptual sensory attenuation and occurred 422ms before the auditory GO signal to start matching (Figure 3.5). As perceptual sensory attenuation increased, i.e. matching became less veridical (self condition), the power of oscillatory activity within the gamma frequency band decreased.

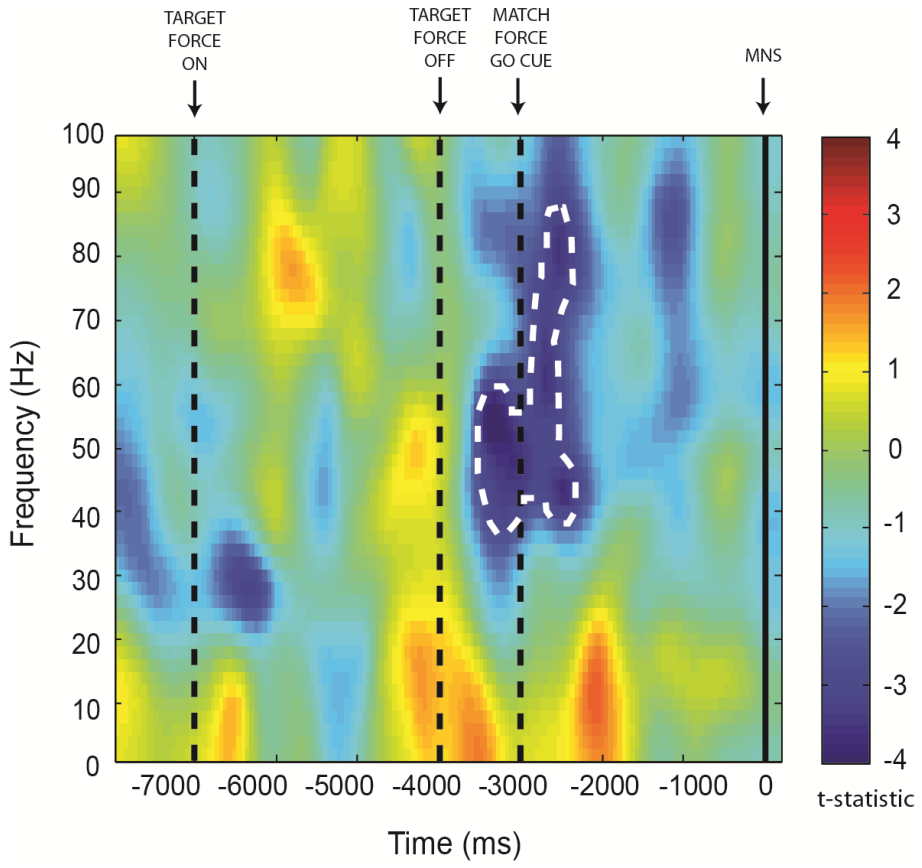

Figure 3.5. Negative correlation between gamma band oscillatory activity and the magnitude of perceptual sensory attenuation prior to force matching. *Time-frequency plot averaged over a preselected ROI showing the value of the t-statistic resulting from a one sample t-test at the group level of beta images from regression analyses between EEG data and behavioural data at the single subject level. This data represents a negative contrast i.e. in which voxels the mean regression across subjects was negative. Gamma oscillatory activity (peak 54Hz) significantly negatively correlated with perceptual sensory attenuation in the time period just before the auditory GO cue to match the target force was produced (-3422ms before the first MNS). A non-parametric permutation analysis using the SnPM toolbox revealed a significant cluster of activity (outlined in a white dotted line) at the corrected p<0.05 level.*

3.4. DISCUSSION

It has previously been proposed that movement-induced cortical gating of SEPs may be the mechanism underlying perceptual somatosensory attenuation measured using a force-matching paradigm. This study aimed to correlate physiological somatosensory attenuation of cortical SEPs with perceptual somatosensory attenuation to test this hypothesis. Primary, N20-P30, and secondary, P45-N55, components of the SEP showed significant attenuation during the behavioural task with force production, but this attenuation was not significantly modulated by task condition. This suggests physiological attenuation of early SEP components does not underlie perceptual somatosensory attenuation. However, analysis of a later SEP component, N55-P100, demonstrated an overall decrease in mean amplitude throughout the self-condition compared to the external condition, which suggests attenuation of this component may have a causal influence over perception in the force matching task.

Cortical SEP attenuation of the primary and secondary complexes was clearly seen during a movement control task and during the force matching paradigm. Previous research has demonstrated that SEP attenuation is greatest 200-400ms after EMG onset (Starr and Cohen, 1985; Wasaka et al., 2012) and increases with the velocity and magnitude of the movement (Rushton et al., 1981); therefore, I hypothesised, and subsequently demonstrated, significant attenuation of SEPs (over sensorimotor cortex contralateral to the moving hand) generated during force production (phasic stimuli) compared to an isometric force (hold stimuli). Interestingly, SEP attenuation of the secondary component, P45-N55, was also identified in the right hemisphere, ipsilateral to the moving hand and contralateral to the hand receiving the matched force. Previous research has found no attenuation of SEPs in the hemisphere ipsilateral to movement (Cohen and Starr, 1987; Kakigi, 1986); but have shown attenuation of early SEP components in response to tactile stimulation (Kakigi and Jones, 1986, 1985). When phasic stimuli were given, the force on the left index finger was increasing compared to hold stimuli where the force did not change. This suggests that applying a changing force to the periphery modulates sensory gating.

We further hypothesised that if this physiological somatosensory attenuation was the mechanism underlying perceptual somatosensory attenuation then there would be an interaction between the amplitude of SEP components at these time points and the behavioural task condition with greater SEP attenuation in the self-condition. However, we found no modulation of the early SEP components with behavioural task condition.

This result is consistent with the hypothesis that these are two distinct forms of somatosensory attenuation.

Interestingly, there was a significant decrease in the mean amplitude of the later N55-P100 SEP component throughout the self-condition compared to the external condition. It is perhaps not surprising that this later component is differentially modulated compared to the earlier components because there is more time for the signal to be influenced by interconnected cortical areas. MEG studies in humans have highlighted that the earliest components of the SEP originate in contralateral area 3b, which has dense thalamocortical projections, and adjacently connected area 1 within the primary somatosensory cortex (Hoshiyama et al., 1997; Kakigi, 1994). Connections between area 3b and the primary motor cortex (M1) and the supplementary motor area (SMA) provide a physiological pathway by which early SEP components can be attenuated in response to movement preparation and execution (Krubitzer and Kaas, 1990) or could alternatively drive changes in motor cortex for movement initiation in accordance with the active inference framework. In contrast, later SEP components are thought to originate from bilateral dipoles in SII (Hoshiyama et al., 1997; Kakigi, 1994); therefore attenuation of the N55-P100 SEP component may be driven by activity in SII.

It has previously been shown that self-generated movement resulting in tactile sensation causes a significant decrease in the BOLD signal in bilateral SII (Blakemore et al., 1999) and is decreased as the sensory input becomes less predictable (Shergill et al., 2013). This is thought to be driven by activity in the cerebellum, which is thought to represent the prediction error signal from comparing predicted and actual sensory input. This mechanism may be reflected in the attenuation of the N55-P100 SEP component. It could be argued that the N55-P100 attenuation is confounded by the greater force produced in the self-condition compared to the external condition, however this is unlikely as this component is not significantly modulated by force level. Attenuation of this component may demonstrate a change in the state of the somatosensory cortex which then modulates subsequent perception. It is harder to interpret the functional role of later components as there is more time to be modulated by other inputs and the peaks are less distinct and more difficult to quantify. Nevertheless, the dissociation between the source of the early and late SEP components and the behavioural outcomes of physiological and perceptual somatosensory attenuation suggests that these forms of sensory gating are not only dissociable but have distinct functional roles.

SEPs provide an assay to measure modulations in somatosensory activity however analysis is limited to the time in which median nerve stimuli were given. In order to

investigate modulations in somatosensory activity that may correlate with perceptual somatosensory attenuation throughout the entire trial, exploratory time-frequency analyses measuring oscillatory activity over sensorimotor cortex were conducted. Time-frequency analyses highlighted a significant negative correlation between gamma band activity (~40-90Hz) and the magnitude of perceptual somatosensory attenuation over the right sensorimotor cortex contralateral to the hand receiving the matched force. This occurred before the auditory cue to start matching rather than during the matching period as might be expected. This signal may therefore be in a position to causally modulate the gain of incoming somatosensory information in preparation for receiving the matched force, which in turn may modulate subsequent perception, rather than representing the perception itself. It could be argued that this result is confounded by the increased force produced in the self-condition, however this is unlikely due to the location of the activity (ipsilateral to the hand producing the force) and the timing of this modulation (before force production).

Interestingly, this oscillatory finding supports theoretical accounts of perceptual somatosensory attenuation, which posit that the difference in somatosensory attenuation between the self and external task conditions is due to a difference in the ability to predict the sensory consequences of our own actions, but not others (Blakemore et al., 1999). When our predictions are highly accurate (as in the self-condition) prediction error is low and somatosensory attenuation is high and vice versa when our predictions are not accurate (external condition). Therefore, it follows that the magnitude of prediction error will negatively correlate with the magnitude of somatosensory attenuation. If we assume that gamma oscillations represent the forward (ascending) connections carrying prediction errors, as has been previously suggested (Arnal and Giraud, 2012; Bastos et al., 2012; Bauer et al., 2014), then this data supports the hypothesis that a changing prediction error, represented by gamma band activity, is underlying the perceptual differences measured. Trials with less perceptual somatosensory attenuation have higher gamma band activity prior to matching the force and have lower prediction error in line with the theory.

However, it is important to note that prediction errors are precision-weighted. This means that an estimate of the (inverse) variance of the predicted and actual sensory input is incorporated into the prediction error signal. In line with the alternative hypothesis which posits that sensory attenuation is caused by a reduction in sensory precision represented by a decrease in the synaptic gain of superficial pyramidal cells transmitting prediction error signals (Adams et al., 2013b; Brown et al., 2013), we can see that there would also be a negative correlation between somatosensory precision and perceptual

somatosensory attenuation, which could explain this oscillatory finding. It has been proposed that gamma band oscillations are responsible for altering the synaptic gain of cells transmitting prediction errors, which in turn decreases somatosensory precision (Friston et al., 2015). Whether the gamma band activity represents changes in precision, or prediction error, or the precision-weighted prediction error, the same result would be found. However, these exploratory analyses were post-hoc therefore specific hypothesis-driven experimental work, optimally using patient populations, is needed to elucidate the necessity and sufficiency of this neural signal for perceptual somatosensory attenuation. Moreover, there are many different neuronal mechanisms besides changes in synaptic gain that can modulate the amplitude of evoked potentials and oscillatory activity, such as differences in synchronisation and recruitment; therefore, simultaneous invasive and non-invasive electrophysiological recordings are needed to better elucidate the underlying neuronal mechanisms.

In this thesis, I hypothesise that sensorimotor beta oscillations may represent changes in sensory precision necessary for movement initiation. In the current study there was no significant correlation between perceptual somatosensory attenuation and beta oscillatory activity. However, this study also found no relationship between physiological somatosensory attenuation and perceptual sensory attenuation. This suggests that these two phenomena may be functionally distinct and thus may be controlled by different frequencies of population activity. One hypothesis is that gamma oscillatory activity modulates the synaptic gain of cells transmitting prediction error signals for perception, however sensorimotor beta oscillations act to modulate the gain of pyramidal cells transmitting proprioceptive prediction errors for action; there may be a differentiation depending on whether the prediction error relates to exteroceptive or proprioceptive input and this may be reflected in the cortical source of the oscillatory activity. Although this does not fit with current predictive coding ideas, the sensorimotor system may not conform to the canonical message passing that has been shown in the visual system. Alternatively, sensorimotor beta oscillations may represent the precision of proprioceptive predictions, which would be increased following a decrease in sensory precision. The literature shows that cortical beta oscillations are coherent with beta activity in the periphery; therefore sensorimotor beta oscillations may play a particularly specialised role in controlling this descending peripheral circuit for movement.

In this study I have demonstrated that physiological somatosensory attenuation of the primary and secondary SEP components in response to movement is not correlated with perceptual somatosensory attenuation. This is consistent with the hypothesis that these two forms of somatosensory attenuation are functionally distinct. The active inference

framework suggests that gating of the afferent signal may be due to a reduction in somatosensory precision which is a necessary step in movement initiation (K. Friston et al., 2011). This same mechanism has also been used to explain perceptual somatosensory attenuation (Brown et al., 2013). However, it is clear from this study that at the level of the primary somatosensory cortex any gating of the afferent signal or theorised modulation of somatosensory precision does not explain behavioural attenuation in the force matching task. That said, it may be the case that perceptual somatosensory attenuation occurs via the same mechanism (a reduction in somatosensory precision) but at a different level of the cortical hierarchy, for example SII. Indeed the later SEP component, N55-P100, thought to originate in SII, was significantly modulated by perceptual somatosensory attenuation in the current study, which supports this hypothesis.

Abnormal perceptual somatosensory attenuation has been highlighted in patients with schizophrenia (Shergill et al., 2005) and functional movement disorders (Pareés et al., 2014) and abnormal physiological somatosensory attenuation has been highlighted in patients with functional movement disorders (A Macerollo et al., 2015) and Parkinson's Disease patients (Macerollo et al., 2016). Identifying how these deficits in somatosensory gating interact and where they dissociate to cause particular cognitive and motor symptoms in differing patient populations will be invaluable for highlighting the key functional role(s) of somatosensory gating and may give novel insights into the neurobiological mechanisms of these symptoms. In the following chapters I aim to modulate sensory precision in the proprioceptive and visual domains to determine the effect of this on behaviour and oscillatory activity over sensorimotor cortex.

CHAPTER 4

Study Two: Investigating the effect of a peripheral vibrating stimulus on oscillatory activity over sensorimotor cortex

4.1. INTRODUCTION

In the previous chapter, I showed that perceptual and physiological somatosensory attenuation did not have the same underlying neurophysiological correlate, therefore may be functionally distinct phenomena. Physiological somatosensory attenuation is thought to play an important and necessary role in motor initiation. The active inference framework posits that a decrease in sensory precision (increase in sensory uncertainty) must occur in order to allow proprioceptive predictions to incite movement (Brown et al., 2013; K. Friston et al., 2011; Friston et al., 2010). The decrease in the amplitude of the somatosensory evoked potential (SEP) with movement is thought to reflect this down-weighting of somatosensory information via a change in synaptic gain on superficial pyramidal cells in the primary somatosensory cortex. However, evoked potentials only reflect the activation of particular circuits at a very specific time point and, in this case, in response to an artificial stimulus. SEPs therefore lack the ability to describe how activity over a population of neurons varies over time during a particular behaviour. Moreover, it has been suggested that oscillatory activity could causally modulate synaptic efficacy (Chawla et al., 1999; Friston et al., 2015), therefore identifying the neurophysiological correlate of physiological somatosensory attenuation in the spectral domain could further our understanding of the potential mechanism by which this change in synaptic gain could affect motor control. In the introduction I have outlined the correlative and theoretical evidence that suggests sensorimotor beta oscillations may encode this decrease in somatosensory precision and therefore could be the oscillatory correlate of physiological somatosensory attenuation necessary for movement initiation. This chapter aims to test this theory.

There is a plethora of evidence to suggest that modulations in beta power over sensorimotor cortex prior to and during movement may represent changes in somatosensory precision. Firstly, the time course of this modulation is very similar to the time course of SEP attenuation with movement (Cohen and Starr, 1987; Jasper and

Penfield, 1949; Pfurtscheller, 1981; Seki and Fetz, 2012). Secondly, during periods of active holding, beta power increases (Baker et al., 1997) as does the amplitude of cutaneous SEPs over sensorimotor cortex (Rushton et al., 1981; Seki and Fetz, 2012), Thirdly, beta bursts have been shown to enhance SEP amplitude following peripheral nerve stimulation (Lalo et al., 2007) and enhance transcortical stretch reflexes (Gilbertson et al., 2005). Finally, recent evidence suggests that beta power may reflect different types of uncertainty, which is the inverse of precision (Tan et al., 2016; Tzagarakis et al., 2015, 2010).

Moreover, the evidence demonstrating that sensorimotor beta power may be mechanistically involved in motor control supports the hypothesis that this frequency of oscillatory activity could mediate somatosensory gating, which according to the active inference framework is necessary for movement (reviewed in introduction). Abnormally high resting beta power is a prominent feature of Parkinson's Disease (PD) and correlates with motor symptoms, such as an inability to initiate movement (akinesia) and a slowness of movement (bradykinesia) (Little and Brown, 2014). High frequency deep brain stimulation (DBS) of the STN improves motor symptoms in PD and has a greater efficacy when paired with an adaptive algorithm in which the stimulation is triggered by peaks in beta power (Little et al., 2013), which suggests beta oscillatory activity may play a causal role in the motor symptoms of PD. Moreover, SEP attenuation is impaired in patients with functional movement disorders (A Macerollo et al., 2015) and PD patients (Macerollo et al., 2016) and improves with dopaminergic medication (Macerollo et al., 2016).

In order to determine the necessity of somatosensory attenuation for movement initiation I designed an experiment to manipulate somatosensory precision and sought to determine its effect on a motor control task and on sensorimotor beta power. Estimates of sensory precision in the brain can be reduced either by making the sensory input more uncertain or by a top-down attentional mechanism. In this study I used high frequency peripheral vibration to increase the uncertainty in the proprioceptive state, which would in turn reduce estimates of somatosensory precision. Previous research (outlined in the introduction) demonstrates that vibration, specifically at high frequencies, increases firing of 1a afferents (Ribot-Ciscar et al., 1998; Roll et al., 1989) and induces kinaesthetic illusions by activating muscle spindles in the vibrated muscle that signal to the cortex that the muscle is lengthening when it is not (Goodwin et al., 1972; McCloskey, 1973). This therefore creates uncertainty in the perceived position of the limb and generates an unexpected afferent input. Peripheral vibration also causes a decrease in SEP amplitudes (Cohen and Starr, 1985), which supports the assumption that this manipulation would decrease estimates of somatosensory precision in the cortex.

Previous work in the lab demonstrated that giving a peripheral vibrating stimulus at 80Hz significantly improved task performance on a number of standardised movement tasks including a simple RT task and the clinically well characterised nine-hole peg task (Grice et al., 2003) (under submission). However, vibration at 20Hz did not have the same effect, potentially due to muscle spindles not being optimally activated at this frequency. In this study I hypothesized that peripheral vibration at 80Hz would: 1) decrease completion time on the nine-hole peg task, replicating this previous result; 2) decrease beta power over sensorimotor cortex during and post-vibration; 3) and that this decrease would correlate with improvements in motor performance on the behavioural task.

4.2. METHODS

4.2.1. Participants

18 healthy participants (male=5; female=13) aged 18-55 years old (mean ±SD: 26.06 ±9.64) took part in this study. Participants had no self-reported history of neurological or psychiatric illness. All participants were right handed and gave written informed consent prior to taking part. This study was approved by the UCL Research Ethics Committee and all testing took place at the UCL Institute of Neurology, Queen Square. One subject was excluded for noisy EEG data.

4.2.2. Apparatus

An upright vibrating stimulator resting on a surface was used to provide the vibratory stimulus throughout the task. Participants were asked to rest the posterior surface of their wrist on top of the vibrating stimulus, just proximal to the crease in the wrist, so it was lightly touching. The frequency was either 80Hz or 20Hz. The gain was always 1. A 128 active electrode Biosemi system was used to collect the EEG data at a sampling frequency of 2048Hz. Triggers indicating the start of each trial were sent to the data acquisition PC using MATLAB 2013a.

4.2.3. Task Procedure

During the EEG recording participants were asked to fixate on a small white cross on a black background and stay relaxed. Their arm was positioned on the vibrating stimulus and supported using a pillow. Recording was divided into 4 blocks of 10 minutes with 5 trials in each block. Each trial consisted of 30s rest followed by 30s peripheral vibration followed by 60s rest. Two blocks used 80Hz vibration and the other two blocks used 20Hz

vibration. The order in which vibration was given was counterbalanced across participants.

To provide a measure of the effect of vibration on motor performance, participants completed the 9-hole peg task (Grice et al., 2003). In this task participants were instructed to place 9 pegs, held within a small well, into 9 holes as fast and as accurately as possible. Participants completed this task 3 times in 3 conditions: 1) after 80Hz vibration; 2) 20Hz vibration; and, 3) no vibration. The order in which vibration was given was counterbalanced across participants.

4.2.4. EEG Preprocessing and Analysis

The data were high-passed filtered at 0.1 Hz, low pass filtered at 100 Hz and down-sampled to 400 Hz. The data were epoched around the onset of the vibration in a 120s time window of -30s to 90s. Prior to time-frequency analysis, the data for each of the 10 trials for both vibration conditions were concatenated into one file. To calculate the power spectra, for each of the 10 trials, the time series was divided into 5 second non-overlapping windows (24 total) and the power spectra were calculated over each window using Welch's averaged periodogram method. This resulted in a time-frequency power spectrum with a power spectrum every 5 seconds with 1 Hz resolution. The resulting power spectra were then averaged over trials, log-transformed and were baseline corrected by subtracting the mean power in the 15 seconds before vibration onset for each frequency.

An initial analysis focused on modulations in beta power. To this end for each subject for each electrode the time-frequency data were averaged over the 15-30 Hz frequency range across both vibration conditions and converted to an image, creating one scalp map for each of the 24 power spectra over time. These 3D images were smoothed and analysed in SPM12. To test for differences in beta power between the conditions over the scalp for each participant the scalp-time images of the beta power modulation for the 80 Hz vibration was subtracted from the 20 Hz vibration and any difference between the two was tested using the standard mass univariate approach in SPM12. The results of this analysis revealed where on the scalp beta power was modulated during vibration and, from this, electrodes of interest were selected (Figure 4.1A-C). Subsequent analyses were conducted on the average time-frequency images over these electrodes of interest. To test for time-frequency differences between the conditions for each subject the time-frequency images for the 80 Hz vibration were subtracted from the 20 Hz vibration and any difference between the two was tested using the standard mass univariate approach in

SPM12. In addition, modulations in the 80 Hz vibration condition were compared to the baseline power by testing for differences from 0 for just the 80 Hz condition using the standard mass univariate approach in SPM12. All statistical thresholds were corrected for multiple comparisons using random field theory approach on the peak voxel using a small volume correction over 15-30Hz (J. M. Kilner et al., 2005).

A Pearson correlation analysis was used to test if there was any relationship between beta power modulation and behavioural performance following the peripheral vibration. Beta power was averaged over 15-30Hz in the 10s following 80Hz vibration for each participant; this represents the change in beta power from the baseline period 15s before vibration onset. This was correlated against the change in completion time on the nine-hole peg task following 80Hz peripheral vibration: the average completion time following 80Hz vibration minus the average baseline completion time.

4.3. RESULTS

4.3.1. Beta oscillations were significantly decreased during 80Hz but not 20Hz peripheral vibration

An initial analysis tested the hypothesis that there was a significant attenuation of power in the 15-30 Hz range during the period when 80 Hz vibration was applied compared with 20 Hz vibration. Beta power was significantly lower at the onset of 80 Hz vibration compared with onset of 20 Hz vibration specifically at electrodes overlying the left sensorimotor cortex (peak voxel $t(1,16) = 4.87$, $p<0.05$ corrected for FWE; Figure 4.1A-C).

Subsequent analyses focused on the average time-frequency plots overlying the electrodes of interest where beta power was significantly attenuated. The time course of beta power modulation averaged over the electrodes of interest and across the beta frequency range (15-30 Hz) revealed that beta power was attenuated at the onset and offset of the 30 seconds vibration period (Figure 4.1F). To investigate this further, the time frequency plots averaged over the electrodes of interest were compared. This analysis revealed a significant attenuation of oscillatory power at 20 Hz at the onset of 80 Hz vibration compared with 20 Hz vibration ($t(1,16) = 5.13$, $p<0.05$ FWE corrected; Figure 4.1D). One possible explanation for these results is that the decrease in power in the beta frequency range reflects an increase in beta power during the 20 Hz vibration, reflecting the power at the frequency of vibration. To exclude this hypothesis, we tested whether there was a significant attenuation of power in the 80Hz condition compared to baseline. This analysis

revealed two clusters of significant attenuation one at the onset of the vibration ($t(1,16) = 4.7$ peak at 27 Hz and one at the offset ($t(1,16) = 4.59$ peak at 23 Hz; $p<0.05$ FWE corrected) (Figure 4.1E).

4.3.2. 80Hz peripheral vibration increased movement speed in the nine-hole peg task

A one way repeated measures ANOVA revealed a significant main effect of vibration, $F(2,34)=32.75, p<0.001, Eta^2=0.66$. Post-hoc pairwise comparisons corrected for multiple comparisons with the Bonferroni method revealed a significant difference between mean completion time following 80 Hz vibration (M±SD=10.71±1.40s) and no vibration (M±SD=12.36 ± 1.04seconds), $t(17)=7.480$, $p< 0.05$, and 80 Hz vibration and 20 Hz vibration (M±SD=11.87 ± 1.22 seconds), $t(17)=-5.529$, $p<0.05$. There was no significant difference between mean completion time following baseline and 20Hz vibration ($p=0.069$). Participants completed the task quicker following 80Hz vibration compared to the other conditions (Figure 4.2A+B).

4.3.3. No significant correlation between beta power modulation and behavioural performance following 80Hz peripheral vibration

I hypothesise that the decrease in beta power seen following 80Hz vibration was potentially responsible for the behavioural improvements seen the nine-hole peg task following 80Hz vibration. I correlated the modulation in beta power from baseline averaged over 10s following vibration for each participant against the change in completion time following 80Hz vibration compared to baseline on the nine-hole peg task. There was no significant correlation: $r=0.012$, $p=0.965$ (Figure 4.2C).

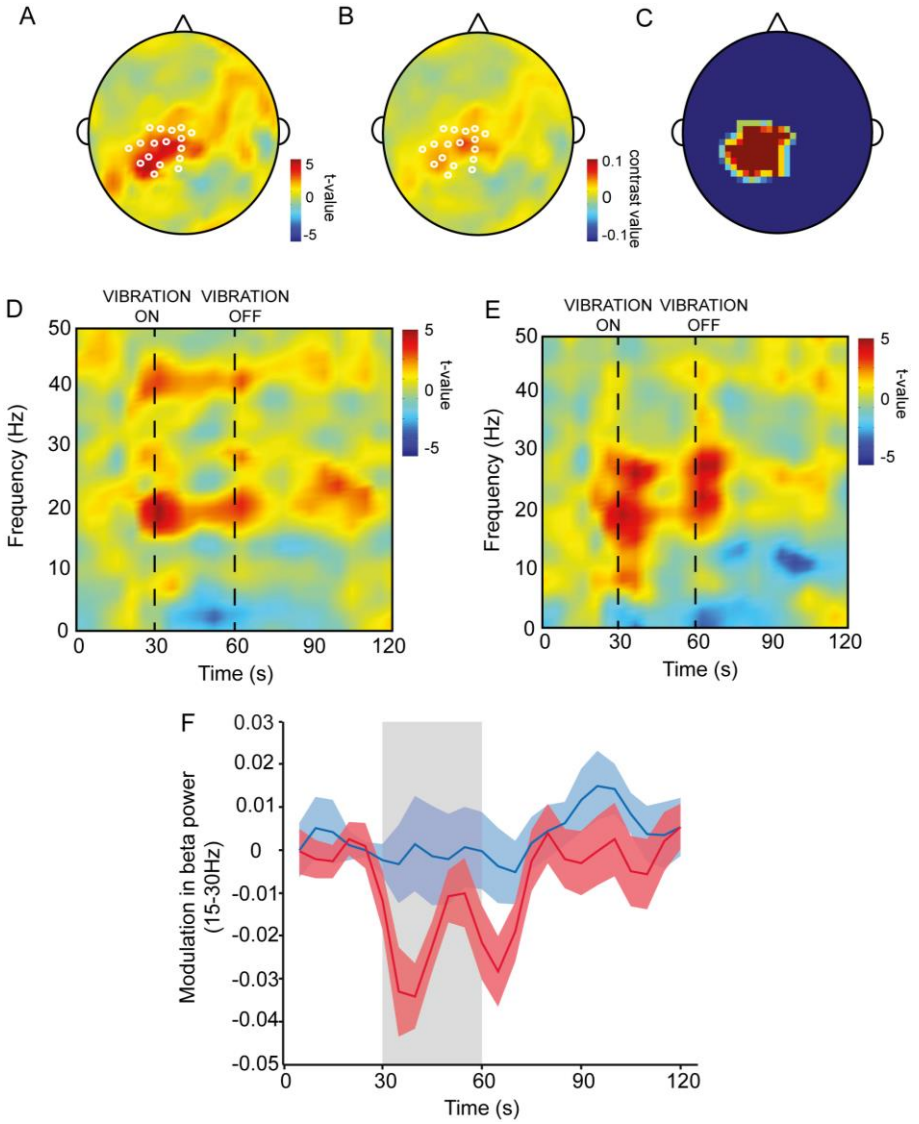

Figure 4.1. Beta power over sensorimotor cortex decreased at the onset and offset of 80Hz peripheral vibration. *A&B) Topography of the EEG activity averaged over 15-30Hz during vibration. White circles show electrodes which showed a significant attenuation of beta power during vibration superimposed on (A) the t-statistic scalp image and (B) the contrast image. C) ROI selected for subsequent time-frequency analyses. (D-E) Time-frequency t-statistic images within an ROI over contralateral sensorimotor cortex for (D) the difference between 80Hz and 20Hz vibration conditions, and (E) the difference between 80Hz vibration and a baseline window. Data is shown in the period prior to, during and following vibration. F) Change in beta power relative to the average beta power in a 15s time window prior to vibration onset shown across time before, during and after 80Hz vibration (red) and 20Hz vibration (blue). The shaded block represents the time when vibration was on.*

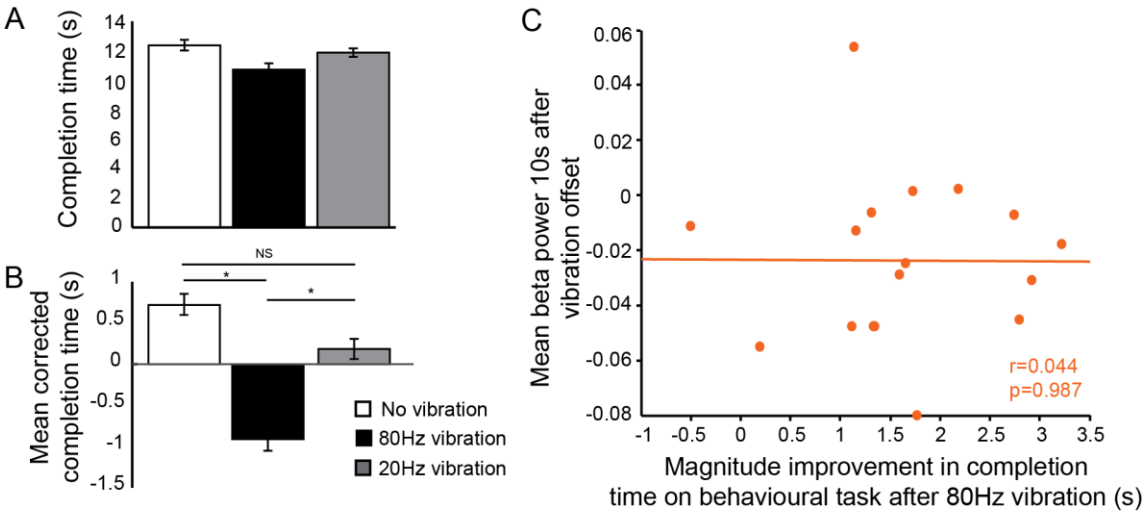

Figure 4.2. Behavioural effect of peripheral vibration. *A+B) Bar graphs showing (A) the completion time and (B) mean-corrected completion time for the nine hole peg task. C) Correlation between the mean beta power over the 10s following 80Hz peripheral vibration (relative to the average beta power over the 15s prior to vibration onset) and the magnitude of improvement in completion time on the nine hole peg task following 80Hz vibration compared to baseline.*

4.4. DISCUSSION

In this study I aimed to modulate somatosensory precision in order to determine the effect of this on sensorimotor beta power and motor control. Sensory precision can be modulated in two ways: 1) by making the afferent input noisier and thus more uncertain; or, 2) through a top-down attentional mechanism. Here I hypothesised that the peripheral vibrating stimulus would increase the uncertainty in the proprioceptive state and thus decrease somatosensory precision. I hypothesised that this would be reflected in a decrease in beta power and lead to enhanced motor initiation in line with the active inference framework. Indeed, 80Hz peripheral vibration applied to the wrist of healthy participants improved performance on a dextrous motor task. The EEG data revealed a significant decrease in beta oscillatory activity (15-30Hz) over the contralateral sensorimotor cortex at the onset and offset of 80Hz vibration. In contrast, peripheral vibration at 20Hz had no effect on motor performance and caused no modulation in beta oscillatory activity. This data suggests that the mechanism by which high frequency vibration improved behavioural performance could be through the modulation of sensorimotor beta oscillations. This supports the hypothesis that sensorimotor beta oscillations may represent changes in somatosensory precision.

In this study, modulations in behaviour and oscillatory activity were only seen with 80Hz vibration and not 20Hz vibration. As muscle spindles are optimally activated at 80Hz, one hypothesis is that the results in this study were driven by a decrease specifically in the precision of the proprioceptive input (Ribot-Ciscar et al., 1998; Roll et al., 1989). Muscle afferent fibres provide an essential source of information about the dynamic position of the muscle necessary for optimal proprioceptive feedback. Previous studies have shown that 80Hz peripheral vibration impairs performance on a number of proprioceptive tasks (Bullen and Brunt, 1986; Capaday and Cooke, 1981; Cordo et al., 1995; Inglis and Frank, 1990; Tsay et al., 2016), which is thought to be driven by an increase in the uncertainty in the proprioceptive input. Indeed, activating these muscle spindles at 80Hz produces the illusion that the implicated muscle is contracting in the absence of any EMG activity by transmitting incorrect kinesthetic information to the brain and spinal cord (Cordo et al., 2005; Craske, 1977; Naito et al., 1999; Seizova-Cajic et al., 2007). The modulation of beta oscillations with high frequency vibration in the current study supports the hypothesis that this beta activity may reflect changes in uncertainty in the proprioceptive input. This is in line with the hypothesis that sensorimotor beta oscillations encode modulations in somatosensory precision. Although there was no direct measure of uncertainty or proprioceptive illusions in this study, I assume that proprioceptive uncertainty has been modulated. The next chapter will aim to directly quantify the effect of peripheral vibration on proprioceptive uncertainty.

In the current study I found a significant decrease in beta oscillatory activity at the onset and offset of 80Hz peripheral vibration. Muscle spindles in general are rapidly adapting and respond to relative changes in muscle stretch rather than sustained stretch, potentially reflecting this pattern of activity. However, microneurographic studies have shown that 1a afferents respond to vibration in a 1:1 mapping such that the afferent firing rate matches that of the vibration frequency and this remains constant throughout the period of vibration (Ribot-Ciscar et al., 1998; Roll et al., 1989); therefore, it is unlikely that this beta modulation directly reflects this afferent firing rate. There is evidence that the motor system adapts to a constant vibratory stimulus and this potential top-down adaptation may be reflected in the modulation of beta power in this study. For example, there is a clear reduction in muscle spindle activity up to 40s following the offset of vibration compared to baseline (pre-vibration) (Ribot-Ciscar et al., 1998) and during this period participants often experience illusory aftereffects i.e. the vibrated muscle appears to move in the opposite direction to that experienced during the vibration (Seizova-Cajic et al., 2007). This adaptation likely occurs via a central mechanism. The modulations in

beta power at the onset and offset of the vibratory stimulus in the current study may represent this central adaptation process.

Indeed, this pattern of oscillatory activity could represent the updating of estimates of sensory precision that are likely to occur with this adaptation process. For example, at the onset of vibration an unexpected proprioceptive input causes a decrease in estimates of sensory precision; as the constant vibratory stimulus then becomes predictable, estimates of sensory precision are increased over time as the sensorimotor system adapts to the stimulus; another update is then required when the stimulus is turned off. This modulation in the sensorimotor beta power may therefore represent a top-down adaptation command, which may be used to gate afferent input depending on its uncertainty. This supports my hypothesis that sensorimotor beta oscillations modulate with changes in sensory precision. This also suggests that beta oscillatory activity may represent estimates of somatosensory precision at a higher level of the cortical hierarchy. This idea is explored later in this thesis.

Vibration also activates cutaneous mechanoreceptors, therefore it is difficult to rule out the possibility that the changes in sensorimotor beta power recorded reflect an adaptation to the cutaneous input. Indeed, previous research has shown that beta power is modulated by a purely tactile stimulus (Cheyne et al., 2003; Gaetz and Cheyne, 2006). However, mechanoreceptors are generally activated at either lower frequencies (30-50Hz) or much higher frequencies of vibration (250-350Hz; Purves et al., 2001a) and it is unlikely that this effect would be specific to 80Hz vibration. Muscle oscillatory activity in the beta frequency range has been shown to be coherent with 1a afferent firing, but not cutaneous afferent firing (Baker et al., 2006), and there is coherence between the EMG and cortical oscillatory activity in the beta band (Kilner et al., 1999); this suggests that the effects recorded in this study are likely due to muscle spindle activity. Microneurographic studies are needed to determine the effect of peripheral vibration on the firing of specific types of afferent fibers and EEG to elucidate the contribution of cutaneous vs muscle afferent input on cortical oscillatory activity.

The active inference framework posits that in order to initiate a movement, we must decrease the certainty in our current sensory state through attenuation of the afferent signal (Brown et al., 2013; K. Friston et al., 2011). Here I have shown that high frequency peripheral vibration thought to activate 1a afferents decreases completion time on the nine-hole peg task and it has previously been shown to decrease reaction times across a number of motor control tasks (under submission), which supports this hypothesis. However, any improvements on this task during the current study were not correlated

with the decrease in beta power that occurred following 80Hz peripheral vibration. This is not surprising as these two measures were taken at different time points during testing. This finding merely suggests that individuals do not show a consistent trait-like modulation of beta power following vibration, which can explain the average behavioural improvement seen on a separate motor control task. It will be important to correlate trial-wise modulations in beta power following vibration and subsequent response times or completion times from a behavioural task in order to conclude whether the change in beta power following vibration may be causally modulating behavior on a trial-by-trial basis.

According to the active inference theory, the behavioural changes seen here are due to increased sensory attenuation (which may be driven by sensorimotor beta oscillations). Indeed, previous research has demonstrated that high frequency peripheral vibration causes somatosensory attenuation, as indicated by a decrease in the amplitude of SEPs evoked by electrical stimulation of the afferent nerve. Peripheral vibration at 60Hz causes an attenuation of early components of the cortical and cervical SEP (Abbruzzese et al., 1980; Cohen and Starr, 1985). Yet, 50 Hz cutaneous vibration between the thumb and finger and 20 Hz vibration at the wrist does not produce significant somatosensory attenuation (Kakigi and Jones, 1986; Legon and Staines, 2006). However, another study found the opposing result with no attenuation of the cortical SEP to 60Hz tendon vibration, but clear attenuation with 60Hz cutaneous stimulation (Hoshiyama and Kakigi, 2000). Nevertheless, in the spinal cord afferent input is attenuated with peripheral vibration demonstrated by a decrease in the tendon jerk reflex and the electrically stimulated H-reflex (De Gail et al., 1966; Delwaide, 1973) and a similar inhibition is seen in the cat (Gillies et al., 1969). This is thought to be driven by a top-down presynaptic inhibition of the 1a afferent volley. The introduction of an unexpected firing pattern in 1a afferents using peripheral vibration may therefore activate this top-down inhibition providing a neurophysiological pathway by which peripheral vibration could modulate sensory gating. It would be interesting to measure SEPs at different time points throughout prolonged vibration in order to quantify whether changes in cortical SEP amplitude match the pattern of modulation of sensorimotor beta power measured here to further elucidate the role of sensorimotor beta power in sensory gating. Indeed, this cortical adaptation to vibration may explain opposing results in the literature describing the effect of peripheral vibration on SEP amplitudes: previous studies have either only measured SEPs at a single time point during vibration or averaged over multiple SEPs given throughout the vibratory period, which would hide any temporal modulation of SEP amplitudes that may correlate with the changes in beta power seen here. However, the

need for multiple peripheral nerve stimuli to generate a reliable average SEP makes this difficult to conduct practically.

Moreover, the relationship between SEP attenuation and motor initiation again supports that this is likely to be the mechanism by which movements are improved following vibration and the mechanism by which changes in sensorimotor beta power could modulate movement. During normal gait initiation the H-reflex of the soleus is inhibited, however the magnitude of this inhibition reduces with symptom severity in PD (Hiraoka et al., 2005; Morita et al., 2000). In addition, attenuation of the primary and secondary components of the SEP is reduced in PD and improves with dopaminergic medication (Macerollo et al., 2016). This supports the idea that the attenuation of somatosensory input is closely involved in motor control. The basal ganglia is placed in a prime location to integrate motor commands and afferent input and therefore could control this top-down gating mechanism. Indeed, electrophysiological evidence from primates suggests that proprioceptive information is represented within the basal ganglia and that the synchrony of neural activity in this brain region may modulate this gain control (Klockgether et al., 1995). Due to these findings vibration has been employed as a therapeutic intervention for PD, but the results have been inconsistent (Arias et al., 2009; Chouza et al., 2011; Ebersbach et al., 2008; Haas et al., 2006; Kapur et al., 2012; King et al., 2009). A better mechanistic understanding of how peripheral vibration could modulate movement could help refine and extend these studies to improve the clinical potential of peripheral vibration for symptom management in PD.

In summary, this study showed that high frequency peripheral vibration increased movement speed on a motor control task and decreased sensorimotor beta power. With the assumption that this stimulus reduced somatosensory precision, these findings support the prediction from the active inference framework that a reduction in the estimate of somatosensory precision is necessary for movement initiation. The temporal modulation of beta power at the onset and offset of movement suggests that beta oscillations may play a role in the adaptation of the motor system to an unexpected proprioceptive stimulus. This supports the hypothesis that sensorimotor beta power may represent estimates of somatosensory precision. This neuroimaging result sheds some light on the mechanism underlying the behavioural improvement seen following 80Hz peripheral vibration. One hypothesis is that the decrease in beta power at the offset of movement attenuates the afferent input to the cortex, therefore placing the sensorimotor cortex in a more “ready-to-move” state; this may then increase the participant’s ability to subsequently initiate a movement. However, more work is needed to elucidate the relationship between beta power modulation and changes in sensory uncertainty.

Moreover, in this study there was no direct measure of the effect of high frequency vibration on proprioceptive uncertainty, therefore this will be addressed in the following chapter.

CHAPTER 5

Study Three: Investigating the effect of a peripheral vibrating stimulus on proprioceptive accuracy

5.1. INTRODUCTION

In the previous chapter I showed that sensorimotor beta power was reduced at the onset and offset of 80Hz peripheral vibration. Participants were also quicker to complete a dextrous motor task following 80Hz peripheral vibration compared to baseline or 20Hz vibration. I hypothesise that the changes in sensorimotor beta power with vibration likely underlie this behavioural change. I argue that the increased movement speed following vibration was due to changes in estimates of somatosensory precision. This is in line with the active inference framework, which states that in order to move we must reduce our estimate of sensory precision to allow proprioceptive predictions to incite movement (Brown et al., 2013). Therefore, I argue that peripheral vibration specifically at 80Hz reduces somatosensory precision by making the proprioceptive input to the cortex more uncertain. However, in the previous study there was no direct measure of proprioceptive uncertainty to support this mechanism. In the current study I aimed to quantify proprioceptive accuracy in order to determine the effect of peripheral vibration of different frequencies on proprioceptive uncertainty.

In the current study participants were asked to direct a robot arm to specific targets on a horizontal plane with no visual feedback after 80Hz, 40Hz or no peripheral vibration. I hypothesised that participants would be less accurate at this task following 80Hz vibration due to the increase in proprioceptive uncertainty. This accuracy was measured in two ways: 1) by the overall error magnitude from the target to each end point; and, 2) by the variability in end point errors. In order to probe how specific these effects might be to 80Hz vibration and provide an active vibration control, I included trials with 40Hz vibration. In this condition 1a afferents, responsible for transmitting proprioceptive information to the brain, should be activated to a lesser extent than 80Hz vibration; I therefore expected to find a reduced behavioural effect following 40Hz vibration. There have been a number of studies that have shown a decrease in proprioceptive accuracy following high frequency vibration supporting the hypotheses put forward here (Cordo et al., 1995, 2005; Inglis and Frank, 1990; Tsay et al., 2016).

In this task, unlike the previous studies, I also asked participants to rate how confident they were in the accuracy of their end position after each trial. These ratings determined how aware participants were of their proprioceptive state and of the accuracy of their reaching movements. The reason for including this measure was to determine if conscious estimates of the proprioceptive state are dissociable from the true proprioceptive state. For Bayesian inference we compute an estimate of the distribution of our prior state and the likelihood of our current state. If our estimates are accurate they will readily reflect the true nature of the behavioural or neural data from which they were made; however, if our estimates are inaccurate there may be a dissociation between the true and estimated states. In order to measure this dissociation experimentally we could assume that the true state is reflected in our behavioural or neural data, but our estimated state is reflected in our conscious awareness or belief about this data. It is unknown whether our cortical estimates of sensory precision accurately reflect our actually sensory state i.e. if the actual afferent input is made more uncertain, does our estimate of that state readily reflect this? This creates interesting hypotheses for the role of sensorimotor beta oscillations. Modulations in sensorimotor beta power with vibration appear to reflect a central adaptation process; therefore, this activity may more readily reflect estimates of sensory precision, which can be determined through confidence judgements, rather than true changes to the precision of the afferent input in the periphery. In the current study I aimed to determine if I could accurately record these two estimates of sensory precision and determine the relationship between these facets in healthy participants. Future work will aim to continue this into PD patients where the exact role of sensorimotor beta power has important implications; the application of this idea to PD will be discussed in the general discussion.

5.2. METHODS

5.2.1. Participants

19 healthy participants completed the study (15 female; mean age: 23; range: 20-40). All participants were right-handed and naïve to the purpose of the task. Written, informed consent was obtained from all participants. 2 participants were excluded from all analyses. 1 participant had a large proportion of missing data due to a technical problem and 1 participant had a large proportion of bad trials (19.8% bad; the mean percentage of bad trials for all other participants was 0.1%). Bad trials were defined in two ways: 1) if the end point error magnitude from the target was greater than 3 standard deviations away from the mean end point error (collapsed across conditions); or, 2) if the position of

the end point on the Z axis was more than 1cm away from the virtual horizontal plane on which participants were instructed to move. All subsequent analyses were carried out with 17 participants.

5.2.2. Experimental setup

Participants were seated at a table with a Phantom Haptik robot directly in front of them (Figure 5.1A). The robot had a mechanical arm that could move freely in all directions within a 3D space. Participants held a spherical attachment fixed to the end of the robot arm and used their thumb and index finger to manoeuvre the robot arm. A horizontal mirror was fixed above the robot at a ~45^{o} angle to the table and reflected the contents of a computer screen hung directly above the mirror in parallel. The computer task was then reflected onto a virtual plane directly above the robot and horizontal to the table. In this way participants could move the robot to positions in space that directly corresponded to the position of targets on this virtual plane without being able to see their hand or the robot. A foam headrest and arm rest were used to ensure all participants were sat in the same position with the same view of the virtual plane. A vibration device (Vibrasens VB115, Technoconcept) was attached to the right wrist of the participant throughout the experiment.

5.2.3. Experimental Design

Participants completed a computer task coded in MATLAB (version 2013b). Before each trial, 5s of vibration or rest was given dependent on the experimental condition of the block. Participants completed 4 blocks of 32 trials. The first block was a training block in which participants had visual feedback of the position of the robot throughout the task and received no vibration. Data from this block was not analysed. For the 3 experimental blocks no visual feedback of the robot was given during the task except for when finding the start position at the beginning of each trial. The vibration conditions of the 3 experimental blocks were: 1) no vibration; 2) 40Hz vibration; 3) 80Hz vibration. The presentation order of the 3 experimental blocks was counter balanced across participants. Short rest breaks were given halfway through each block and between blocks.

5.2.4. Task Design

The task was coded in MATLAB (version 2013b) using Cogent and Haptik Lib toolboxes. At the start of each trial a fixation cross was presented in the centre of the screen for 5 seconds whilst participants either received peripheral vibration or rested. A home

position (blue square) then appeared at the bottom of the screen and participants were instructed to move the robot arm so that they were directly beneath the home square. A cursor representing the end of the robot arm was used to guide participants into the start position, however this only appeared when participants moved to within a 2.5cm radius circle of the home position to avoid giving participants additional feedback about where they were at the end of the previous trial. After 1 second of being positioned in the home square a target (red square) appeared at one of four possible locations. All targets were positioned 4cm from the central home position and arranged on an arc at the following angles: -150^{o}, -110^{o}, 110^{o} and 150^{o}. Participants were instructed to move the robot arm so that the spherical attachment at the end of the arm was directly beneath the target. There was no visual feedback of the position of the robot. Once the participant had positioned the robot they verbalised this to the experimenter who recorded the final position using the MATLAB script. The participants were then asked to report how confident they were that they had placed the robot arm directly beneath the target location on a scale of 0-100 (Figure 5.1B).

Throughout the experiment a virtual plane was created by generating a force output from the robot at a specific point in the Z axis. Participants were instructed to move the robot arm up to this plane and move along it. This created the illusion that any target on the screen was resting on this plane to make it easier to match the target location and remove any participant error in the Z axis. Participants would only be recorded as being in the correct start position if they held the robot arm in the correct location on this virtual plane. Any trials in which the Z coordinate of the final position recorded was greater than 1cm away from this plane were discounted as bad trials.

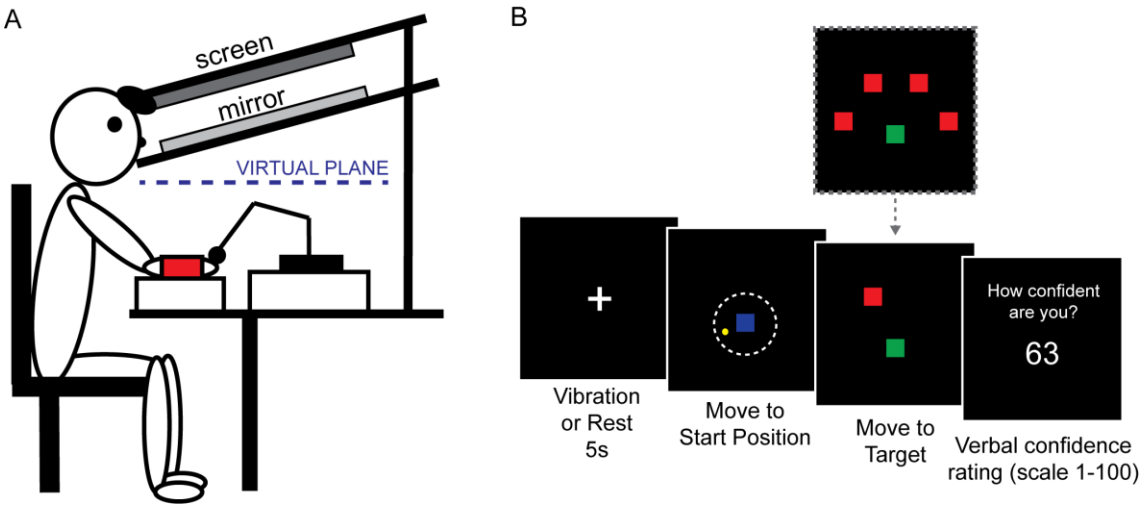

Figure 5.1. Experimental set up and task design. *A) Participants were seated at a table and held the robot arm in their right hand. The vibrating device was attached to the wrist and their arm was rested on a support. A computer screen was placed parallel to a mirror which reflected the contents of the computer screen onto the dotted line marked virtual plane. Participants looked at this through the mirror as shown. The robot produced a downward force at this height to create a horizontal plane for the participants to move along so that proprioceptive errors could only occur in 2 dimensions. B) Schematic of the visual stimuli seen by participants throughout the task.*

5.2.5. Data analysis

5.2.5.1. Vibration and Proprioceptive Error Analysis

For each trial I recorded: 1) the end-point coordinate of the position of the robot arm when the participant reported they were directly matched with the target location; 2) the confidence rating of the participant; and 3) the participant's movement trajectory and velocity from the start position. The first analysis aimed to determine if vibration had any effect on the end point of participant's movements. Firstly, end point errors were calculated by determining the Euclidean distance between the target location and each end point. The median of these values was compared across condition and target. I also calculated error values separately along the X and Y axes in Cartesian space relative to the targets in order to determine if there were any consistent shifts in these errors in a particular direction. Secondly, the variability in the distribution of end-point coordinates was analysed. A custom written MATLAB function (by Marco Davare) generated a confidence variability ellipse around the distribution of end-point coordinates for each target for each condition. From this I extracted the surface area of the ellipse at 95% confidence limits as a measure of the variability of the distribution of end-points. Error differences were positive for an overshoot (movement outside the arc that the targets were located on) and negative for an undershoot (movement towards the central start position). All dependent variables were analysed using a 3x4 (vibration: no vibration, 40Hz vibration, 80Hz vibration; x target: targets 1-4) repeated measures ANOVA.

5.2.5.2. Confidence, Proprioceptive Error and Vibration Analyses

The mean confidence rating for each target for each condition for each participant was also analysed in a 3x4 (vibration x target) repeated measures ANOVA. I then aimed to confirm whether confidence ratings were related to proprioceptive error in a more specific analysis. I calculated error values using four different methods then measured the relationship between confidence and error. The four types of error were as follows: 1) Actual Error (the Euclidean distance between the end point and the actual target location); 2) Precision-weighted Actual Error (the Euclidean distance between the end point and the actual target normalised by the standard deviation of the distribution of end points; 3) Perceived Error (the Euclidean distance between the end point and the median of the distribution of end points); 4) Precision-weighted Perceived Error (the Euclidean distance between the end point and the median of the distribution of end points normalised by the standard deviation of the distribution). All errors were ranked across trials and grouped into 4 bins from high to low end-point error separately for each condition, but collapsed across targets. Confidence ratings were mean corrected across all trials to account for any between subject differences in how participants used the scale. Corresponding confidence ratings in each bin were averaged. I conducted four 3x4 (vibration x bin) repeated measures ANOVAs for mean confidence binned according to each error calculation method to determine if there was any consistent modulation of confidence with error across participants.

5.2.5.3. Analysis of Distribution of End Points

The Euclidean distance from the target location to each end point was calculated separately for end points around each target. A 30x30mm grid with 5mm bins was created and centred upon the true target location. I calculated the number of end points that fell within each bin in the grid to create a 2D representation of the spread of end points from each target. I then converted this number to a percentage of the total number of end points that fell within the grid and averaged each grid across participants for each target. To determine if there was a significant difference in the width of these distributions in the X and Y axes I conducted a paired sample t-test on the standard deviation of the X values of all the end points and the Y values of all the end points across participants. To plot the probability density functions (PDFs) I fitted a probability distribution to the X and Y values for each end point (separately for each target) using the MATLAB function 'fitdist'. I then normalised this by dividing the PDF by the maximum value of the PDF.

5.2.5.4. Vibration and Movement Parameters Analysis

In order to determine if there were any other effects of vibration on participants' movements in the task I calculated three movement parameters: initial velocity, reaction time (RT) and average velocity. Velocity was calculated by dividing the change in the robot position at each sample point by the change in time between samples. This was then convolved with a Gaussian kernel with a FWHM of 80ms. A circular boundary of 2cm diameter was generated around the start position. RT was recorded as the time in which a participant crossed this boundary with the robot arm and initial velocity was recorded as the velocity at this point. Average velocity was calculated as the total path length from the point of crossing this boundary to the end point divided by the total movement time minus the RT. These parameters were then analysed using a 3x4 (vibration x target) repeated measures ANOVA.

5.3. RESULTS

5.3.1. Vibration increases proprioceptive error by causing participants to overshoot the target

In this experiment I hypothesised that high frequency peripheral vibration would increase participants' uncertainty in their proprioceptive state resulting in either increased error or increased variability in movement end points. Firstly, I calculated error magnitude as the Euclidean distance between the target and the end point on each trial and found the median error value for each condition and target location. A vibration (no vibration, 40Hz vibration, 80Hz vibration) by target (1 to 4) repeated measures ANOVA demonstrated a significant main effect of vibration, $F(2,32)=4.17$, $p=0.025$, $\eta_p^2=0.21$ (Figure 5.2A). Although none of the pairwise comparisons were significant when corrected for multiple comparisons, there was a trend towards a significant difference between the no vibration condition (M±SD=20.14±6.11mm) and the 80Hz vibration condition (M±SD=24.22±9.00mm; $p=0.083$). There was no significant main effect of target ($p=0.483$; Figure 5.2B) and no significant interaction between target and vibration ($p=0.627$).

High frequency vibration significantly increased error magnitude from the target to each end point, however this analysis does not dissociate if the errors produced were in a consistent direction. I therefore calculated the distance between the target and each end point separately along the X and Y axes. There was a significant main effect of vibration for the median end point error calculated along the Y axis, $F(2,32)=5.65$, $p=0.008$, $\eta_p^2=0.26$ (Figure 5.2C). This was driven by a significantly greater error for the 80Hz vibration

condition (M±SD=19.87±9.80mm) compared to the no vibration condition (M±SD=14.17±7.67mm; p=0.024 Bonferroni corrected). There was a trend towards a significant difference between the 40Hz vibration condition (M±SD=18.87±9.34mm) and the no vibration condition (p=0.082), however there was no significant difference between the 40Hz vibration condition and the 80Hz vibration condition (p>0.9). The positive mean values mean that participants were on average overshooting the targets along the Y axis. There was no significant main effect of target (p=0.186; Figure 5.2D) and no significant interaction (p=0.381). For the median end point error along the X axis, there were no significant main effects of vibration (p=0.641; Figure 5.2E) or target (p=0.234) and there was a trend towards a significant interaction between vibration and target (p=0.092). From these results I conclude that vibration caused participants to significantly overshoot the targets compared to no vibration.

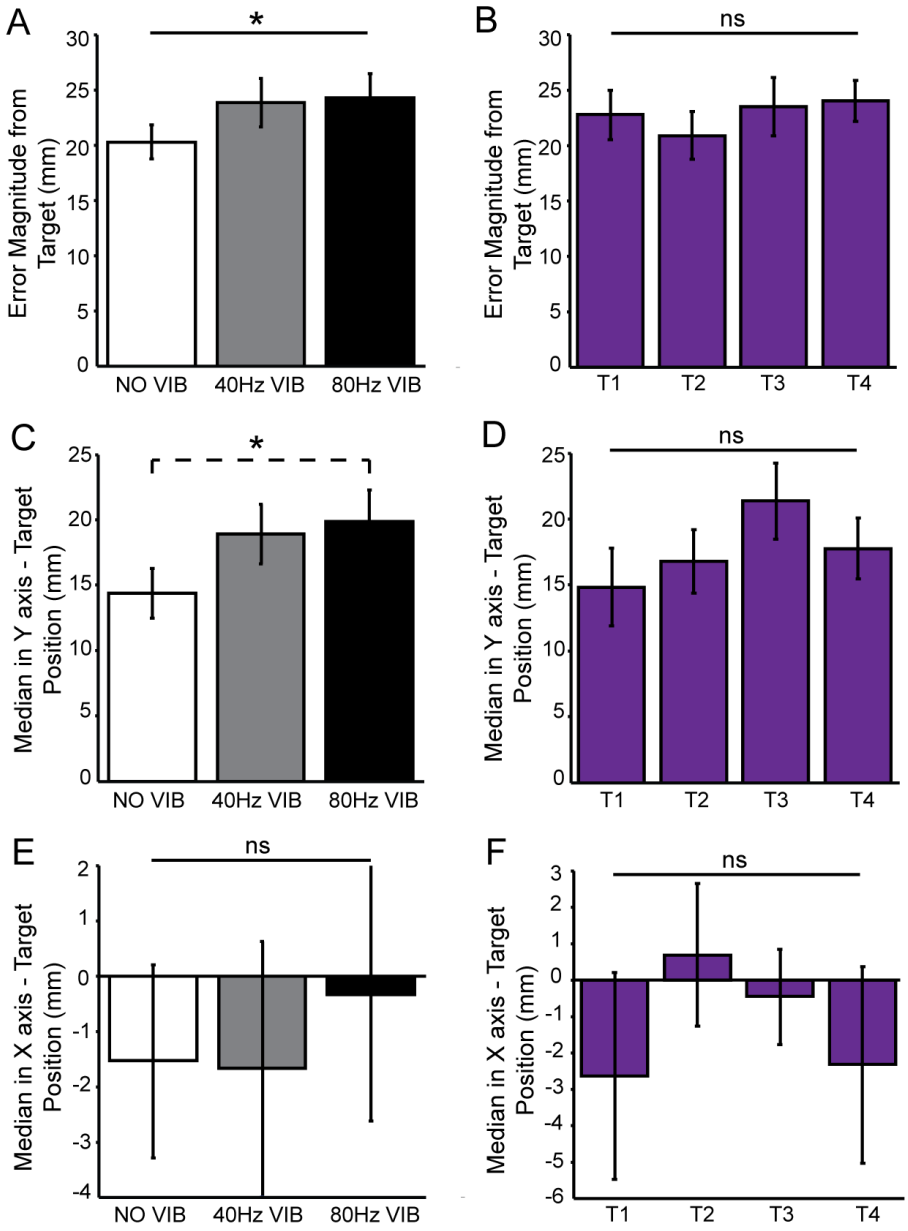

Figure 5.2. 80Hz peripheral vibration increased overshooting along the Y axis. *To measure the effect of vibration and target location on proprioceptive error a repeated measures ANOVA with factors vibration and target was used. The bar graphs in the left column (A,C,E) represent the main effect of vibration (80Hz vibration (black bar), 40Hz vibration (grey bar) and no vibration (white bar)) on a number of different error measurements. The bar graphs in the right column (B,D,F) represent the main effect of target on a number of different error measurements. Solid lines represent main effects. Dotted lines represent significant pairwise comparisons. The different measures of error analysed were: A+B) median error magnitude (Euclidean distance) calculated from the target to each end point; C+D) median error from the target to each end point along the Y axis; and, E+F) median error from the target to each end point along the X axis. There was a significant main effect of vibration on the error magnitude (A; p=0.025) and errors along the Y axis (C; p=0.008). This latter effect was driven by a larger overshoot of the target along the Y axis following 80Hz vibration compared to no vibration (p=0.024, corrected). There were no significant main effects of target (p>0.05).*

Secondly, I hypothesised that high frequency vibration would lead to an increased variability in the distribution of end points. To measure this, I conducted a variability analysis in which I produced a confidence variability ellipse around the distribution of end-point coordinates for each condition and target. Here the surface area of the ellipse at 95% confidence limits provided a measure of the spread of the end-point coordinates (see Figure 5.3A for example participant). A vibration (no vibration, 40Hz vibration, 80Hz vibration) by target (1 to 4) repeated measures ANOVA demonstrated no significant main effect of vibration ($p=0.864$; Figure 5.3B) and no significant interaction between vibration and target ($p=0.999$). There was a significant main effect of target ($F(3,48)=4.16$, $p=0.011$, $\eta_p^2=0.21$). This was driven by a significant difference between target 1 and target 3 ($p=0.038$, Bonferroni corrected) where target 1 ($M\pm SD=869\pm527mm^2$) had more variability than target 3 ($M\pm SD=531\pm296mm^2$). Qualitatively, the two outer targets (1 and 4) appeared to have greater variability than the inner targets (2 and 3) (Figure 5.3C); however, this was not modulated by vibration.

Overall, peripheral vibration did not modulate error variability, however across vibration conditions end point errors were more variable for the outer targets compared to the inner targets. In addition, on average, high frequency vibration caused participants to overshoot the targets particularly in the Y direction.

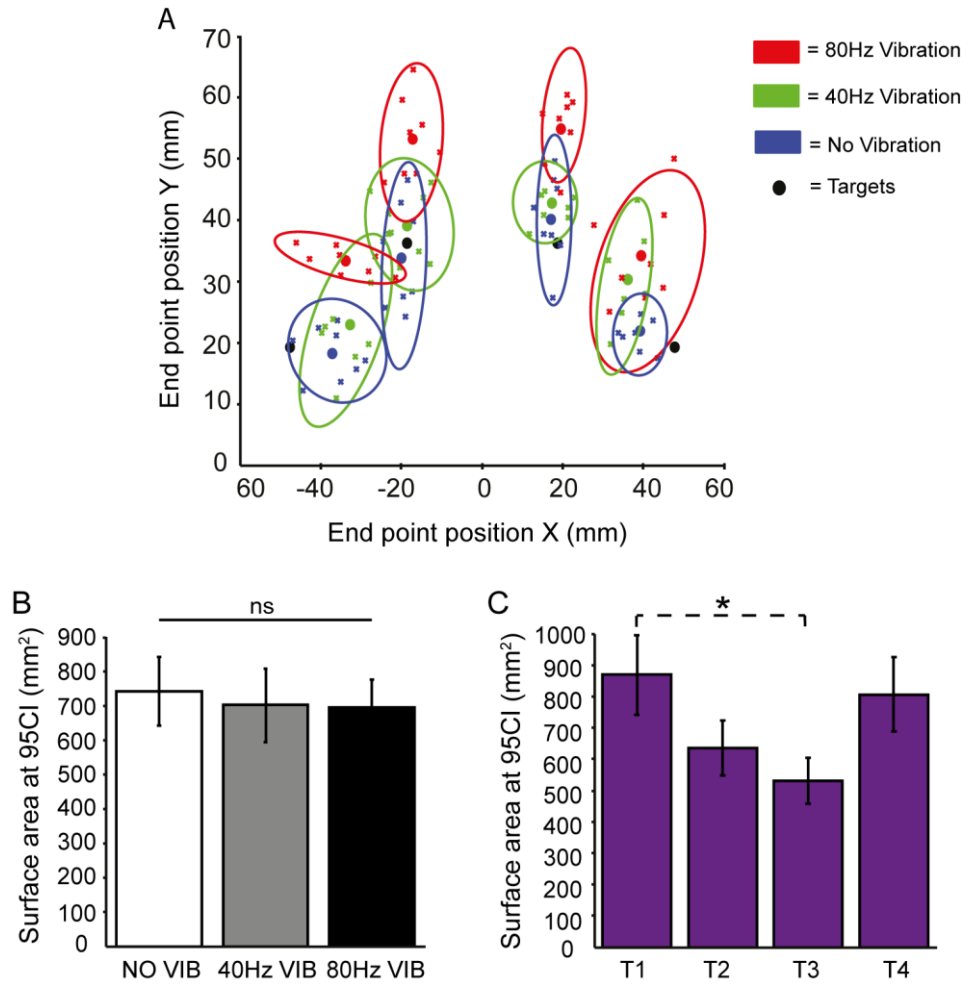

Figure 5.3. Effect of vibration and target on error variability. *A) End points across trials for example participant. Black circles represent the targets numbered from 1-4 from left to right. Crosses show the end points for each trial colour coded by condition (red = 80Hz vibration; green = 40Hz vibration; blue = no vibration). Error variability analysis which produces ellipses around each distribution of end points at the 95% confidence limits. B) Bar graph showing no significant main effect of vibration on the mean surface area of the ellipses (at 95% CI) across participants (p>0.05). C) Bar graph showing the significant main effect of target on the mean surface area of the ellipses (at 95% CI) across participants (p=0.011). This was driven by a significant difference between target 1 and target 3 after Bonferroni correction for multiple comparisons (p=0.038).*

5.3.2. Confidence ratings are modulated by precision-weighted proprioceptive errors

Participants were asked to report their confidence in how accurately they had placed the robot under the target on each trial. I hypothesised that any increases in proprioceptive end-point error with vibration would be associated with a decrease in confidence. Here I conducted a vibration by target repeated measures ANOVA on participant's mean confidence ratings. Despite the increased error seen with 80Hz vibration, there was no significant main effect of vibration (p=0.186; Figure 5.4A) and no significant interaction between vibration and target (p=0.235). There was a significant main effect of target,

F(3,48)=3.61, p=0.02, η_p^2=0.18 (Figure 5.4B), however none of the pairwise comparisons were significant following correction for multiple comparisons. There was however a trend towards a significant difference between targets 1 and 3 (p=0.074) where participants were on average more confident for target 3 (M±SD: 63.08±12.98) compared to target 1 (M±SD: 58.04±14.50. This may reflect the changes in error variability seen between targets. There were also no significant effects of vibration or target on the variability of participant's confidence ratings as measured using the standard deviation of confidence across trials for each condition (vibration main effect: p=0.797; target main effect: p=0.147; vibration-x-target interaction: p=0.439; Figure 5.4C+D). Therefore, despite 80Hz vibration causing participants to overshoot the targets, participants did not modulate their confidence ratings accordingly.

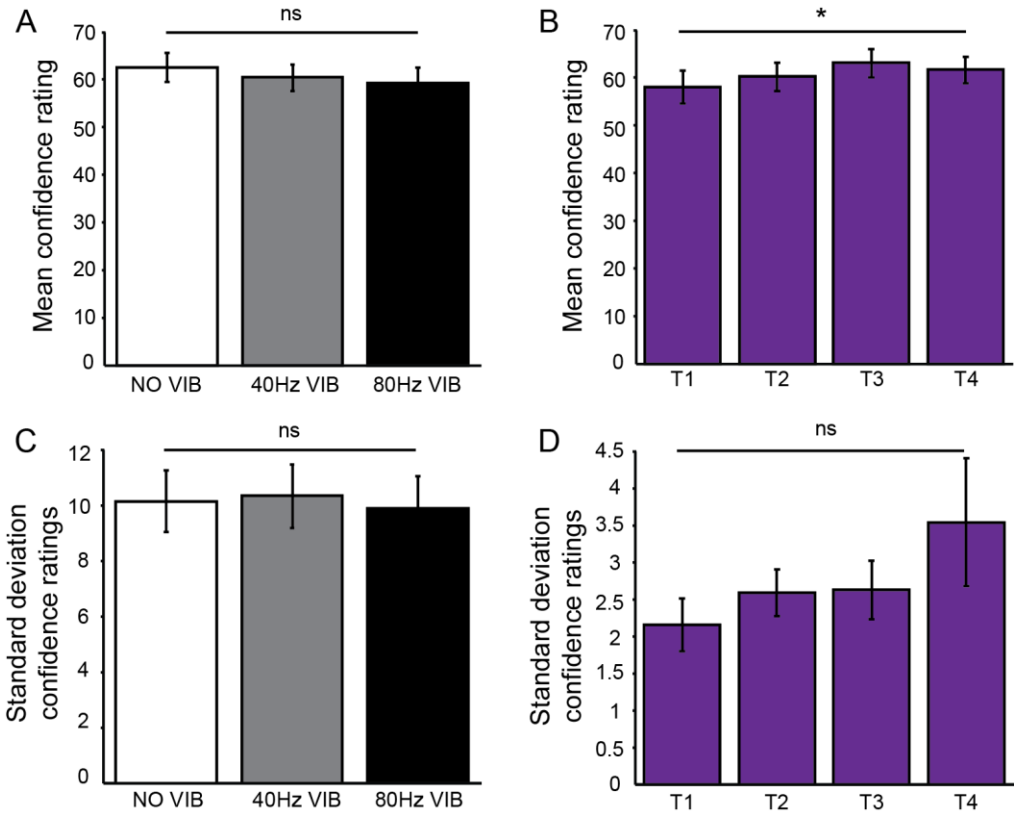

Figure 5.4. High frequency peripheral vibration did not modulate mean confidence ratings. *To measure the effect of vibration and target location on confidence a repeated measures ANOVA with factors vibration and target was used. The bar graphs in the left column (A+C) represent the main effect of vibration (80Hz vibration (black bar), 40Hz vibration (grey bar) and no vibration (white bar)) on the mean confidence ratings (A) and the standard deviation of confidence ratings (C). The bar graphs in the right column (B+D) represent the main effect of target on the mean confidence ratings (B) and the standard deviation of confidence ratings (D). Solid lines represent main effects. There were no significant main effects of vibration on the mean or standard deviation of confidence ratings (p>0.05). There was only a significant main effect of target for the mean confidence ratings (p=0.02); however, there were no significant pairwise comparisons after correction for multiple comparisons.*

The above result is surprising as it suggests that participants did not readily modulate their confidence ratings with changes in error. However, the change in error between the no vibration and 80Hz vibration condition was small in magnitude; therefore it may be that a larger error was required before participants modulated their confidence accordingly. I therefore carried out a series of subsequent analyses to determine if there was a relationship between confidence ratings and proprioceptive error across all trials. Proprioceptive error in this task can be calculated in a number of ways. By comparing the relationship between error and confidence calculated under different models of error, I could determine what information was being used to generate confidence ratings. Previous work suggests that confidence ratings reflect the perceived probability of being correct on a given task (Kepecs and Mainen, 2012; Meyniel et al., 2015; Navajas et al., 2017; Pouget et al., 2016). Confidence ratings in this task may therefore more readily correlate with error values calculated from the median of the participant's distribution of end points (where they think the target is; 'Perceived Error') compared to error values calculated from actual target location ('Actual Error'). In addition, other work has suggested that confidence judgements can reflect the precision of the sensory evidence presented during perceptual decision-making tasks (Aitchison et al., 2015; Friston and Kiebel, 2009; Meyniel et al., 2015; Navajas et al., 2017). Indeed, in this task there was a significant difference in the mean width of the distribution of end points around targets 2 and 3 for the X axis compared to the Y axis and a trend towards significance for targets 1 and 4 (paired sample t-tests at the group level - target 1: $p=0.09$; target 2: $p<0.001$; target 3: $p<0.001$; target 4: $p=0.057$; Figure 5.5). This suggests that end point errors were more varied along the Y axis compared to the X axis and therefore confidence judgements may be modulated in accordance with the inverse of these variances: the precision.

I tested the relationship between confidence ratings and four different models of error: 1) Actual Error (Euclidian distance from target location to end points); 2) Precision-weighted Actual Error (median Euclidian distance from target location to end points normalised by the standard deviation of the of the distribution of end points; 3) Perceived Error (distance from the centre (median) of the distribution of end points); 4) Precision-weighted Perceived Error (distance from the median of the distribution of end points normalised by the standard deviation of the distribution). For each model I divided the error values into 4 bins from smallest to largest and averaged the confidence ratings for all the trials within each bin separately for each condition. I then conducted a repeated measures ANOVA with vibration and bin number as factors. I hypothesised that if confidence ratings were dependent on proprioceptive error then there would be a significant modulation of confidence with bin number. The effect size of this relationship

would then determine which method of error calculation explained the most variance in the modulation of confidence ratings.

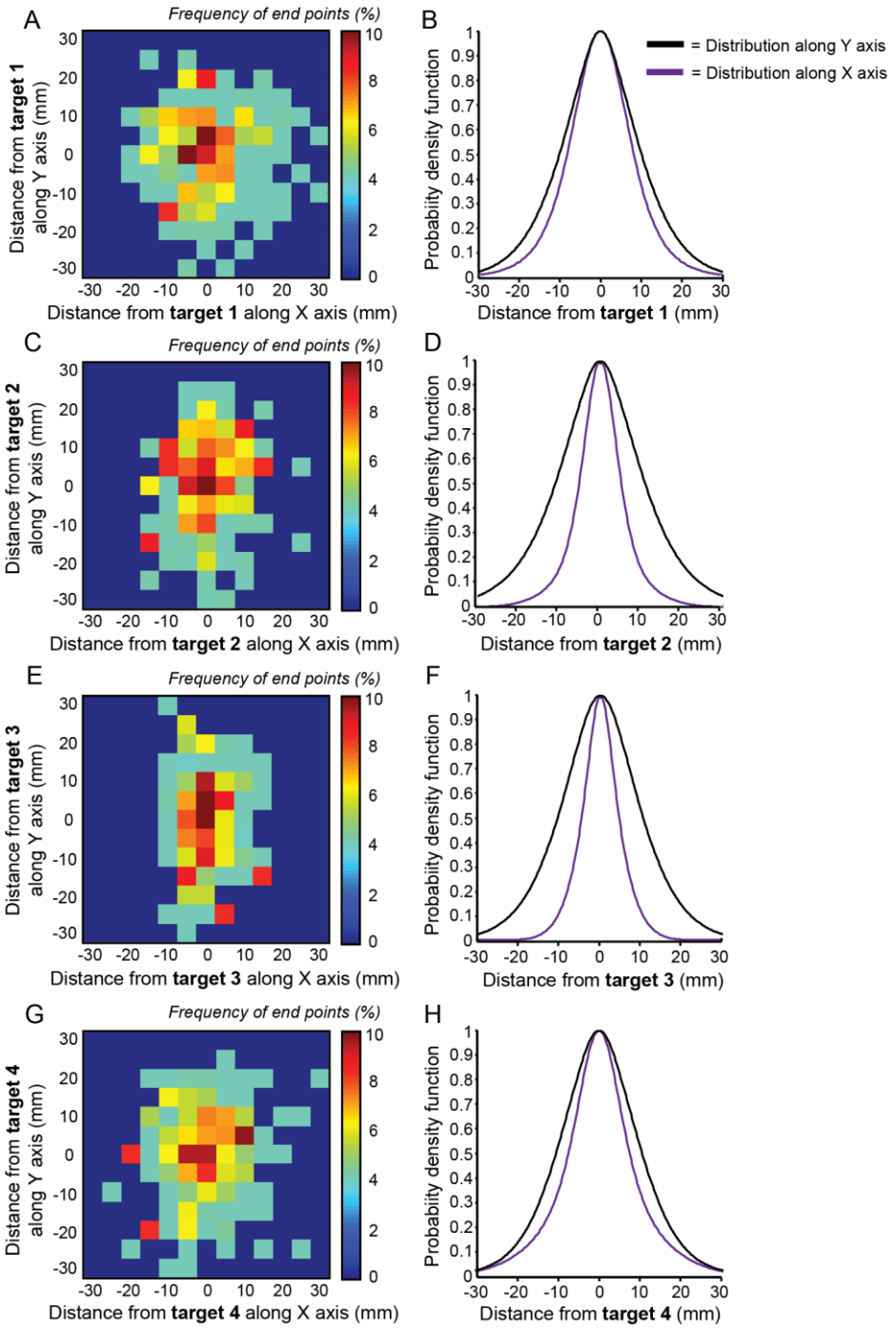

Figure 5.5. Distribution of end points across participants has a greater precision in the X axis compared to the Y axis. *A,C,E,G) Heat maps show the frequency of end points (percentage of total number of end points) that occurred within 5mm bins arranged in a 30x30mm grid representing the distance in mm from the actual target location for target 1 (A), target 2 (C), target 3 (E) and target 4 (G). The centre of the grid (0,0) represents the true location of the target. B,D,F,H) Probability density functions of the distribution of end points along the Y axis of the 30x30mm grid (black line) and the X axis (purple line) for target 1 (B), target 2 (D), target 3 (F) and target 4 (H). There was a significant difference between the width of the X and Y axis distributions for targets 2 and 3 ($p<0.001$) and a trend towards significance for target 1 ($p=0.09$) and target 4 ($p=0.057$).*

For the first analysis confidence ratings were binned based on actual error. I averaged the confidence ratings for all the trials in each bin and conducted a 3x4 (vibration by bin) repeated measures ANOVA. I hypothesised that if confidence ratings were dependent on proprioceptive error then there would be a significant modulation of confidence with bin number. There was no significant main effect of vibration ($p=0.182$), no significant main effect of bin number ($p=0.763$; Figure 5.6A) and no significant interaction ($p=0.260$). This suggests that confidence was not modulated by absolute error magnitude from the target. However, it may be the case that more variance in the modulation of confidence ratings would be explained if these judgements were binned based on the Precision-weighted Actual Error. For this second model, there was no significant main effect of bin ($p=0.148$; Figure 5.6B), however, the p-value was closer to reaching significance compared to the statistical test using non-normalised error values and the effect size was larger. There was also no significant main effect of vibration ($p=0.190$) and no significant interaction ($p=0.164$).

Models 1 (Actual Error) and 2 (Precision-weighted Actual Error) assume that a participant's own representation of where they think the target is, is the same as its true location. As hypothesised above, changes in confidence may be more readily based on differences in error from a prior location of where the participant thinks the target is rather than the error distance from the actual target. For the third analysis I binned confidence judgements based on participant's Perceived Error. A 3x4 repeated measures ANOVA showed that there was a significant main effect of bin number, $F(3,48)=3.95$, $p=0.013$, $\eta_p^2=0.20$ (Figure 5.6C). This was driven by a significantly lower confidence in bin 4 compared to bin 3 (mean difference in confidence: 3.07; $p=0.037$, corrected). This suggests that on average confidence ratings were significantly lower when error was greater. The interaction between vibration and bin trended towards significance ($p=0.056$). There was no significant main effect of vibration ($p=0.190$). It is clear that modulations in confidence were more readily modulated by Perceived Error rather than Actual Error.

As before, I hypothesised that the precision of the distribution of end points may also be important in determining subjective confidence ratings. For the fourth analysis, I binned confidence ratings based on Precision-weighted Perceived Error. There was a significant main effect of bin number, $F(3,48)=5.49$, $p=0.003$, $\eta_p^2=0.26$ (Figure 5.6D). This again was driven by a significantly lower mean confidence rating for bin 4 (largest error) compared to bin 3 (mean difference: 3.41; $p=0.005$, corrected). There was also a significant interaction between vibration and bin number, $F(6,96)=2.53$, $p=0.026$, $\eta_p^2=0.14$. For the no vibration condition there were no significant pairwise differences between bins;

however, following 40Hz vibration, mean confidence ratings were significantly reduced in bin 4 compared to bin 1 (mean difference: 4.53; p=0.017, corrected) and bin 3 (mean difference: 3.99; p=0.007, corrected); and following 80Hz vibration, mean confidence ratings were significantly reduced in bin 4 compared to bin 3 (mean difference: 4.27; p=0.021, corrected). There was no significant main effect of vibration (p=0.193).

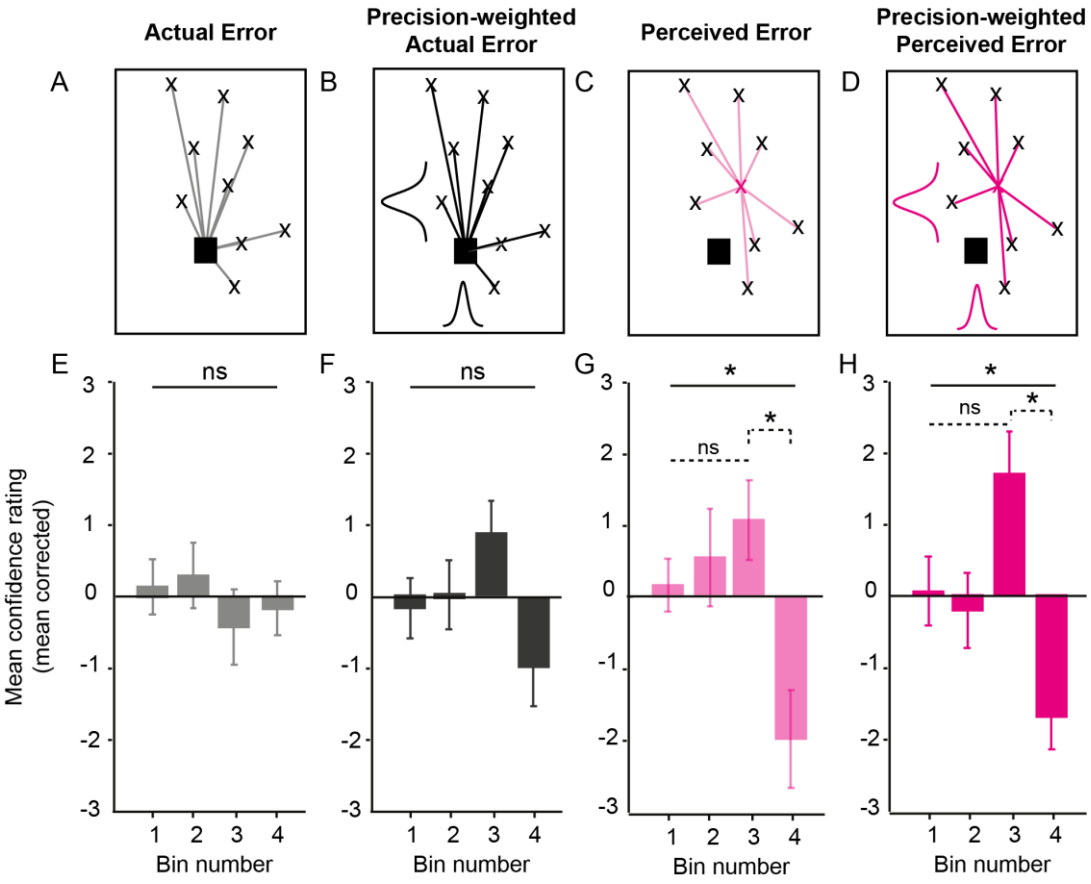

Figure 5.6. Mean confidence was most readily modulated by errors relative to the median and precision of the distribution of end points. *A-D) The four different models used to calculate proprioceptive error to compare with mean confidence ratings: A) Actual Error (error magnitude from each target); B) Precision-weighted Actual Error (error magnitude from each target weighted by the standard deviation of the distribution); C) Perceived Error (error magnitude from the median of the distribution of end points); D) Precision-weighted Perceived Error (error magnitude from the median of the distribution of end points weighted by the standard deviation of the distribution). E-H) Bar graphs show the modulation of mean confidence (mean corrected) binned relative to absolute errors calculated according to the corresponding model shown. Solid lines represent the significance of the main effect of confidence and bin number. Dotted lines show the significance of post-hoc pairwise comparisons between bins corrected for multiple comparisons with the Bonferroni method. The effect sizes of the main effects represented in the graphs increased from left to right. The most variance in the modulation of confidence with error was explained when confidence was binned based on precision weighted errors calculated from the median of the distribution of end points (D).*

Table 5.1 shows the effect sizes of the results of the effect of bin number on mean confidence ratings for the four models tested. It is clear from this summary that, on average, the effect size for the modulation of confidence with bin number was greater when error values were calculated based on each participant's prior distribution of end points and these errors were weighted by the precision of that distribution. This suggests that confidence ratings in this task were more readily based on the size of precision-weighted proprioceptive errors relative to the participant's own distribution of end points rather than absolute errors.

	ERROR MODEL	EFFECT SIZE
1	***Actual Error*** *calculated from target locations*	0.024
2	***Precision-weighted Actual Error*** *calculated from target locations*	0.11
3	***Perceived Error*** *calculated from median end point*	**0.20***
4	***Precision-weighted Perceived Error*** *calculated from median end point*	**0.26***

Table 5.1. Effect sizes depicting the variance of the modulation in mean confidence ratings explained by bin number organised by different types of proprioceptive error. *Rows show the different models used to calculate the error values. Effect sizes are of the main effect of bin number from the 3x4 (vibration x bin number) ANOVA used to analyse mean confidence values. *=significant main effect of bin number on mean confidence.*

5.3.3. Vibration did not modulate any other movement parameters

Based on previous literature and our previous work I hypothesised that high frequency vibration would decrease movement time. However, this task was not optimal for testing this hypothesis as participants were not under any time pressure and end-point accuracy was the only factor stipulated in the instructions to participants. Nevertheless, for completeness I analysed initial and average movement velocity and RT to determine if these parameters were modulated by the vibration conditions. These parameters were averaged over vibration condition and target for each participant and analysed in a 3x4 (vibration x target) repeated measures ANOVA. For initial velocity, there was no significant main effect of vibration ($p=0.19$) and no significant interaction between vibration and target ($p=0.549$); however, there was a significant main effect of target ($F(3,48)=5.74$, $p=0.002$, $\eta_p^2=0.26$). Post-hoc pairwise comparisons showed that initial

velocity was greater for target 4 (M±SD: 75.65±49.64mm/s) compared to target 2 (M±SD: 65.98±46.66mm/s; p=0.006, Bonferroni corrected) and trended towards a significant difference with target 1 (M±SD: 66.71±42.90mm/s; p=0.071). Similar results were found for RT. There was no significant main effect of vibration (p=0.726) and no significant interaction between vibration and target (p=0.661); however, there was a significant main effect of target ($F(3,48)=5.30$, p=0.003, $\eta_p^2=0.25$). Post-hoc pairwise comparisons showed that RTs were significantly slower for target 1 (M±SD: 0.70±0.28s) compared to target 4 (M±SD: 0.63±0.21s; p=0.046; Bonferroni corrected). Unlike with RT and initial velocity, average velocity showed no significant effects (main effect of vibration: p=0.785; main effect of target: p=0.877; interaction effect: p=0.539). These results demonstrated that on average participants had slower initial movements and reacted more slowly towards targets presented on the left compared to targets presented on the right, but this was not reflected in the average velocity. There was no effect of vibration on any movement parameters.

5.4. DISCUSSION

The main hypothesis for this study was that peripheral vibration would increase the uncertainty in the proprioceptive state and this would lead to an increase in proprioceptive errors or error variability on a proprioceptive reaching task. I have shown that, across all conditions, participants overshot the targets in the Y axis and this occurred to a significantly greater extent following 80Hz peripheral vibration compared to the no vibration condition. There was no effect of vibration on error variability or on a number of movement parameters, such as RT, initial velocity and average velocity. Participants rated how confident they were that they had accurately placed the robot under the target following each trial. There was no significant modulation of confidence with vibration despite an increase in proprioceptive error. Confidence ratings were most readily modulated by perceived errors from the centre of each participant's distribution of where they thought the target was rather than the true location of the target. Moreover, the most variance in the modulation of confidence ratings was explained when confidence was binned based on errors weighted by the precision of the prior distribution of end points.

Across all conditions participants consistently overshot the targets in the Y direction, which is consistent with previous studies using a very similar matching task (Beers et al., 1999; van Beers et al., 1998). In these studies, participants were asked to match visual and proprioceptive targets by placing their left finger on the underside of the table beneath a target. In the visual condition they could see the target, but not their matching

hand; in the proprioceptive condition, the participant's right hand acted as a target on top of the table and participants were blindfolded. This research showed that when the visual target was available to guide movements the variance in the distribution of end points in the azimuth (~X axis) dimension was very small, but the variance in the radial plane (~Y axis) was larger. The authors suggest that this was due to the angle at which the person was viewing the target and the movement of the hand away from the body; we are less accurate when reaching to visual targets that are far away (Bays and Wolpert, 2007). In the current study, the distribution of end points for targets 2 and 3 was narrow along the X axis and wide along the Y axis, which reflects this result and suggests that participants were using a visually guided motor plan to guide the robot arm towards the targets. In addition, in the previous study, when participants were blindfolded and only able to use proprioceptive information, the opposite result was found. There was a greater variability of end points in the azimuth (~X axis) dimension due to the geometry and precision of the angles of our joints, but a much lower variability of end points in the radial (~Y-axis) dimension. In the current study, there was more variability along the X axis for targets 1 and 4 compared to targets 2 and 3, which was most likely due to the greater change in the angle of the wrist required to move to these targets.

According to this previous literature, we weight visual and proprioceptive information differently depending on the direction of movement. Therefore, when reaching along the Y axis in the current study, proprioceptive information would have been relatively more precise than the prior visuomotor plan and would have been weighted to a greater extent. This generates an interesting explanation for why high frequency peripheral vibration generated proprioceptive errors specifically along the Y axis. According to Bayesian inference, we weight our sensory estimates and prior beliefs differently depending on their uncertainty and this relative precision-weighting determines whether the posterior distribution more closely represents our sensory or prior estimates (Körding and Wolpert, 2004). One hypothesis is that the vibration increased the uncertainty in the proprioceptive feedback, therefore participants relied more on their prior visuomotor plan about where the target was to determine when to stop moving in the Y axis. This would cause them to overshoot the targets. However, in the current task the prior and likelihood estimates cannot be separated and I did not model the integration between visual and proprioceptive information, therefore it is difficult to confirm this hypothesis. It would be interesting to repeat this study by training participants to have a specific prior distribution of end points (using a similar method to Körding and Wolpert, (2004)) and then manipulate the uncertainty in the proprioceptive feedback. Bayesian modelling can then be used to determine how increasing proprioceptive uncertainty effects the posterior

distribution of end points. It is important to note that the previous studies described here measured the distribution of end points along the axis of movement relative to the participant; however, in this study I have measured the distributions relative to the targets in external space. It will therefore be useful to repeat these analyses using an egocentric frame of reference for a more precise exploration of how vibration affects end point accuracy.

It is also important to hypothesise how vibration induced proprioceptive errors from a neurophysiological perspective. I suggested in the previous chapter that estimates of sensory input are represented within beta oscillatory activity over sensorimotor cortex. Therefore, one hypothesis would be that vibration modulated sensorimotor beta power by activating 1a afferents unexpectedly, which then decreased the gain of proprioceptive information relative to visual information used to generate a motor plan. An alternative hypothesis would be that vibration modulated the perception of the initial start position of the hand due to the kinesthetic illusions caused by the activation of muscle spindles. Previous tasks have shown that tendon vibration causes the illusory percept that the muscle being vibrated is lengthening in the absence of any EMG activity; therefore, when the muscle extensor is vibrated for example, participants consistently undershoot targets in the extension direction; the opposite result is found when flexor muscles are vibrated (Capaday and Cooke, 1981; Cordo et al., 1995, 2005; Goodwin et al., 1972; McCloskey, 1973). Following vibration offset, after effects have been recorded such that participants perceived an illusory movement in the opposite direction to that perceived during vibration (Seizova-Cajic et al., 2007). In this task, vibration was applied to the inside of the wrist before each movement, therefore an illusory aftereffect would have created the perception of wrist flexion. If participants perceived the initial position of their hand to be in this orientation then they would overshoot the targets as recorded, which suggests that this illusion could underlie participant's behaviour. However, I did not record the presence or magnitude of any vibration-induced illusions in this study, therefore it is difficult to confirm whether an altered perception of this start position was the reason for the increased proprioceptive errors seen in this task. Moreover, participants had to orientate their hand to the start position using a cursor on the screen after vibration prior to each trial, which makes this hypothesis unlikely; however, this cursor only specified the location of the robot arm, therefore it is feasible that participants thought their wrist was more flexed than it was when in this start position.

It is difficult to determine from the current results whether there was a frequency specific effect of vibration. There was a trend towards a significant difference between 40Hz vibration and no vibration and there was no significant pairwise difference between the

40Hz and 80Hz vibration conditions. Therefore, no firm conclusions can be made about the effect of vibration frequency on proprioceptive errors. It is known that 80Hz vibration optimally stimulates 1a afferents (Roll et al., 1989), therefore it is likely that 40Hz vibration did activate muscle spindles, but to a lesser extent, which may explain the slight but reduced behavioural effect. Alternatively, the similarity between the behaviour in the 40Hz and 80Hz conditions may suggest that proprioceptive errors were driven by the transmission of unexpected cutaneous rather than muscle reafferance to the cortex. Indeed, it has been argued that slowly adapting mechanoreceptors in the skin may play a role in proprioception. Interestingly, in the rubber hand illusion synchronous tactile stimulation of a rubber hand and the real hidden hand causes the perception that the rubber hand belongs to the participant, such that the participant reports a perceived shift in their real hand towards the position of the rubber hand (Botvinick and Cohen, 1998; Kammers et al., 2009; Tsakiris and Haggard, 2005). This proprioceptive drift supports the hypothesis that position sense is generated by an integration of exteroceptive, somatosensory and proprioceptive inputs. Indeed, in the current task participants moved the robot arm along a virtual plane, therefore could also have been using somatosensory information from the force feedback of the robot along this plane to determine when to stop moving. Based on the distribution of end points and the previous literature, it appears that in this task participants were integrating visual information with either proprioceptive and/or somatosensory information to determine the final end position, therefore a disruption in either of these two latter domains could have potentially generated the behavioural errors seen.

In addition to proprioceptive error, confidence ratings were recorded on each trial to provide a measure of how accurately participants thought they had placed the robot under the target. This determined how aware participants were of their proprioceptive state. As this study was conducted with young, healthy individuals, I hypothesised that participants would have a high awareness of their proprioceptive state and thus any increase in errors that occurred as a result of the high frequency peripheral vibration would be associated with a decrease in confidence ratings. However, there was no significant main effect of vibration on mean confidence scores. There are a number of reasons why this may be the case. Firstly, the overshooting error caused by the 80Hz vibration was very small (~5mm on average), therefore one hypothesis is that this error was not large enough for participants to consciously notice. Interestingly, this error was within the mean standard deviation of all errors in the Y axis across participants, therefore although vibration caused a consistent overshoot, this was within the normal distribution of movements. This supports the hypothesis that confidence ratings were more readily based on

perceived error from their own distribution of end points. Secondly, the peripheral system may be more sensitive to changes in afferent input than our conscious awareness of that input. Reflexes are constantly activated in the body without our conscious awareness of them, which demonstrates a dissociation between the sensitivity of different levels of the cortical hierarchy to changes in afferent input. Thirdly, this method of assessing confidence may not be sensitive enough within the current experimental design. As the task difficulty didn't change from trial to trial and no feedback was given throughout the task, there were limited reasons why a participant would modulate their confidence trial-by-trial within a block. However, the random sequence in which different targets were presented added some variability within blocks. Finally, previous research has highlighted individual differences in metacognitive ability across a sample of participants with similar performance accuracy (Fleming et al., 2010). Therefore, the lack of an effect here could be due to between subject variance in metacognitive awareness.

Confidence judgements are traditionally used within the decision-making literature to calculate scores of metacognitive sensitivity, which describe how well a participant knows when they are correct or incorrect following a perceptual decision. This is often based on a direct read out from the quality or strength of the stimuli perceived such that when this signal is degraded beyond a certain threshold or the accumulation of evidence for a particular decision threshold is slower a decision is made with lower confidence (Galvin et al., 2003; Kiani and Shadlen, 2009; Lau and Rosenthal, 2011). Within this literature choice certainty is very closely related to performance accuracy and the sensory input. However, the analyses used in these studies cannot be applied to the current task as the dependent variable (end point error) is continuous, therefore no binary decision is made and end point errors cannot be classed as correct or incorrect. In order to use these analyses, the current task will need to be repeated in a two-alternate choice discrimination paradigm in which participants must determine if they are closer or further away from two targets.

Nevertheless, the current results showed that confidence judgements were related to participant's perceived error from where they thought the target was normalised by the precision of the distribution of end points. This result fits with hierarchical predictive coding frameworks, which hypothesise that confidence is related to the precision (inverse variance) of higher-order beliefs about internal states and external sensations (Friston and Kiebel, 2009). Previous research has shown that confidence can be modulated whilst performance accuracy is maintained, which suggests a domain-general mechanism used to calculate confidence, which is separate from the primary task (Fleming et al., 2015). For example, increasing sensory noise in the task stimuli whilst maintaining task difficulty has been associated with decreased confidence ratings for the same task performance (Spence

et al., 2016). In addition, Friston and colleagues suggest that neuromodulatory circuits modulate the sensory gain on pyramidal cells transmitting bottom-up input such that this gain modulation determines the precision of the estimates encoded by those connections and this precision can therefore modulate confidence ratings. In support of this, recent evidence has found that noradrenergic systems and bodily arousal modulate confidence without disrupting task performance potentially be modulating the precision surrounding afferent input (Allen et al., 2016; Hauser et al., 2017).

The results in the current study provide novel evidence that confidence ratings in the sensorimotor domain (and in a task that does not involve explicit decision-making) are also related to the precision of the afferent input (i.e. are readily modulated in line with the distribution of movements) adding to this body of work, which suggests there is a global mechanism used to generate metacognitive judgements based on precision. However, a recent study argues that confidence ratings based on the precision of sensory input are domain-specific as they rely on the variance along a particular dimension: the precision in one domain will not necessarily be the same as in another domain. Indeed the authors found that confidence judgements calculated using an equivalent method were not correlated across two tasks in different domains: orientation discrimination and numerical discrimination (Navajas et al., 2017). Nonetheless, the mechanism underlying how that confidence rating is generated may be domain-general i.e. across domains the same computation may be used dependent on the synaptic gain across the neuronal population encoding the domain-specific sensation being reported on. In the current study, I did not formally model how confidence ratings were generated or quantify how this could vary between individuals. However, this would be an important next step to determine the underpinnings of confidence values about the proprioceptive state. It would be especially interesting to find a task or patient population in which confidence ratings and task performance were dissociable within the proprioceptive domain. From this we could determine whether sensorimotor beta oscillations more readily correlate with changes in sensory precision at the lowest level or represent our conscious estimate of sensory precision driven by frontal areas involved in metacognitive judgements. The application of this to PD is discussed in the general discussion.

In summary, this chapter demonstrates that high frequency peripheral vibration increases proprioceptive error by causing participants to overshoot visual targets. One mechanism for this effect is that vibration increases the uncertainty (decreases the precision) of bottom-up proprioceptive input, therefore more weight is placed on the prior visuomotor plan to determine the movement end point. A specially designed task with Bayesian modelling is required to test this hypothesis. Despite inducing a proprioceptive error,

peripheral vibration did not cause a decrease in confidence ratings as hypothesised. This is most likely due to the size of the error remaining within the normal distribution of end points across participants. Confidence ratings were readily modulated by precision-weighted end point errors from the median of each participant's distribution of end points rather than absolute error values from the target locations. This provides evidence to support global theories of metacognition, which suggest confidence judgements are based on the precision of internal and external states.

CHAPTER 6

Study Four: Orthogonalising the parameters of predictive coding using a visuomotor adaptation task and the Hierarchical Gaussian Filter (HGF)

6.1. INTRODUCTION

The active inference framework aims to create a unifying hypothesis that can explain perception and action in the brain by generalising the principles of predictive coding to the sensorimotor system. It is hypothesised that a hierarchical generative model exists in the motor cortex that predicts the sensory consequences of movement. Proprioceptive predictions are compared with ascending reafferent input to generate prediction errors (PE) at multiple levels of the sensorimotor system from the spinal cord to the cortex. PEs are precision-weighted, meaning that the generative model uses an estimate of the variance (uncertainty or inverse precision) of the sensory input to dictate how readily the PE will update the model. This precision-weighting determines the relative influence of descending proprioceptive predictions compared to ascending proprioceptive PEs, which is hypothesised to be integral for the initiation of movement.

At the neuronal level, it is hypothesised that this precision-weighting is determined by the post-synaptic gain on superficial pyramidal cells thought to transmit PEs up the cortical hierarchy (Friston and Kiebel, 2009). It is therefore difficult to independently measure precision and PE. However, the magnitude of the PE and the precision estimate serve different functions in Bayesian inference, therefore it is highly likely that the brain has a mechanism to dissociate these. For this study I have designed a paradigm to orthogonalise the parameters involved in Bayesian inference, namely predictions, PE and sensory precision, in order to determine their neurophysiological correlates.

In the introduction I highlighted the recent evidence that sensorimotor beta oscillations (~12-30Hz) appear to be correlated with parameters of Bayesian inference. In brief, previous studies have demonstrated that the post-movement beta synchronisation (PMBS) correlated with both changes in PE and uncertainty in the predictions produced by the internal model (Tan et al., 2016, 2014b, 2014a; Torrecillos et al., 2015) and the increase in beta power seen prior to a task-related movement has been shown to correlate

with the adjustment of the motor command necessary to produce a more accurate movement on the next trial (Torrecillos et al., 2015).

In this thesis, I specifically hypothesise that modulations in sensorimotor beta oscillations with movement may be explained by modulations in sensory precision. Indeed, in study two (chapter four) I demonstrated that sensorimotor beta power decreased in response to a decrease in proprioceptive precision. The reasoning for this hypothesis (outlined in full in the introduction) is demonstrated by the close correlation between the modulation of beta power and sensory attenuation with movement (Cohen and Starr, 1987; Davis et al., 2012; Engel and Fries, 2010; Starr and Cohen, 1985). Moreover, evidence suggests beta power is modulated by somatosensory information, therefore may not be solely related to movement parameters (Baker, 2007; Baker et al., 2006; Lalo et al., 2007).

In order to test this hypothesis, I recorded EEG whilst participants carried out a modified visuomotor adaptation task. It is thought that adaptation in these tasks occurs via a model-based mechanism involving error feedback (Thoroughman and Shadmehr, 1999). Angular visuomotor rotations of differing sizes were added into the feedback of a cursor to generate PEs throughout the task. Each perturbation would remain constant for 10-15 repetitions before a new perturbation was introduced in order to allow for behavioural adaptation. Sensory precision was modulated in blocks by altering the amount of noise, or uncertainty, in the sensory feedback given; this aimed to decrease the influence of the precision-weighted PEs on updating the internal model leading to a decreased behavioural adaptation rate as shown previously (Burge et al., 2008; Wei and Körding, 2010). In addition, prior precision was independently modulated by altering the probability with which the next trial in a sequence would require the same movement. For example, participants were told that a new angular perturbation would be introduced on a random trial following at least 7 repetitions of the same perturbation (see *Task Procedure: Visuomotor Adaptation Task* for more details). The probability of a new perturbation occurring increased following 7 repetitions of the same perturbation, therefore I hypothesised that participant's prior precision would track this probability. In many active inference and predictive coding schemes precision-weighting is afforded only to PEs; however, the hierarchical model employed in this study dissociates between the precision of prior predictions and the precision of sensory input both of which are used to determine the precision-weighting of PEs.

I hypothesised that behaviour would be updated on a trial-by-trial basis using Bayes theorem and thus the task parameters I modulated would represent hidden beliefs involved in Bayesian updating. For example, I hypothesised that the initial angular error

of the movement would decrease over repetitions of the same perturbation with adaptation; therefore, repetition number could be used as a proxy for PE. In addition, the block wise changes in visual noise represented a proxy for sensory uncertainty (inverse sensory precision) used to weight the PE. Under high visual noise there would be lower sensory precision, therefore PEs would have less impact on changing the motor prediction on the next trial. The task design variables that served as proxies for these hidden beliefs were regressed with EEG data before and after each trial in order to determine their neurophysiological correlates.

For a more specific measure of how these hidden beliefs actually evolved over time, the Hierarchical Gaussian Filter (HGF) was used to model these beliefs using each participant's behavioural data. The HGF is a hierarchical generative model that estimates how specific hidden beliefs about hidden states of the world (pertaining to estimates of predictions, PEs, and their precision) at different levels of the established hierarchy evolve over time based on specific task demands and individual participant's behavioural responses. It incorporates a perceptual model, which is used to estimate hidden beliefs, and a response model, which maps these hidden beliefs onto behavioural responses. The trajectories of how these hidden beliefs changed over time were then regressed against EEG data in a second regression analysis to verify and extend the original findings based on the design variables. Using this method this study aimed to deduce the neurophysiological correlates underlying the trial-wise modulation of a number of hidden beliefs involved in Bayesian inference during a visuomotor adaptation task.

6.2. METHODS

6.2.1. Participants

24 healthy participants (female=12) aged 21-37 years old (mean ±SD: 25.46 ±4.56) took part in this study. Participants had no history of neurological or psychiatric illness by self-report. All participants were right handed and gave written informed consent prior to taking part. This study was approved by the UCL Research Ethics Committee and all testing took place at the UCL Institute of Neurology, Queen Square. 5 participants were excluded for showing no visuomotor adaptation in the behavioural task (no significant difference in angular error between the error trial and the following tenth trial, $p>0.1$; see *Behavioural Data Analysis* for more details). This suggested they were not following the task instructions correctly. All subsequent analyses were carried out on 19 participants (female=9) aged 21-34 years old (mean ±SD: 25.53±4.03).

6.2.2. Experimental Setup

Participants were seated in front of a laptop with their dominant hand resting on a trackpad (Sway MultiTouch Trackpad, Speedlink, London) under a box, which hid their arm from view. The sampling rate was capped at the 60Hz refresh rate of the monitor. The position of the tip of their finger on the trackpad was shown as a circular cursor on the screen during the task. Participants completed a visuomotor adaptation task (custom code using Cogent 2000 in Matlab 2013b). EEG data were recorded using a BioSemi 128 active electrode system at a sampling frequency of 2048Hz. Two external reference electrodes were placed on the participants' earlobes.

6.2.3. Task Procedure: Visuomotor Adaptation Task

The task design can be seen in Figure 6.1 and was adapted from similar tasks used previously (Tan et al., 2016, 2014a, 2014b; Torrecillos et al., 2015). A start position (red circle) was presented at the bottom of a black screen at the start of a trial for 4s. The start position turned orange indicating a READY signal and remained on screen for 1.5s. At the GO signal, the start position disappeared and a single target appeared 20cm above the start position. The target consisted of a small filled in circle at the centre of a larger outer circle. A circular cursor appeared on screen at the position of the tip of the participants' index finger on the trackpad. Participants were instructed to move the cursor into the target zone following the most direct path as quickly and accurately as possible. On reaching the target participants were instructed to remain still for 2s and then when given the RETURN signal were instructed to return to the start position without visual feedback. A tactile marker on the track pad indicated to the participant that they were back in the start position. The ISI between the RETURN signal and the READY signal for the next trial was 4s. There were 387 trials in total with 43 trials per block and 9 blocks. The first block was a training block and was not included in subsequent analyses. Participants were given a few minutes rest between blocks.

The visual feedback of the cursor given during the trial was perturbed in two ways, which were independent from each other. Firstly, an angular rotation was introduced on certain trials such that the position of the cursor on the screen did not always directly emulate the position of the participant's finger on the trackpad. The angular rotation in the cursor was either 30 degrees, 60 degrees or was veridical with the participant's finger position. When an angular rotation was introduced this remained constant for 10 trials and then at a random trial number between 11 and 15 a new angular rotation was introduced. However, participants were told that a new angular rotation could be introduced at any

point after 7 trials. The sequence of angular rotations was pseudorandomised but the number of different changes in angular rotation was controlled such that there were an equal number of small and large error trials. Change in angular rotation was considered large if the rotation changed from 0° to 60° or vice versa and was considered small if the rotation changed from 0° to 30° or 30° to 60° and vice versa. Secondly, a random displacement in the X-axis was added into the visual feedback of the cursor in "high visual noise" blocks. This made it difficult to accurately determine the exact position of the cursor. In "no visual noise" blocks the cursor accurately tracked the participant's finger position without any added displacement except for the angular rotation. The type of block alternated and the noise level of the first block was counterbalanced across participants, except for the training block which was always a "no visual noise" block.

The sequence of changes in angular rotation was pseudorandomised to ensure it was different for each participant, but there were an equal number of small and large changes. Each block started with the adapted angular rotation from the previous block and a new rotation was given after 3 trials. This was to ensure that the noise perturbation and an angular perturbation did not occur at the same time. Participants were explicitly told this and the first 3 trials of each block were excluded from data analysis.

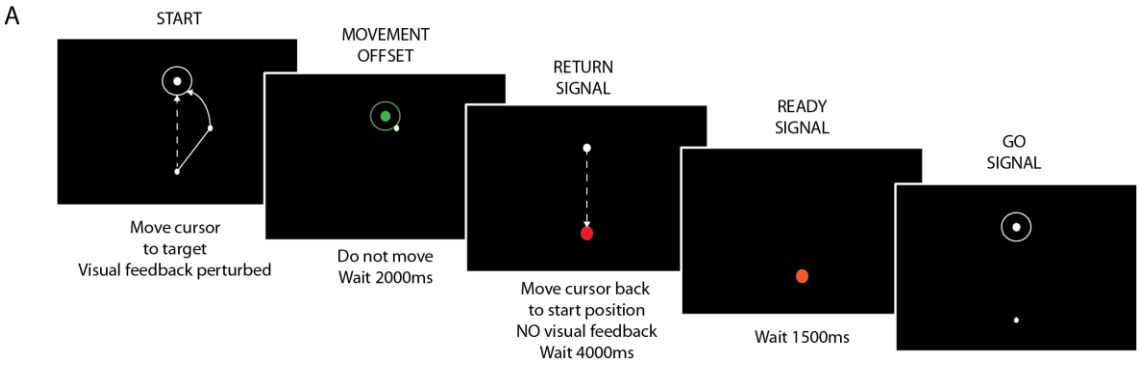

Figure 6.1. Visuomotor adaptation task design. *Participants were instructed to move the cursor from the start position to the target via the most direct path using a touchpad. A visuomotor rotation was added to the feedback of the cursor. Participants were told to wait at the target until the return signal when participants were asked to move back to the start position, which was signalled with a tactile marker: no visual feedback was given. Participants then waited for 4s until the ready signal was given then another 1.5s until the go signal was given for the next trial.*

6.2.4. Behavioural Data Analysis

Data were analysed using custom code written in MATLAB (version 2013b; MathWorks). The main dependent variable in this task was angular error at maximum velocity. Velocity was calculated from the differentiated cursor position and convolved with a Gaussian

kernel with a FWHM of 40ms. Angular error was calculated as the angle between a line connecting the start position and the target and a line connecting the start position and the point of maximum velocity. Movement initiation was calculated as the point in which the cursor crossed a semi-circular boundary with a radius of 5mm from the start position. Movement offset was defined as the time at which the cursor reached the outer circle of the target zone. Movement time was calculated as the difference between the time of movement offset and the time of movement initiation. Path length was calculated as the sum of the differentiated cursor position from the time of movement initiation to the time of movement offset. A 2x2x10 repeated measures ANOVA with factors change in angular rotation, visual noise and repetition number was used to analyse each dependent variable. All comparisons were corrected for multiple comparisons using the Bonferroni method where applicable. Where assumptions of sphericity were not met the Greenhouse-Geisser correction was applied.

6.2.5. Behavioural modelling using the Hierarchical Gaussian Filter (HGF)

I aimed to determine the neurophysiological correlates of hidden beliefs modelled using a two-level HGF (Figure 6.2). In this model Bayesian updating occurs at multiple levels in a hierarchy and the volatility, or uncertainty, at each level of the hierarchy is determined by the volatility of the hidden state at the level below. Hidden states evolve over time at each level via a Gaussian random walk and the variance (volatility or step size) of this is coupled to the level above such that different levels of uncertainty are represented at different levels of the hierarchy. The HGF consists of two models. The perceptual model determines how beliefs evolve over time given specific task inputs. The response model then maps those beliefs onto actions by determining how a subject should behave given those inputs. This model uses participant's behavioural data to estimate specific parameter values that best explain how these beliefs influence that individual's behaviour. For example, individual estimates of learning rate based on the behavioural data determine how quickly a participant will adapt to changes in perturbation level across trials. The output of the HGF is several time-series, which demonstrate the trial-wise evolution of hidden beliefs throughout the task that are individual to each subject. These trajectories were then correlated with neurophysiological data to understand how these beliefs were represented in the brain in this task.

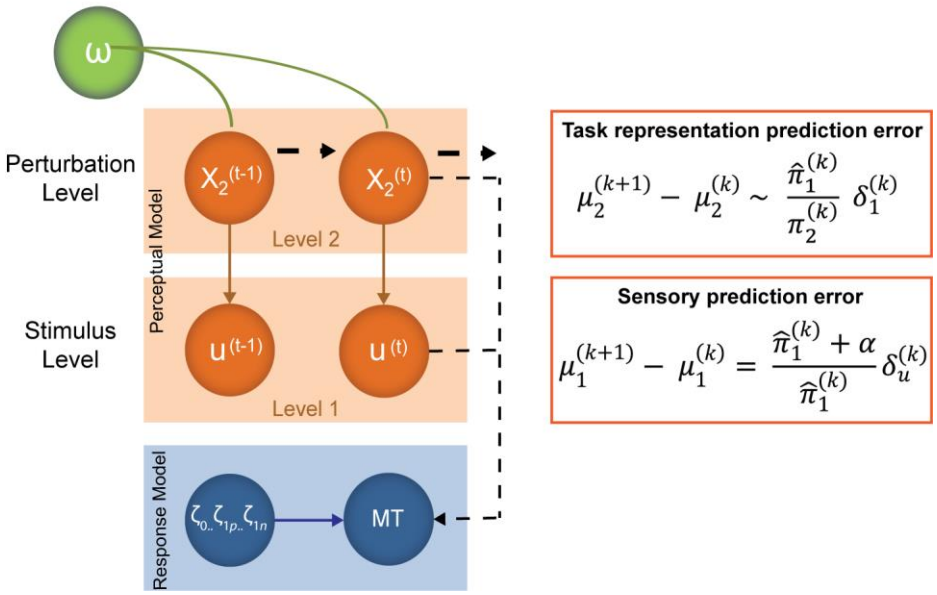

Figure 6.2. Overview of the HGF used in this study. *In this study a 2 level HGF was employed. At the first level, the perceptual model estimates how participant's beliefs about the perturbation level u modulate trial-by-trial i.e. what perturbation level governs that trial. This prediction depends on the current task representation level and the magnitude of noise in the visual feedback α (assumed to be constant for a given block). Sensory PEs at this level represent the error between this prediction and the actual perturbation level that is weighted by the sensory uncertainty. At the second level, the perceptual model estimated the probability with which the perturbation level would change over trials, x2. Participants were told this would occur after at least 7 repetitions of a given perturbation level, however the change in perturbation occurred implicitly. This level describes the validity of the perturbation level and the variance of this depends on the individualised learning step size ω. Task representation PEs produced at this level are weighted by the predicted precision from the level below and the precision at the second level. The response model maps these hidden beliefs onto observed movement times in order to estimate individual parameters that dictate learning rate based on Vossel et al (2014).*

6.2.5.1. The Perceptual Model

In this model beliefs about hidden states were updated over time using Bayes theorem. Hierarchical levels were linked by the predictions of hidden states at lower levels, and the ensuing precision-weighted PEs updated the predictions at higher levels. Estimates of uncertainty and individual learning rates were used to weight PEs at different levels of the hierarchy to explain the behavioural data. In this task, the manipulation of uncertainty was twofold: (1) which visuomotor perturbation level would govern a given trial; and (2) how much noise there would be in the visual feedback. The perturbation level changed implicitly over the course of the experiment, while feedback noise was manipulated explicitly and presented in separate blocks. The model estimated the participants' trial-by-trial beliefs about the perturbation level, corresponding to the lowest level in the model, denoted by u. Participants were told that the perturbation would change on a random trial between 7-15 trials after it was introduced. Over the course of the experiment, participants could learn when the perturbation level was more likely to change; accordingly, the beliefs about the higher-level structure of the task are denoted by

x_2. The inferred beliefs constitute the hidden states of an observation model (Mathys et al., 2011) and evolve as a Gaussian random walk. The generative model is hierarchical, i.e., the hidden states at a given level determine the variance of the random walk at the level below:

$$(1)\ p\left(u\middle|x_2^{(k)}\right) = N\left(u; x_2^{(k)}, \alpha\right),$$

$$(2)\ p\left(x_2^{(k)}\middle|x_2^{(k-1)}\right) = N\left(x_2^{(k)}; x_2^{(k-1)}, \exp(\omega)\right).$$

At the lower level (Eq. 1), the prediction of the visuomotor rotation depended on the current task representation level and visual feedback noise α (assumed to be constant for a given block). At the higher level (Eq. 2), the inferred task representation level in a given trial $x_2^{(k)}$ was normally distributed around the validity level from the previous trial $x_2^{(k-1)}$, with the variance of this distribution depending on the learning step size □. In this paradigm the validity of the visuomotor perturbation was fixed at 100% (i.e., all trials governed by e.g. a 30° rotation required a 30° displacement of the motor action relative to the visual input to accurately hit the target), however the second level of the observation model can efficiently learn about probabilistic validity levels (cf. e.g.(Vossel et al., 2014)). This model can in principle be extended with further hierarchical levels (Mathys et al., 2014) describing e.g. the volatility of the perturbation level; however, in our paradigm no further manipulations of uncertainty were introduced.

During the fitting of the model to the data, one can estimate the trial-by-trial time-series (at each level i) of the participants' beliefs $\mu_i^{(k)}$ (i.e., posterior means of states $x_i^{(k)}$) and the updates on these beliefs $\varepsilon_i^{(k)}$ (precision-weighted PEs) after observing an outcome. The variational approximation in the HGF provides analytic update equations describing these time-series:

$$(3)\ \mu_2^{(k+1)} - \mu_2^{(k)} \sim \psi_2^{(k)}\delta_1^{(k)} = \varepsilon_2^{(k)},$$

$$(4)\ \psi_2^{(k)} = \frac{\hat{\pi}_1^{(k)}}{\pi_2^{(k)}},$$

$$(5)\ \pi_2^{(k)} = \frac{1}{\sigma_2^{(k)}},$$

$$(6)\ \delta_1^{(k)} = \frac{\sigma_1^{(k)} + \left(\mu_1^{(k)} - \mu_1^{(k-1)}\right)^2}{\sigma_1^{(k-1)}} - 1.$$

As shown in equations 3-6, in each trial, a belief update at the second level, about the task representation $\mu_2^{(k+1)} - \mu_2^{(k)}$ is proportional to the PE at the level below $\delta_1^{(k)}$, weighted by

a precision ratio $\psi_2^{(k)}$. This precision ratio depends on the precision (inverse variance) of the prediction at the level below, $\hat{\pi}_1^{(k)}$, and the precision at the current level $\pi_2^{(k)}$. The superscript ^ denotes the prediction before observing the trial outcome; accordingly, $\hat{\pi}_i^{(k)}$ is the precision of this prediction. At the lower level, the updates take a similar form. The numerator of the precision term includes the parameter of sensory uncertainty and therefore the precision weighting modulates according to the noise level of the visual feedback.

$$(7)\ \mu_1^{(k+1)} - \mu_1^{(k)} = \frac{\hat{\pi}_1^{(k)}+\alpha}{\hat{\pi}_1^{(k)}}\delta_u^{(k)},$$

$$(8)\ \hat{\pi}_1^{(k)} = \frac{1}{\sigma_1^{(k-1)}+e^{\omega}},$$

$$(9)\ \delta_u^{(k)} = u^{(k)} - \hat{\mu}_1^{(k)} = u^{(k)} - \mu_1^{(k-1)}.$$

At the lower level, the PE about the observed perturbation level $\delta_u^{(k)}$ is simply the difference between the actual and the predicted outcome, where the prediction is inherited from the previous trial (Eq. 9). This PE, weighted by its variance and sensory noise *alpha*, is used to update the predictions about the outcome in the next trial (Eq. 7). At the higher level, the PE about the visuomotor perturbation level is used to update the prediction of its validity in the next trial (Eq. 3). These HGF-derived time-series – fitted to each participant's behavioural data – were used as regressors in subsequent analysis of EEG data. Prior variance $\log(\sigma_{1,2}^{(0)})$ were treated as free parameters.

6.2.5.2. <u>The Response Model</u>

To map the estimated hidden states (beliefs) onto the observed behavioural data, I specified a response model for the measured movement time (MT). Visuomotor adaptation studies have previously controlled for movement speed, such that the only variable to vary from trial to trial is angular error, and this is used as a measure of adaptation. However, the speed in which a participant moves contains a lot of important information related to how confident they are, which is thought to reflect estimates of precision. I therefore decided to use movement time as our dependent variable for the response model as this encompasses both speed and accuracy in a single variable and therefore produces a more holistic summary of how participants behaved. The response model was based on the trial-by-trial estimate of surprise, *S* (Vossel et al., 2014):

$$(10)\quad MT = \zeta_0 + u(\zeta_p + \zeta_2 S) + (1-u)(\zeta_n + \zeta_2(1-S)),$$

$$(11)\quad S = \frac{1}{1+surprise(\hat{\mu}_1)} = \frac{1}{1-\log_2(\hat{\mu}_1)}.$$

Inputs *u* were coded such that they mapped onto a range {0, 1} corresponding to {0°, 60°} displacement. Responses MT were calculated as response speed, i.e., the reciprocal of reaction times. A time-resolved value *S* represents attentional resources, scales with Shannon surprise associated with the target stimulus, and respects the same boundary conditions as responses and inputs, i.e., is confined to the {0,1} interval with $S = 0.5$ when $\hat{\mu}_1 = 0.5$. Parameters ζ quantify each participant's MT values (ζ_0: baseline; ζ_{1p} and ζ_{1n}: MT contribution after increasing and decreasing the perturbation level respectively), with ζ_2 denoting the weight of the attentional resources onto a given trial's estimated MT.

6.2.5.3. <u>Model comparison</u>

To test whether the participants' behaviour in this task can be assumed to follow Bayesian learning, I compared two observation models (HGF and a standard reinforcement learning model; cf. Rescorla and Wagner, (1972)) using Bayesian Model Selection. The Rescorla-Wagner (RW) learning model demonstrates how the association between a conditioned stimulus (CS) and an unconditioned stimulus (US) is learned over time. This association is updated in a trialwise manner depending on a prediction error weighted by a constant salience term that does not vary over time, but allows the learning rate to vary on an individual basis. In this experiment the CS can be likened to the angular rotation in the visuomotor mapping and the US is the subsequent motor action; on each trial the subject predicts the optimal motor action from the visual feedback from the previous trial. In the RW learning model equations below (eq 12 and 13) a prediction error, δ, is generated on each trial from the difference between the sensory input, u , and the change in association between the CS and US on the previous trial, $v^{(k-1)}$, (eq 12). The change in association for the current trial, $v^{(k)}$, is determined by weighting the prediction error by the salience of the CS, α , and adding this to the change in association from the previous trial (eq 13). This update equation modulates the association between the CS and US based on the given sensory input and a constant, individual learning rate.

$$\delta^{(k)} = u^{(k)} - v^{(k-1)} \quad (12)$$

$$v^{(k)} = v^{(k-1)} + \alpha * \delta^{(k)} \quad (13)$$

Each model provides a goodness of fit measurement, which states how well the model predicted each participant's behavioural data. In this study, this was the log model evidence (LME), which is calculated based on the negative variational free energy. I compared the LME across participants and these two models using the function "SPM_BMS" (Stephan et al., 2009).

6.2.6. EEG Data Analysis: Pre-processing

Data were pre-processed using SPM 12. EEG data were filtered using a highpass filter at 1Hz and a low pass filter at 100Hz and downsampled to 400Hz. Bad channels were identified using the 'threshold z-scored difference data' detection algorithm in SPM with a threshold of 8. If 20% of the continuous data for a channel was above this threshold, it was flagged as a bad channel and removed from analysis at a later stage. Due to the length of the trials being analysed topography-based artefact correction was applied to the continuous data to remove eyeblinks. Epoched EEG data were aligned to: 1) the onset of the GO signal with a time window of -6000ms to 1000ms to investigate foreperiod EEG activity, and 2) to movement offset, defined as the time the participant reached the target, with a time window of -1000ms to 2000ms to investigate post-movement EEG activity. For the time-frequency analysis the power of the EEG signal at each frequency from 1 to 99Hz was estimated using the wavelet transform in SPM. A Morlet wavelet with 7 cycles for each frequency was used.

To measure topographic changes in beta oscillatory activity over time, time frequency data was averaged over 15-30Hz. Data was log transformed and mean corrected such that the data at each sample point represented the change in beta power from the total average beta power for each channel. A region of interest (ROI) over sensorimotor cortex was selected by highlighting electrodes in which there was a significant event-related decrease in beta power during motor preparation at the onset of the GO signal and also a significant event-related increase in beta power at 1000ms post-movement (Figure 6.3). To measure time-frequency changes over sensorimotor cortex, EEG data were averaged over the ROI electrodes selected, log transformed and mean corrected such that the data at each sample point at each frequency band represented the change in the power from the total average power for that frequency.

For 18 subjects a technical error during recording meant that the rebound period for one condition (no angular perturbation, high visual noise) was 1s less than the other conditions; therefore, these trials (n=53) were removed from the EEG analysis for movement offset only for these participants. However, this did not affect the main results as regression analyses were used and there was still a large number of remaining trials. It is important to note that this did not affect the pre-movement results.

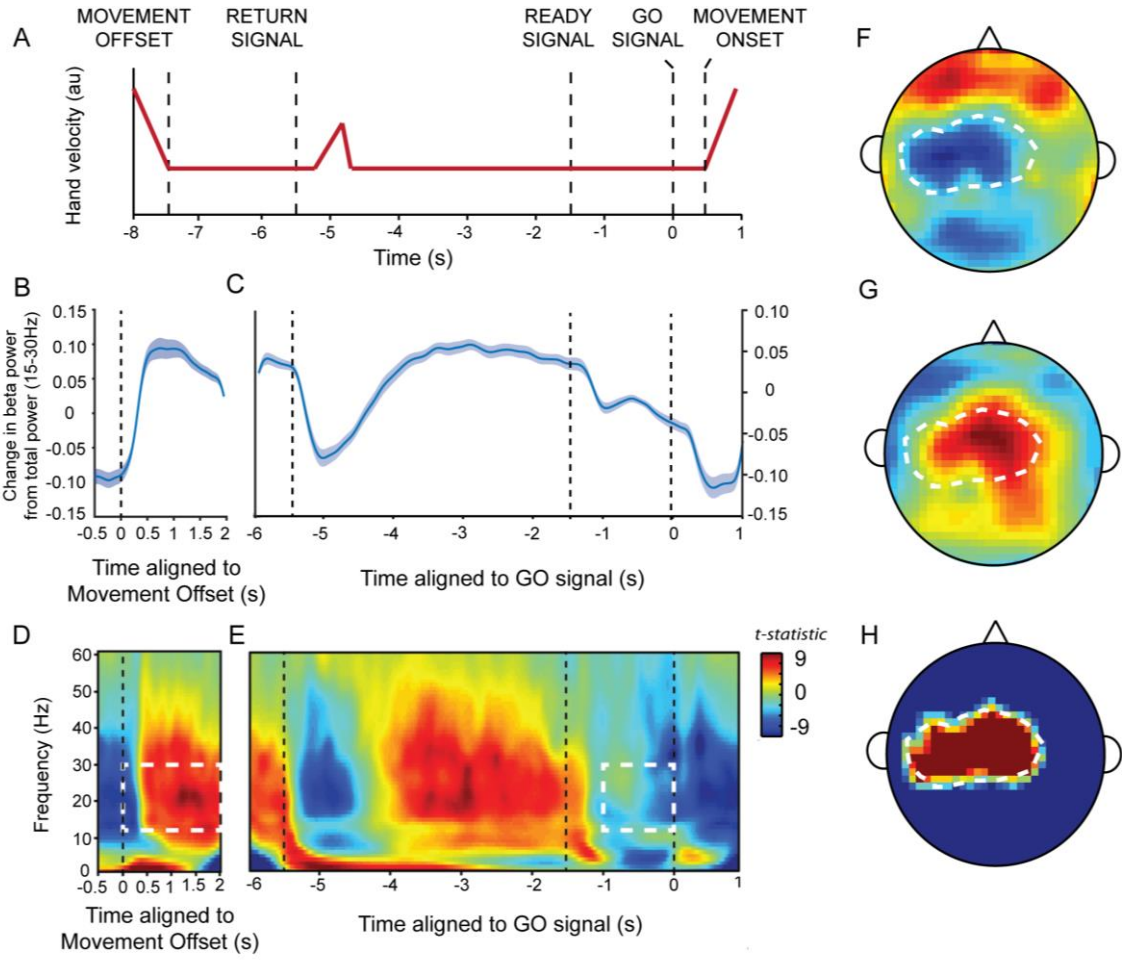

Figure 6.3. Beta power (15-30Hz) modulated over sensorimotor cortex with movement. *A) A schematic demonstrating the change in hand velocity throughout the task with each signal. This highlights the points at which participants were moving and the points they remained still. B+C) Solid line represents the change in beta power (15-30Hz) from the total average beta power for each channel averaged over all trials over a selected ROI and over all subjects in an epoch aligned to movement offset (B) and the GO signal (C). Shaded area represents ±s.e.m across subjects. D+E) Time-frequency plots demonstrating the average change in power over time across 1Hz frequency bands from 1-60Hz averaged over subjects. EEG data were epoched around movement offset (D) and the GO signal (E). F-H) An ROI was selected over sensorimotor cortex. The white dotted line represents the ROI selected as shown in H. This incorporated both the average ERD over subjects at the onset of the GO signal (F) and the average ERS over subjects 1s after movement offset (G). The white dotted squares indicate the windows of interest that were used for small volume correction for statistical analyses.*

6.2.7. EEG Data Analysis: Statistical analysis

The time-frequency data files for each trial were converted into images for statistical analysis in SPM. At the single subject level, images aligned to the GO signal or movement offset were regressed against the behavioural task trajectories of either the design variables or the HGF variables using a GLM (see Figure 6.4 for details of the regressors used). For the images aligned to the GO signal, the first trial of the EEG data was deleted and the last trial of each behavioural regressor was deleted in order to see the effect of the behaviour from the previous trial on the EEG activity in the foreperiod of the next trial.

For the design trajectories, both GLMs included regressors of repetition number, noise level and visuomotor rotation. For the HGF trajectories, specific regressors from each level of the hierarchy were used to analyse EEG data before and after a movement. For images aligned to movement offset the following HGF trajectories were used at the first level: sensory PE (δ_u), precision (ψ_1) and the posterior mean of the prediction (u_1); and from the second level: task representation PE (δ_1), precision (ψ_2) and the posterior mean of the prediction (x_2). For images aligned to the GO signal the following HGF trajectories were used at the first level: the prediction mean regarding the expected visuomotor rotation for the current trial ($\hat{u}_1$) and prior precision ($\hat{\pi}_1$). The prediction ($\hat{x}_2$) and prior precision ($\hat{\pi}_2$) at the second level lacked any probabilistic structure, therefore these regressors were not analysed. The contrast images from these analyses for each participant were smoothed used the "SPM_smooth" function with a Gaussian kernel with a FWHM of 2Hz and 150ms. The smoothed contrast images for each regressor of interest were then analysed at the group level using a one sample t-test to identify any EEG activity in the time-frequency domain that showed a consistent correlation with each regressor of interest across participants.

I hypothesised that there would be correlations between the regressors of interest and beta power within the frequency band 12-30Hz in two windows of interest based on the task design and the average change in beta power over time across participants. For images aligned to the GO signal, a window of interest was selected between the ready signal and GO signal in order to measure activity in this time period that may be relevant for motor preparation, therefore a small volume correction with a 18Hz by 1000ms window centered at -500ms and 21Hz (mid-way between 12Hz and 30Hz) was used. For images aligned to movement offset the average time-frequency spectrum showed a significant increase in beta power post-movement with the peak voxel at 21Hz and 1133ms therefore a small volume correction in a 18Hz by 2000ms window centred on here was used to include the whole rebound period (see Figure 6.3).

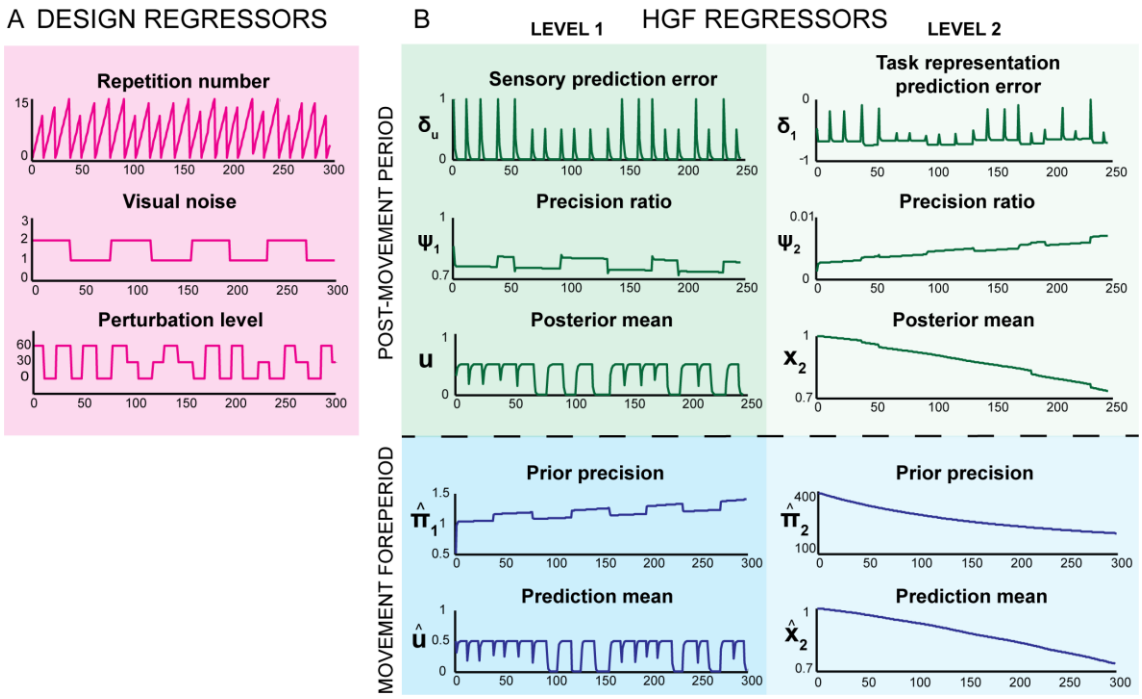

Figure 6.4. The trial-wise trajectories of task inputs or hidden beliefs estimated by the HGF. *A) The task was designed to manipulate perturbation level and visual noise orthogonally. Repetition number follows the implicit changes in perturbation level. Repetition 1 is the first introduction of a new perturbation: the error trial. Visual noise was modulated in blocks of high and low visual noise. Angular rotation denotes the size of the perturbation level introduced (0°, 30° or 60°), which stayed constant over subsequent repetitions of that perturbation. These regressors were used in a GLM to explain sensorimotor beta power following a movement and before a movement. B) The HGF estimated trajectories for how different hidden beliefs evolved over time throughout the task are shown for an example participant. Hidden beliefs estimated after sensory input was received were used to explain the post-movement beta synchronisation (upper panels) and predictions made before sensory input was received were used to explain preparatory beta power before movement onset (lower panels). These trajectories were produced at both the first level (left panels) and second level (right panels) of the HGF.*

6.3. RESULTS

6.3.1. Behavioural results: Participants behaved differently under high and low visual noise

Out of 24 participants, 19 successfully adapted their behaviour to the visuomotor rotation as shown by a significant mean decrease in initial angular error from the first error trial to the tenth repetition of that perturbation (all $p<0.05$). The 5 participants that did not show a significant difference in angular error by the tenth repetition were excluded from subsequent analyses for not completing the task appropriately. In the remaining sample of 19 participants, a 2x2x10 repeated measures ANOVA, comparing visual noise (no or

high), size of change in angular rotation on an error trial (small, 30° or large, 60°) and repetition number, was conducted for initial angular error. As expected there was a significant main effect of repetition number ($F(2.58,46.48)=104.15$, $p<0.001$, $\eta_p^2=0.85$; Figure 6.5A). Participants adapted quickly to the perturbation over repetitions of the same visual rotation: overall mean angular error significantly decreased from repetition 1 to repetition 3 and then remained stable for subsequent repetitions. Angular error was also modulated by the size of the perturbation as expected i.e. a large change in perturbation (0° to 60° or vice versa) generated a larger angular error than a small change in perturbation (0° to 30° or 30° to 60° and vice versa), but this was only significant for the error trial and the subsequent trial (size of angular rotation x repetition number: $F(4.68,84.30)=30.32$, $p<0.001$, $\eta_p^2=0.63$; large change in rotation: M±SD on error trial=47±6.7; small change in rotation: M±SD on error trial=26.9±5.1).

Similar results were found for the other behavioural variables measured. Movement time was greatest on error trials and decreased with adaptation ($F(2.02,36.39)=29.24$, $p<0.001$, $\eta_p^2=0.62$; Figure 6.5B). This was driven by a decrease in average velocity and an increase in path length on error trials. Movement time was longer following a large change in perturbation compared to a small change ($F(1,18)=11.17$, $p=0.004$, $\eta_p^2=0.38$) and this was significantly different for the error trial and the subsequent two trials (angular rotation x repetition number: $F(9,162)=6.58$, $p<0.001$, $\eta_p^2=0.27$).

Path length was greatest on error trials and decreased with adaptation ($F(2.37,42.73)=71.16$, $p<0.001$, $\eta_p^2=0.80$; Figure 6.5C). Path length was greatest following a large change in angular rotation compared to a small change ($F(1,18)=8.90$, $p=0.008$, $\eta_p^2=0.33$) and this was only significant for the error trial and repetition 3 (angular rotation x repetition number: $F(4.66,83.94)=16.46$, $p<0.001$, $\eta_p^2=0.48$). Average velocity was not significantly modulated by the size of the change in perturbation ($p=0.069$), however this was significantly modulated by repetition number ($F(2.2,40.26)=7.57$, $p<0.001$, $\eta_p^2=0.30$). Participants significantly slowed down on error trials and sped up over subsequent trials (Figure 6.5D).

I hypothesised that introducing uncertainty into the visual feedback of the cursor would lead to reduced movement speeds and a decreased rate of adaptation. Indeed under high visual noise compared to no visual noise mean movement time increased (main effect of noise: $F(1,18)=64.10$, $p<0.001$, $\eta_p^2=0.78$) and overall average velocity decreased (main effect of noise: $F(1,18)=11.75$, $p=0.003$, $\eta_p^2=0.40$). The rate of increase in average velocity after an error trial was smaller under high visual noise compared to no visual noise. I infer that under high visual noise participants were not as confident in their movements and

therefore moved slower. Indeed, participants did not adapt as quickly or as fully under high visual noise as demonstrated by an overall increase in initial angular error (main effect of noise: $F(1,18)=11.47$, $p=0.003$, $\eta_p^2=0.39$) and path length (main effect of noise: $F(1,18)=31.81$, $p<0.001$, $\eta_p^2=0.64$) throughout high noise blocks.

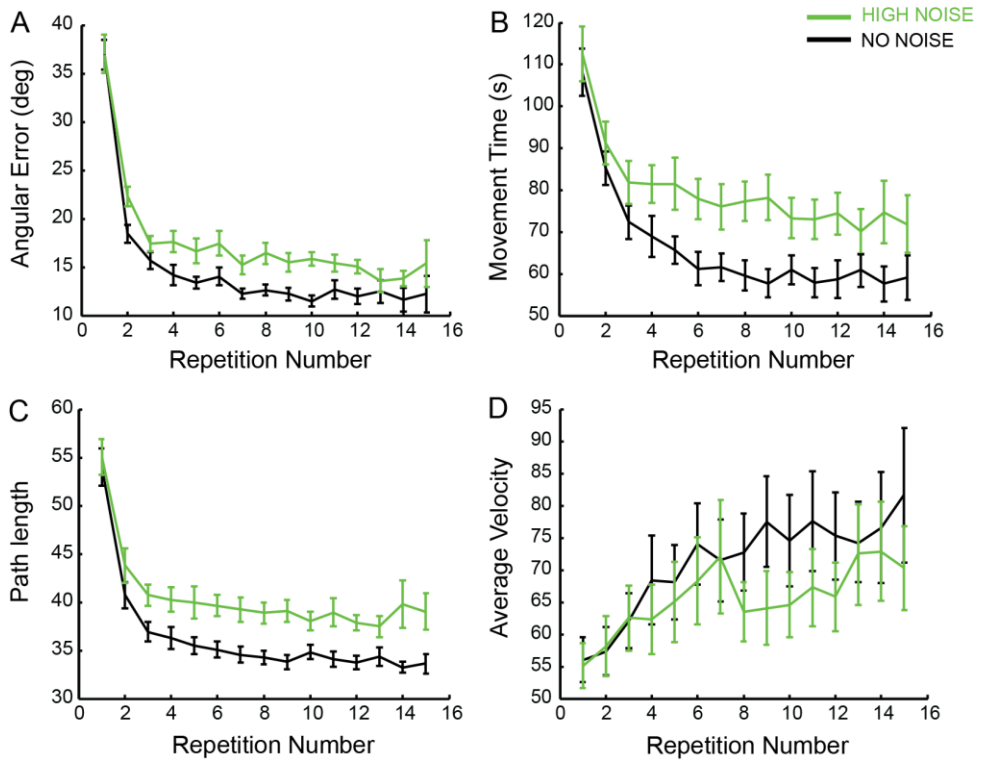

Figure 6.5. The visuomotor rotation and visual noise significantly modulated behaviour. *All behavioural variables were averaged over all perturbation sizes for the noise (green) and no noise (black) blocks and for each repetition of a perturbation. A) Angular error was maximal on an error trial and decreased over subsequent repetitions with adaptation. B) Movement time was on average greater for high visual noise compared to no visual noise conditions. C) Path length modulated in a very similar way to angular error decreasing with repetition number. On average path length was significantly greater for high visual noise compared to no visual noise conditions. D) Average velocity decreased on error trials and increased over subsequent repetitions with adaptation. Average velocity was significantly less under high visual noise compared to no visual noise.*

I designed the current task so that all the experimental manipulations were independent from each other in order to determine the specific neurophysiological correlates for each task parameter. In particular, I aimed to dissociate the effects of PE and sensory precision on sensorimotor beta oscillatory activity. Errors were introduced using visuomotor rotations and, as can be seen from the behavioural data, were reduced over subsequent repetitions under blocks of high and no visual noise. I entered regressors of the task parameters (repetition number, visual noise and perturbation level) into a GLM to identify the neurophysiological correlates of these independent parameters prior to movement and at the end of each movement.

6.3.2. Neurophysiological result: post-movement beta synchronisation (PMBS) increased over repetition number with adaptation

Across participants, there was a significant positive correlation between repetition number and the PMBS such that beta power was decreased following an error trial and increased with subsequent repetitions of the same perturbation (Figure 6.6A,D; peak voxel at 12Hz, 545ms: t=7.10, p=0.001 FWE). There was a significant positive correlation between beta power and visual noise such that high noise blocks had higher post-movement beta power than no noise blocks; however this did not survive correction for multiple comparisons (peak voxel 23Hz, 828ms: t=3.77, p=0.080 FWE, p=0.001 uncorrected; Figure 6.6B,E). There was no significant correlation between post-movement beta power and the perturbation level (Figure 6.6C,F). Here the majority of the variance in the PMBS could be explained by repetition number; however, some variance was also accounted for by visual noise.

6.3.3. Neurophysiological result: pre-movement beta power decreased more following an error trial and increased with adaptation

Task parameters from the previous trial were used to identify the neurophysiological effects of these on preparation for the next trial. I found a significant positive correlation between repetition number and beta power in the preparatory period following the ready signal and prior to the GO signal (peak voxel at 21Hz, -420ms, t=4.76, p=0.018 FWE; Figure 6.6G,J). Beta power was significantly reduced in this preparatory period following an error trial and increased with subsequent repetitions. There was no significant effect of visual noise and no significant effect of the perturbation level on beta power (p>0.1 FWE; Figure 6.6H,I,K,L).

These results demonstrate that beta desynchronisation prior to movement and beta synchronisation post-movement were significantly reduced following an error trial and increased over subsequent repetitions of the same perturbation. To formally probe the relationship between PE and precision further I modelled the behaviour from this task using the HGF in order to produce individual trajectories of how hidden beliefs evolved throughout the task. In particular, I modelled prediction, PE, precision and the posterior mean of the prediction and then repeated the EEG analyses to determine the neurophysiological correlates of these estimated beliefs.

6.3.4. Modelling result: the HGF readily explained participant's behaviour compared to a non-Bayesian learning model

The task used in this study involves integrating uncertainty estimates to optimise behaviour, therefore it is likely that a Bayesian learning model would readily describe participant's behaviour. However, it is important to compare the Bayesian HGF used in this study with an alternative non-Bayesian learning model (e.g. the Rescorla-Wagner model, (Rescorla and Wagner, 1972)) to confirm that the HGF captured more variance in participant's behaviour that would otherwise be unaccounted for. The log model evidence (LME) from each model was compared across participants using the Bayesian Model Selection function in SPM. The behavioural data used for these models was movement time as this encapsulated both the size of the angular error (due to increased path length) and any uncertainty in the movement that may be captured in participant's movement speed. Across participants, movement time was better explained using the HGF compared to the RW model (protected exceedance probability = 0.89 i.e. the HGF was 89% more likely to explain the data better). This suggests that participants behaved in a Bayesian manner and this justifies the use of the HGF for subsequent analyses.

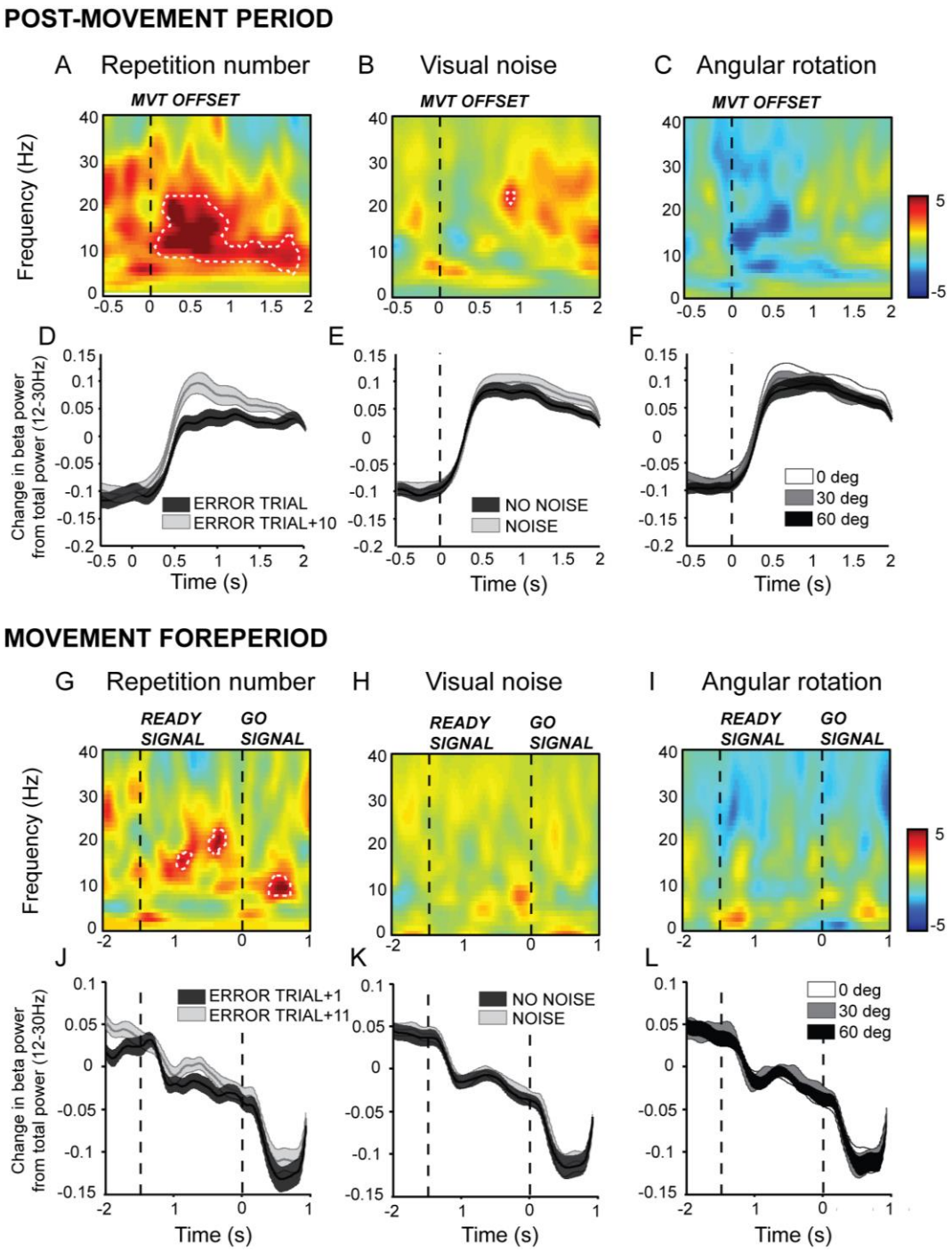

Figure 6.6. Beta power before and after a movement correlated with repetition number. *A-C, G-I) A GLM involving the design regressors (repetition number, visual noise and angular rotation) measured the correlation between EEG activity and each regressor of interest for each subject individually for the time period after each movement (A-C) and before each movement (G-I). Here the time-frequency plots show the t-statistic from a series of one sample t-tests measuring the consistency of these relationships across participants. The results show areas in which the data was consistently positively correlated (warm colours) or negatively correlated (cool colours) with the regressor of interest across participants. D-F, J-L) These graphs display the change in beta power (12-30Hz) from the total average beta power in each channel averaged over the ROI and across participants over trials in a particular condition. D+J) Beta power averaged over error trials (or error trials+1 for pre-movement period) and adapted trials (error trial+10 or error trials+11 for pre-movement period) to compare activity on trials with a large error and no error. E+K) Beta power averaged over high visual noise and low visual noise blocks. F+L) Beta power averaged over all trials with a particular sized angular rotation: 0 degrees, 30 degrees or 60 degrees. The upper two rows show data corresponding to the post-movement period and the bottom two rows correspond to the pre-movement period. White dotted lines show significant activity thresholded at t=3.61, p<0.001 uncorrected.*

6.3.5. Modelling and neurophysiology: post-movement beta synchronisation (PMBS) correlated with parameters involved in Bayesian updating at the sensory level

GLMs were used to identify the neurophysiological correlates of model parameters at each level of the HGF. For the post-movement period, for the first level of the HGF, a GLM including the following regressors was used: sensory PE (δ_u), precision ratio (ψ_1) and the posterior mean of the prediction (x_1). There was a significant negative correlation between the PMBS and sensory PE (peak at 15Hz, 768ms; t=6.72, p=0.001 FWE; Figure 6.7A). Beta power was significantly reduced following an error trial and increased with adaptation as PE decreased; this mirrors the finding with repetition number. Beta power was also significantly negatively correlated with the precision ratio (peak at 16Hz, 1788ms; t=5.44, p=0.005 FWE; Figure 6.7B). When sensory precision was low, for example during blocks of high visual noise, the beta rebound was much larger. In addition, the posterior mean indicating the updated belief about the size of the visuomotor rotation (which is then used as the prediction for the next trial) significantly negatively correlated with the PMBS (peak at 18Hz, 508ms; t=4.94, p=0.016 FWE; Figure 6.7C). The data provides evidence that the parameters involved in Bayesian updating following a movement may be encoded within the PMBS.

At the second level of the HGF, a GLM including the following regressors was used: task representation PE (δ_1), precision ratio (ψ_2) and the posterior mean of the prediction (x_2). The only regressor that showed a significant correlation with the PMBS was the precision ratio (peak at 23Hz, 813ms; t=4.23, p=0.037 FWE; Figure 6.7E). Here, as for the first level, the PMBS was larger when this precision-weighting was low. There was no significant correlation between beta power and the task representation PE or the posterior mean of the prediction at the second level (p>0.05; Figure 6.7D,F). This suggests that beta power over the sensorimotor cortex most likely encodes parameters of Bayesian updating at the lowest sensory level of Bayesian updating relevant to the magnitude of PE rather than its validity, or that the task did not introduce enough variability in validity over time.

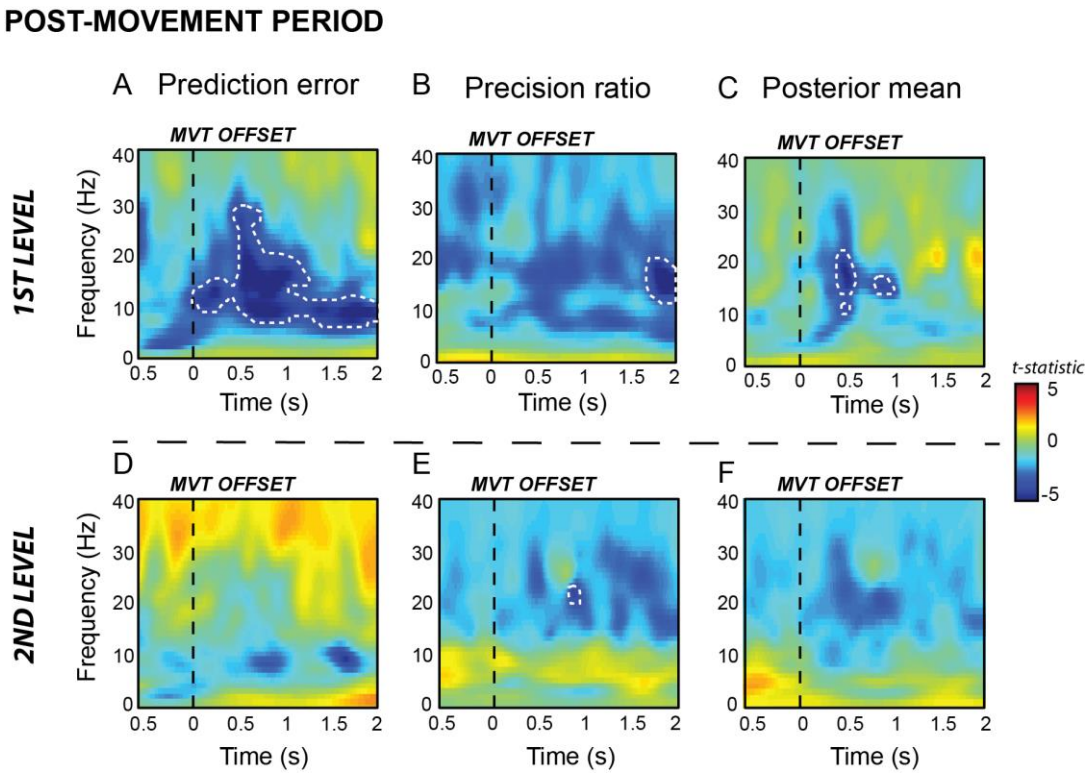

Figure 6.7. Post-movement beta synchronisation correlates with multiple components of Bayesian updating. *Two GLMs involving regressors estimated from the first level of the HGF (upper row) or the second level of the HGF (lower row) measured the correlation between EEG activity following a movement and each regressor of interest for each subject individually. Here the time-frequency plots show the t-statistic from a series of one sample t-tests measuring the consistency of these relationships across participants. There was a significant consistent negative correlation between the PMBS and prediction error (A), the precision ratio (B) and the posterior mean (C) estimated at the first level of the HGF across participants. There was a significant consistent correlation between the precision ratio (E) and high frequency beta power in the PMBS. There was no significant correlation between the PMBS and prediction error (D) and posterior mean (F) estimated at the second level. White dotted lines show significant activity thresholded at t=3.61, p<0.001 uncorrected.*

6.3.6. Modelling and neurophysiology: preparatory beta power inversely correlated with precision

I hypothesised that beta power in the preparatory period before a trial would be correlated with both the model prediction of the visuomotor rotation for that trial and the predicted precision surrounding this. Here I focused my analysis on the period between the ready signal (-1500ms) and the GO signal (0ms) where there was a gradual decrease in beta power in preparation to make the upcoming movement. A GLM using the following regressors at the first level was analysed: predicted visuomotor rotation before any sensory input ($\hat{x}_1$) and prior precision ($\hat{\pi}_1$). I found a significant negative correlation between prior precision and beta power in this time window (peak at 14Hz, -250ms; t=4.66, p=0.011 FWE; Figure 6.8A), showing that beta power was suppressed to a greater

extent under high prior precision (least uncertainty). There was no significant correlation between beta power and the estimated prediction mean ($p>0.05$, Figure 6.8B).

The prior precision value in the HGF is taken from the variance of the posterior from the previous trial, which is updated based on the previous trial PE; therefore, the prior precision value incorporates the magnitude of the previous PE and an estimate of sensory uncertainty. I wanted to explore further the relationship between beta power, uncertainty and error in this preparatory period. In order to do this I conducted a series of exploratory analyses to look at the interaction between error, visual noise and beta power. For this I extracted the values of beta power in the significant cluster highlighted above (Figure 6.8A white dotted outline; 12-20Hz, -500-0ms) for trials immediately following an error trial and trials 10 repetitions after an error trial (behaviour fully adapted) under both high and no visual noise. A 2x2 repeated measures ANOVA revealed a significant interaction between trial number and visual noise at this time point ($F(1,18)=5.19$, $p=0.035$, $\eta_p^2=0.22$), but no significant main effects ($p>0.1$). Under no visual noise there was a significant difference in the preparatory suppression of beta power following an error trial compared to the later repetition ($p=0.036$, corrected); beta suppression was greatest following an error trial and increased with adaptation. There was no significant modulation of beta power with trial number for the high noise blocks ($p=0.32$, corrected) (Figure 6.8C). A correlation analysis of beta power over repetitions following an error trial revealed a significant positive correlation between the beta power and repetition number for no noise blocks ($r=0.63$, $p=0.026$; one-tailed) and no significant correlation for high noise blocks ($r=0.19$, $p=0.31$; one-tailed) (Figure 6.8D). This analysis dissociates the precision-weighting from the magnitude of the previous error and therefore supports the hypothesis that preparatory beta power in the 500ms prior to the GO signal readily modulates depending on movement uncertainty or prior precision.

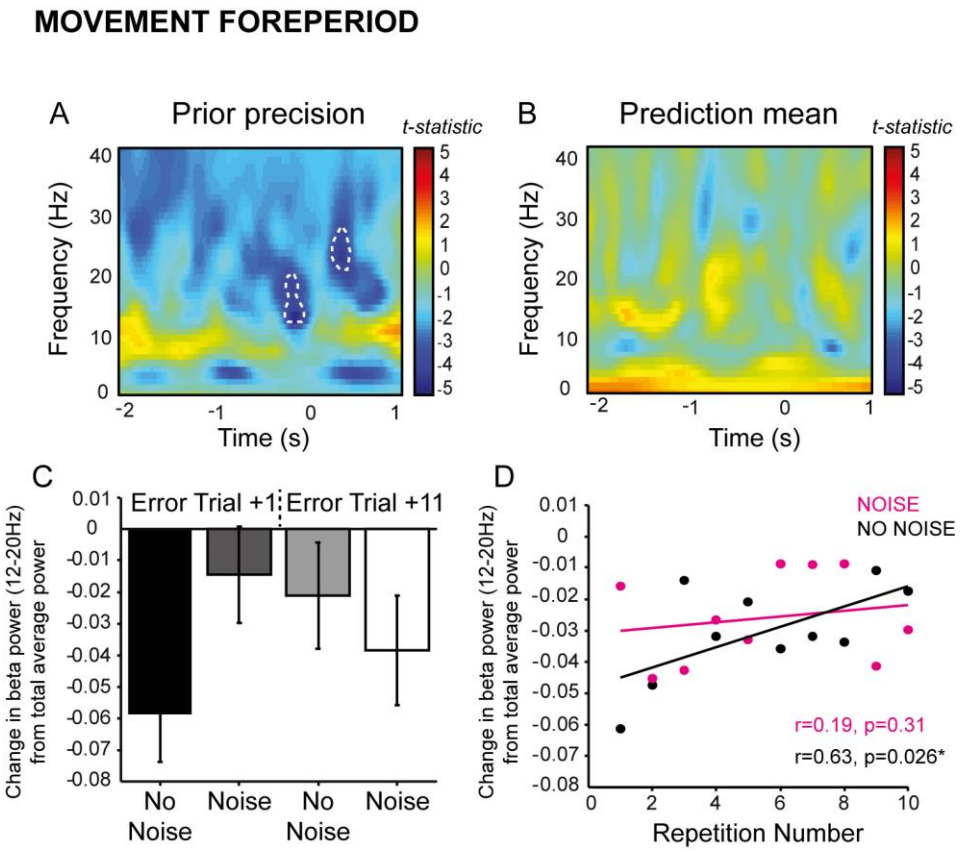

Figure 6.8. Preparatory beta power inversely correlated with prior precision. *A+B) Time-frequency plots showing the results of a one sample t-test measuring the consistency of the correlation between the estimated parameters of the HGF and the EEG data. Low-frequency beta power (12-20Hz) was consistently negatively correlated across participants with prior precision (A). There were no significant consistent correlations for the prediction mean (B). C) Beta power (12-30Hz) represented as a change in beta power from the total average beta power in each channel was averaged over the ROI and time window of interest (-500-0ms; white dotted line in A). The bar graph shows the mean (±s.e.m) beta power across participants for four conditions in a 2x2 factorial design (visual noise level (high vs low); repetition number (error trial +1 vs error trial +11). There was a significant interaction between visual noise and repetition number (p=0.035, Eta2=0.22). D) There was a significant correlation between repetition number and beta power for the no noise condition (r=0.63, p=0.026; one-tailed): beta power increased with adaptation over repetitions of the same perturbation. There was no significant correlation between repetition and beta power for the high noise condition (r=0.19, p=0.31; one-tailed). White dotted lines show significant activity thresholded at t=3.61, p<0.001 uncorrected.*

6.4. DISCUSSION

The aim of this study was to orthogonalise the parameters of predictive coding in a visuomotor adaptation paradigm in order to determine their neurophysiological correlates within the sensorimotor system. I modulated visual noise independently from an angular perturbation and used the HGF to estimate trial-wise modulations in hidden beliefs (prediction, PEs and precision), which explained the effect of these task inputs on participant's behaviour. I found that beta power prior to and following a movement readily correlated with angular error and estimates of sensory PE, which is consistent with

previous literature (Tan et al., 2016, 2014a, 2014b; Torrecillos et al., 2015). In addition, the variance in the PMBS following a movement was also explained by trial-wise changes in the precision-weighting of PEs and the posterior mean of the prediction. This suggests that the PMBS does not solely modulate with PE, which also supports previous research (Tan et al., 2016). Moreover, the preparatory decrease in beta power prior to a movement correlated with uncertainty in the motor prediction, which was readily modulated by sensory uncertainty. Overall, the data suggests that sensorimotor beta power may readily reflect the precision-weighting afforded to PEs, which are used to update future predictions about the sensory consequences of a movement.

Participants readily adapted to the angular perturbation within 10-15 repetitions and participants, on average, fully adapted by the third repetition of a perturbation. This suggests that the task was quite easy, therefore to make the task more difficult multiple targets in different positions could have been used as seen in previous tasks (Tan et al., 2016, 2014a, 2014b); however, for this task it was important that adaptation occurred over a small number of trials in order to include multiple error trials without having a very lengthy testing session. The addition of visual noise to the feedback of participant's movements caused participants to move slower. Unlike previous studies, I chose not to restrict participant's movement speed. This is more ecologically valid and can provide important information regarding participant's model confidence: previous research has shown that people move slower when they are less confident in a task or decision (A. Macerollo et al., 2015; C. E. Palmer et al., 2016; Patel et al., 2012). I hypothesised that participants would modulate their movement speed with repetition number following a U shape based on the confidence in their movements (model precision): i.e. movement velocity would increase with adaptation and then decrease again in anticipation that a new perturbation would be introduced. In this way PE and model precision would be orthogonal; however, this latter decrease in velocity did not occur suggesting that participants were not tracking trial number and were simply waiting to respond to the perturbation. Making the trial number explicit or adding a penalty for responding to a perturbation may have ensured participants adjusted their model precision in anticipation of a change in visuomotor mapping. It is therefore difficult to dissociate angular error and model precision in the current design as they modulated in the same way across trials. However, importantly, sensory precision was modulated orthogonally to angular error (or model precision), which was the main aim for this study.

Compared to the RW learning model, the HGF better explained participant's behaviour in this task. This supports previous work that suggests humans are Bayesian learners and confirms that estimates of uncertainty were used in this task. The RW learning model uses

a fixed learning rate across time whereas the HGF, more optimally, estimates an individual learning rate based on each participant's behavioural data that depends on trial-by-trial PE magnitude. From this, individualised trajectories of hidden beliefs were estimated from the HGF. These trajectories of how each hidden belief evolved over the course of the task were then correlated with the EEG data, which aimed to provide compelling evidence for a relationship between parameters of Bayesian inference and sensorimotor beta power. In the current study the response model in the HGF used participant's movement time to map the hidden beliefs produced by the perceptual model onto actions. For this I adjusted a previous response model based on reaction times (Vossel et al., 2014). Movement time was selected because it indirectly incorporates both angular error (through increased path length) and movement speed information in a single variable providing more information for parameter estimation.

Previous studies have consistently found a correlation between the PMBS and PE during sensorimotor learning tasks, which is supported by the findings here. The PMBS was modulated by repetition number suggesting, as in previous studies, that the PMBS tracks adaptation error. Indeed, the PMBS significantly negatively correlated with sensory PE, from the first level of the HGF, across participants. There was no corrected significant correlation between visual noise and the PMBS, however there was a consistent negative correlation between the precision ratio and the PMBS. The significant relationship with the precision ratio, but not the visual noise regressor may be due to individual differences in how participants responded to the visual noise; therefore, using the output from the HGF explained more variance in the PMBS than the design regressor. This demonstrates the potential advantage of estimating latent variables from experimental manipulations using computational modelling; these estimates offer a more specific interpretation for how the experimental perturbations could modulate behaviour and a mechanism by which the brain could be processing these task inputs.

It has previously been suggested that the PMBS more readily correlates with uncertainty than PE (C. Palmer et al., 2016; Tan et al., 2016) and indeed I found that both were represented in the PMBS. However, it is particularly difficult to dissociate which form of uncertainty may be encoded due to the relationship between these parameters in this model. The precision ratio produced by the HGF is a ratio of sensory precision from the level below (numerator) and prior precision from the level being updated (denominator), which denotes the weighting given to the PE and dictates how readily the model will be updated. Manipulating sensory and prior precision has opposing effects on this precision-weighting. Tan et al (2016) found that increasing model uncertainty correlated with a decrease in the average power of the PMBS. According to the HGF, decreasing prior

precision in this way would increase the precision-weighting of PEs creating a negative relationship between precision-weighting and the PMBS. Indeed, in the current study where sensory precision was modulated, there was also a negative correlation between the precision-weighting and the PMBS. This suggests that despite whether the model uncertainty or sensory uncertainty is modulated, the PMBS negatively correlates with the resultant precision-weighting afforded to PEs. Sensorimotor beta oscillations may therefore represent the summation of these different uncertainty values, which are potentially encoded by different inputs into the sensorimotor cortex.

One hypothesis is that decreasing sensory precision at the first level, increases the relative contribution of model precision at higher levels of the cortical hierarchy. It may be possible to test this by separating these types of uncertainty using different levels of a model, such as the HGF. In the HGF a different type of PE is produced at each level of the hierarchy and this is weighted by a precision ratio consisting of different precision terms. At the first level, sensory PEs are heavily influenced by uncertainty within the sensory input (sensory precision), whereas at the second level task representation PEs reflect learned probabilistic stimulus transitions modulated by estimation uncertainty (prior precision). In this study, beta power appeared to more readily correlate with hidden beliefs at the first level, which suggests that sensorimotor beta power may more readily reflect bottom-up processing of sensory stimuli. This is supported by the location of the activity over primary sensorimotor cortices. It has also been suggested that dopamine is important in responding to low-level sensory PEs in stimulus outcomes (Bestmann et al., 2014; Iglesias et al., 2013). Evidence from PD patients demonstrates a link between the loss of dopamine and increased beta power, which supports the proposal that beta power is related to the processing of low-level sensory PEs.

There was also a significant correlation between the precision ratio and beta power at the second level of the HGF, however the regressors here lacked a probabilistic structure. The behavioural data and the HGF model regressors show no evidence that model precision was modulated across repetition number as expected at this level (Figure 6.4). This precision term appeared to decrease gradually across the course of the experiment suggesting that inferences at the second level were not as useful in completing the task and more attention was placed on the first level inferences. It will be interesting to repeat this study with independent manipulations at higher levels of this computational hierarchy to determine whether different brain areas or different frequencies of oscillatory activity correlate with parameters of Bayesian inference at different hierarchical levels. Indeed, a recent study which involved a complex implicit probabilistic RT task found that a pharmacological manipulation of dopamine altered estimates of

volatility at the third level of the HGF (Marshall et al., 2016). Perhaps for more complex tasks beta power is more readily modulated by estimation uncertainty whereas for simpler tasks differences in sensory uncertainty may have a greater influence over beta power.

As PE magnitude, the precision ratio and the posterior mean of the prediction all correlated with the PMBS in this study, it could be suggested that the computations involved in Bayesian updating occur within this frequency band of oscillatory activity at this time point. Although the oscillatory activity at the macro-scale can be modelled with these equations and therefore we infer that Bayesian updating most likely occurs within this post-movement time window and frequency band of activity, there is little evidence to demonstrate exactly how the brain computes these variables and equations at a cellular level and how these components are then represented in synchronous activity across the population. This will be discussed in more depth in the general discussion. However, all of the components required for Bayesian updating appear to be present in the PMBS, therefore we can infer that this computation or the results of this computation are represented in some manner within this frequency band of activity.

It is important to note, however, that results of the correlation between PE and the PMBS could be confounded by differences in behaviour: movement time and path length modulated over trials in a very similar way to this regressor, therefore it is difficult to determine if it was PE (or prior precision) rather than a movement execution parameter, which was responsible for the modulation of beta power. However, the current findings support those of other studies in which these parameters have been controlled for. Importantly, these behavioural differences do not affect results regarding the modulation of pre-movement beta power. Another movement was required to move back to the home position (with no visual feedback) after the PMBS and the inter-trial interval was very long (4s), therefore EEG results in the pre-movement time window cannot be confounded by any execution parameters of the previous movement and this is where the novel results of this study were found.

Pre-movement preparatory beta power between the ready signal and the GO signal correlated with precision in the prediction of the sensory consequences of movement, but not with the estimated prediction mean. Following the ready signal there was a decrease in beta power in preparation to move and this decrease was greater for trials with higher prior precision (less model uncertainty). This is in line with previous findings that beta power during motor preparation was dependent on directional uncertainty such that beta power decreased more when there was less uncertainty (Tzagarakis et al., 2015). This

prior precision parameter produced by the HGF is the predicted model precision before any sensory input has been received and comes from the posterior precision from the previous trial. This regressor therefore readily modulated with the precision-weighting of the previous PE, which was heavily influenced by the external changes in sensory uncertainty, therefore does not purely represent prior precision without any influence of sensory uncertainty. Indeed, this regressor modulated very closely with the block-wise changes in visual noise.

To probe the relationship between error, uncertainty and preparatory beta power further, I carried out additional analyses in this time window by comparing beta power on trials with high and low error and high and low visual noise in a 2x2 factorial design. This aimed to orthogonalise the effects of error and noise on beta power. I found a significant interaction between these factors over a 500ms time window before the GO signal to move. Beta power was suppressed significantly more under no visual noise than high visual noise on the trial immediately following an error trial despite the same initial angular error being produced in the previous trial; however, this difference disappeared with adaptation. This suggests that preparatory beta power was not specifically modulated by sensory uncertainty or error. As model uncertainty is thought to modulate with error in this task, these results, in line with the HGF findings, suggest that pre-movement beta power reflects the relative contribution of sensory and model uncertainty estimates as represented in the precision ratio. When there is no visual uncertainty, a new perturbation immediately increases the weighting on sensory information such that the precision-weighted PE more readily updates the model and adapts to the new context. This is associated with a large decrease in beta power, which then increases with adaptation. However, under high visual noise, sensory precision is suppressed such that model precision remains high despite the introduction of an angular perturbation and does not change as readily over subsequent trials due to the decreased precision-weighting of PEs. Beta power remains high over subsequent trials despite the magnitude of the PE changing with adaptation. This suggests that beta power more readily tracks this precision-weighting (in an inverse relationship) rather than the magnitude of the PE.

A recent study by Vilares and Kording, (2017) found that dopamine depletion in PD patients caused patients off medication to place less weight on the current sensory information needed to make Bayes optimal decisions in a visual discrimination task. Giving dopaminergic medication increased this sensory weighting. Moreover, a lack of dopamine reduced patient's ability to react to changes in sensory uncertainty. This is supported by another study suggesting that dopamine is important for motor flexibility (Galea et al., 2012). Dopamine depletion in PD patents is associated with an increase in

resting beta power and a lack of modulation of beta power with movement (Little et al., 2012). Here I found that beta power negatively correlated with the precision-weighting afforded to sensory information, therefore PD patients with increased beta power should place less weight on sensory information in line with the results by Vilares and Kording (2017).

According to this hypothesis it would be expected that PD patients would adapt more slowly to changes in visuomotor mapping compared to controls due to this decreased weighting on sensory information. However, the results are mixed. Some studies suggest that PD patients have impaired visuomotor adaptation (Contreras-Vidal and Buch, 2003; Paquet et al., 2008), others suggest PD patients adapt the same as controls (Marinelli et al., 2009; Weiner et al., 1983), but have impaired consolidation when retested (Marinelli et al., 2009), and another suggested that PD patients actually adapt quicker than controls (Semrau et al., 2014). However, there are multiple different types of adaptation protocols that are used. Indeed it seems that PD patients are only impaired when sudden perturbations are introduced (in a similar way to the current study) compared to a gradual implicit perturbation task (Mongeon et al., 2013; Venkatakrishnan et al., 2011). This suggests that PD patients may lack the conscious awareness to explicitly respond to a perturbation by selecting a high cost action that is necessary to adapt. In the current task, perturbations were implicit, but were obvious and introduced suddenly, therefore we can infer that sensorimotor beta power may be involved in the explicit adaptation process. Pharmacological and neuroimaging studies in PD patients and healthy controls are required to probe this idea further.

This study demonstrates that sensorimotor beta oscillations may play an important role in Bayesian updating during visuomotor adaptation tasks. Modulations in beta power both prior to a movement and following a perturbed movement correlate with precision estimates, which supports hypotheses that sensorimotor beta oscillations may encode uncertainty. However, it is not clear from this study whether beta oscillations actually have an active role in processing uncertainty or reflect an epiphenomenon of the underlying cognitive processes. Here I conclude that sensorimotor beta oscillations most likely represent the precision-weighting of PEs, which is represented following a movement during Bayesian updating and in the precision surrounding the predictions of a movement before the next trial. However, this negative correlation between precision-weighting and beta power is the opposite to what I have proposed given the predictions of the active inference framework. In this thesis I posit that a decrease in the precision-weighting of PEs (which is thought to be necessary for movement) will correlate with a decrease in sensorimotor beta power. Indeed, in study two (chapter four) a decrease in

proprioceptive precision caused a decrease in sensorimotor beta power; whereas in this study a decrease in precision-weighting caused an increase in beta power. This is likely due to the specific domain in which sensory precision was modulated in both of these studies. The sensorimotor cortex has been proposed to act as a multisensory hub integrating exteroceptive and proprioceptive information to readily predict the sensory consequences of movement (Adams et al., 2013a). Therefore, modulating precision in the visual domain compared to the proprioceptive domain appears to have different effects on beta power. An interrogation of the different results in this thesis may provide a novel interpretation of the role of sensorimotor beta power in motor control. This will be discussed in detail in the general discussion.

CHAPTER 7

DISCUSSION

In this thesis I have tested the hypothesis that sensory attenuation is a necessary step for movement initiation to occur. Prior to and during movement, sensory input to the cortex is reduced. The active inference framework posits that this sensory attenuation "is a necessary consequence of reducing the precision of sensory evidence during movement to allow the expression of proprioceptive predictions that incite movement" (Brown et al., 2013; K. Friston et al., 2011; Friston et al., 2010). Estimates of sensory precision (inverse of uncertainty) must be down-weighted by reducing the synaptic gain on superficial pyramidal cells transmitting prediction errors up the cortical hierarchy; this occurs in order to allow the proprioceptive predictions that incite movement to prevail. In this thesis, I carried out a series of experiments using different behavioural tasks and EEG to test specific predictions that emerge from this hypothesis. Below I will summarise the hypotheses and main findings from each study.

In study one (chapter three), I aimed to determine if the two forms of somatosensory attenuation referred to in the literature were neurophysiologically distinct. I found that the decrease in SEP amplitude that occurs with force production did not correlate with perceptual somatosensory attenuation measured in a force matching paradigm; however, a later component of the SEP did. This demonstrated a dissociation between physiological and perceptual somatosensory attenuation and suggested that these may occur at different levels of the cortical hierarchy with separable functions. Previous research suggests that perceptual somatosensory attenuation plays an important role in dissociating externally and internally generated sensations for the correct perception of agency and most likely occurs in the secondary somatosensory cortex. Physiological somatosensory attenuation on the other hand appears to occur in the primary somatosensory cortex and has been hypothesised to play an important role in movement initiation. One hypothesis is that SEP attenuation represents a reduction in estimates of somatosensory precision, which is necessary for movement initiation. Due to the close correlation between the time course of SEP attenuation with movement and the decrease in sensorimotor beta power with movement, I hypothesised that modulations in sensorimotor beta oscillations may represent changes in estimates of somatosensory precision that are predicted to be necessary for movement initiation.

In study two (chapter four), I aimed to modulate estimates of somatosensory precision in order to determine the effect of this on motor control and sensorimotor oscillatory activity. High frequency (80Hz) peripheral vibration was applied to the wrist of participants to increase uncertainty in the proprioceptive state by activating muscle spindles in the absence of any overt muscle lengthening and thus generating uncertainty in the position of the limb. In line with previous results from our lab and predictions from the active inference framework, I hypothesised that increasing proprioceptive uncertainty using this method would decrease estimates of somatosensory precision and lead to decreased reaction times (RTs) on a motor task. In addition, I hypothesised that this decrease in the estimate of somatosensory precision would be associated with a decrease in sensorimotor beta power. I demonstrated that high frequency peripheral vibration readily decreased participants' completion time on a motor control task. Moreover, I showed that the same peripheral vibrating stimulus caused a significant decrease in sensorimotor beta power at the onset and offset of the stimulus. The adaptation of sensorimotor beta power that occurred may reflect the adaptation of estimates of somatosensory precision that would occur in response to the unexpected firing of 1a afferents. This result provides evidence that modulations in somatosensory precision are important for movement initiation and that sensorimotor beta oscillations readily reflect changes in sensory precision. However, there was no direct measure that the vibrating stimulus used in this experiment did modulate somatosensory precision.

In study three (chapter five), I tested the hypothesis that a peripheral high frequency vibrating stimulus applied to the wrist would increase proprioceptive uncertainty on a proprioceptive reaching task. This aimed to test whether a modulation in proprioceptive uncertainty was the mechanism by which movement times and sensorimotor beta power were decreased in the previous study. In a reaching task with no visual feedback, I found that vibration caused participants to significantly overshoot the targets demonstrating that peripheral vibration decreased proprioceptive accuracy, but had no effect on error variability. The distribution of end points around the targets was consistent with previous literature suggesting that participants weight visuomotor information and proprioceptive feedback in a direction dependent manner. The overshooting errors produced were consistent with a reduced weighting of proprioceptive information compared to a prior visuomotor prediction when determining the end point of the movement. This result suggests that the vibratory stimulus decreased the precision in estimates of proprioceptive feedback. In this study I also showed that the modulation of confidence ratings readily reflected the distribution of precision-weighted end point errors relative to the participant's own model of where the target was. This suggests that confidence ratings

may be generated based on the precision-weighting of sensory estimates in line with previous research in other domains (Aitchison et al., 2015; Friston and Kiebel, 2009; Navajas et al., 2017). However, the lack of modulation of confidence with vibration suggests that the central nervous system is more sensitive to changes in precision than our conscious awareness of those estimates. This may also suggest that confidence judgements are likely based on precision terms at higher levels of the cortical hierarchy.

Active inference posits that there is a hierarchical generative model in sensorimotor cortex that produces proprioceptive predictions that incite movement. This prediction comes from the generalisation of the predictive coding framework to the sensorimotor system. Moreover, active inference suggests that sensory attenuation occurs across all sensory channels during movement. In study four (chapter six), I aimed to test whether a hierarchical generative model, based on the free energy principle, could readily predict motor behaviour in response to changes in visual uncertainty in a visuomotor adaptation paradigm. I then measured the neurophysiological correlates of estimates from this model to determine whether these hidden beliefs were represented within the sensorimotor system. I manipulated sensory precision by adding visual noise to the feedback of a participant's movement and generated prediction errors by adding an angular rotation between the true position of the participant's hand and the cursor on the screen. I modelled the parameters of Bayesian predictive coding using the Hierarchical Generative Filter (HGF). I demonstrated that both the post-movement beta synchronisation (PMBS) and the pre-movement beta desynchronization negatively correlated with the precision-weighting afforded to sensory prediction errors. This confirmed my hypotheses and supported findings in the literature, which have suggested that components necessary for predictive coding are represented within sensorimotor beta oscillatory activity (Tan et al., 2016, 2014a, 2014b; Torrecillos et al., 2015).

However, the pre-movement beta power decrease and the precision-weighting term were negatively correlated in this study; this was the inverse relationship to predicted where a decrease in beta power was hypothesised to correlate with a decrease in sensory precision prior to movement. However, it may be hypothesised that increasing uncertainty in the visual domain increased the reliance on proprioceptive information; this would therefore support the hypothesis that sensorimotor beta power is positively correlated specifically with changes in proprioceptive precision. Despite sensory attenuation occurring across all sensory modalities during movement, it is likely that a reduction specifically in somatosensory precision is represented by sensorimotor beta power and is necessary for motor initiation.

In summary, the results in this thesis provide support for some of the predictions that emerge from the active inference framework. Firstly, I have shown that modulating proprioceptive uncertainty using a high frequency peripheral vibrating stimulus can decrease movement times on a motor control task providing support for the hypothesis that a decrease in sensory precision is necessary for movement initiation to occur. Secondly, I have shown that sensorimotor beta oscillations may reflect modulations in estimates of sensory precision. Beta power was decreased in response to the peripheral vibrating stimulus and correlated with estimates of precision produced by a hierarchical generative model. Beta power was also differentially modulated by proprioceptive and visual uncertainty; I suggest that beta power more readily reflects the precision afforded to proprioceptive reafferance, which is modulated by the integration between proprioceptive and visual information in sensorimotor cortex. The role of beta oscillations in motor control further provides support that modulations in sensory precision may have an important role in controlling movement as hypothesised by the active inference framework.

7.1. Is sensory attenuation necessary for movement initiation?

The active inference framework predicts that a decrease in estimates of sensory precision are necessary in order to initiate a movement. In order to test this hypothesis, it is important to assess whether sensory precision can be experimentally manipulated and measured using a behavioural or neurophysiological correlate; this was one of the main focuses of this PhD. Active inference posits that precision is determined by the post-synaptic gain of superficial pyramidal cells that transmit precision-weighted prediction error signals up the cortical hierarchy (Friston, 2005; Friston and Kiebel, 2009). This is thought to be controlled by neuromodulators, such as dopamine and acetylcholine, and/or synchronous neural activity that modulates synaptic gain via spike-timing dependent plasticity(Friston et al., 2015; K. J. Friston et al., 2011). Both of these mechanisms can be modulated through top-down attentional processes or by increasing the uncertainty in the afferent input used to generate prediction errors. In this thesis I used the latter option and chose to modulate sensory precision in two ways: by adding noise into visual feedback used to guide movements and using high frequency peripheral vibration to increase uncertainty in the proprioceptive state. It is difficult to directly measure synaptic gain in healthy humans at the macroscale, therefore I used changes in behaviour, Bayesian modelling and recorded EEG in order to determine whether the manipulations used

readily modulated sensory precision. This could then provide support for specific predictions from the active inference framework. However, it must be noted that the behavioural and neural data recorded in this thesis may have been modulated by an alternative neuronal mechanism to a change in synaptic gain, such as an increase in neuronal synchronisation or recruitment; therefore, simultaneous invasive and non-invasive electrophysiological recordings are needed to better elucidate the underlying neuronal mechanism employed.

In study four (chapter six), adding noise into the visual feedback of visually-guided movements in a visuomotor adaptation task caused participants to adapt more slowly to the visuomotor perturbation, which suggests that the increased uncertainty reduced the precision-weighting of sensory prediction errors. Indeed, this was confirmed by estimates produced by the HGF, which showed that the precision ratio used to weight sensory prediction errors at the first level decreased when visual uncertainty increased. In study three (chapter five), I showed that increasing proprioceptive uncertainty using high frequency peripheral vibration decreased proprioceptive accuracy on a behavioural task. Based on previous literature (Bays and Wolpert, 2007; van Beers et al., 1999, 1998), the overshooting errors in this behavioural task can be explained by a reduction in proprioceptive precision relative to precision in the prior visuomotor plan, which supports the hypothesis that this stimulus modulated proprioceptive precision. However, Bayesian modelling is needed to simulate the effect of modulating proprioceptive and visual precision in this behavioural task in order to provide evidence that this was the mechanism by which vibration affected behaviour.

The most direct evidence for the role of sensory precision in motor initiation comes from study two (chapter four). Here I showed that high frequency peripheral vibration reduced completion time on a motor control task replicating previous results found in the lab (under submission). However, the task used here (nine-hole peg task) required coordination across a number of modalities, therefore it is difficult to deduce that the vibration specifically altered motor initiation; it could have equally affected motor preparation. The decreased precision in the proprioceptive state may have caused participants to rely more on a prepared movement trajectory and less on the afferent feedback, which could explain the improved performance. However, a previous study from the lab did find a significant decrease in reaction times on a simple reaction time task following high frequency peripheral vibration, which suggests the mechanism involved in movement initiation may have been modulated.

Peripheral nerve stimulation can be used to determine synaptic efficacy. SEP attenuation with movement is thought to reflect changes in synaptic gain that may reflect modulations in estimates of sensory precision. Previous studies have shown that high frequency peripheral vibration decreased SEP amplitudes (Cohen and Starr, 1985), which supports the prediction that peripheral vibration reduced sensory precision. It would have been useful to confirm the effect of vibration and visual noise on synaptic efficacy by giving peripheral nerve stimuli throughout the experiments used in this thesis. Moreover, correlating SEP attenuation in response to vibration with changes in reaction time on a simple motor task will be important to determine whether this behavioural effect was driven by a change in synaptic efficacy in somatosensory cortex. However, in order to produce a reliable SEP the response from multiple stimuli must be averaged, therefore hundreds of movement trials averaged across different experimental conditions will be necessary. Determining alternative neurophysiological correlates of sensory precision that can be easily recorded in humans at the macroscale will be essential to testing the hypothesis that reducing sensory precision is important for motor control.

The role of vibration in these studies has been to directly modulate proprioceptive uncertainty. However, cortical somatosensory prediction errors from S1 to M1 that are proposed to be attenuated prior to movement represent a broad reafferent signal including both proprioceptive and cutaneous information (Adams et al., 2013a; Brown et al., 2013). It is difficult to determine whether peripheral vibration in these studies influenced behaviour by attenuating activity of muscle afferents or cutaneous afferents or both and whether dissociating between these is important. According to the active inference theory proprioceptive prediction errors in the spinal cord are resolved via the classical motor reflex arc; however, a descending control signal from the sensorimotor cortex directly modulates the gain of this reflex and somatosensory attenuation prior to movement occurs at multiple levels of the cortical hierarchy (Adams et al., 2013a). It is therefore difficult to determine the necessity of attenuating proprioceptive vs cutaneous information for motor initiation. Previous work using peripheral vibration has shown that muscle spindles are optimally activated at 80Hz and the increased firing of 1a afferents is associated with kinesthetic illusions (Ribot-Ciscar et al., 1998; Roll et al., 1989). However, in this thesis there was no direct measure of muscle spindle activity or of the presence or magnitude of kinesthetic illusions. I inferred that the reduction in beta oscillatory power following peripheral vibration was due to a specific down-weighting of proprioceptive prediction errors in the sensorimotor cortex, however this could equally be explained by a reduction in the precision of cutaneous reafferance.

Using different frequencies of vibration served to act as an active control for the cutaneous effect of vibration and to determine the specificity of muscle spindle activity on the outcomes measured. In study two (chapter four), 20Hz vibration had no effect on behaviour or on sensorimotor beta power; however, 20Hz is within the beta frequency range analysed in the cortex, therefore it is difficult to know whether this confounded the EEG result. In study three (chapter five), there was no behavioural difference between proprioceptive accuracy following 40Hz compared to 80Hz vibration, but there was also no significant difference between 40Hz and no vibration. This suggests that the 40Hz vibration potentially activated muscle spindles but not as efficiently as the optimal vibration frequency of 80Hz; however, it equally could suggest that there was no frequency specific effect, therefore the optimal activation of muscle spindles may not be integral for reducing beta power and estimates of somatosensory precision. It will be important to repeat the experiments in chapters two and three directly comparing a purely cutaneous peripheral stimulation with a purely proprioceptive one (if possible) and include microneurographic recordings from 1a afferents; this will aim to determine the specificity of reducing cutaneous vs proprioceptive precision for the modulation of sensorimotor beta power and movement initiation and thus further inform the predictions of the active inference framework.

There are other methods of manipulating sensory precision, which were not used in this thesis but could offer an important insight to assess the veracity of the predictions from the active inference framework. Dopamine has been highlighted as a potential candidate to modulate synaptic gain and thus sensory precision (Friston, 2005; K. J. Friston et al., 2011); therefore, future experiments using pharmacological manipulations of dopamine or measuring the behaviour of PD patients, in which dopamine in the basal ganglia is depleted, may offer a greater insight into the role of sensory precision in movement initiation. Interestingly, however, the current literature exploring the role of dopamine in predictive coding and motor control suggests that reducing dopamine reduces the precision-weighting of sensory prediction errors and this is associated with increased reaction times and bradykinetic symptoms in PD; this is the opposite to that hypothesised by the active inference framework. Dopamine has been highlighted as a potential modulator of motor flexibility, such as the ability to inhibit a prepared response and replace it with the correct action (Bestmann et al., 2014; Galea et al., 2012). PD patients with a specific loss of dopamine have impaired motor flexibility, which is improved with dopaminergic medication (Galea et al., 2012). Moreover, pharmacological D1 and D2 receptor blockade in healthy subjects specifically impaired participant's ability to react to unexpected events that generated large sensory prediction errors by replacing a prepared

action with another action (Bestmann et al., 2014). The authors suggest that dopamine depletion leads to an overreliance on top-down predictions, therefore there is a diminished response to low-level sensory prediction errors. This can be likened to a reduction in the precision-weighting of sensory prediction errors. In order to reconcile these findings with predictions from the active inference framework it is important to address the exact neurobiological connections that are modulated and the role of prediction errors in the tasks used.

Friston et al (2012) created a generative model across a number of motor areas with dopaminergic projections acting to modulate the synaptic gain on cortical projections transmitting prediction errors. The authors simulated dopaminergic depletion as a reduction in synaptic gain at multiple levels of this hierarchical model and found differential effects depending on the location of the reduction in gain. Reducing the gain in the motor cortex (encoding proprioception) and superior colliculus (encoding salience) lead to increased RTs. This task simulated reaching movements to a learned sequence of visual cues that was then altered. Similarly, the above tasks describe motor flexibility and selecting appropriate actions in response to visual information. Therefore, in these contexts dopamine may be acting to reduce the precision-weighting of exteroceptive information in the motor cortex. If this information is useful, such as in a cued reaction time task, reducing the weighting of this information with a dopaminergic block will increase RTs as shown. It is likely that a reduction in precision-weighting of somatosensory reafferance from S1 to M1 is most important specifically for motor initiation. For proprioceptive predictions to be preferentially selected, prediction errors from somatosensory cortex must be down-weighted; if the precision afforded to these prediction errors is too high than the cortex will try to resolve these by changing the prediction to move. One hypothesis is that beta oscillations specifically represent the modulation of somatosensory precision which is modulated directly by highe frequency vibration or indirectly through visual noise.

Synaptic gain can also be modulated by synchronous neuronal activity and the synaptic gain of coupled neuronal populations determines the frequency of their oscillatory behaviour, therefore EEG can be a useful tool to identify a neurophysiological correlate of sensory precision. In this thesis I hypothesise that sensorimotor beta oscillations may correlate with changes in sensory precision. Determining whether this oscillatory activity can represent a robust marker of sensory precision, therefore offers another method to modulate and measure this precision estimate to test the hypothesis that changes in sensory precision are important for movement initiation. Indeed, modulations in sensorimotor beta power with movement readily correlate with SEP attenuation: both of

these neurophysiological markers decrease prior to and during movement and increase after movement (Cohen and Starr, 1987; Davis et al., 2012; Engel and Fries, 2010; Starr and Cohen, 1985). In Parkinson's Disease (PD) a loss of dopamine in the basal ganglia results in increased resting beta power across the cortico-striatal loop (Little et al., 2012; Little and Brown, 2014) and dopaminergic medication is associated with a decrease in beta power and improved motor symptoms (Kühn et al., 2006b). As previously stated, it is posited that dopamine may play a role in modulating synaptic gain: changes in beta power and motor control may therefore directly reflect changes in sensory precision driven by this neuromodulator. How well the evidence in this thesis supports this hypothesis is discussed in the next section. With the assumption that sensorimotor beta power readily reflects sensory precision, the well characterised relationship between sensorimotor beta oscillations and motor control in patients with PD and healthy controls supports the prediction that sensory precision may play an important role in movement. However, more work is needed to better elucidate the specific relationship between beta oscillatory activity and sensory precision. Moreover, it is important to model and understand how beta oscillations may be generated at the cellular level; from this we can determine whether this oscillatory activity can causally modulate synaptic gain and thus have a mechanistic role in information processing or simply reflects an epiphenomenon of population activity.

7.2. Does sensorimotor beta power reflect estimates of sensory precision?

Circumstantial evidence regarding the similar relationship between SEP attenuation and the beta ERD with movement suggests that sensorimotor beta oscillations may reflect estimates of sensory precision in accordance with the active inference framework. In this PhD, I aimed to directly test this hypothesis by modulating sensory precision and measuring the effect of this on sensorimotor beta oscillations. Oscillations measured at a macroscopic level using M/EEG represent the cumulative summation of synchronous post-synaptic potentials on a group of apical dendrites of pyramidal cells in layer V of the cortex, which are thought to transmit prediction errors up the cortical hierarchy (Friston, 2005; Friston and Kiebel, 2009). The magnitude of these post-synaptic potentials will be modulated by the post-synaptic gain thought to represent changes in precision. From this it has been suggested that precision can only be measured at the macroscale by its effect on the prediction error signal; therefore, synchronous oscillatory activity from these cells most likely represents precision-weighted prediction errors.

Indeed, in study four (chapter six) of this thesis beta power readily correlated with both prediction error and precision following a movement. However, inferences from this data are limited by the resolution of EEG. Biophysical modelling and multi-unit recordings in primates will give a better understanding of how neuronal firing rates and population dynamics can encode precision and prediction error and therefore determine how independent these parameters are in the brain. This will be useful to determine exactly what is being represented by sensorimotor beta activity measured at the scalp. Moreover, it will be important to determine whether sensorimotor beta oscillatory activity has a specific role in modulating synaptic gain in order to suggest that this activity specifically encodes sensory precision. Transcranial alternating current stimulation (tACS) has been used to entrain the motor cortex in a beta rhythm and caused participants to move slower in a motor task (Pogosyan et al., 2009). The mechanism by which beta oscillatory activity reduced movement speed may be through increasing sensory precision in accordance with the active inference framework. By recording SEPs during and following beta tACS, it may be possible to determine whether sensorimotor beta oscillatory activity can actually modulate synaptic gain and provide further evidence that changes in movement that correlate with changes in beta power are driven by changes in synaptic gain.

In this thesis I found evidence to support the hypothesis that sensorimotor beta power would be positively correlated with changes in sensory precision. In study two (chapter four), a reduction in proprioceptive precision caused by high frequency vibration to the wrist led to a decrease in sensorimotor beta power in line with this hypothesis. In study four (chapter six), the post-movement beta synchronisation (PMBS) negatively correlated with estimates of prediction error, the posterior mean and the precision-weighting attributed to sensory prediction errors at the first level of the HGF; and the beta power decrease prior to movement negatively correlated with estimates of the precision-weighting of prediction errors. This relationship was the opposite to hypothesised. There are three different explanations that can reconcile these results.

Firstly, in study two (chapter four) I modulated uncertainty in the somatosensory domain, whereas in study four (chapter six) I modulated uncertainty in the visual domain. The active inference framework posits that the generative model in the motor cortex converts visuospatial predictions in extrinsic coordinates into proprioceptive predictions in intrinsic coordinates; therefore, the motor cortex acts as a multisensory integration hub and incorporates information from exteroceptive and proprioceptive inputs to predict the sensory consequences of subsequent movements (Adams et al., 2013a). If we assume that exteroceptive and proprioceptive information are integrated in a Bayesian manner within the motor cortex (as has been previously suggested; Bays and Wolpert, 2007), then

decreasing precision in the exteroceptive domain would increase the relative precision in the somatosensory domain. Therefore, if sensorimotor beta oscillations are positively correlated with somatosensory precision, then preparatory beta power should inversely correlate with visual precision as shown. It has previously been shown that the end point accuracy of reaching movements is influenced by visuomotor and proprioceptive information differently depending on the precision weighting of these inputs (van Beers et al., 1999); indeed, the behavioural effect in study three (chapter five) was explained in light of this idea. To test the hypothesis that beta oscillations specifically represent the relative precision of proprioceptive inputs compared to other exteroceptive inputs to motor cortex, M/EEG should be recorded during a behavioural task in which these inputs need to be integrated and can be independently modulated.

Secondly, an alternative explanation for the findings in this thesis is that beta power actually correlates with the precision surrounding proprioceptive predictions produced in the motor cortex rather than prediction errors. Previous research suggests that beta power correlates readily with uncertainty in the forward model that generates motor commands (Tan et al., 2016). In addition, studies in the visual domain have suggested that predictive coding occurs via a canonical circuit in the brain in which predictions are transmitted via backward connections in the beta frequency band and prediction errors are transmitted via forward connections in theta and gamma frequency bands (Bastos et al., 2012; Bauer et al., 2014). This hypothesis therefore fits with other models of predictive coding in the brain that beta power should represent predictions and not prediction errors. In study four (chapter six), reducing the precision in visual information used to guide movement would theoretically increase the reliance on top-down prior proprioceptive information to inform predictions about the sensory consequences of the movement; therefore, if beta power more readily reflects the precision of these predictions, this would explain the inverse correlation between pre-movement beta power and visual precision.

However, when somatosensory precision is reduced (using vibration) in a context where only proprioceptive information is needed to inform proprioceptive predictions, as in study two (chapter four) (at rest with no task), then paradoxically this could reduce the precision of subsequent proprioceptive predictions. This is because empirical priors are posterior distributions passed down from the level above (here I hypothesise that this is from S1 to M1) and the precision of this posterior will already have been influenced by the proprioceptive input. Therefore, the decrease in sensorimotor beta power with peripheral vibration may actually reflect changes in the precision of proprioceptive predictions. The relative precision of prior and sensory information is hypothesised to be combined into a

single modulation of post-synaptic gain, therefore it is difficult to dissociate these forms of uncertainty neurobiologically and is further complicated by the multisensory integration necessary to form accurate proprioceptive predictions. One method to tease apart the neurophysiological correlates of these forms of uncertainty would be to independently modulate or correlate estimates of precision at different hierarchical levels with oscillatory activity. In study four (chapter six) sensorimotor beta power correlated readily with estimates from the first level of the HGF; however, it is difficult to know if this was simply because the task did not effectively modulate parameters at the second level.

A final hypothesis is that there is not a single unifying hypothesis for the functional role of sensorimotor beta oscillations. The correlation between precision and beta power in study four (chapter six) occurred prior to the GO signal in the visuomotor adaptation task and was the inverse relationship to that predicted by the active inference framework. This suggests that modulations in precision may not have been necessary for motor initiation. Sensorimotor beta power at this time point more likely represent computations involved in motor preparation that are effected by visual uncertainty; however, this could be separate from the computations that occur at movement initiation during the beta ERD. Recent behavioural evidence suggests that motor preparation and motor initiation are independent processes that likely involve different neural computations (Haith et al., 2016). As oscillatory activity represents the summation of post-synaptic potentials across pyramidal neurons in a cortical region, one could assume that different inputs to those pyramidal neurons could create the same oscillatory signal; however, this activity may be dominated more by inputs from different cortical regions at slightly different time points. In line with this, beta power could represent both changes in precision that are associated with motor preparation and those associated with motor initiation. This would suggest that beta power in the motor cortex more readily reflects an epiphenomenon of the computational processes occurring in the region rather than being mechanistically involved in the processes.

Importantly, I have assumed that the beta power measured in chapters two and four has the same cortical source; however, neurophysiological evidence suggests that the machinery is present in both primary motor and primary somatosensory cortices to generate beta oscillations. Beta power could theoretically represent precision in both cortical areas; however, this precision could relate to a different input. In somatosensory cortex, afferent feedback providing somatosensory prediction errors is likely to be the most important input; therefore, beta power in this area may reflect the precision of this signal. This could be what was reflected in the modulation of beta power with peripheral vibration. The primary motor cortex, on the other hand, has a primary role in generating

motor commands or in this case proprioceptive predictions for movement. Therefore, beta power in this region could directly reflect the precision of proprioceptive predictions for movement. This may have been modulated in the visuomotor adaptation task in study four (chapter six). It will be interesting to carry out studies manipulating different forms of exteroceptive and proprioceptive uncertainty using high-spatial resolution MEG (Bonaiuto et al., 2017; Meyer et al., 2017). This could potentially isolate sources of different components of beta power that may be modulated differently depending on the type of sensory uncertainty manipulated and thus have differential effects on behaviour. These recent techniques have even been able to dissociate sources of activity from superficial and deep layers of the cortex, which would provide even more information regarding the functional role of beta power in predictive coding in the sensorimotor system.

To further elucidate whether sensorimotor beta oscillations may reflect changes in sensory precision and potentially whether this activity could causally modulate sensory precision, it is important to understand how this activity can be generated in the brain at the cellular level. As we can only record macroscopic changes in oscillatory activity on the scalp using M/EEG in healthy human participants, mathematical models are key to hypothesising how this activity might be generated. A number of biophysical models based on the intrinsic membrane properties and neuronal firing rates of specific types of neurons within a network demonstrate that the neuronal machinery exists within both the motor and somatosensory cortices to produce beta oscillatory activity (McCarthy et al., 2008; Roopun et al., 2006). These models are supported by electrophysiological recordings from animal studies measuring single cell firing and local field potentials (LFPs) simultaneously. The abnormal increase in sensorimotor beta oscillations following dopamine depletion in PD patients has led to the hypothesis that beta oscillations are generated subcortically. The STN-GPe pacemaker hypothesis describes how reciprocal connections between excitatory STN neurons and inhibitory GPe neurons with synaptic transmission delays equivalent to a beta period can generate beta oscillations. This system requires a strong excitatory drive from the cortex (Holgado et al, 2010), which has been confirmed by extracellular recordings from the STN and GPe in Parkinsonian rats (Holgado et al, 2014). In humans, simultaneous MEG and STN-LFP recordings revealed a strong functional drive from the cortex to the STN (Litvak et al., 2011); however, this coherence was in the upper beta band (25-30Hz), whereas pathological increases in beta power in PD occur in the lower beta band (18-20Hz). This suggests that different frequencies of beta oscillatory activity may represent different functions within the sensorimotor system. DCM studies have been used to demonstrate that pathological beta

activity in PD is caused by an increase in the cortical drive to the STN and this is associated with changes in the coupling between STN and GP neurons (Marreiros et al., 2013; Moran et al., 2011). Interestingly, the abnormal neuromodulation in the basal ganglia caused by a loss of dopaminergic input into the striatum was associated with changes in synaptic gain on DCMs that produced beta synchrony in the STN. This supports the hypothesis that changes in beta activity in PD may represent modulations in precision caused by changes in synaptic gain. However, it is not known how changes in beta activity in the basal ganglia and the STN can then actually modulate movements.

An interesting new theory regarding the generation of beta oscillations in the cortex suggests that cortical beta oscillatory activity is driven by an exogenous drive likely to come from the thalamus. (Sherman et al., 2016) have proposed that beta oscillations do not represent a sustained network rhythmicity as inferred from time-locked data averaged over multiple trials; instead MEG and LFP recordings from humans, mice and monkeys have revealed transient beta events (<150ms) that have a consistent, stereotypical waveform and duration. The authors generated a biophysical model of the somatosensory cortex that could produce post-synaptic currents in apical dendrites of pyramidal neurons that could be directly compared with M/EEG and LFP data. The model revealed that a weak and broad proximal drive from layer IV to the proximal dendrites of pyramidal neurons and coupled inhibitory interneurons in layers 2/3 and layer V, alongside a simultaneous strong drive to the distal dendrites of those neurons could produce beta events with the exact waveform seen in the experimental data. Giving a 20Hz drive indicative of entrainment of the cortex from beta activity in the basal ganglia did not produce the same beta events nor did introducing an M-current. This study suggests that beta oscillatory activity can be produced in the cortex independently from the basal ganglia and has a number of implications for our understanding of the generation and function of sensorimotor beta power.

Firstly, the authors stipulate the requirement of two exogenous drives to the cortex to generate beta oscillations and postulate two distinct pathways from the thalamus to the cortex in primates, which could provide these inputs: 1) “a focally projecting…”driving” pathway that carries sensory information from the periphery”; and, 2) “a widespread, nonspecific modulatory pathway projecting directly to supragranular layers.” One hypothesis is that the first input represents sensory prediction errors, whereas the second input serves to set the precision of the prediction errors. Indeed, the second neuromodulatory pathway has been suggested to modulate overall activity without eliciting any spikes in the recipient area in line with the role of precision in active inference. This suggests that somatosensory beta power could readily represent

precision-weighted prediction errors and is supported by the finding in study two (chapter four) where the variance in sensorimotor beta power was explained by both modulations in the magnitude and precision-weighting of prediction errors. Moreover, the ventromedial or pallidal thalamus has been shown to project to the supragranular layers in sensory and motor cortex, therefore offers a pathway whereby an aberrant signal from the basal ganglia in PD could increase beta power in the cortex (Herkenham, 1980); however, as stipulated by Sherman et al (2016) the beta events described do not occur via a 20Hz entrainment of the cortex by the basal ganglia.

Secondly, this paper suggests that current analyses of oscillatory activity in the brain incorrectly suggest that oscillations are rhythms which are sustained over time for multiple cycles, which therefore has implications for hypotheses regarding the mechanism by which this activity may influence information processing. This paper, and others (Feingold et al., 2015; Jones et al., 2010; Lundqvist et al., 2016; Parkkonen et al., 2015) demonstrate that oscillatory activity occurs as discrete, transient events across trials. When these events are averaged across trials in the spectral domain, the averaged signal represents the accumulation of these induced signals, because power is non-negative and therefore the signals do not cancel out. This suggests that high power activity in the average likely reflects the frequency of oscillatory events occurring at that time point over trials. The role of oscillatory activity in cognitive and motor tasks may therefore be best explained by the probability with which these bursts occur. This mechanism lends itself readily to encoding parameters in Bayesian inference, which are represented as probability distributions. One hypothesis could be that the probability of a beta event occurring in M1, potentially generated by a forward drive from S1, may represent the precision-weighting of the prediction error signal; a decreased likelihood of these beta events may reflect decreased precision-weighting such that the forward signal has less influence over other computational processes and may therefore allow, for example, the activation of the descending proprioceptive signal that will then initiate movement in the spinal cord. In line with this research, future work should aim to characterise the presence and frequency with which these beta events occur on a trial-by-trial basis and correlate this with trial-wise performance on a simple motor task.

The study by Sherman et al (2016) is a seminal piece of work that highlights a number of important fundamental issues in neuroimaging that have been recently explored by De Wit et al (2017). It is very common for neural signals to be analysed and interpreted from the perspective of the experimenter without an informed understanding of how the brain could receive and decode those signals. Shannon's original formulation of information states that information can only be quantified relative to a transmitter and receiver;

therefore, without tracking the flow of neural activity between cortical areas and understanding how a different brain region could interpret the recorded signal, inferences regarding the functional role of the neural signal in information processing are obsolete. Averaging over trials of neuroimaging data highlights this misunderstanding: the brain will only ever see and respond to trial-wise changes in neural activity. Indeed, beta oscillatory activity is wrongly assumed to occur as a sustained rhythm in the brain due to an artefact of averaging power (Sherman et al., 2016) and ERPs are likely a by-product of averaging caused by the interaction of travelling waves (Alexander et al., 2013). The neuroimaging results in this thesis can be criticised for being interpreted with the "experimenter-as-receiver".

To understand whether beta oscillations have a mechanistic impact on information processing, and in this case motor initiation, it is important to use effective connectivity analyses to determine whether the changes to beta power in M1 readily predict changes in oscillatory activity in other cortical regions. In addition, it is important to track how feedforward activity transmitting visual or proprioceptive prediction errors, or neuromodulatory activity, could modulate beta activity in sensorimotor cortex. There have been a number of DCM studies to determine how predictions and prediction errors may be transmitted in different frequencies of oscillatory activity throughout the cortex (Bastos et al., 2012; Kerkoerle et al., 2014), but this work is missing from the sensorimotor system. In particular, more work with high-spatial resolution techniques is needed to understand the connectivity between somatosensory and motor cortices either side of the central sulcus and potentially dissociate the functional role of beta oscillations separately in each area by determining the effect of this activity on downstream targets. Moreover, all the work in this thesis has focused on beta power, however previous studies have suggested that more information is carried in the phase of oscillatory activity (Schyns et al., 2011). Future work should dissociate whether phase, power or frequency of this oscillatory activity is most important for predicting activity in downstream targets that are important for motor initiation.

7.3. Implications for understanding and treating Parkinson's Disease (PD)

According to the hypothesised relationship between sensory precision, sensorimotor beta power and motor initiation, I hypothesise that PD patients have increased precision in their proprioceptive state and this explains the akinetic and bradykinetic symptoms typical of PD. By placing too much weight on their current proprioceptive state,

proprioceptive predictions about the sensory consequences of movement are not fulfilled. In support of this hypothesis, SEP attenuation is reduced in PD patients and dopaminergic medication normalises SEP attenuation and improves motor symptoms (Macerollo et al., 2016). Similar results have been found in patients with functional movement disorders (A Macerollo et al., 2015). Moreover, PD patients have abnormal gating of 1a afferents in the spinal cord: it is this circuitry that is hypothesised to play a central role in movement initiation in active inference and be mediated by modulations of precision in the cortex. The central control of descending inputs on 1a afferents can be measured using the size of the H-reflex: this is a reactionary muscle contraction elicited by electrical stimulation of Ia afferents from muscle spindles, which activates the monosynaptic stretch reflex (Angel and Hofmann, 1963; Purves et al., 2001b). Descending presynaptic inhibition of the Ia afferent volley onto alpha motor neurons in the spinal cord modulates the gain of this reflex (Delwaide, 1973; Zehr and Stein, 1999). During gait initiation, the H-reflex of the soleus muscle is reduced, which suggests the gain of this circuit is reduced. The magnitude of this reduction inversely correlated with disease severity in PD such that those with more severe symptoms showed less H-reflex attenuation, similar to that seen with SEPs at the scalp (Hiraoka et al., 2005). Moreover, using a specifically designed conditioning paradigm, (Morita et al., 2000) showed that PD patients have less presynaptic inhibition of Ia afferents compared to healthy controls (suggesting an increase in the gain of the H-reflex) and found that the degree of presynaptic inhibition correlated with bradykinesia and the time to walk 10m in PD patients. In addition, the amount of presynaptic inhibition increased with levodopa treatment along with an improvement in bradykinesia, which suggests that dopamine may modulate this central descending afferent gating in the spinal cord. Stimulation of the sensorimotor cortex in the cat has been shown to decrease presynaptic inhibition at Ia afferent terminals (Lundberg and Vyklický, 1963; Rudomín et al., 1983), which suggests that this gain is modulated by a central descending signal. Indeed, Adams et al (2013) posit that modulations of precision are transmitted from the somatosensory cortex to the spinal cord via a descending input, which supports that PD patients may have increased somatosensory precision and this may influence their motor symptoms.

Based on these studies, the experiments in this thesis could be extended by measuring the effects of modulating sensory precision on the H reflex, the SEP, cortical oscillatory activity and motor initiation simultaneous. In this way the mechanism by which somatosensory precision can causally effect motor control can be better understood. Importantly, testing novel mechanisms by which motor symptoms could occur in PD generates novel avenues for therapeutic interventions. Deep Brain Stimulation (DBS) is currently the leading

treatment for PD, however this is extremely invasive and is not suitable for all PD patients (Okun et al., 2004; Okun and Foote, 2010). One hypothesis is that this high frequency stimulation in the basal ganglia interferes with the reafferant signal reaching the somatosensory cortex and reduces the precision of somatosensory prediction errors. Indeed, DBS of the pedunculopontine nucleus has been shown to reduce the amplitude of the H reflex (Pierantozzi et al., 2008). However, much more work needs to be done to test this hypothesis especially as the exact pathways affected by DBS will depend on the site of stimulation. Modulating somatosensory precision, non-invasively in the periphery, may offer an alternative method for symptom management in PD for those who cannot receive DBS. Indeed, there has been a long history of using vibration to treat PD since Charcot's "Vibrating Chair" (Charcot, 1892), but the results have been mixed (Arias et al., 2009; Chouza et al., 2011; Ebersbach et al., 2008; Haas et al., 2006; Kapur et al., 2012; King et al., 2009). This is likely due to differences in the vibration protocols used, the muscles targeted, the behaviors being measured and the patient groups studied. A better understanding of the mechanism by which this therapy could work and the advancement in wearable technology may allow this method to be refined offering a novel therapeutic avenue for PD.

However, the pathology in PD suggests that these patients may have reduced rather than increased proprioceptive precision. Numerous psychophysical studies suggest that kinesthesia (the conscious awareness of the position or movement of the limb) is reduced in PD: patients with PD have a decreased sensitivity to detect small changes in limb position (Maschke et al., 2003), finger position (Putzki et al., 2006) and limb motion (Konczak et al., 2007) compared to healthy controls and this impairment has been shown to correlate with disease severity (Maschke et al., 2003). Interestingly, patients with spinocerebellar ataxia do not show the same impairment and perform comparably to healthy controls, which suggests that the basal ganglia may play an important role in kinesthesia (Maschke et al., 2003). Electrophysiological recordings from primate models of PD and PD patients demonstrate that the processing of proprioceptive information in the basal ganglia is noisier and less precise in PD. Pallidal cells in a Parkinsonian primate model show increased firing during passive movement at multiple joints compared to healthy primates demonstrating a lack of specificity in the tuning of pallidal cells to specific joints (Filion et al., 1988). The tuning of the receptive field of thalamic neurons receiving input from the basal ganglia is also broadened in PD suggesting noisier and less differentiated proprioceptive information is sent to cortical regions (Pessiglione et al., 2005). Moreover, neurons within the basal ganglia are more synchronised in PD, which suggests a reduced responsiveness to signals related to a particular context or action

further implying that the SNR of basal ganglia neural processing is reduced in PD (Bar-Gad and Bergman, 2001).

It has previously been suggested that PD is a disorder of gain control of sensorimotor integration (Kaji, 2001; Kaji et al., 2005) and that dopamine may act to modulate a gain control for the responsiveness of the organism to the environment (Schultz, 2007), which supports ideas within the active inference framework. However, this evidence suggests PD patients have reduced rather than increased precision-weighting of afferent signals from the basal ganglia. In order to reconcile this with the hypothesis that PD patients have increased proprioceptive precision in the cortex and spinal cord, I hypothesise that cortical estimates of sensory precision in PD do not readily reflect the true proprioceptive state. There are two mechanisms by which this could occur. Firstly, this may be part of the pathology; the increased synchronicity in the beta band in the basal ganglia may lead to abnormal increased beta in the cortex, which is interpreted as an increased estimate of somatosensory precision. Secondly, the brain may attempt to resolve the state of disorder caused by the aberrant input from the basal ganglia by increasing the estimate of sensory precision in the cortex via a top-down mechanism. According to the active inference framework, reduced proprioceptive precision caused by dopamine depletion in the basal ganglia would increase the relative weighting on top-down proprioceptive predictions to move. This biases the system towards the top-down predictions, which would most likely result in aberrant movements; therefore, the Parkinsonian state may reflect the brain trying to overcompensate and correct for this by increasing the precision weighting of other sensory inputs to the cortex. In this way the increased beta power acts as a brake on movement and indeed previous research has shown that increasing beta power has an inhibitory effect on motor control (Pogosyan et al., 2009). Interestingly, the deafferented patient IW reports "suddenly I found myself in a hospital bed to all intents and purposes paralysed from the neck down" ("Pride and a Daily Marathon," n.d.). This is perhaps an example of the brain trying to correct for the sudden uncertain afferent input and the result is an inability to move. After a short-time the brain adapts to the lack of a clear afferent input by placing more weight on visual information to be able to move.

However, it is difficult to test this idea experimentally as patients already have the disease when they are tested. One hypothesis would be that this increased somatosensory precision in the sensorimotor cortex, potentially modulated by frontal areas, would be reflected in higher-order measures of precision, such as confidence ratings. PD patients may produce large proprioceptive errors, but may be unaware and overly confident in those movements. A recent study showed that OCD patients had a dissociation between their confidence judgements and actions, such that they were able to integrate the history

of sensory evidence to accurately estimate confidence ratings, but their actions were based only on the most recent sensory evidence (Vaghi et al., 2017). This suggests that it is feasible in a diseased state to have an uncoupling between these facets. To my knowledge, there is currently no evidence to suggest that PD patients have intact metacognitive awareness of their proprioceptive ability. It will be interesting to repeat the proprioceptive target matching task in study three (chapter five) in PD patients to quantify this relationship.

Moreover, it will be important to further quantify the role of sensorimotor beta power in representing sensory precision by determining if this information readily contributes to the generation of confidence ratings. This will aim to determine exactly what level of the hierarchy sensorimotor beta oscillations represent the processing of motor information. Indeed, within the sensorimotor system the sensorimotor cortex is at the higher end of the hierarchy, therefore it is likely that activity in this area could mediate conscious awareness of the sensorimotor state, which is dissociable from activity in downstream areas of this. It has recently been reported that individual differences in confidence ratings can be determined by the relative weighting individuals give to two computations of confidence: 1) the probability of the given decision or action being correct; 2) the precision of the sensory evidence used to make the decision (Navajas et al., 2017). The precision term used has a specific dimension relevant to the task measured, therefore the authors suggest this represents a domain-specific computation, which is likely fed-forward to frontal areas involved in generating metacognitive judgements. In this thesis, I found that mean confidence judgements across participants in a proprioceptive reaching task were based on precision-weighted proprioceptive errors, which suggests that the proprioceptive precision is likely used to generate metacognitive judgements in the sensorimotor domain. It will be important to correlate confidence ratings and beta power particularly in a task and population where confidence and performance may dissociate. Moreover, it will be important to determine whether this oscillatory activity predicts, or is predicted by, activity in frontal areas, which have been shown to be important for metacognition (Fleming et al., 2010; Fleming and Dolan, 2012). This “cortex-as-receiver” design will provide evidence that this beta power is mechanistically important and that it plays a functional role in generating domain-specific confidence judgements about the sensorimotor system. It may also be important to extend this further to include a task that dissociates confidence within the somatosensory system and motor system to determine whether sensorimotor beta power more readily reflects one of these domains.

7.4. The role of modelling in cognitive neuroscience

In this thesis I have used computational modelling to understand the function of neuronal oscillations in the brain. The integration of computational neuroscience into functional neuroimaging has allowed us to access latent variables, assumed to have a functional role in neuronal processing, and use these to predict neural responses observable with M/EEG or fMRI. This method therefore extends previous work in which experimental variables are used as proxies for computational estimates in order to provide more specific hypotheses about the mechanisms underlying particular behaviours and their neurophysiological correlates. However, this method cannot address the underlying neuronal dynamics which play an integral role in neuronal processing. Biophysical models aim to understand the causes of neural responses by modelling the intrinsic and extrinsic connections within and between cortical sources of activity. DCMs therefore allow experimenters to hypothesise how experimental perturbations influence effective connectivity between regions and the balance of excitatory and inhibitory connections within brain areas. Sophisticated neural mass models are based on electrophysiological data and therefore provide a more realistic inference about the mechanisms that explain observed neuronal responses. This is an important step to advance our current understanding of the brain and ensure that we focus our interpretations of neuroimaging data in terms of what information *the brain* can see, use and communicate.

DCMs use Bayesian inversion to determine the efficacy of the generative model, therefore Bayesian model comparison can be used to determine the model that best explained the data based on the Bayesian model evidence. However, this highlights a fundamental problem with the current use of modelling in neuroimaging and cognitive neuroscience: there is no guarantee that the true model was amongst those tested. It is therefore difficult to conclude anything about how the brain actually works from these methods. We rely on the assumptions of the models we use being correct with no guarantee that they are. The use of biophysical models has the advantage that the models are built in accordance with current empirical evidence from electrophysiological studies; however, these will only be as accurate as the latest cellular evidence and recording techniques.

The models referred to in this thesis are Bayesian, therefore the inferences I have made allude to the brain acting as a Bayesian inference machine. However, there is a lack of understanding of how Bayesian inference is computed in the brain. Bayesian models have proved very useful at predicting people's behaviour across a number of contexts including sensorimotor control (Ernst and Banks, 2002; Gopnik et al., 2004; Knill, 1998; Körding and Wolpert, 2004; Tenenbaum et al., 2006; van Beers et al., 1999; Wolpert et al., 1995).

However, these studies do not demonstrate that the brain actually uses Bayesian statistics to integrate information; non-Bayesian models could also be used to explain the integration of information (Gigerenzer and Brighton, 2009; Juslin et al., 2009). In order to determine if the brain uses Bayesian inference, it is imperative to demonstrate that neurons encode uncertainty or probability distributions, however the current literature is not conclusive (Deneve, 2007; Knill and Pouget, 2004; Ma et al., 2006; Rao, 2004). In this thesis, I have demonstrated that sensorimotor beta oscillations correlate with uncertainty estimates, which supports previous studies regarding the role of this activity (Tan et al., 2016); however, this work fails to demonstrate whether and how the brain utilises this information. Even if the machinery is present for the brain to be able to compute Bayesian statistics, this doesn't mean that the brain actually does. More work needs to focus on identifying how neuronal firing rates can integrate information at the neuronal and population levels across different domains and how this information is transmitted between cortical regions potentially by using DCMs. Before these fundamental studies have been completed, we cannot confirm that Bayes-optimal behaviours are actually Bayesian.

One issue with Bayesian models, and a key criticism of the active inference framework, is that they are so flexible, they cannot be falsified. Bayesian models have numerous free parameters and degrees of freedom, which allow the modeller to generate any predictions they want. Indeed, Brown et al (2013) created a generative model designed to explain how a decrease in sensory precision is necessary for movement by linking these parameters such that an increased expectation of an internally generated force would decrease sensory precision. In this way, the authors could guarantee the model would be able to explain existing evidence of perceptual and physiological sensory attenuation based on this hypothesis. Indeed, the active inference framework was built upon existing literature about the neurophysiology of connections within the sensorimotor system, therefore novel empirical work to test the model will most likely confirm these findings and thus the model becomes self-fulfilling. Moreover, the framework accommodates new data to generate and extend the model; it is therefore difficult to design an experiment that will definitively disprove this theory. Nevertheless, this theory generates a number of novel predictions, which will increase the number of new paradigms developed and can only enhance our understanding of the brain further. It is imperative that we acknowledge the flexibility of many models in cognitive neuroscience and therefore design stringent and constrained experiments to provide empirical evidence for well-defined experimental predictions.

7.5. CONCLUSION

In this thesis, I tested a specific prediction from the active inference framework that a reduction in sensory precision is necessary to allow movement initiation to occur. The evidence in this thesis supports this hypothesis, but is far from conclusive. I have shown that sensory attenuation can occur at different levels of the cortical hierarchy and the level at which this modulation in sensory precision occurs will determine the functional impact of this change in synaptic efficacy. I have also shown that sensorimotor beta oscillations readily correlate with modulations in proprioceptive and visual uncertainty and computational estimates of sensory precision. I have shown that those changes in uncertainty modulate behaviour in accordance with the active inference framework. However, there are a number of underlying assumptions of the work in this thesis that must be corroborated before conclusions can be drawn about the validity of the predictions from the active inference framework. Firstly, it is not clear whether or how changes in the uncertainty of afferent input modify synaptic gain, and thus sensory precision. It will be important to use brain stimulation, microneurography and in vivo electrophysiological recordings in primates to determine the effect of peripheral vibration on synaptic efficacy in the cortex and spinal cord. Secondly, it will be important to determine whether beta oscillatory activity, potentially transmitted from another cortical region, plays a role in modulating synaptic gain or is a consequence of a change in synaptic gain caused by a cellular mechanism, such as spike-timing dependent plasticity. Finally, it will be important to use a wide range of alternative Bayesian and non-Bayesian models to explain the integration of visual and proprioceptive information in sensorimotor cortex under different levels of uncertainty to determine whether generative models designed to optimise free energy optimally explain behavioural data and neural oscillations.

The active inference framework is a novel theory that aims to produce a unifying hypothesis for how the brain integrates sensory information for perception and action. The framework uses a hierarchical generative model, which incorporates the computational principles of predictive coding and Bayesian inference, to understand the causes of sensory input and motivate behaviour. Unlike other models of sensorimotor control, this theory attempts to map the components of this computational mechanism onto the machinery of the brain in order to determine how the brain functions. The flexibility of this computational work makes this model difficult to falsify; however, the complexity of the brain requires a framework that can be moulded to explain new data.

One major challenge caused by the incorporation of computational modelling into our understanding of how the brain works is that we move further away from recording and

understanding what is actually happening in the brain; instead we infer functionality from parameters and estimates that we as modellers have crafted. It is imperative that we use multi-modal neuroimaging, from single cell recordings to M/EEG, to ensure that the fundamental assumptions underlying the models we use are accurate and combine these with connectivity analyses to ensure the information we are measuring from the brain is interpretable and useful for the brain.

REFERENCES

Abbruzzese, G., Abbruzzese, M., Favale, E., Ivaldi, M., Leandri, M., Ratto, S., 1980. The effect of hand muscle vibration on the somatosensory evoked potential in man: an interaction between lemniscal and spinocerebellar inputs? J. Neurol. Neurosurg. Psychiatry 43, 433–437.

Adams, R.A., Shipp, S., Friston, K.J., 2013a. Predictions not commands: active inference in the motor system. Brain Struct. Funct. 218, 611–643. https://doi.org/10.1007/s00429-012-0475-5

Adams, R.A., Stephan, K.E., Brown, H.R., Frith, C.D., Friston, K.J., 2013b. The computational anatomy of psychosis. Front. Psychiatry 4, 47. https://doi.org/10.3389/fpsyt.2013.00047

Aitchison, L., Bang, D., Bahrami, B., Latham, P.E., 2015. Doubly Bayesian Analysis of Confidence in Perceptual Decision-Making. PLOS Comput. Biol. 11, e1004519. https://doi.org/10.1371/journal.pcbi.1004519

Alegre, M., Alvarez-Gerriko, I., Valencia, M., Iriarte, J., Artieda, J., 2008. Oscillatory changes related to the forced termination of a movement. Clin. Neurophysiol. Off. J. Int. Fed. Clin. Neurophysiol. 119, 290–300. https://doi.org/10.1016/j.clinph.2007.10.017

Alegre, M., Gurtubay, I.G., Labarga, A., Iriarte, J., Malanda, A., Artieda, J., 2003. Alpha and beta oscillatory changes during stimulus-induced movement paradigms: effect of stimulus predictability. Neuroreport 14, 381–385.

Alegre, M., Imirizaldu, L., Valencia, M., Iriarte, J., Arcocha, J., Artieda, J., 2006. Alpha and beta changes in cortical oscillatory activity in a go/no go randomly-delayed-response choice reaction time paradigm. Clin. Neurophysiol. Off. J. Int. Fed. Clin. Neurophysiol. 117, 16–25. https://doi.org/10.1016/j.clinph.2005.08.030

Alexander, D.M., Jurica, P., Trengove, C., Nikolaev, A.R., Gepshtein, S., Zvyagintsev, M., Mathiak, K., Schulze-Bonhage, A., Ruescher, J., Ball, T., van Leeuwen, C., 2013. Traveling waves and trial averaging: The nature of single-trial and averaged brain responses in large-scale cortical signals. NeuroImage 73, 95–112. https://doi.org/10.1016/j.neuroimage.2013.01.016

Alexander, D.M., Trengove, C., van Leeuwen, C., 2015. Donders is dead: cortical traveling waves and the limits of mental chronometry in cognitive neuroscience. Cogn. Process. 16, 365–375. https://doi.org/10.1007/s10339-015-0662-4

Allen, M., Frank, D., Schwarzkopf, D.S., Fardo, F., Winston, J.S., Hauser, T.U., Rees, G., 2016. Unexpected arousal modulates the influence of sensory noise on confidence. eLife 5, e18103. https://doi.org/10.7554/eLife.18103

Angel, R.W., Hofmann, W.W., 1963. The H Reflex in Normal, Spastic, and Rigid Subjects: Studies. Arch. Neurol. 8, 591–596. https://doi.org/10.1001/archneur.1963.00460060021002

Arias, P., Chouza, M., Vivas, J., Cudeiro, J., 2009. Effect of whole body vibration in Parkinson's disease: a controlled study. Mov. Disord. Off. J. Mov. Disord. Soc. 24, 891–898. https://doi.org/10.1002/mds.22468

Ariff, G., Donchin, O., Nanayakkara, T., Shadmehr, R., 2002. A Real-Time State Predictor in Motor Control: Study of Saccadic Eye Movements during Unseen Reaching Movements. J. Neurosci. 22, 7721–7729.

Arnal, L.H., Giraud, A.-L., 2012. Cortical oscillations and sensory predictions. Trends Cogn. Sci. 16, 390–398. https://doi.org/10.1016/j.tics.2012.05.003

Arnal, L.H., Wyart, V., Giraud, A.-L., 2011. Transitions in neural oscillations reflect prediction errors generated in audiovisual speech. Nat. Neurosci. 14, 797–801. https://doi.org/10.1038/nn.2810

Babiloni, C., Babiloni, F., Carducci, F., Cincotti, F., Cocozza, G., Del Percio, C., Moretti, D.V., Rossini, P.M., 2002. Human Cortical Electroencephalography (EEG) Rhythms

during the Observation of Simple Aimless Movements: A High-Resolution EEG Study. NeuroImage 17, 559–572. https://doi.org/10.1006/nimg.2002.1192
Baker, S.N., 2007. Oscillatory interactions between sensorimotor cortex and the periphery. Curr. Opin. Neurobiol. 17, 649–655. https://doi.org/10.1016/j.conb.2008.01.007
Baker, S.N., Chiu, M., Fetz, E.E., 2006. Afferent encoding of central oscillations in the monkey arm. J. Neurophysiol. 95, 3904–3910. https://doi.org/10.1152/jn.01106.2005
Baker, S.N., Olivier, E., Lemon, R.N., 1997. Coherent oscillations in monkey motor cortex and hand muscle EMG show task-dependent modulation. J. Physiol. 501, 225–241.
Baker, S.N., Pinches, E.M., Lemon, R.N., 2003. Synchronization in monkey motor cortex during a precision grip task. II. effect of oscillatory activity on corticospinal output. J. Neurophysiol. 89, 1941–1953. https://doi.org/10.1152/jn.00832.2002
Bar-Gad, I., Bergman, H., 2001. Stepping out of the box: information processing in the neural networks of the basal ganglia. Curr. Opin. Neurobiol. 11, 689–695.
Barnes, C.D., Pompeiano, O., 1970. Effects of muscle vibration on the pre- and postsynaptic components of the extensor monosynaptic reflex. Brain Res. 18, 384–388.
Bäss, P., Jacobsen, T., Schröger, E., 2008. Suppression of the auditory N1 event-related potential component with unpredictable self-initiated tones: evidence for internal forward models with dynamic stimulation. Int. J. Psychophysiol. Off. J. Int. Organ. Psychophysiol. 70, 137–143. https://doi.org/10.1016/j.ijpsycho.2008.06.005
Bastian, A.J., 2006. Learning to predict the future: the cerebellum adapts feedforward movement control. Curr. Opin. Neurobiol., Motor systems / Neurobiology of behaviour 16, 645–649. https://doi.org/10.1016/j.conb.2006.08.016
Bastos, A.M., Usrey, W.M., Adams, R.A., Mangun, G.R., Fries, P., Friston, K.J., 2012. Canonical Microcircuits for Predictive Coding. Neuron 76, 695–711. https://doi.org/10.1016/j.neuron.2012.10.038
Bauer, M., Stenner, M.-P., Friston, K.J., Dolan, R.J., 2014. Attentional modulation of alpha/beta and gamma oscillations reflect functionally distinct processes. J. Neurosci. Off. J. Soc. Neurosci. 34, 16117–16125. https://doi.org/10.1523/JNEUROSCI.3474-13.2014
Bays, P.M., Flanagan, J.R., Wolpert, D.M., 2006. Attenuation of Self-Generated Tactile Sensations Is Predictive, not Postdictive. PLoS Biol. 4, e28. https://doi.org/10.1371/journal.pbio.0040028
Bays, P.M., Wolpert, D.M., 2007. Computational principles of sensorimotor control that minimize uncertainty and variability. J. Physiol. 578, 387–396.
Bays, P.M., Wolpert, D.M., Flanagan, J.R., 2005. Perception of the Consequences of Self-Action Is Temporally Tuned and Event Driven. Curr. Biol. 15, 1125–1128. https://doi.org/10.1016/j.cub.2005.05.023
Beers, R.J. van, Sittig, A.C., Gon, J.J.D. van der, 1999. Integration of Proprioceptive and Visual Position-Information: An Experimentally Supported Model. J. Neurophysiol. 81, 1355–1364.
Behrens, T.E.J., Hunt, L.T., Woolrich, M.W., Rushworth, M.F.S., 2008. Associative learning of social value. Nature 456, 245–249. https://doi.org/10.1038/nature07538
Behrens, T.E.J., Woolrich, M.W., Walton, M.E., Rushworth, M.F.S., 2007. Learning the value of information in an uncertain world. Nat. Neurosci. 10, 1214–1221. https://doi.org/10.1038/nn1954
Beilock, S.L., Carr, T.H., 2001. On the fragility of skilled performance: what governs choking under pressure? J. Exp. Psychol. Gen. 130, 701–725.
Bestmann, S., Ruge, D., Rothwell, J., Galea, J.M., 2014. The Role of Dopamine in Motor Flexibility. J. Cogn. Neurosci. 27, 365–376. https://doi.org/10.1162/jocn_a_00706
Betz, 1874. Anatomischer Nachweis zweier Gehirncentra. Centralblatt für die medizinische Wissenschaften 578=580, 595-599.
Blakemore, S., Frith, C., Wolpert, D., 1999. Spatio-temporal prediction modulates the perception of self-produced stimuli. J. Cogn. Neurosci. 11, pp.551-559.

Blakemore, S.-J., Sirigu, A., 2003. Action prediction in the cerebellum and in the parietal lobe. Exp. Brain Res. 153, 239–245. https://doi.org/10.1007/s00221-003-1597-z
Blakemore, S.-J., Wolpert, D., Frith, C., 2000. Why can't you tickle yourself? Neuroreport 11, R11–R16.
Blakemore, S.-J., Wolpert, D.M., Frith, C.D., 1998. Central cancellation of self-produced tickle sensation. Nat. Neurosci. 1, 635–640.
Bonaiuto, J.J., Rossiter, H.E., Meyer, S.S., Adams, N., Little, S., Callaghan, M.F., Dick, F., Bestmann, S., Barnes, G.R., 2017. Non-invasive laminar inference with MEG: Comparison of methods and source inversion algorithms. bioRxiv 147215. https://doi.org/10.1101/147215
Botvinick, M., Cohen, J., 1998. Rubber hands "feel" touch that eyes see. Nature 391, 756. https://doi.org/10.1038/35784
Bressler, S.L., Richter, C.G., 2015. Interareal oscillatory synchronization in top-down neocortical processing. Curr. Opin. Neurobiol. 31, 62–66. https://doi.org/10.1016/j.conb.2014.08.010
Brovelli, A., Battaglini, P.P., Naranjo, J.R., Budai, R., 2002. Medium-range oscillatory network and the 20-Hz sensorimotor induced potential. NeuroImage 16, 130–141. https://doi.org/10.1006/nimg.2002.1058
Brovelli, A., Ding, M., Ledberg, A., Chen, Y., Nakamura, R., Bressler, S.L., 2004. Beta oscillations in a large-scale sensorimotor cortical network: directional influences revealed by Granger causality. Proc. Natl. Acad. Sci. U. S. A. 101, 9849–9854.
Brown, H., Adams, R.A., Parees, I., Edwards, M., Friston, K., 2013. Active inference, sensory attenuation and illusions. Cogn. Process. 14, 411–427. https://doi.org/10.1007/s10339-013-0571-3
Brown, M.C., Engberg, I., Matthews, P.B.C., 1967. The relative sensitivity to vibration of muscle receptors of the cat. J. Physiol. 192, 773–800.
Brown, P., 2007. Abnormal oscillatory synchronisation in the motor system leads to impaired movement. Curr. Opin. Neurobiol., Motor systems / Neurobiology of behaviour 17, 656–664. https://doi.org/10.1016/j.conb.2007.12.001
Brown, P., 2003. Oscillatory nature of human basal ganglia activity: Relationship to the pathophysiology of Parkinson's disease. Mov. Disord. 18, 357–363. https://doi.org/10.1002/mds.10358
Bullen, A.R., Brunt, D., 1986. Effects of tendon vibration on unimanual and bimanual movement accuracy. Exp. Neurol. 93, 311–319. https://doi.org/10.1016/0014-4886(86)90192-5
Burge, J., Ernst, M.O., Banks, M.S., 2008. The statistical determinants of adaptation rate in human reaching. J. Vis. 8, 20.1-19. https://doi.org/10.1167/8.4.20
Burke, D., Hagbarth, K.E., Löfstedt, L., Wallin, B.G., 1976. The responses of human muscle spindle endings to vibration of non-contracting muscles. J. Physiol. 261, 673–693.
Capaday, C., Cooke, J.D., 1983. Vibration-induced changes in movement-related EMG activity in humans. Exp. Brain Res. 52, 139–146.
Capaday, C., Cooke, J.D., 1981. The effects of muscle vibration on the attainment of intended final position during voluntary human arm movements. Exp. Brain Res. 42, 228–230.
Cardoso-Leite, P., Mamassian, P., Schütz-Bosbach, S., Waszak, F., 2010. A new look at sensory attenuation. Action-effect anticipation affects sensitivity, not response bias. Psychol. Sci. 21, 1740–1745. https://doi.org/10.1177/0956797610389187
Cassim, F., Monaca, C., Szurhaj, W., Bourriez, J.L., Defebvre, L., Derambure, P., Guieu, J.D., 2001. Does post-movement beta synchronization reflect an idling motor cortex? Neuroreport 12, 3859–3863.
Cassim, F., Szurhaj, W., Sediri, H., Devos, D., Bourriez, J.-L., Poirot, I., Derambure, P., Defebvre, L., Guieu, J.-D., 2000. Brief and sustained movements: differences in event-related (de)synchronization (ERD/ERS) patterns. Clin. Neurophysiol. 111, 2032–2039. https://doi.org/10.1016/S1388-2457(00)00455-7

Chapman, C.E., Jiang, W., Lamarre, Y., 1988. Modulation of lemniscal input during conditioned arm movements in the monkey. Exp. Brain Res. 72, 316–334. https://doi.org/10.1007/BF00250254
Charcot, J., 1892. La medicine vibratoire: Application des vibrations rapides et continues a traitement de quelques maladies du systeme nerveux. Prog Med 149–151.
Chawla, D., Lumer, E.D., Friston, K.J., 1999. The relationship between synchronization among neuronal populations and their mean activity levels. Neural Comput. 11, 1389–1411.
Chen, R., Yaseen, Z., Cohen, L.G., Hallett, M., 1998. Time course of corticospinal excitability in reaction time and self-paced movements. Ann. Neurol. 44, 317–325. https://doi.org/10.1002/ana.410440306
Cheyne, D., Gaetz, W., Garnero, L., Lachaux, J.-P., Ducorps, A., Schwartz, D., Varela, F.J., 2003. Neuromagnetic imaging of cortical oscillations accompanying tactile stimulation. Cogn. Brain Res. 17, 599–611. https://doi.org/10.1016/S0926-6410(03)00173-3
Chouza, M., Arias, P., Viñas, S., Cudeiro, J., 2011. Acute effects of whole-body vibration at 3, 6, and 9 hz on balance and gait in patients with Parkinson's disease. Mov. Disord. Off. J. Mov. Disord. Soc. 26, 920–921. https://doi.org/10.1002/mds.23582
Cohen, L.G., Starr, A., 1987. Localization, timing and specificity of gating of somatosensory evoked potentials during active movement in man. Brain J. Neurol. 110 (Pt 2), 451–467.
Cohen, L.G., Starr, A., 1985. Vibration and muscle contraction affect somatosensory evoked potentials. Neurology 35, 691–698.
Cohen, M.X., 2014. Analyzing neural time series data: theory and practice. MIT Press.
Contreras-Vidal, J.L., Buch, E.R., 2003. Effects of Parkinson's disease on visuomotor adaptation. Exp. Brain Res. 150, 25–32. https://doi.org/10.1007/s00221-003-1403-y
Cordo, P., Gurfinkel, V.S., Bevan, L., Kerr, G.K., 1995. Proprioceptive consequences of tendon vibration during movement. J. Neurophysiol. 74, 1675–1688.
Cordo, P.J., Gurfinkel, V.S., Brumagne, S., Flores-Vieira, C., 2005. Effect of slow, small movement on the vibration-evoked kinesthetic illusion. Exp. Brain Res. 167, 324–334. https://doi.org/10.1007/s00221-005-0034-x
Craske, B., 1977. Perception of impossible limb positions induced by tendon vibration. Science 196, 71–73. https://doi.org/10.1126/science.841342
Crone, N.E., Miglioretti, D.L., Gordon, B., Sieracki, J.M., Wilson, M.T., Uematsu, S., Lesser, R.P., 1998. Functional mapping of human sensorimotor cortex with electrocorticographic spectral analysis. I. Alpha and beta event-related desynchronization. Brain J. Neurol. 121 (Pt 12), 2271–2299.
Curio, G., Neuloh, G., Numminen, J., Jousmäki, V., Hari, R., 2000. Speaking modifies voice-evoked activity in the human auditory cortex. Hum. Brain Mapp. 9, 183–191.
Davis, N.J., Tomlinson, S.P., Morgan, H.M., 2012. The Role of Beta-Frequency Neural Oscillations in Motor Control. J. Neurosci. 32, 403–404. https://doi.org/10.1523/JNEUROSCI.5106-11.2012
Dayan, P., Hinton, G.E., Neal, R.M., Zemel, R.S., 1995. The Helmholtz machine. Neural Comput. 7, 889–904.
De Gail, P., Lance, J.W., Neilson, P.D., 1966. Differential effects on tonic and phasic reflex mechanisms produced by vibration of muscles in man. J. Neurol. Neurosurg. Psychiatry 29, 1–11.
DeLong, M.R., Wichmann, T., 2007. Circuits and circuit disorders of the basal ganglia. Arch. Neurol. 64, 20–24. https://doi.org/10.1001/archneur.64.1.20
Delwaide, P.J., 1973. Human Monosynaptic Reflexes and Presynaptic Inhibition 3, 508–522. https://doi.org/10.1159/000394164
Deneve, S., 2007. Bayesian Spiking Neurons I: Inference. Neural Comput. 20, 91–117. https://doi.org/10.1162/neco.2008.20.1.91

Desantis, A., Weiss, C., Schütz-Bosbach, S., Waszak, F., 2012. Believing and Perceiving: Authorship Belief Modulates Sensory Attenuation. PLOS ONE 7, e37959. https://doi.org/10.1371/journal.pone.0037959
Doya, K., 2007. Bayesian Brain: Probabilistic Approaches to Neural Coding. MIT Press.
Doyle, L.M.F., Yarrow, K., Brown, P., 2005. Lateralization of event-related beta desynchronization in the EEG during pre-cued reaction time tasks. Clin. Neurophysiol. 116, 1879–1888. https://doi.org/10.1016/j.clinph.2005.03.017
Drevets, W.C., Burton, H., Videen, T.O., Snyder, A.Z., Simpson, J.R., Raichle, M.E., 1995. Blood flow changes in human somatosensory cortex during anticipated stimulation. Nature 373, 249–252. https://doi.org/10.1038/373249a0
Ebersbach, G., Edler, D., Kaufhold, O., Wissel, J., 2008. Whole body vibration versus conventional physiotherapy to improve balance and gait in Parkinson's disease. Arch. Phys. Med. Rehabil. 89, 399–403. https://doi.org/10.1016/j.apmr.2007.09.031
Ehringer, H., Hornykiewicz, O., 1960. Verteilung Von Noradrenalin Und Dopamin (3-Hydroxytyramin) Im Gehirn Des Menschen Und Ihr Verhalten Bei Erkrankungen Des Extrapyramidalen Systems. Klin. Wochenschr. 38, 1236–1239. https://doi.org/10.1007/BF01485901
Engel, A.K., Fries, P., 2010. Beta-band oscillations--signalling the status quo? Curr. Opin. Neurobiol. 20, 156–165. https://doi.org/10.1016/j.conb.2010.02.015
Ernst, M.O., Banks, M.S., 2002. Humans integrate visual and haptic information in a statistically optimal fashion. Nature 415, 429–433. https://doi.org/10.1038/415429a
Ernst, M.O., Bülthoff, H.H., 2004. Merging the senses into a robust percept. Trends Cogn. Sci. 8, 162–169. https://doi.org/10.1016/j.tics.2004.02.002
Feingold, J., Gibson, D.J., DePasquale, B., Graybiel, A.M., 2015. Bursts of beta oscillation differentiate postperformance activity in the striatum and motor cortex of monkeys performing movement tasks. Proc. Natl. Acad. Sci. U. S. A. 112, 13687–13692. https://doi.org/10.1073/pnas.1517629112
Feldman, A.G., 1986. Once More on the Equilibrium-Point Hypothesis (λ Model) for Motor Control. J. Mot. Behav. 18, 17–54. https://doi.org/10.1080/00222895.1986.10735369
Feldman, H., Friston, K.J., 2010. Attention, Uncertainty, and Free-Energy. Front. Hum. Neurosci. 4. https://doi.org/10.3389/fnhum.2010.00215
Filion, M., Tremblay, L., Bédard, P.J., 1988. Abnormal influences of passive limb movement on the activity of globus pallidus neurons in parkinsonian monkeys. Brain Res. 444, 165–176. https://doi.org/10.1016/0006-8993(88)90924-9
Fleming, S.M., Dolan, R.J., 2012. The neural basis of metacognitive ability. Phil Trans R Soc B 367, 1338–1349. https://doi.org/10.1098/rstb.2011.0417
Fleming, S.M., Maniscalco, B., Ko, Y., Amendi, N., Ro, T., Lau, H., 2015. Action-Specific Disruption of Perceptual Confidence. Psychol. Sci. 26, 89–98. https://doi.org/10.1177/0956797614557697
Fleming, S.M., Weil, R.S., Nagy, Z., Dolan, R.J., Rees, G., 2010. Relating introspective accuracy to individual differences in brain structure. Science 329, 1541–1543. https://doi.org/10.1126/science.1191883
Franklin, D.W., Wolpert, D.M., 2011. Computational Mechanisms of Sensorimotor Control. Neuron 72, 425–442. https://doi.org/10.1016/j.neuron.2011.10.006
Friston, K., 2011. What Is Optimal about Motor Control? Neuron 72, 488–498. https://doi.org/10.1016/j.neuron.2011.10.018
Friston, K., 2008. Hierarchical models in the brain. PLoS Comput. Biol. 4, e1000211. https://doi.org/10.1371/journal.pcbi.1000211
Friston, K., 2005. A theory of cortical responses. Philos. Trans. R. Soc. Lond. B. Biol. Sci. 360, 815–836. https://doi.org/10.1098/rstb.2005.1622

Friston, K., Kiebel, S., 2009. Predictive coding under the free-energy principle. Philos. Trans. R. Soc. B Biol. Sci. 364, 1211–1221. https://doi.org/10.1098/rstb.2008.0300
Friston, K., Mattout, J., Kilner, J., 2011. Action understanding and active inference. Biol. Cybern. 104, 137–160. https://doi.org/10.1007/s00422-011-0424-z
Friston, K.J., Bastos, A.M., Pinotsis, D., Litvak, V., 2015. LFP and oscillations—what do they tell us? Curr. Opin. Neurobiol. 31, 1–6. https://doi.org/10.1016/j.conb.2014.05.004
Friston, K.J., Daunizeau, J., Kilner, J., Kiebel, S.J., 2010. Action and behavior: a free-energy formulation. Biol. Cybern. 102, 227–260. https://doi.org/10.1007/s00422-010-0364-z
Friston, K.J., Shiner, T., Fitzgerald, T., Galea, J.M., Adams, R., Brown, H., Dolan, R.J., Moran, R., Stephan, K.E., Bestmann, S., 2011. Dopamine, Affordance and Active Inference.
Gaetz, W., Cheyne, D., 2006. Localization of sensorimotor cortical rhythms induced by tactile stimulation using spatially filtered MEG. NeuroImage 30, 899–908. https://doi.org/10.1016/j.neuroimage.2005.10.009
Gaetz, W., Edgar, J.C., Wang, D.J., Roberts, T.P.L., 2011. Relating MEG measured motor cortical oscillations to resting γ-Aminobutyric acid (GABA) concentration. NeuroImage 55, 616–621. https://doi.org/10.1016/j.neuroimage.2010.12.077
Galea, J.M., Bestmann, S., Beigi, M., Jahanshahi, M., Rothwell, J.C., 2012. Action Reprogramming in Parkinson's Disease: Response to Prediction Error Is Modulated by Levels of Dopamine. J. Neurosci. 32, 542–550. https://doi.org/10.1523/JNEUROSCI.3621-11.2012
Galvin, S.J., Podd, J.V., Drga, V., Whitmore, J., 2003. Type 2 tasks in the theory of signal detectability: Discrimination between correct and incorrect decisions. Psychon. Bull. Rev. 10, 843–876.
Gastaut, H., 1952. [Electrocorticographic study of the reactivity of rolandic rhythm]. Rev. Neurol. (Paris) 87, 176–182.
George, J.S., Strunk, J., Mak-McCully, R., Houser, M., Poizner, H., Aron, A.R., 2013. Dopaminergic therapy in Parkinson's disease decreases cortical beta band coherence in the resting state and increases cortical beta band power during executive control. NeuroImage Clin. 3, 261–270. https://doi.org/10.1016/j.nicl.2013.07.013
Gigerenzer, G., Brighton, H., 2009. Homo Heuristicus: Why Biased Minds Make Better Inferences. Top. Cogn. Sci. 1, 107–143. https://doi.org/10.1111/j.1756-8765.2008.01006.x
Gilbertson, T., Lalo, E., Doyle, L., Lazzaro, V.D., Cioni, B., Brown, P., 2005. Existing Motor State Is Favored at the Expense of New Movement during 13-35 Hz Oscillatory Synchrony in the Human Corticospinal System. J. Neurosci. 25, 7771–7779. https://doi.org/10.1523/JNEUROSCI.1762-05.2005
Gillies, J.D., Lance, J.W., Neilson, P.D., Tassinari, C.A., 1969. Presynaptic inhibition of the monosynaptic reflex by vibration. J. Physiol. 205, 329–339.
Goodwin, G.M., McCloskey, D.I., Matthews, P.B.C., 1972. Proprioceptive Illusions Induced by Muscle Vibration: Contribution by Muscle Spindles to Perception? Science 175, 1382–1384. https://doi.org/10.1126/science.175.4028.1382
Gopnik, A., Glymour, C., Sobel, D.M., Schulz, L.E., Kushnir, T., Danks, D., 2004. A theory of causal learning in children: causal maps and Bayes nets. Psychol. Rev. 111, 3–32. https://doi.org/10.1037/0033-295X.111.1.3
Gregory, R.L., 1980. The psychology of vision - Perceptions as hypotheses. Phil Trans R Soc Lond B 290, 181–197. https://doi.org/10.1098/rstb.1980.0090
Grice, K.O., Vogel, K.A., Le, V., Mitchell, A., Muniz, S., Vollmer, M.A., 2003. Adult Norms for a Commercially Available Nine Hole Peg Test for Finger Dexterity. Am. J. Occup. Ther. 57, 570–573. https://doi.org/10.5014/ajot.57.5.570

Gruber, T., Müller, M.M., 2005. Oscillatory brain activity dissociates between associative stimulus content in a repetition priming task in the human EEG. Cereb. Cortex N. Y. N 1991 15, 109–116. https://doi.org/10.1093/cercor/bhh113
Haas, C.T., Turbanski, S., Kessler, K., Schmidtbleicher, D., 2006. The effects of random whole-body-vibration on motor symptoms in Parkinson's disease. NeuroRehabilitation 21, 29–36.
Hagbarth, K.-E., Eklund, G., 1966. Tonic vibration reflexes (TVR) in spasticity. Brain Res. 2, 201–203. https://doi.org/10.1016/0006-8993(66)90029-1
Haith, A.M., Pakpoor, J., Krakauer, J.W., 2016. Independence of Movement Preparation and Movement Initiation. J. Neurosci. 36, 3007–3015. https://doi.org/10.1523/JNEUROSCI.3245-15.2016
Hari, R., Forss, N., Avikainen, S., Kirveskari, E., Salenius, S., Rizzolatti, G., 1998. Activation of human primary motor cortex during action observation: a neuromagnetic study. Proc. Natl. Acad. Sci. 95, 15061–15065.
Hari, R., Salmelin, R., 1997. Human cortical oscillations: a neuromagnetic view through the skull. Trends Neurosci. 20, 44–49. https://doi.org/10.1016/S0166-2236(96)10065-5
Harris, C.M., Wolpert, D.M., 1998. Signal-dependent noise determines motor planning. Nature 394, 780–784. https://doi.org/10.1038/29528
Haruno, M., Wolpert, D.M., 2005. Optimal control of redundant muscles in step-tracking wrist movements. J. Neurophysiol. 94, 4244–4255. https://doi.org/10.1152/jn.00404.2005
Hatsopoulos, N.G., Suminski, A.J., 2011. Sensing with the motor cortex. Neuron 72, 477–487. https://doi.org/10.1016/j.neuron.2011.10.020
Hauser, T.U., Allen, M., Purg, N., Moutoussis, M., Rees, G., Dolan, R.J., 2017. Noradrenaline blockade specifically enhances metacognitive performance. eLife 6, e24901. https://doi.org/10.7554/eLife.24901
Helmholtz, H. von, König, A.P., 1896. Handbuch der physiologischen Optik / von H. von Helmholtz. L. Voss, Hamburg.
Herkenham, M., 1980. Laminar organization of thalamic projections to the rat neocortex. Science 207, 532–535.
Hiraoka, K., Matsuo, Y., Abe, K., 2005. Soleus H-reflex inhibition during gait initiation in Parkinson's disease. Mov. Disord. 20, 858–864. https://doi.org/10.1002/mds.20448
Holmes, A.P., Blair, R.C., Watson, J.D., Ford, I., 1996. Nonparametric analysis of statistic images from functional mapping experiments. J. Cereb. Blood Flow Metab. Off. J. Int. Soc. Cereb. Blood Flow Metab. 16, 7–22. https://doi.org/10.1097/00004647-199601000-00002
Hoshiyama, M., Kakigi, R., 2000. Vibratory stimulation of proximal muscles does not affect cortical components of somatosensory evoked potential following distal nerve stimulation. Clin. Neurophysiol. 111, 1607–1610. https://doi.org/10.1016/S1388-2457(00)00369-2
Hoshiyama, M., Kakigi, R., Koyama, S., Watanabe, S., Shimojo, M., 1997. Activity in posterior parietal cortex following somatosensory stimulation in man: magnetoencephalographic study using spatio-temporal source analysis. Brain Topogr. 10, 23–30.
Huffman, K.J., Krubitzer, L., 2001. Thalamo-cortical connections of areas 3a and M1 in marmoset monkeys. J. Comp. Neurol. 435, 291–310. https://doi.org/10.1002/cne.1031
Hughes, G., Desantis, A., Waszak, F., 2013. Attenuation of auditory N1 results from identity-specific action-effect prediction. Eur. J. Neurosci. 37, 1152–1158. https://doi.org/10.1111/ejn.12120
Hughes, G., Waszak, F., 2011. ERP correlates of action effect prediction and visual sensory attenuation in voluntary action. NeuroImage 56, 1632–1640. https://doi.org/10.1016/j.neuroimage.2011.02.057

Iglesias, S., Mathys, C., Brodersen, K.H., Kasper, L., Piccirelli, M., den Ouden, H.E.M., Stephan, K.E., 2013. Hierarchical prediction errors in midbrain and basal forebrain during sensory learning. Neuron 80, 519–530. https://doi.org/10.1016/j.neuron.2013.09.009
Inglis, J.T., Frank, J.S., 1990. The effect of agonist/antagonist muscle vibration on human position sense. Exp. Brain Res. 81, 573–580. https://doi.org/10.1007/BF02423506
Jackson, A.F., Bolger, D.J., 2014. The neurophysiological bases of EEG and EEG measurement: A review for the rest of us. Psychophysiology n/a-n/a. https://doi.org/10.1111/psyp.12283
Jasper, H., Penfield, W., 1949. Electrocorticograms in man: Effect of voluntary movement upon the electrical activity of the precentral gyrus. Arch. Für Psychiatr. Nervenkrankh. 183, 163–174. https://doi.org/10.1007/BF01062488
Jasper, H.H., Andrews, H.L., 1936. Human Brain Rhythms: I. Recording Techniques and Preliminary Results. J. Gen. Psychol. 14, 98–126. https://doi.org/10.1080/00221309.1936.9713141
Jenkinson, N., Brown, P., 2011. New insights into the relationship between dopamine, beta oscillations and motor function. Trends Neurosci. 34, 611–618. https://doi.org/10.1016/j.tins.2011.09.003
Jiang, W., Chapman, C.E., Lamarre, Y., 1990. Modulation of somatosensory evoked responses in the primary somatosensory cortex produced by intracortical microstimulation of the motor cortex in the monkey. Exp. Brain Res. 80, 333–344.
Johansen-Berg, H., Christensen, V., Woolrich, M., Matthews, P.M., 2000. Attention to touch modulates activity in both primary and secondary somatosensory areas. Neuroreport 11, 1237–1241.
Jones, S.R., Kerr, C.E., Wan, Q., Pritchett, D.L., Hämäläinen, M., Moore, C.I., 2010. Cued spatial attention drives functionally relevant modulation of the mu rhythm in primary somatosensory cortex. J. Neurosci. Off. J. Soc. Neurosci. 30, 13760–13765. https://doi.org/10.1523/JNEUROSCI.2969-10.2010
Joundi, R.A., Jenkinson, N., Brittain, J.-S., Aziz, T.Z., Brown, P., 2012. Driving Oscillatory Activity in the Human Cortex Enhances Motor Performance. Curr. Biol. 22, 403–407. https://doi.org/10.1016/j.cub.2012.01.024
Jueptner, M., Stephan, K.M., Frith, C.D., Brooks, D.J., Frackowiak, R.S., Passingham, R.E., 1997. Anatomy of motor learning. I. Frontal cortex and attention to action. J. Neurophysiol. 77, 1313–1324.
Juravle, G., Spence, C., 2011. Juggling reveals a decisional component to tactile suppression. Exp. Brain Res. 213, 87–97. https://doi.org/10.1007/s00221-011-2780-2
Jurkiewicz, M.T., Gaetz, W.C., Bostan, A.C., Cheyne, D., 2006. Post-movement beta rebound is generated in motor cortex: evidence from neuromagnetic recordings. NeuroImage 32, 1281–1289. https://doi.org/10.1016/j.neuroimage.2006.06.005
Juslin, P., Nilsson, H., Winman, A., 2009. Probability theory, not the very guide of life. Psychol. Rev. 116, 856–874. https://doi.org/10.1037/a0016979
Kaji, R., 2001. Basal ganglia as a sensory gating devise for motor control. J. Med. Investig. JMI 48, 142–146.
Kaji, R., Urushihara, R., Murase, N., Shimazu, H., Goto, S., 2005. Abnormal sensory gating in basal ganglia disorders. J. Neurol. 252, iv13-iv16. https://doi.org/10.1007/s00415-005-4004-9
Kakigi, R., 1994. Somatosensory evoked magnetic fields following median nerve stimulation. Neurosci. Res. 20, 165–174. https://doi.org/10.1016/0168-0102(94)90034-5
Kakigi, R., 1986. Ipsilateral and contralateral SEP components following median nerve stimulation: effects of interfering stimuli applied to the contralateral hand. Electroencephalogr. Clin. Neurophysiol. 64, 246–259.

Kakigi, R., Jones, S.J., 1986. Influence of concurrent tactile stimulation on somatosensory evoked potentials following posterior tibial nerve stimulation in man. Electroencephalogr. Clin. Neurophysiol. 65, 118–129.
Kakigi, R., Jones, S.J., 1985. Effects on median nerve SEPs of tactile stimulation applied to adjacent and remote areas of the body surface. Electroencephalogr. Clin. Neurophysiol. 62, 252–265.
Kammers, M.P.M., de Vignemont, F., Verhagen, L., Dijkerman, H.C., 2009. The rubber hand illusion in action. Neuropsychologia 47, 204–211. https://doi.org/10.1016/j.neuropsychologia.2008.07.028
Kapur, S.S., Stebbins, G.T., Goetz, C.G., 2012. Vibration therapy for Parkinson's disease: Charcot's studies revisited. J. Park. Dis. 2, 23–27. https://doi.org/10.3233/JPD-2012-12079
Keinrath, C., Wriessnegger, S., Müller-Putz, G.R., Pfurtscheller, G., 2006. Post-movement beta synchronization after kinesthetic illusion, active and passive movements. Int. J. Psychophysiol. 62, 321–327. https://doi.org/10.1016/j.ijpsycho.2006.06.001
Kepecs, A., Mainen, Z.F., 2012. A computational framework for the study of confidence in humans and animals. Philos. Trans. R. Soc. Lond. B Biol. Sci. 367, 1322–1337. https://doi.org/10.1098/rstb.2012.0037
Kerkoerle, T. van, Self, M.W., Dagnino, B., Gariel-Mathis, M.-A., Poort, J., Togt, C. van der, Roelfsema, P.R., 2014. Alpha and gamma oscillations characterize feedback and feedforward processing in monkey visual cortex. Proc. Natl. Acad. Sci. 111, 14332–14341. https://doi.org/10.1073/pnas.1402773111
Kersten, D., Mamassian, P., Yuille, A., 2004. Object perception as Bayesian inference. Annu. Rev. Psychol. 55, 271–304. https://doi.org/10.1146/annurev.psych.55.090902.142005
Khudados, E., Cody, F., O'Boyle, D., 1999. Proprioceptive regulation of voluntary ankle movements, demonstrated using muscle vibration, is impaired by Parkinson's disease. J. Neurol. Neurosurg. Psychiatry 67, 504–510.
Kiani, R., Shadlen, M.N., 2009. Representation of Confidence Associated with a Decision by Neurons in the Parietal Cortex. Science 324, 759–764. https://doi.org/10.1126/science.1169405
Kilner, J., Bott, L., Posada, A., 2005. Modulations in the degree of synchronization during ongoing oscillatory activity in the human brain. Eur. J. Neurosci. 21, 2547–2554. https://doi.org/10.1111/j.1460-9568.2005.04069.x
Kilner, J.M., 2013. Bias in a common EEG and MEG statistical analysis and how to avoid it. Clin. Neurophysiol. 124, 2062–2063. https://doi.org/10.1016/j.clinph.2013.03.024
Kilner, J.M., Baker, S.N., Salenius, S., Jousmäki, V., Hari, R., Lemon, R.N., 1999. Task-dependent modulation of 15-30 Hz coherence between rectified EMGs from human hand and forearm muscles. J. Physiol. 516, 559–570. https://doi.org/10.1111/j.1469-7793.1999.0559v.x
Kilner, J.M., Kiebel, S.J., Friston, K.J., 2005. Applications of random field theory to electrophysiology. Neurosci. Lett. 374, 174–178. https://doi.org/10.1016/j.neulet.2004.10.052
King, L.K., Almeida, Q.J., Ahonen, H., 2009. Short-term effects of vibration therapy on motor impairments in Parkinson's disease. NeuroRehabilitation 25, 297–306. https://doi.org/10.3233/NRE-2009-0528
Klimesch, W., Hanslmayr, S., Sauseng, P., Gruber, W.R., 2006. Distinguishing the evoked response from phase reset: a comment to Mäkinen et al. NeuroImage 29, 808–811. https://doi.org/10.1016/j.neuroimage.2005.08.041
Klockgether, T., Borutta, M., Rapp, H., Spieker, S., Dichgans, J., 1995. A defect of kinesthesia in Parkinson's disease. Mov. Disord. 10, 460–465.
Knight, R.T., Richard Staines, W., Swick, D., Chao, L.L., 1999. Prefrontal cortex regulates inhibition and excitation in distributed neural networks. Acta Psychol. (Amst.) 101, 159–178. https://doi.org/10.1016/S0001-6918(99)00004-9

Knill, D.C., 1998. Surface orientation from texture: ideal observers, generic observers and the information content of texture cues. Vision Res. 38, 1655–1682.
Knill, D.C., Pouget, A., 2004. The Bayesian brain: the role of uncertainty in neural coding and computation. Trends Neurosci. 27, 712–719. https://doi.org/10.1016/j.tins.2004.10.007
Koelewijn, T., van Schie, H.T., Bekkering, H., Oostenveld, R., Jensen, O., 2008. Motor-cortical beta oscillations are modulated by correctness of observed action. NeuroImage 40, 767–775. https://doi.org/10.1016/j.neuroimage.2007.12.018
Konczak, J., Corcos, D.M., Horak, F., Poizner, H., Shapiro, M., Tuite, P., Volkmann, J., Maschke, M., 2009. Proprioception and motor control in Parkinson's disease. J. Mot. Behav. 41, 543–552. https://doi.org/10.3200/35-09-002
Konczak, J., Krawczewski, K., Tuite, P., Maschke, M., 2007. The perception of passive motion in Parkinson's disease. J. Neurol. 254, 655–663. https://doi.org/10.1007/s00415-006-0426-2
Körding, K.P., Wolpert, D.M., 2006. Bayesian decision theory in sensorimotor control. Trends Cogn. Sci., Special issue: Probabilistic models of cognition 10, 319–326. https://doi.org/10.1016/j.tics.2006.05.003
Körding, K.P., Wolpert, D.M., 2004. Bayesian integration in sensorimotor learning. Nature 427, 244–247. https://doi.org/10.1038/nature02169
Krubitzer, L.A., Kaas, J.H., 1990. The organization and connections of somatosensory cortex in marmosets. J. Neurosci. 10, 952–974.
Kühn, A.A., Doyle, L., Pogosyan, A., Yarrow, K., Kupsch, A., Schneider, G.-H., Hariz, M.I., Trottenberg, T., Brown, P., 2006a. Modulation of beta oscillations in the subthalamic area during motor imagery in Parkinson's disease. Brain 129, 695–706. https://doi.org/10.1093/brain/awh715
Kühn, A.A., Kupsch, A., Schneider, G.-H., Brown, P., 2006b. Reduction in subthalamic 8-35 Hz oscillatory activity correlates with clinical improvement in Parkinson's disease. Eur. J. Neurosci. 23, 1956–1960. https://doi.org/10.1111/j.1460-9568.2006.04717.x
Lalo, E., Gilbertson, T., Doyle, L., Lazzaro, V.D., Cioni, B., Brown, P., 2007. Phasic increases in cortical beta activity are associated with alterations in sensory processing in the human. Exp. Brain Res. 177, 137–145. https://doi.org/10.1007/s00221-006-0655-8
Lau, H., Rosenthal, D., 2011. Empirical support for higher-order theories of conscious awareness. Trends Cogn. Sci. 15, 365–373. https://doi.org/10.1016/j.tics.2011.05.009
Legon, W., Staines, W.R., 2006. Predictability of the target stimulus for sensory-guided movement modulates early somatosensory cortical potentials. Clin. Neurophysiol. Off. J. Int. Fed. Clin. Neurophysiol. 117, 1345–1353. https://doi.org/10.1016/j.clinph.2006.02.024
Little, S., Brown, P., 2014. The functional role of beta oscillations in Parkinson's disease. Parkinsonism Relat. Disord. 20, S44–S48. https://doi.org/10.1016/S1353-8020(13)70013-0
Little, S., Pogosyan, A., Kuhn, A.A., Brown, P., 2012. β band stability over time correlates with Parkinsonian rigidity and bradykinesia. Exp. Neurol. 236, 383–388. https://doi.org/10.1016/j.expneurol.2012.04.024
Little, S., Pogosyan, A., Neal, S., Zavala, B., Zrinzo, L., Hariz, M., Foltynie, T., Limousin, P., Ashkan, K., FitzGerald, J., Green, A.L., Aziz, T.Z., Brown, P., 2013. Adaptive deep brain stimulation in advanced Parkinson disease. Ann. Neurol. 74, 449–457. https://doi.org/10.1002/ana.23951
Litvak, V., Jha, A., Eusebio, A., Oostenveld, R., Foltynie, T., Limousin, P., Zrinzo, L., Hariz, M.I., Friston, K., Brown, P., 2011. Resting oscillatory cortico-subthalamic connectivity in patients with Parkinson's disease. Brain J. Neurol. 134, 359–374. https://doi.org/10.1093/brain/awq332

Luft, C.D.B., Takase, E., Bhattacharya, J., 2014. Processing graded feedback: electrophysiological correlates of learning from small and large errors. J. Cogn. Neurosci. 26, 1180–1193. https://doi.org/10.1162/jocn_a_00543
Lundberg, A., Vyklický, L., 1963. Inhibitory interaction between spinal reflexes to primary afferents. Experientia 19, 247–248. https://doi.org/10.1007/BF02151360
Lundqvist, M., Rose, J., Herman, P., Brincat, S.L., Buschman, T.J., Miller, E.K., 2016. Gamma and Beta Bursts Underlie Working Memory. Neuron 90, 152–164. https://doi.org/10.1016/j.neuron.2016.02.028
Ma, W.J., Beck, J.M., Latham, P.E., Pouget, A., 2006. Bayesian inference with probabilistic population codes. Nat. Neurosci. 9, 1432–1438. https://doi.org/10.1038/nn1790
Macerollo, A., Bose, S., Ricciardi, L., Edwards, M.J., Kilner, J.M., 2015. Linking differences in action perception with differences in action execution. Soc. Cogn. Affect. Neurosci. https://doi.org/10.1093/scan/nsu161
Macerollo, A., Chen, J.-C., Korlipara, P., Foltynie, T., Rothwell, J., Edwards, M.J., Kilner, J.M., 2016. Dopaminergic treatment modulates sensory attenuation at the onset of the movement in Parkinson's disease: A test of a new framework for bradykinesia. Mov. Disord. n/a-n/a. https://doi.org/10.1002/mds.26493
Macerollo, A, Chen, J.-C., Pareés, I., Kassavetis, P., Kilner, J.M., Edwards, M.J., 2015. Sensory Attenuation Assessed by Sensory Evoked Potentials in Functional Movement Disorders. PloS One 10, e0129507. https://doi.org/10.1371/journal.pone.0129507
Makeig, S., Westerfield, M., Jung, T.P., Enghoff, S., Townsend, J., Courchesne, E., Sejnowski, T.J., 2002. Dynamic brain sources of visual evoked responses. Science 295, 690–694. https://doi.org/10.1126/science.1066168
Mäkinen, V., Tiitinen, H., May, P., 2005. Auditory event-related responses are generated independently of ongoing brain activity. NeuroImage 24, 961–968. https://doi.org/10.1016/j.neuroimage.2004.10.020
Marinelli, L., Crupi, D., Di Rocco, A., Bove, M., Eidelberg, D., Abbruzzese, G., Ghilardi, M.F., 2009. Learning and consolidation of visuo-motor adaptation in Parkinson's disease. Parkinsonism Relat. Disord. 15, 6–11. https://doi.org/10.1016/j.parkreldis.2008.02.012
Marreiros, A.C., Cagnan, H., Moran, R.J., Friston, K.J., Brown, P., 2013. Basal ganglia–cortical interactions in Parkinsonian patients. Neuroimage 66, 301–310. https://doi.org/10.1016/j.neuroimage.2012.10.088
Marshall, L., Mathys, C., Ruge, D., de Berker, A.O., Dayan, P., Stephan, K.E., Bestmann, S., 2016. Pharmacological Fingerprints of Contextual Uncertainty. PLoS Biol. 14, e1002575. https://doi.org/10.1371/journal.pbio.1002575
Martikainen, M.H., Kaneko, K., Hari, R., 2005. Suppressed Responses to Self-triggered Sounds in the Human Auditory Cortex. Cereb. Cortex 15, 299–302. https://doi.org/10.1093/cercor/bhh131
Maschke, M., Gomez, C.M., Tuite, P.J., Konczak, J., 2003. Dysfunction of the basal ganglia, but not the cerebellum, impairs kinaesthesia. Brain J. Neurol. 126, 2312–2322. https://doi.org/10.1093/brain/awg230
Mathys, C., Daunizeau, J., Friston, K.J., Stephan, K.E., 2011. A bayesian foundation for individual learning under uncertainty. Front. Hum. Neurosci. 5, 39. https://doi.org/10.3389/fnhum.2011.00039
Mathys, C.D., Lomakina, E.I., Daunizeau, J., Iglesias, S., Brodersen, K.H., Friston, K.J., Stephan, K.E., 2014. Uncertainty in perception and the Hierarchical Gaussian Filter. Front. Hum. Neurosci. 8. https://doi.org/10.3389/fnhum.2014.00825
Matyas, F., Sreenivasan, V., Marbach, F., Wacongne, C., Barsy, B., Mateo, C., Aronoff, R., Petersen, C.C.H., 2010. Motor Control by Sensory Cortex. Science 330, 1240–1243. https://doi.org/10.1126/science.1195797
Mazaheri, A., Jensen, O., 2006. Posterior alpha activity is not phase-reset by visual stimuli. Proc. Natl. Acad. Sci. U. S. A. 103, 2948–2952. https://doi.org/10.1073/pnas.0505785103

Mazaheri, A., Picton, T.W., 2005. EEG spectral dynamics during discrimination of auditory and visual targets. Brain Res. Cogn. Brain Res. 24, 81–96. https://doi.org/10.1016/j.cogbrainres.2004.12.013
McCarthy, M.M., Brown, E.N., Kopell, N., 2008. Potential network mechanisms mediating electroencephalographic beta rhythm changes during propofol-induced paradoxical excitation. J. Neurosci. Off. J. Soc. Neurosci. 28, 13488–13504. https://doi.org/10.1523/JNEUROSCI.3536-08.2008
McCloskey, D.I., 1973. Differences between the senses of movement and position shown by the effects of loading and vibration of muscles in man. Brain Res. 61, 119–131. https://doi.org/10.1016/0006-8993(73)90521-0
McFarland, D.J., Miner, L.A., Vaughan, T.M., Wolpaw, J.R., 2000. Mu and beta rhythm topographies during motor imagery and actual movements. Brain Topogr. 12, 177–186.
Meyer, G., 1987. Forms and spatial arrangement of neurons in the primary motor cortex of man. J. Comp. Neurol. 262, 402–428. https://doi.org/10.1002/cne.902620306
Meyer, S.S., Bonaiuto, J., Lim, M., Rossiter, H., Waters, S., Bradbury, D., Bestmann, S., Brookes, M., Callaghan, M.F., Weiskopf, N., Barnes, G.R., 2017. Flexible head-casts for high spatial precision MEG. J. Neurosci. Methods 276, 38–45. https://doi.org/10.1016/j.jneumeth.2016.11.009
Meyniel, F., Sigman, M., Mainen, Z.F., 2015. Confidence as Bayesian Probability: From Neural Origins to Behavior. Neuron 88, 78–92. https://doi.org/10.1016/j.neuron.2015.09.039
Miall, R.C., Weir, D.J., Wolpert, D.M., Stein, J.F., 1993. Is the cerebellum a smith predictor? J. Mot. Behav. 25, 203–216. https://doi.org/10.1080/00222895.1993.9942050
Mongeon, D., Blanchet, P., Messier, J., 2013. Impact of Parkinson's disease and dopaminergic medication on adaptation to explicit and implicit visuomotor perturbations. Brain Cogn. 81, 271–282. https://doi.org/10.1016/j.bandc.2012.12.001
Moore, A.P., 1987. Impaired sensorimotor integration in parkinsonism and dyskinesia: a role for corollary discharges? J. Neurol. Neurosurg. Psychiatry 50, 544–552.
Moran, R.J., Mallet, N., Litvak, V., Dolan, R.J., Magill, P.J., Friston, K.J., Brown, P., 2011. Alterations in Brain Connectivity Underlying Beta Oscillations in Parkinsonism. PLoS Comput. Biol. 7, e1002124. https://doi.org/10.1371/journal.pcbi.1002124
Morita, H., Shindo, M., Ikeda, S., Yanagisawa, N., 2000. Decrease in presynaptic inhibition on heteronymous monosynaptic Ia terminals in patients with Parkinson's disease. Mov. Disord. 15, 830–834. https://doi.org/10.1002/1531-8257(200009)15:5<830::AID-MDS1011>3.0.CO;2-E
Müller, G.R., Neuper, C., Rupp, R., Keinrath, C., Gerner, H.J., Pfurtscheller, G., 2003. Event-related beta EEG changes during wrist movements induced by functional electrical stimulation of forearm muscles in man. Neurosci. Lett. 340, 143–147.
Muthukumaraswamy, S. d., Johnson, B. w., 2004. Changes in rolandic mu rhythm during observation of a precision grip. Psychophysiology 41, 152–156. https://doi.org/10.1046/j.1469-8986.2003.00129.x
Naito, E., Ehrsson, H.H., Geyer, S., Zilles, K., Roland, P.E., 1999. Illusory Arm Movements Activate Cortical Motor Areas: A Positron Emission Tomography Study. J. Neurosci. 19, 6134–6144.
Nakagawa, K., Aokage, Y., Fukuri, T., Kawahara, Y., Hashizume, A., Kurisu, K., Yuge, L., 2011. Neuromagnetic beta oscillation changes during motor imagery and motor execution of skilled movements. Neuroreport 22, 217–222. https://doi.org/10.1097/WNR.0b013e328344b480
Navajas, J., Hindocha, C., Foda, H., Keramati, M., Latham, P.E., Bahrami, B., 2017. The idiosyncratic nature of confidence. Nat. Hum. Behav. 1. https://doi.org/10.1038/s41562-017-0215-1
Nichols, T.E., Holmes, A.P., 2002. Nonparametric permutation tests for functional neuroimaging: a primer with examples. Hum. Brain Mapp. 15, 1–25.

Ohara, S., Ikeda, A., Kunieda, T., Yazawa, S., Baba, K., Nagamine, T., Taki, W., Hashimoto, N., Mihara, T., Shibasaki, H., 2000. Movement-related change of electrocorticographic activity in human supplementary motor area proper. Brain J. Neurol. 123 (Pt 6), 1203–1215.
Okun, M.S., Fernandez, H.H., Pedraza, O., Misra, M., Lyons, K.E., Pahwa, R., Tarsy, D., Scollins, L., Corapi, K., Friehs, G.M., Grace, J., Romrell, J., Foote, K.D., 2004. Development and initial validation of a screening tool for Parkinson disease surgical candidates. Neurology 63, 161–163.
Okun, M.S., Foote, K.D., 2010. Parkinson's disease DBS: what, when, who and why? The time has come to tailor DBS targets. Expert Rev. Neurother. 10, 1847–1857.
Palmer, C., Zapparoli, L., Kilner, J.M., 2016. A New Framework to Explain Sensorimotor Beta Oscillations. Trends Cogn. Sci. 0. https://doi.org/10.1016/j.tics.2016.03.007
Palmer, C.E., Bunday, K.L., Davare, M., Kilner, J.M., 2016. A Causal Role for Primary Motor Cortex in Perception of Observed Actions. J. Cogn. Neurosci. 28, 2021–2029. https://doi.org/10.1162/jocn_a_01015
Palmer, C.E., Macerollo, A., 2015. Predictive Coding: How Many Faces? J. Neurosci. Off. J. Soc. Neurosci. 35, 14689–14690. https://doi.org/10.1523/JNEUROSCI.3093-15.2015
Papakostopoulos, D., 1980. A no-stimulus, no-response, event-related potential of the human cortex. Electroencephalogr. Clin. Neurophysiol. 48, 622–638.
Paquet, F., Bedard, M.A., Levesque, M., Tremblay, P.L., Lemay, M., Blanchet, P.J., Scherzer, P., Chouinard, S., Filion, J., 2008. Sensorimotor adaptation in Parkinson's disease: evidence for a dopamine dependent remapping disturbance. Exp. Brain Res. 185, 227–236. https://doi.org/10.1007/s00221-007-1147-1
Pareés, I., Brown, H., Nuruki, A., Adams, R.A., Davare, M., Bhatia, K.P., Friston, K., Edwards, M.J., 2014. Loss of sensory attenuation in patients with functional (psychogenic) movement disorders. Brain J. Neurol. 137, 2916–2921. https://doi.org/10.1093/brain/awu237
Parkkonen, E., Laaksonen, K., Piitulainen, H., Parkkonen, L., Forss, N., 2015. Modulation of the ∽20-Hz motor-cortex rhythm to passive movement and tactile stimulation. Brain Behav. 5, e00328. https://doi.org/10.1002/brb3.328
Pastötter, B., Berchtold, F., Bäuml, K.-H.T., 2012. Oscillatory correlates of controlled speed-accuracy tradeoff in a response-conflict task. Hum. Brain Mapp. 33, 1834–1849. https://doi.org/10.1002/hbm.21322
Patel, D., Fleming, S.M., Kilner, J.M., 2012. Inferring subjective states through the observation of actions. Proc. R. Soc. B Biol. Sci. 279, 4853–4860. https://doi.org/10.1098/rspb.2012.1847
Paulin, M.G., 1993. The role of the cerebellum in motor control and perception. Brain. Behav. Evol. 41, 39–50.
Penny, W.D., Kiebel, S.J., Kilner, J.M., Rugg, M.D., 2002. Event-related brain dynamics. Trends Neurosci. 25, 387–389.
Pessiglione, M., Guehl, D., Rolland, A.-S., François, C., Hirsch, E.C., Féger, J., Tremblay, L., 2005. Thalamic Neuronal Activity in Dopamine-Depleted Primates: Evidence for a Loss of Functional Segregation within Basal Ganglia Circuits. J. Neurosci. 25, 1523–1531. https://doi.org/10.1523/JNEUROSCI.4056-04.2005
Pfurtscheller, G., 1981. Central beta rhythm during sensorimotor activities in man. Electroencephalogr. Clin. Neurophysiol. 51, 253–264. https://doi.org/10.1016/0013-4694(81)90139-5
Pfurtscheller, G., Woertz, M., Supp, G., Lopes da Silva, F.H., 2003. Early onset of post-movement beta electroencephalogram synchronization in the supplementary motor area during self-paced finger movement in man. Neurosci. Lett. 339, 111–114.
Pierantozzi, M., Palmieri, M.G., Galati, S., Stanzione, P., Peppe, A., Tropepi, D., Brusa, L., Pisani, A., Moschella, V., Marciani, M.G., Mazzone, P., Stefani, A., 2008. Pedunculopontine nucleus deep brain stimulation changes spinal cord excitability

in Parkinson's disease patients. J. Neural Transm. 115, 731–735. https://doi.org/10.1007/s00702-007-0001-8
Pogosyan, A., Gaynor, L.D., Eusebio, A., Brown, P., 2009. Boosting Cortical Activity at Beta-Band Frequencies Slows Movement in Humans. Curr. Biol. 19, 1637–1641. https://doi.org/10.1016/j.cub.2009.07.074
Pouget, A., Drugowitsch, J., Kepecs, A., 2016. Confidence and certainty: distinct probabilistic quantities for different goals. Nat. Neurosci. 19, 366–374. https://doi.org/10.1038/nn.4240
Pride and a Daily Marathon [WWW Document], n.d. . MIT Press. URL https://mitpress.mit.edu/books/pride-and-daily-marathon (accessed 10.11.17).
Purves, D., Augustine, G.J., Fitzpatrick, D., Katz, L.C., LaMantia, A.-S., McNamara, J.O., Williams, S.M., 2001a. Mechanoreceptors Specialized to Receive Tactile Information.
Purves, D., Augustine, G.J., Fitzpatrick, D., Katz, L.C., LaMantia, A.-S., McNamara, J.O., Williams, S.M., 2001b. The Spinal Cord Circuitry Underlying Muscle Stretch Reflexes.
Putzki, N., Stude, P., Konczak, J., Graf, K., Diener, H.-C., Maschke, M., 2006. Kinesthesia is impaired in focal dystonia. Mov. Disord. 21, 754–760. https://doi.org/10.1002/mds.20799
Rao, R.P.N., 2004. Bayesian Computation in Recurrent Neural Circuits. Neural Comput. 16, 1–38. https://doi.org/10.1162/08997660460733976
Rao, R.P.N., Ballard, D.H., 1999. Predictive coding in the visual cortex: a functional interpretation of some extra-classical receptive-field effects. Nat. Neurosci. 2, 79–87. https://doi.org/10.1038/4580
Rathelot, J.-A., Strick, P.L., 2009. Subdivisions of primary motor cortex based on cortico-motoneuronal cells. Proc. Natl. Acad. Sci. U. S. A. 106, 918–923. https://doi.org/10.1073/pnas.0808362106
Rathelot, J.-A., Strick, P.L., 2006. Muscle representation in the macaque motor cortex: an anatomical perspective. Proc. Natl. Acad. Sci. U. S. A. 103, 8257–8262. https://doi.org/10.1073/pnas.0602933103
Rescorla, R., Wagner, A., 1972. A theory of pavlovian conditioning: variations in the effectiveness of reinforcement and nonreinforcement, in Clsssical Conditioning II: Current Research and Theory. Appleton Century Crofts, New York, pp. 64–99.
Ribot-Ciscar, E., Rossi-Durand, C., Roll, J.-P., 1998. Muscle spindle activity following muscle tendon vibration in man. Neurosci. Lett. 258, 147–150. https://doi.org/10.1016/S0304-3940(98)00732-0
Rickards, C., Cody, F.W., 1997. Proprioceptive control of wrist movements in Parkinson's disease. Reduced muscle vibration-induced errors. Brain J. Neurol. 120 (Pt 6), 977–990.
Rijn, A.C.M. van, Peper, A., Grimbergen, C.A., 1990. High-quality recording of bioelectric events. Med. Biol. Eng. Comput. 28, 389–397. https://doi.org/10.1007/BF02441961
Roll, J.P., Vedel, J.P., Ribot, E., 1989. Alteration of proprioceptive messages induced by tendon vibration in man: a microneurographic study. Exp. Brain Res. 76, 213–222. https://doi.org/10.1007/BF00253639
Roopun, A.K., Middleton, S.J., Cunningham, M.O., LeBeau, F.E.N., Bibbig, A., Whittington, M.A., Traub, R.D., 2006. A beta2-frequency (20–30 Hz) oscillation in nonsynaptic networks of somatosensory cortex. Proc. Natl. Acad. Sci. 103, 15646–15650. https://doi.org/10.1073/pnas.0607443103
Roussel, C., Hughes, G., Waszak, F., 2014. Action prediction modulates both neurophysiological and psychophysical indices of sensory attenuation. Front. Hum. Neurosci. 8. https://doi.org/10.3389/fnhum.2014.00115
Rudomín, P., Jiménez, I., Solodkin, M., Dueñas, S., 1983. Sites of action of segmental and descending control of transmission on pathways mediating PAD of Ia- and Ib-afferent fibers in cat spinal cord. J. Neurophysiol. 50, 743–769.

Rushton, D.N., Roghwell, J.C., Craggs, M.D., 1981. Gating of somatosensory evoked potentials during different kinds of movement in man. Brain 104, 465–491.
Saleh, M., Reimer, J., Penn, R., Ojakangas, C.L., Hatsopoulos, N.G., 2010. Fast and Slow Oscillations in Human Primary Motor Cortex Predict Oncoming Behaviorally Relevant Cues. Neuron 65, 461–471. https://doi.org/10.1016/j.neuron.2010.02.001
Salmelin, R., Hämäläinen, M., Kajola, M., Hari, R., 1995. Functional segregation of movement-related rhythmic activity in the human brain. NeuroImage 2, 237–243.
Salmelin, R., Hari, R., 1994. Spatiotemporal characteristics of sensorimotor neuromagnetic rhythms related to thumb movement. Neuroscience 60, 537–550.
Salmelin, R.H., Hämäläinen, M.S., 1995. Dipole modelling of MEG rhythms in time and frequency domains. Brain Topogr. 7, 251–257.
Sanes, J.N., Donoghue, J.P., 1993. Oscillations in local field potentials of the primate motor cortex during voluntary movement. Proc. Natl. Acad. Sci. U. S. A. 90, 4470–4474.
Schroeder, C.E., Mehta, A.D., Foxe, J.J., 2001. Determinants and mechanisms of attentional modulation of neural processing. Front. Biosci. J. Virtual Libr. 6, D672-684.
Schultz, W., 2007. Multiple dopamine functions at different time courses. Annu. Rev. Neurosci. 30, 259–288. https://doi.org/10.1146/annurev.neuro.28.061604.135722
Schyns, P.G., Thut, G., Gross, J., 2011. Cracking the Code of Oscillatory Activity. PLOS Biol. 9, e1001064. https://doi.org/10.1371/journal.pbio.1001064
Seizova-Cajic, T., Smith, J.L., Taylor, J.L., Gandevia, S.C., 2007. Proprioceptive movement illusions due to prolonged stimulation: reversals and aftereffects. PloS One 2, e1037. https://doi.org/10.1371/journal.pone.0001037
Seki, K., Fetz, E.E., 2012. Gating of Sensory Input at Spinal and Cortical Levels during Preparation and Execution of Voluntary Movement. J. Neurosci. 32, 890–902. https://doi.org/10.1523/JNEUROSCI.4958-11.2012
Semrau, J.A., Perlmutter, J.S., Thoroughman, K.A., 2014. Visuomotor adaptation in Parkinson's disease: effects of perturbation type and medication state. J. Neurophysiol. 111, 2675–2687. https://doi.org/10.1152/jn.00095.2013
Shah, A.S., Bressler, S.L., Knuth, K.H., Ding, M., Mehta, A.D., Ulbert, I., Schroeder, C.E., 2004. Neural dynamics and the fundamental mechanisms of event-related brain potentials. Cereb. Cortex N. Y. N 1991 14, 476–483. https://doi.org/10.1093/cercor/bhh009
Shergill, S.S., Bays, P.M., Frith, C.D., Wolpert, D.M., 2003. Two eyes for an eye: the neuroscience of force escalation. Science 301, 187–187.
Shergill, S.S., Samson, G., Bays, P.M., Frith, C.D., Wolpert, D.M., 2005. Evidence for Sensory Prediction Deficits in Schizophrenia. Am. J. Psychiatry 162, 2384–2386. https://doi.org/10.1176/appi.ajp.162.12.2384
Shergill, S.S., White, T.P., Joyce, D.W., Bays, P.M., Wolpert, D.M., Frith, C.D., 2013. Modulation of somatosensory processing by action. NeuroImage 70, 356–362. https://doi.org/10.1016/j.neuroimage.2012.12.043
Sherman, M.A., Lee, S., Law, R., Haegens, S., Thorn, C.A., Hämäläinen, M.S., Moore, C.I., Jones, S.R., 2016. Neural mechanisms of transient neocortical beta rhythms: Converging evidence from humans, computational modeling, monkeys, and mice. Proc. Natl. Acad. Sci. 113, E4885–E4894. https://doi.org/10.1073/pnas.1604135113
Sochůrková, D., Rektor, I., Jurák, P., Stancák, A., 2006. Intracerebral recording of cortical activity related to self-paced voluntary movements: a Bereitschaftspotential and event-related desynchronization/synchronization. SEEG study. Exp. Brain Res. 173, 637–649. https://doi.org/10.1007/s00221-006-0407-9
Spence, M.L., Dux, P.E., Arnold, D.H., 2016. Computations underlying confidence in visual perception. J. Exp. Psychol. Hum. Percept. Perform. 42, 671–682. https://doi.org/10.1037/xhp0000179
Staines, W.R., Brooke, J.D., McIlroy, W.E., 2000. Task-relevant selective modulation of somatosensory afferent paths from the lower limb. Neuroreport 11, 1713–1719.

Staines, W.R., Graham, S.J., Black, S.E., McIlroy, W.E., 2002. Task-Relevant Modulation of Contralateral and Ipsilateral Primary Somatosensory Cortex and the Role of a Prefrontal-Cortical Sensory Gating System. NeuroImage 15, 190–199. https://doi.org/10.1006/nimg.2001.0953

Stancák, A., Pfurtscheller, G., 1995. Desynchronization and recovery of β rhythms during brisk and slow self-paced finger movements in man. Neurosci. Lett. 196, 21–24. https://doi.org/10.1016/0304-3940(95)11827-J

Starr, A., Cohen, L.G., 1985. "Gating" of somatosensory evoked potentials begins before the onset of voluntary movement in man. Brain Res. 348, 183–186. https://doi.org/10.1016/0006-8993(85)90377-4

Stephan, K.E., Penny, W.D., Daunizeau, J., Moran, R.J., Friston, K.J., 2009. Bayesian model selection for group studies. NeuroImage 46, 1004–1017. https://doi.org/10.1016/j.neuroimage.2009.03.025

Sutton, R.S., Barto, A.G., 1998. Introduction to Reinforcement Learning, 1st ed. MIT Press, Cambridge, MA, USA.

Szurhaj, W., Derambure, P., Labyt, E., Cassim, F., Bourriez, J.-L., Isnard, J., Guieu, J.-D., Mauguière, F., 2003. Basic mechanisms of central rhythms reactivity to preparation and execution of a voluntary movement: a stereoelectroencephalographic study. Clin. Neurophysiol. Off. J. Int. Fed. Clin. Neurophysiol. 114, 107–119.

Tan, H., Jenkinson, N., Brown, P., 2014a. Dynamic Neural Correlates of Motor Error Monitoring and Adaptation during Trial-to-Trial Learning. J. Neurosci. 34, 5678–5688. https://doi.org/10.1523/JNEUROSCI.4739-13.2014

Tan, H., Wade, C., Brown, P., 2016. Post-Movement Beta Activity in Sensorimotor Cortex Indexes Confidence in the Estimations from Internal Models. J. Neurosci. Off. J. Soc. Neurosci. 36, 1516–1528. https://doi.org/10.1523/JNEUROSCI.3204-15.2016

Tan, H., Zavala, B., Pogosyan, A., Ashkan, K., Zrinzo, L., Foltynie, T., Limousin, P., Brown, P., 2014b. Human subthalamic nucleus in movement error detection and its evaluation during visuomotor adaptation. J. Neurosci. Off. J. Soc. Neurosci. 34, 16744–16754. https://doi.org/10.1523/JNEUROSCI.3414-14.2014

Tenenbaum, J.B., Griffiths, T.L., Kemp, C., 2006. Theory-based Bayesian models of inductive learning and reasoning. Trends Cogn. Sci. 10, 309–318. https://doi.org/10.1016/j.tics.2006.05.009

Teufel, C., Kingdon, A., Ingram, J.N., Wolpert, D.M., Fletcher, P.C., 2010. Deficits in sensory prediction are related to delusional ideation in healthy individuals. Neuropsychologia 48, 4169–4172. https://doi.org/10.1016/j.neuropsychologia.2010.10.024

Thoroughman, K.A., Shadmehr, R., 1999. Electromyographic correlates of learning an internal model of reaching movements. J. Neurosci. Off. J. Soc. Neurosci. 19, 8573–8588.

Todorov, E., 2004. Optimality principles in sensorimotor control. Nat. Neurosci. 7, 907–915. https://doi.org/10.1038/nn1309

Todorov, E., Jordan, M.I., 2002. Optimal feedback control as a theory of motor coordination. Nat. Neurosci. 5, 1226–1235. https://doi.org/10.1038/nn963

Torrecillos, F., Alayrangues, J., Kilavik, B.E., Malfait, N., 2015. Distinct Modulations in Sensorimotor Postmovement and Foreperiod β-Band Activities Related to Error Salience Processing and Sensorimotor Adaptation. J. Neurosci. 35, 12753–12765. https://doi.org/10.1523/JNEUROSCI.1090-15.2015

Tsakiris, M., Haggard, P., 2005. The rubber hand illusion revisited: visuotactile integration and self-attribution. J. Exp. Psychol. Hum. Percept. Perform. 31, 80–91. https://doi.org/10.1037/0096-1523.31.1.80

Tsay, A.J., Giummarra, M.J., Allen, T.J., Proske, U., 2016. The sensory origins of human position sense. J. Physiol. 594, 1037–1049. https://doi.org/10.1113/JP271498

Tzagarakis, C., Ince, N.F., Leuthold, A.C., Pellizzer, G., 2010. Beta-band activity during motor planning reflects response uncertainty. J. Neurosci. Off. J. Soc. Neurosci. 30, 11270–11277. https://doi.org/10.1523/JNEUROSCI.6026-09.2010

Tzagarakis, C., West, S., Pellizzer, G., 2015. Brain oscillatory activity during motor preparation: effect of directional uncertainty on beta, but not alpha, frequency band. Front. Neurosci. 9. https://doi.org/10.3389/fnins.2015.00246

Vaghi, M.M., Luyckx, F., Sule, A., Fineberg, N.A., Robbins, T.W., Martino, B.D., 2017. Compulsivity Reveals a Novel Dissociation between Action and Confidence. Neuron 0. https://doi.org/10.1016/j.neuron.2017.09.006

van Beers, R.J., Sittig, A.C., Denier van der Gon, J.J., 1998. The precision of proprioceptive position sense. Exp. Brain Res. 122, 367–377.

van Beers, R.J., Sittig, A.C., van Der Gon, J.J.D., 1999. Integration of proprioceptive and visual position-information: An experimentally supported model. J. Neurophysiol. 81, 1355–1364.

Van Hulle, L., Juravle, G., Spence, C., Crombez, G., Van Damme, S., 2013. Attention modulates sensory suppression during back movements. Conscious. Cogn. 22, 420–429. https://doi.org/10.1016/j.concog.2013.01.011

van Wijk, B.C.M., Daffertshofer, A., Roach, N., Praamstra, P., 2009. A Role of Beta Oscillatory Synchrony in Biasing Response Competition? Cereb. Cortex 19, 1294–1302. https://doi.org/10.1093/cercor/bhn174

Venkatakrishnan, A., Banquet, J.P., Burnod, Y., Contreras-vidal, J.L., 2011. Parkinson's disease differentially affects adaptation to gradual as compared to sudden visuomotor distortions. Hum. Mov. Sci., Special Issue: Progress in Graphonomics: A Perceptual Motor Skill Perspective 30, 760–769. https://doi.org/10.1016/j.humov.2010.08.020

Vilares, I., Kording, K.P., 2017. Dopaminergic medication increases reliance on current information in Parkinson's disease. Nat. Hum. Behav. 1, s41562-017-0129–017. https://doi.org/10.1038/s41562-017-0129

Voss, M., Bays, P.M., Rothwell, J.C., Wolpert, D.M., 2007. An improvement in perception of self-generated tactile stimuli following theta-burst stimulation of primary motor cortex. Neuropsychologia 45, 2712–2717. https://doi.org/10.1016/j.neuropsychologia.2007.04.008

Voss, M., Ingram, J.N., Wolpert, D.M., Haggard, P., 2008. Mere Expectation to Move Causes Attenuation of Sensory Signals. PLOS ONE 3, e2866. https://doi.org/10.1371/journal.pone.0002866

Vossel, S., Mathys, C., Daunizeau, J., Bauer, M., Driver, J., Friston, K.J., Stephan, K.E., 2014. Spatial Attention, Precision, and Bayesian Inference: A Study of Saccadic Response Speed. Cereb. Cortex 24, 1436–1450. https://doi.org/10.1093/cercor/bhs418

Wasaka, T., Kida, T., Kakigi, R., 2012. Modulation of somatosensory evoked potentials during force generation and relaxation. Exp. Brain Res. 219, 227–233. https://doi.org/10.1007/s00221-012-3082-z

Wei, K., Körding, K., 2010. Uncertainty of Feedback and State Estimation Determines the Speed of Motor Adaptation. Front. Comput. Neurosci. 4. https://doi.org/10.3389/fncom.2010.00011

Weiner, M.J., Hallett, M., Funkenstein, H.H., 1983. Adaptation to lateral displacement of vision in patients with lesions of the central nervous system. Neurology 33, 766–772.

Weiss, C., Herwig, A., Schütz-Bosbach, S., 2011. The Self in Social Interactions: Sensory Attenuation of Auditory Action Effects Is Stronger in Interactions with Others. PLOS ONE 6, e22723. https://doi.org/10.1371/journal.pone.0022723

Williams, D., Kühn, A., Kupsch, A., Tijssen, M., van Bruggen, G., Speelman, H., Hotton, G., Yarrow, K., Brown, P., 2003. Behavioural cues are associated with modulations of synchronous oscillations in the human subthalamic nucleus. Brain 126, 1975–1985. https://doi.org/10.1093/brain/awg194

Witham, C.L., Baker, S.N., 2007. Network oscillations and intrinsic spiking rhythmicity do not covary in monkey sensorimotor areas. J. Physiol. 580, 801–814. https://doi.org/10.1113/jphysiol.2006.124503
Witham, C.L., Wang, M., Baker, S.N., 2010. Corticomuscular coherence between motor cortex, somatosensory areas and forearm muscles in the monkey. Front. Syst. Neurosci. 4. https://doi.org/10.3389/fnsys.2010.00038
Wolpert, D.M., Ghahramani, Z., 2000. Computational principles of movement neuroscience. Nat. Neurosci. 3, 1212–1217.
Wolpert, D.M., Ghahramani, Z., Jordan, M.I., 1995. An internal model for sensorimotor integration. Science 269, 1880–1882.
Wolpert, D.M., Miall, R.C., 1996. Forward Models for Physiological Motor Control. Neural Netw. Off. J. Int. Neural Netw. Soc. 9, 1265–1279.
Yu, A.J., Dayan, P., 2005. Uncertainty, Neuromodulation, and Attention. Neuron 46, 681–692. https://doi.org/10.1016/j.neuron.2005.04.026
Zehr, E.P., Stein, R.B., 1999. What functions do reflexes serve during human locomotion? Prog. Neurobiol. 58, 185–205. https://doi.org/10.1016/S0301-0082(98)00081-1

APPENDICES

I have attached the two papers I have published as part of this PhD. The first paper is study one (chapter three) from this thesis which was published in the Journal of Neuroscience. The second paper is a commentary on the paper by Tan et al (2016), which was published in Trends In Cognitive Science.

Appendix A

Palmer, C.E., Davare, M., Kilner, J.M., 2016. Physiological and Perceptual Sensory Attenuation Have Different Underlying Neurophysiological Correlates. J. Neurosci. Off. J. Soc. Neurosci. 36, 10803–10812. doi:10.1523/JNEUROSCI.1694-16.2016

Appendix B

Palmer, C., Zapparoli, L., Kilner, J.M., 2016. A New Framework to Explain Sensorimotor Beta Oscillations. Trends Cogn. Sci. 0. doi:10.1016/j.tics.2016.03.007

Behavioral/Cognitive

Physiological and Perceptual Sensory Attenuation Have Different Underlying Neurophysiological Correlates

Clare E. Palmer,[1] Marco Davare,[1,2] and James M. Kilner[1]

[1]Sobell Department of Motor Neuroscience and Movement Disorders, Institute of Neurology, University College London, London WC1N 3BG, United Kingdom, and [2]Movement Control and Neuroplasticity Research Group, Biomedical Sciences Group, Department of Kinesiology, KU Leuven, 3001 Leuven, Belgium

Sensory attenuation, the top-down filtering or gating of afferent information, has been extensively studied in two fields: physiological and perceptual. Physiological sensory attenuation is represented as a decrease in the amplitude of the primary and secondary components of the somatosensory evoked potential (SEP) before and during movement. Perceptual sensory attenuation, described using the analogy of a persons' inability to tickle oneself, is a reduction in the perception of the afferent input of a self-produced tactile sensation due to the central cancellation of the reafferent signal by the efference copy of the motor command to produce the action. The fields investigating these two areas have remained isolated, so the relationship between them is unclear. The current study delivered median nerve stimulation to produce SEPs during a force-matching paradigm (used to quantify perceptual sensory attenuation) in healthy human subjects to determine whether SEP gating correlated with the behavior. Our results revealed that these two forms of attenuation have dissociable neurophysiological correlates and are likely functionally distinct, which has important implications for understanding neurological disorders in which one form of sensory attenuation but not the other is impaired. Time–frequency analyses revealed a negative correlation over sensorimotor cortex between gamma-oscillatory activity and the magnitude of perceptual sensory attenuation. This finding is consistent with the hypothesis that gamma-band power is related to prediction error and that this might underlie perceptual sensory attenuation.

Key words: electroencephalography; force matching; gamma oscillations; median nerve stimulation; sensory attenuation; somatosensory cortex

Significance Statement

We demonstrate that there are two functionally and mechanistically distinct forms of sensory gating. The literature regarding somatosensory evoked potential (SEP) gating is commonly cited as a potential mechanism underlying perceptual sensory attenuation; however, the formal relationship between physiological and perceptual sensory attenuation has never been tested. Here, we measured SEP gating and perceptual sensory attenuation in a single paradigm and identified their distinct neurophysiological correlates. Perceptual and physiological sensory attenuation has been shown to be impaired in various patient groups, so understanding the differential roles of these phenomena and how they are modulated in a diseased state is very important for aiding our understanding of neurological disorders such as schizophrenia, functional movement disorders, and Parkinson's disease.

Introduction

During movement, peripheral sensory receptors are stimulated, which activates sensory pathways in the CNS to relay information about our proprioceptive state and our surrounding environment to the cortex. Sensory attenuation is the top-down filtering of this afferent information to limit how much feedback is received. It has been proposed that the role of this sensory gating is to differentiate between sensations created by one's own move-

Received May 25, 2016; revised July 30, 2016; accepted Aug. 22, 2016.

Author contributions: C.E.P. and J.M.K. designed research; C.E.P. performed research; M.D. contributed unpublished reagents/analytic tools; C.E.P. analyzed data; C.E.P., M.D., and J.M.K. wrote the paper.

C.E.P is funded by a Wellcome Trust doctoral studentship and is in the 4-year doctoral program in neuroscience at University College London. M.D. is funded by a Biotechnology and Biological Sciences Research Council David Phillips fellowship, the Royal Society, and the Research Foundation Flanders (FWO) Odysseus Project (Fonds Wetenschappelijk Onderzoek, Belgium).

The authors declare no competing financial interests.

This article is freely available online through the *J Neurosci* Author Open Choice option.

Correspondence should be addressed to Clare E. Palmer, Institute of Neurology, University College London, 33 Queen Square, London WC1N 3BG, UK. E-mail: clare.palmer.13@ucl.ac.uk.

DOI:10.1523/JNEUROSCI.1694-16.2016

ments and those created from external stimuli to highlight the biologically more salient and less predictable external sensory input (Wolpert et al., 1995; Wolpert and Miall, 1996; Shergill et al., 2005). An alternative hypothesis posits that sensory attenuation is a necessary preparatory step to allow movement initiation to occur (Brown et al., 2013). However, due to the nature in which sensory attenuation has been studied previously, the role of this mechanism remains highly contested. Sensory attenuation has been studied extensively across the perceptual and physiological domains and it has been suggested that "movement-induced somatosensory gating may be the physiological correlate of the decreased sensation associated with self-produced tactile stimuli in humans" (Blakemore et al., 2000); however, the relationship between the two has never been formally tested. This was the aim of the work described here.

Physiological somatosensory attenuation can be explored using electrical stimulation of the median nerve. This produces a somatosensory evoked potential (SEP) recordable at multiple levels of the somatosensory pathway to provide a measure of the magnitude of the afferent volley. Cortical EEG recordings have shown that there is a suppression of the primary and secondary complexes of the SEP during active and passive movement (Rushton et al., 1981). Attenuation of SEPs has also been shown during motor preparation before EMG onset of active movement (Starr and Cohen, 1985; Jiang et al., 1990; Seki and Fetz, 2012), suggesting that this gating occurs via central mechanisms.

Perceptual sensory attenuation is described as a reduction in the perception of the afferent input of a self-produced tactile sensation and is referred to as the inability to tickle oneself. This has been attributed to a central cancellation of the reafferent sensory signal by the efference copy of the motor command before making the tickling action. When someone else is producing the tickling sensation, there is no efference copy to cancel out or reduce the incoming afference, so the sensory information is not attenuated (Blakemore et al., 1998, 2000). This has been proposed to distinguish between self-generated and externally generated sensations. Similar results were found in a force-matching paradigm, which provides a more quantitative method to assess sensory gating at a perceptual level. When asked to match a force by pressing on themselves (self-generated), participants significantly overestimated the matched force compared with when a robot was manipulated to produce the force (externally generated) (Shergill et al., 2003; Pareés et al., 2014). In addition, when the finger receiving the force was given an anesthetic to prevent any reafference from skin and joint receptors, attenuation still occurred, suggesting that, as with SEP gating, the sensory signal was modified using top-down processes (Walsh et al., 2011).

To date, the neurophysiological correlates underlying perceptual sensory attenuation have not been addressed. fMRI studies have attempted to localize the networks involved in somatosensory attenuation and have suggested that perceptual attenuation may be driven by activity in the secondary somatosensory cortex (Blakemore et al., 1998; Shergill et al., 2013). This is distinct from SEP attenuation, in which it is has been shown that the early SEP components that are attenuated during movement originate from activity in SI. Indeed, studies measuring neurophysiological attenuation to action-driven and externally driven sensations in the auditory and visual domains have highlighted differences in the locus and timing of attenuation dependent on the nature of the task (Bäss et al., 2008; Hughes et al., 2013; Roussel et al., 2014); this may demonstrate a potential dissociation in mechanism depending on whether the task is low level (e.g., active movement) or high level (e.g., force matching). Therefore, although it has been suggested that movement-induced SEP attenuation may underlie perceptual sensory attenuation, the relationship between the two may be more complex. Here, we delivered median nerve stimulation at specific time points throughout a force-matching paradigm and recorded the EEG to determine whether physiological sensory attenuation was correlated with perceptual sensory attenuation, as has been proposed previously, or if these two forms of sensory attenuation are dissociable and therefore potentially functionally distinct.

Materials and Methods

Subjects

Eighteen healthy participants (male = 9; female = 9) age 20–56 years (mean ± SD: 28.24 ± 8.53) took part in this study. Participants had no history of neurological or psychiatric illness. All participants were right handed and gave written informed consent before taking part. This study was approved by the University College London (UCL) Research Ethics Committee and all testing took place at the UCL Institute of Neurology. Two subjects were excluded due to noisy EEG data.

Experimental setup

Participants sat at a desk with their left hand supernated and index finger extended under a force transducer. Two haptic robots were positioned in front of the subject (Fig. 1*A*). One robot was stationed above the force transducer and produced forces directly on the left index finger. The second robot was positioned over a pliable object and controlled the force produced by the first robot in the "external" condition (see "Task procedure"). The force transducer recorded all forces exerted on the left finger using Spike2 version 6.17 software. The target forces applied were 1, 1.5, 2, and 2.5 N. A peripheral nerve stimulator was used to stimulate the median nerve at the left or right wrist at specific time points throughout the experiment. EEG data were recorded using a BioSemi 128 active electrode system at a sampling frequency of 2048 Hz. Two external reference electrodes were placed on the subjects' earlobes.

Task procedure

Force-matching task. To measure perceptual sensory attenuation, a classic force-matching task was used (Shergill et al., 2005; Pareés et al., 2014). Subjects received a force (produced by robot 1) on their left index finger for 3 s. They were instructed to match the intensity of that force on the same finger by either pushing down on robot 1 to emulate the force produced ("self" condition) or by pushing down on robot 2 ("external" condition; Fig 1*A*). Robot 2 was linearly connected to robot 1 such that a 1 cm movement in robot 2 produced a 1.25 N downward force on robot 1. Once the subjects had produced the appropriate force, they were instructed to hold the matched force until they heard the stop signal (4.5 s). The intertrial interval was 1 s. Instructions for the behavioral task appeared on a computer screen in front of the participant throughout the experiment. Median nerve stimulation (MNS) was either given while holding the matched force only (×3 every 500 ms from 3 s after the GO signal; 32 trials per block; "Hold stimuli") or additionally during force production (×5 stimuli every 500 ms from GO signal 12 trials per block; "Phasic stimuli"; Fig. 1*B*). Subjects completed alternate blocks of each condition counterbalanced across participants. There were 44 trials in each block containing equal numbers (×11) of each target force (ratio of trials with and without phasic stimuli = 3:8). There were four blocks of each condition in one session. Subjects completed the same behavioral task in 2 sessions (mean ± SD time between sessions: 2.8 ± 3.4 d). The stimulated wrist alternated between sessions and the order was counterbalanced across participants.

Movement control. To record a measure of SEP attenuation during movement independently from the behavioral task, participants completed a movement control task in both sessions. The task consisted of alternating blocks of movement and rest. When subjects saw the word "MOVE" presented on a computer screen accompanied by an auditory "GO" signal, they were instructed to make a rapid, large, and frequent tapping motion of the index finger of the wrist being stimulated. When they saw the word "REST," participants were instructed to remain as still

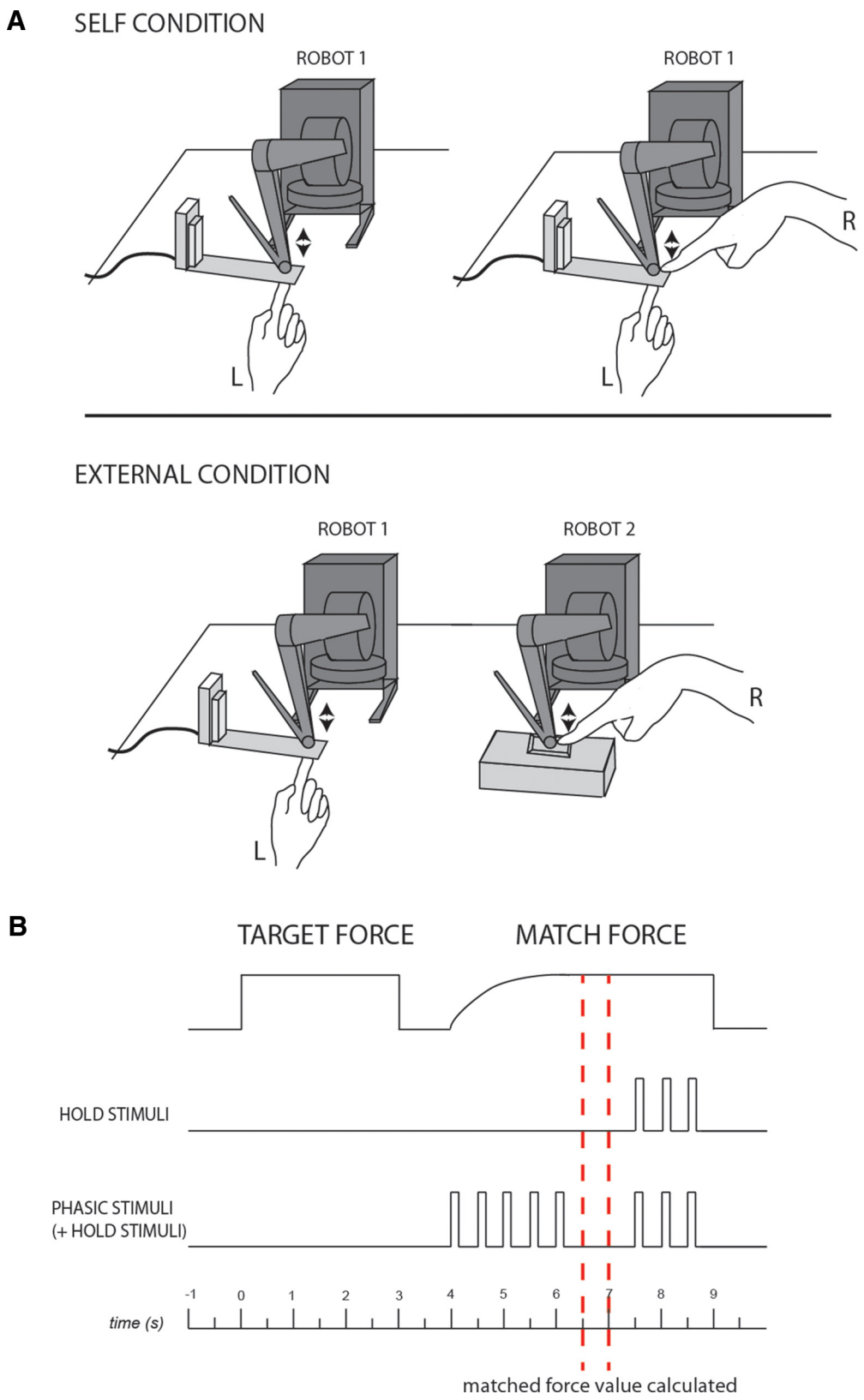

Figure 1. Experimental setup and task design for the force-matching paradigm. ***A***, Self-condition (top): robot 1 was fixed onto a force transducer. Robot 1 produced a target force on the left index finger, which was matched by pushing down on the subject pushing down on robot 1 using the right index finger. External condition (bottom): robot 2 was linearly connected to robot 1 such that any force exerted on robot 2 was felt on the left index finger. The gain was altered so that more force was required in this condition to produce the same force output across conditions. ***B***, Schematic of the trial design for a single trial. The top line is the force output from the force transducer during the target and matched forces. The top middle line shows the timing of the hold stimuli relative to the force output; behavioral data were only used for these trials. The bottom middle line shows trials that additionally received phasic stimuli and the timing of these relative to the force output. The bottom line is a time axis in seconds aligned to the start of the target force at 0 s. The red dotted lines mark the time period in which the magnitude of the matched force for each trial was calculated.

and relaxed as possible. During each block, participants received 25 electrical pulses to the wrist at a frequency of 2 Hz. There were 20 blocks in total in each session (10 rest, 10 movement), resulting in 250 SEPs per condition for each wrist.

Median nerve stimulation

Two electrodes were placed on the surface of the skin in the center of the wrist above the median nerve with the cathode more distal just below the crease of the wrist. The intensity of the stimulation at threshold (slight thumb twitch) was identified and then increased by 1 mA to produce a definite thumb twitch. The intensity remained the same throughout the experiment with a pulse width of 0.2 μm.

Behavioral data analysis

Force values were extracted from Spike into MATLAB. Trials in which median nerve stimulation was given during force production in the matching phase (phasic stimuli) were removed from the behavioral analysis. Mean force output per trial was calculated from a specific time window of 2.5–3 s after the GO signal to start matching (Fig. 1*B*). Median nerve stimuli were not given until 3 s in these trials (no phasic stimuli given), so they would have had no interference with the behavioral data during this time window. The mean force output during the target force was also recorded in the same time window to determine the relationship between the voltage output of the force transducer and the force applied by the robot given in Newtons. A calibration procedure was then used to scale the force output (voltage) to determine the true magnitude difference in Newtons from the given target force.

It has been shown previously that people with schizophrenia are impaired on the force-matching task such that they did not overestimate force in the self-condition (Shergill et al., 2005). In addition, the magnitude of perceptual sensory attenuation in a population of healthy controls negatively correlated with their scores of delusional ideation (a measure of schizotypy). To replicate previous findings, we hypothesized that the magnitude of force matching would be negatively correlated with schizotypy scores. All subjects completed the Peter's Delusion Inventory (PDI) before taking part in the experiment. An overcompensation score for the force-matching task was calculated for each participant by finding the difference between the matched force and the target force in the self-condition. Parametric and nonparametric correlation analyses measured the relationship between overcompensation scores and PDI scores (one-tailed) across subjects.

EEG data analysis

Preprocessing. Data were preprocessed using SPM 12. EEG data were rereferenced by deducting data from two external electrodes attached to the subjects' earlobes. The data were then filtered using a high-pass filter at 0.1 Hz. For analysis of the time × frequency data only, a low-pass filter at 100 Hz was also used. A trigger was sent to the EEG system at the time of every median nerve stimulus. The data were epoched around the time of median nerve stimulation with a time window of −100 ms to 250 ms for the SEP data. For the time–frequency analysis, epochs were generated from the first median nerve stimulus given after force matching in trials with hold stimuli only with a time window of −7500 to 0 ms. In this way, we could ensure that there were no stimulus artifacts in the window of interest. The different experimental blocks were merged into a single file. For the time–frequency analysis, the power of the EEG signal at each frequency from 1 to 99 Hz in steps of 2 was estimated using the multitaper spectral estimation in SPM with a sliding time window of 400 ms that moved in steps of 50 ms. The data were transformed using the log rescale function and baseline corrected using a 50 ms window from the first 100 ms of the epoched time window.

SEP analysis. The epoched EEG data were averaged over trials and the topography examined to determine a ROI over sensorimotor cortex. Individual ROIs over sensorimotor corticies were selected based on electrodes that showed a negative peak at ~20 ms and a positive peak ~30–45 ms after the stimulus. For each subject, electrodes for analysis were selected from SEP data averaged over all conditions and the same ROI was used for all analyses for that subject. Epoched data were subdivided dependent on whether the median nerve stimulation was given during the phasic part of the force matching or while holding the matched force. Five well characterized peaks of the SEP were identified and used for analysis: N20, P30, P45, N55, and P100. For each subject, an average SEP across all conditions over the specified ROI was generated and the latency of each peak was identified from this. The same latencies were then used for all subsequent analyses. Mean latencies of the left hemisphere were as follows (in milliseconds): N20 = 20.4 ± 1.2, P30 = 29.6 ± 3.3, P45 = 45 ± 3.7, N55 = 64 ± 8.0, and P100 = 95.1 ± 10.7. Mean latencies in the right hemisphere were as follows (in milliseconds): N20 = 21.3 ± 3.7, P30 = 31.4 ± 6.2, P45 = 45.2 ± 5.0, N55 = 61.8 ± 8.9, and P100 = 94.6 ± 13.6. These latencies were used to calculate the amplitude of each peak in the SEP for each condition so that there was no experimenter bias in determining peak amplitudes (Kilner, 2013). The amplitude difference between neighboring peaks generated the dependent variable for each component of the SEP: primary complex = N20–P30, secondary complex = P45–N55, and the later component = N55–P100.

To replicate previous neurophysiological data showing SEP attenuation with movement, the mean amplitude difference of each SEP component was compared for MNS given during movement versus rest in the control task. To determine the effect of task condition on SEP attenuation, the mean amplitude difference of each component was compared in a 2 × 2 repeated-measures ANOVA (rmANOVA) with the factors self- versus external task condition and hold versus phasic stimuli. The contrast between hold versus phasic stimuli was included to provide a measure of physiological SEP attenuation (most commonly seen comparing movement and rest) within the behavioral paradigm with the rationale that SEP components should show a greater decrease in amplitude during force generation (phasic stimuli) compared with those produced during an isometric contraction (hold stimuli). A significant interaction between task condition and MNS time point would therefore suggest greater physiological SEP attenuation in one task condition compared with the other.

To further substantiate the relationship between perceptual and physiological sensory attenuation, nonparametric and parametric correlations were also performed between the magnitude of physiological sensory attenuation (difference between SEP amplitudes during the hold phase of force matching and the phasic phase) for each component of the SEP (N20–P30, P45–N55, and N55–P100) and PDI scores for both hemispheres.

Time–frequency analysis. A time–frequency analysis was conducted to investigate whether there was any aspect of the oscillatory neural signal that correlated significantly with the behavioral data. The time–frequency data files were converted into images for statistical analysis in SPM. Images were created of the average of all trials for each condition (self, external) and force level (1, 1.5, 2, or 2.5 N), creating 8 images in total per subject. The time–frequency data were averaged over the ROI selected previously in the SEP analysis to remove the dimension of "scalp" for both hemispheres independently. The EEG data were then regressed against the behavioral outcomes of the task for each condition: the magnitude of sensory attenuation (the target force − the matched force) and the target force given. The latter covariate was used to control for any changes in neural activity as a result of force applied to the left finger. A β-image was created for each subject and used in a one-sample *t* test at the group level to determine in which voxels the regressions at the first level were either positively or negatively significantly different from 0. To test for any significant clusters in the time–frequency images, we ran a permutation analysis using the SnPM toolbox within SPM with 500 permutations.

Results

Behavior: participants overestimated force in the self-condition compared with the external condition

As expected from previous findings, there was significant perceptual sensory attenuation across subjects in the force-matching task, meaning that subjects significantly overestimated the matched force in the self-condition compared with the external condition. A 2 × 4 rmANOVA comparing condition (self vs external) and force level (1, 1.5, 2, or 2.5) for the matched force

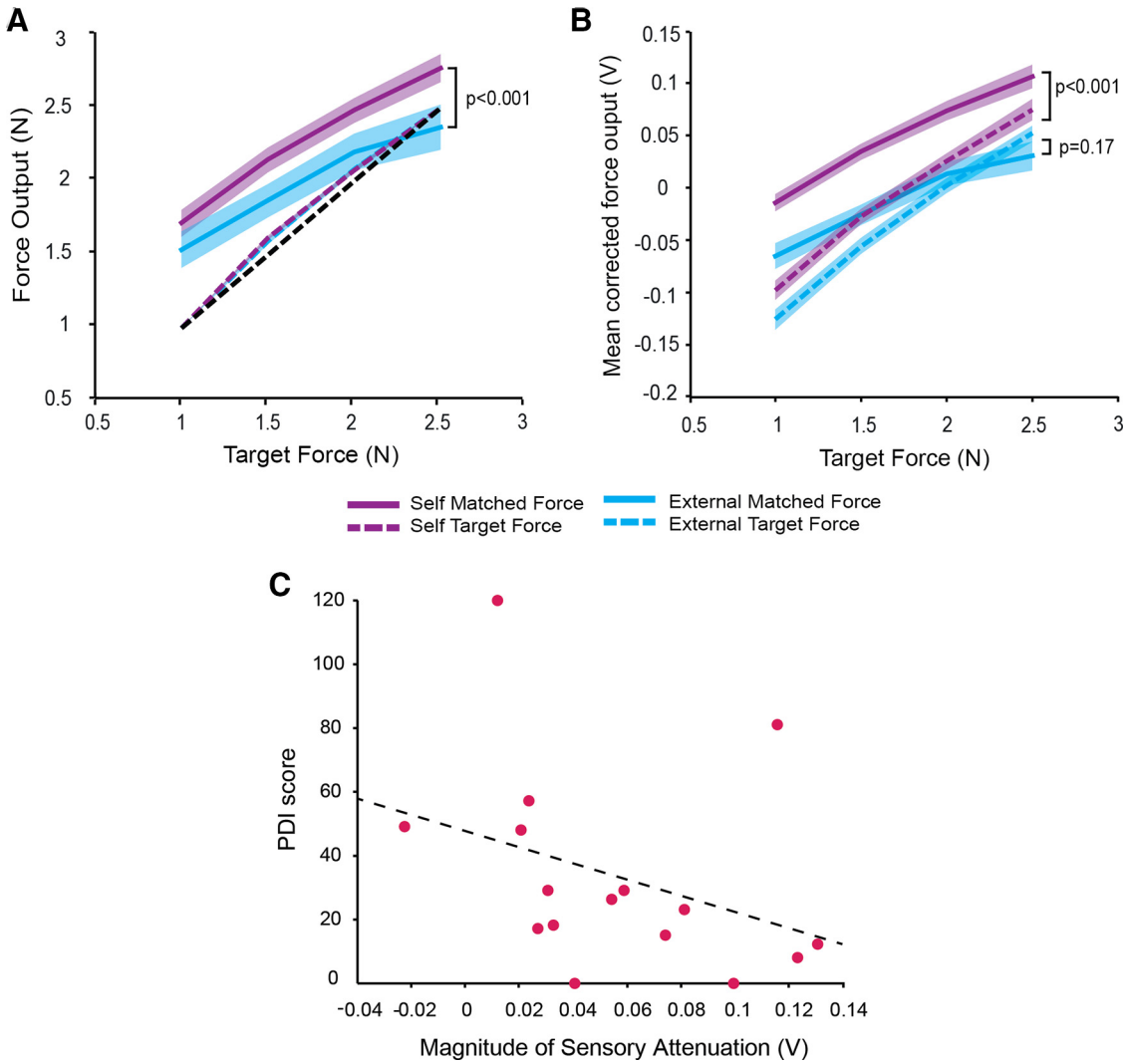

Figure 2. Behavioral data: greater overall force output in the self-condition compared with the external condition. ***A***, Mean matched force for each target force level given (1, 1.5, 2, and 2.5 N) for the self-condition (purple, solid) and the external condition (blue, solid). The dotted black line represents the input target forces and the colored dotted lines represent the mean force output calculated during the target force for each condition. The force output has been converted from voltage (V) to Newtons (N). ***B***, Same data as graph ***A*** before they were converted to Newtons and mean corrected to demonstrate the statistical differences between the conditions. ***C***, Correlation between the magnitude of perceptual sensory attenuation and scores of delusional ideation taken from the PDI replicating Teufel et al. (2010)'s findings (parametric: $r = -0.35$, $p = 0.092$; nonparametric: $r = -0.56$, $p = 0.012$; both one-tailed).

revealed a significant main effect of condition ($F_{(1,15)} = 19.43$, $p < 0.001$), a significant main effect of force level ($F_{(3,45)} = 79.23$, $p < 0.001$), and a significant interaction ($F_{(3,45)} = 3.10$, $p = 0.036$). Overall, participants produced significantly greater force output in the self-condition (mean ± SD = 2.34 ± 0.41 N) compared with the external condition (mean ± SD = 1.80 ± 0.79 N; Fig. 2*A*), demonstrating significant perceptual sensory attenuation. Pairwise comparisons between the two conditions at each force level showed that, despite the significant interaction, the matched force produced in the self-condition was significantly larger than the external condition at each force level ($p < 0.002$, corrected for multiple comparisons). Comparing the matched force and the target force against force level for each condition separately using a 2 × 4 rmANOVA revealed a significant difference between the matched force and the target force in the self-condition ($F_{(1,15)} = 26.31$, $p < 0.001$), but no significant difference between the matched force and the target force in the external condition ($p = 0.168$). Both conditions showed a significant interaction between force level and the difference between the matched and the target force (self: $F_{(3,45)} = 25.19$, $p < 0.001$; external: $F_{(3,45)} = 21.63$, $p < 0.001$). As can be seen in Figure 2*B*, there was a greater difference between the matched force and the target force at lower force levels compared with higher force levels.

Replicating previous findings by Teufel et al. (2010), we found a significant negative correlation between the overall magnitude of perceptual sensory attenuation and scores of delusional ideation using the nonparametric Spearman's correlational analysis ($r_s = -0.56$, $p = 0.012$ one-tailed; Fig. 2*C*).

Here, we were able to demonstrate significant behavioral sensory attenuation, replicating previous results and, critically, demonstrating that MNS given after matching did not abolish this effect.

Neurophysiology: movement attenuated the primary and secondary complexes of the SEP

To ensure that we could measure standard SEP attenuation previously recorded in response to movement, participants performed a simple control task in which we compared SEP amplitudes at rest and during movement. We were able to replicate previous findings successfully. SEPs recorded over sensori-

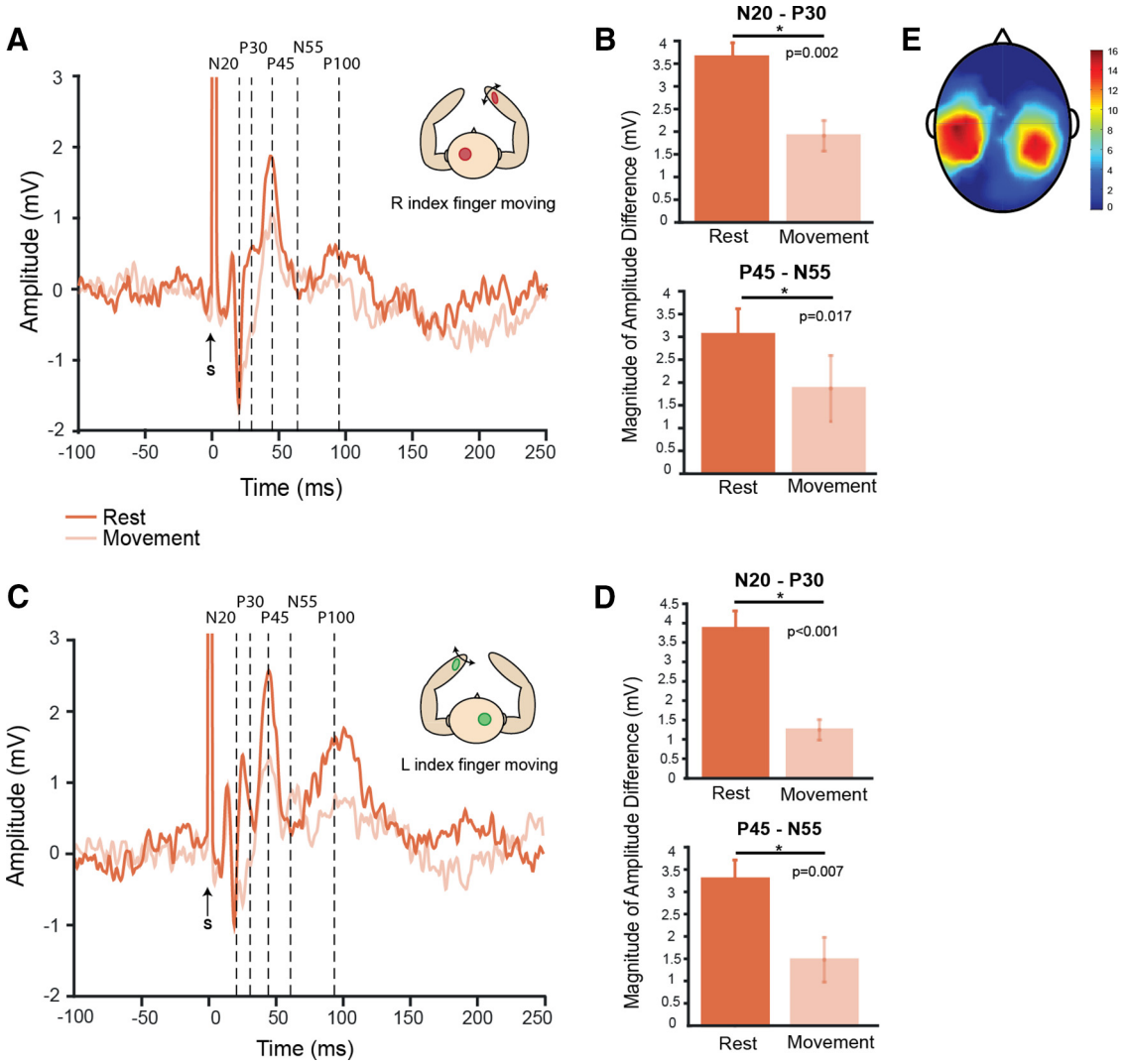

Figure 3. Movement decreases SEP amplitudes relative to baseline. ***A***, ***C***, Average SEP traces in response to median nerve stimulation from a ROI over the right (***A***) and left (***C***) sensorimotor corticies for the rest (orange) and movement (pale orange) conditions of the movement control task. ***B***, ***D***, Magnitude of the mean SEP amplitude for N20 – P30 and P45 – N55 across all subjects is shown for the rest (orange) and movement (pale orange) conditions for the right (***B***) and left (***D***) sensorimotor corticies. ***E***, Individual ROIs were selected for each subject based on SEP data averaged across all conditions; therefore, the scalp map shows the overlap of selected electrodes over each hemisphere. The color bar represents the number of participants for which that electrode (area) was selected for analysis. S, Median nerve stimulus.

motor cortex contralateral to the moving hand being stimulated were attenuated during movement compared with rest in a movement control task (Fig. 3). The mean amplitude of the primary complex, N20–P30, from SEPs recorded over the hemisphere contralateral to movement decreased significantly when the stimulated index finger was moving compared with rest; this was conducted separately for right and left wrist MNS (left hemisphere: $t_{(15)} = -3.83$, $p = 0.002$; right hemisphere: $t_{(15)} = -5.68$, $p < 0.001$). The same result was found for the secondary component, P45–N55 (left hemisphere: $t_{(15)} = 2.70$, $p = 0.017$; right hemisphere: $t_{(15)} = 3.15$, $p = 0.007$). Individual ROIs were selected for each subject based on SEP data averaged across all conditions. Figure 3*E* shows the overlap of selected electrodes over each hemisphere.

Neurophysiology: SEP attenuation of the primary and secondary components was not modulated by behavioral task condition

MNS was given at two time points during the behavioral task: "phasic stimuli" were given directly after the GO cue to start matching during force generation and "hold stimuli" were given during steady-state contraction when the target force was matched (Fig. 1*B*). We hypothesized that mean SEP amplitudes would be smaller for phasic SEPs compared with hold SEPs because it has been shown previously that there is greater physiological sensory attenuation during force generation compared with an isometric contraction. This contrast was used to demonstrate standard physiological SEP attenuation seen with movement during the behavioral task. We then compared mean SEP amplitudes at these time points and across conditions in the behavioral task using a 2 × 2 rmANOVA comparing condition (self vs external) and stimulation time (phasic SEPs vs hold SEPs) with the hypothesis that a significant interaction between stimulation time and task condition would demonstrate a direct modulation of SEP attenuation with task condition.

Over the left sensorimotor cortex contralateral to the moving hand, there was a significant effect of stimulation time for both the primary (N20–P30: $F_{(1,15)} = 15.93$, $p = 0.001$) and secondary (P45–N55: $F_{(1,15)} = 10.62$, $p = 0.005$) components of the SEP. For both components, the mean amplitude was greatest for the

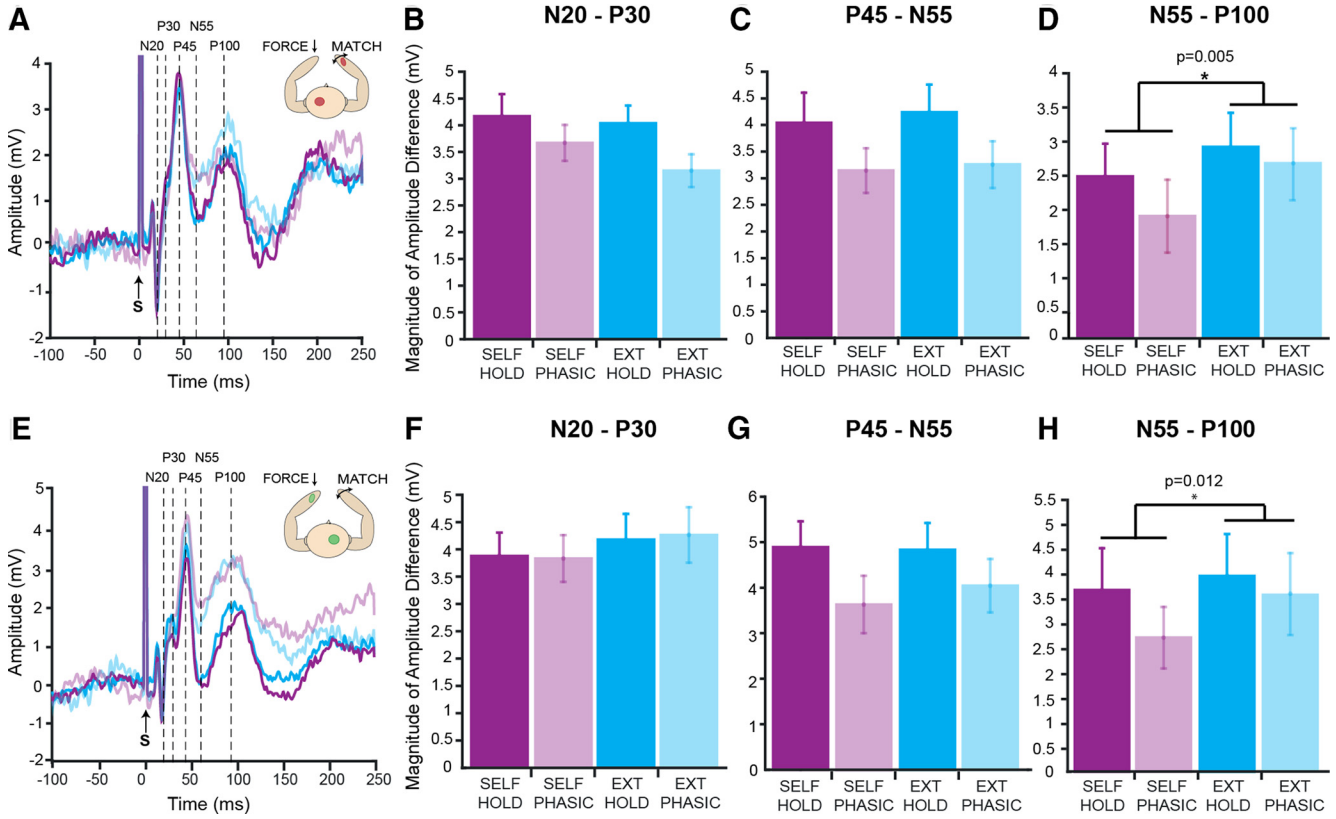

Figure 4. Attenuation of SEP amplitudes with stimulation time and behavioral task condition. ***A–D***, Top, Data taken from left sensorimotor cortex. ***E–H***, Bottom, data taken from right sensorimotor cortex. Graphs ***A*** and ***E*** show the average SEP traces across all subjects for the four experimental conditions: self-condition hold stimuli (dark purple); self-condition phasic stimuli (light purple); external condition hold stimuli (dark blue); and external condition phasic stimuli (light blue). The remaining graphs show the magnitude amplitude difference between adjacent SEP components for each condition for N20–P30 (***B***, ***F***), P45–N55 (***C***, ***G***), and N55–P100 (***D***, ***H***). Graphs ***B***, ***C***, and ***G*** show a significant effect of stimulation time representing significant attenuation, but no significant effect of behavioral task condition. Graphs ***D*** and ***H*** show no significant effect of stimulation time, but a significant effect of behavioral task condition.

hold SEPs compared with the phasic SEPs, demonstrating significant SEP attenuation during the behavioral task (Fig. 4*A–C*). However, there was no significant effect of condition for either component (N20–P30, $p = 0.183$; P45–N55, $p = 0.516$) and no significant interaction (N20–P30, $p = 0.430$; P45–N55, $p = 0.893$), suggesting that SEP attenuation of the primary and secondary components was not modulated by task condition.

Interestingly, similar results were found the over right sensorimotor cortex ipsilateral to the moving hand and contralateral to the finger receiving the matched force. There was no significant effect of stimulation time for the primary component (N20–P30, $p = 0.902$); however, there was a significant effect of stimulation time for the secondary complex (P45–N55, $F_{(1,15)} = 11.94$, $p = 0.004$). The mean amplitude for the hold SEPs was greater than the phasic SEPs (Fig. 4*E–G*). Again, there were no significant effects of condition (N20–P30, $p = 0.157$; P45–N55, $p = 0.565$) and no significant interactions (N20–P30, $p = 0.724$; P45–N55, $p = 0.389$). Attenuation of the primary and secondary components of the SEP was not modulated significantly by the behavioral task condition.

To ensure that there were no specific modulations of SEP attenuation with force level, the same analysis used for the behavioral data were conducted. A 2 × 4 rmANOVA compared the magnitude of SEP attenuation (hold − phasic) at each force level for the self- and external conditions. This was conducted separately for the primary and secondary SEP components and for both hemispheres. There were no significant main effects of condition (left hemisphere: N20–P30, $p = 0.238$; P45–N55, $p = 0.766$; right hemisphere: N20–P30, $p = 0.505$; P45–N55, $p = 0.848$), no significant main effects of force level (left hemisphere: N20–P30, $p = 0.404$; P45–N55, $p = 0.401$; right hemisphere: N20–P30, $p = 0.300$; P45–N55, $p = 0.398$) and no significant interactions between condition and force level (left hemisphere: N20–P30, $p = 0.233$; P45–N55, $p = 0.923$; right hemisphere: N20–P30, $p = 0.890$; P45–N55, $p = 0.563$).

To provide further support that SEP attenuation is not related to perceptual sensory attenuation, we found no significant correlations between attenuation of individual SEP components and scores of delusional ideation across either hemisphere, unlike perceptual sensory attenuation, using nonparametric Spearman's analysis (left hemisphere: N20–P30, $r = 0.093$, $p = 0.73$; P45–N55, $r = -0.040$, $p = 0.88$; right hemisphere: N20–P30, $r = 0.22$, $p = 0.42$; P45–N55, $r = -0.17$, $p = 0.52$).

Neurophysiology: attenuation of a later SEP component, N55–P100, was modulated by behavioral task condition

In contrast to the results regarding the primary and secondary SEP components, analysis of a later SEP component, N55–P100, using the same rmANOVA revealed a significant main effect of condition for both the left sensorimotor cortex ($F_{(1,15)} = 10.72$, $p = 0.005$; Fig. 4*D*) and right sensorimotor cortex ($F_{(1,15)} = 8.25$, $p = 0.012$; Fig. 4*H*). In both hemispheres, the mean N55–P100 amplitude for the self-condition (left hemisphere: mean ± SD = 2.02 ± 1.93; right hemisphere: mean ± SD = 3.17 ± 2.94) was significantly less than in the external condition (left hemisphere: mean ± SD = 2.53 ± 1.86; right hemisphere: mean ± SD =

3.72 ± 3.26). However, there was no significant interaction between the behavioral condition and the stimulation time for either hemisphere (left hemisphere, $p = 0.460$; right hemisphere, $p = 0.216$) and no significant main effect of stimulation time (left hemisphere, $p = 0.059$; right hemisphere, $p = 0.123$). Overall, the mean amplitude of the N55–P100 component was smaller over both hemispheres for the self-condition compared with the external condition, suggesting that attenuation of this later SEP component correlated with perceptual sensory attenuation.

To investigate whether attenuation of this later SEP component was modulated by force level, the same analysis used for the behavioral data and for the early SEP components was conducted. Because the main ANOVA revealed a significant main effect of condition but no interaction or main effect of stimulation time, a 2 × 4 rmANOVA was conducted to compare the mean SEP amplitude across hold and phasic SEPs combined at each force level for the self- and external conditions. For both hemispheres, there was a significant main effect of condition (left hemisphere: $F_{(1,15)} = 6.11$, $p < 0.026$; right hemisphere: $F_{(1,15)} = 4.88$, $p = 0.043$), with a lower SEP magnitude difference for the self-condition (left hemisphere: mean ± SD = 2.01 ± 2.22 mV; right hemisphere: mean ± SD = 3.03 ± 3.05 mV) compared with the external condition (left hemisphere: mean ± SD = 2.55 ± 2.12 mV; right hemisphere: mean ± SD = 3.54 ± 3.59 mV). However, there was no modulation of SEP amplitude with force level ($p = 0.974$) and no significant interaction between condition and force level ($p = 0.426$).

In addition, there was no significant correlation between attenuation of the N55–P100 SEP component and scores of delusional ideation across either hemisphere, unlike perceptual sensory attenuation, using nonparametric Spearman's analysis (left hemisphere: N55–P100, $r = -0.25$, $p = 0.34$; right hemisphere: N55–P100, $r = -0.15$, $p = 0.59$).

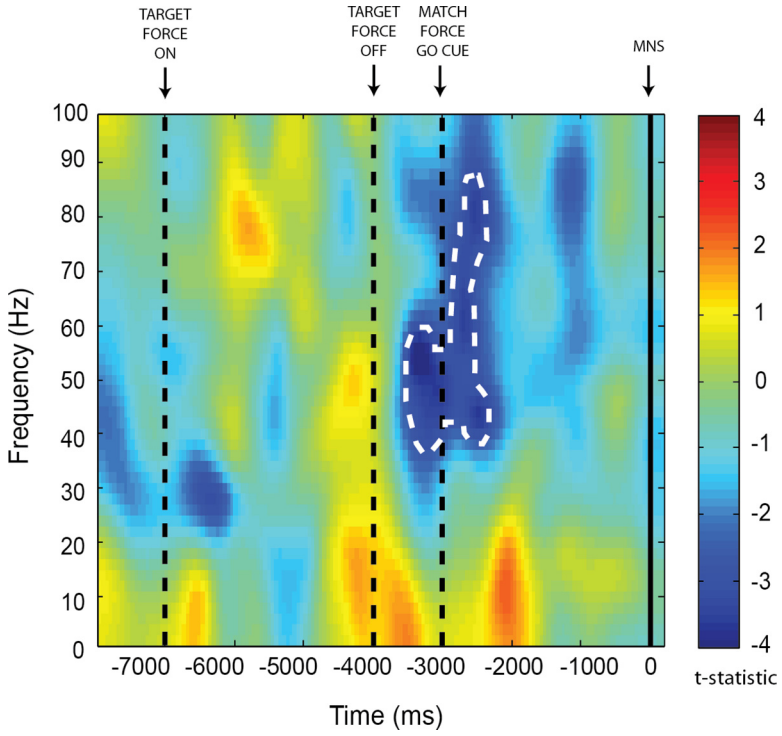

Figure 5. Negative correlation between gamma-band oscillatory activity and the magnitude of perceptual sensory attenuation before force matching. Shown is a time–frequency plot averaged over a preselected ROI showing the value of the *t*-statistic resulting from a one-sample *t* test at the group level of β images from regression analyses between EEG data and behavioral data at the single-subject level. These data represent a negative contrast; that is, in which voxels the mean regression across subjects was negative. Gamma-band oscillatory activity (peak 54 Hz) was significantly negatively correlated with perceptual sensory attenuation in the time period just before the auditory GO cue to match the target force was produced (−3422 ms before the first MNS). A nonparametric permutation analysis using the SnPM toolbox revealed a significant cluster of activity (outlined in a white dotted line) at the corrected $p < 0.05$ level.

Time–frequency analysis: negative correlation between gamma-band activity and the magnitude of perceptual sensory attenuation

Having demonstrated no significant comodulation of the SEP components with the behavioral data, we next tested whether there were any modulations in the time–frequency domain that correlated with the behavior. To this end, a time–frequency analysis was performed to identify whether any oscillatory activity over sensorimotor cortex correlated with the magnitude of perceptual sensory attenuation to provide a potential neurophysiological marker for this behavioral phenomenon. At the single-subject level, the average magnitude of sensory attenuation (difference between the target force and the matched force) for each force level and each condition (2 × 4; average of all trials at each level of each factor; see Materials and Methods for more details) was regressed against the EEG activity in the previously specified ROI across all frequencies and across the full time window of a single trial to determine whether any neurophysiological activity correlated with the behavioral data. The target force averaged over the same trials was also included in the model to regress out the effect of target force. A one-sample *t* test at the second level revealed a significant cluster over the right sensorimotor cortex within the gamma-frequency band with a peak at 54 Hz (cluster-level: $p = 0.004$, corrected; peak-level: $t = 4.24$, $p < 0.001$,uncorrected). A nonparametric permutation analysis run with the SnPM toolbox confirmed this cluster to be significant at the corrected $p < 0.05$ level. This activity was negatively correlated with the magnitude of perceptual sensory attenuation and occurred 422 ms before the auditory GO signal to start matching (Fig. 5). As perceptual sensory attenuation increased, that is, as matching became less veridical (self-condition), the power of oscillatory activity within the gamma-frequency band decreased.

Discussion

It has been proposed previously that movement-induced cortical gating of SEPs may be the mechanism underlying perceptual sensory attenuation measured using a force-matching paradigm. This study aimed to correlate physiological sensory attenuation of cortical SEPs with perceptual sensory attenuation to test this hypothesis. Primary (N20–P30) and secondary (P45–N55) components of the SEP showed significant attenuation during the behavioral task with force production, but this attenuation was not modulated significantly by task condition. This suggests that physiological attenuation of early SEP components does not underlie perceptual sensory attenuation. However, analysis of a later SEP component (N55–P100) demonstrated an overall decrease

in mean amplitude throughout the self-condition compared with the external condition, suggesting that attenuation of this component may have a causal influence over perception in the force-matching task.

Cortical SEP attenuation of the primary and secondary complexes was seen clearly during a movement control task and during the force-matching paradigm. Previous research has demonstrated that SEP attenuation is greatest 200–400 ms after EMG onset (Starr and Cohen, 1985; Wasaka et al., 2012) and increases with the velocity and magnitude of the movement (Rushton et al., 1981); therefore, we hypothesized, and subsequently demonstrated, significant attenuation of SEPs (over sensorimotor cortex contralateral to the moving hand) generated during force production (phasic stimuli) compared with an isometric force (hold stimuli). Interestingly, SEP attenuation of the secondary component, P45–N55, was also identified in the right hemisphere ipsilateral to the moving hand and contralateral to the hand receiving the matched force. Previous research has found no attenuation of SEPs in the hemisphere ipsilateral to movement (Kakigi, 1986; Cohen and Starr, 1987), but has shown attenuation of early SEP components in response to tactile stimulation (Kakigi and Jones, 1985, 1986). When phasic stimuli were given, the force on the left index finger was increasing compared with hold stimuli, in which the force did not change. This suggests that applying a changing force to the periphery modulates sensory gating.

We further hypothesized that, if this physiological sensory attenuation were the mechanism underlying perceptual sensory attenuation, then there would be an interaction between the amplitude of SEP components at these time points and the behavioral task condition with greater SEP attenuation in the self-condition. However, we found no modulation of the early SEP components with behavioral task condition. This result is consistent with the hypothesis that these are two distinct forms of sensory attenuation.

Interestingly, there was a significant decrease in the mean amplitude of the later N55–P100 SEP component throughout the self-condition compared with the external condition. It is perhaps not surprising that this later component is modulated differentially compared with the earlier components because there is more time for the signal to be influenced by interconnected cortical areas. MEG studies in humans have highlighted that the earliest components of the SEP originate in contralateral area 3b, which has dense thalamocortical projections, and adjacently connected area 1 within the primary somatosensory cortex (Kakigi, 1994; Hoshiyama et al., 1997). Connections between area 3b and the primary motor cortex and the supplementary motor area provide a physiological pathway by which early SEP components can be attenuated in response to movement preparation and execution (Krubitzer and Kaas, 1990). In contrast, later SEP components are thought to originate from bilateral dipoles in SII (Kakigi, 1994; Hoshiyama et al., 1997); therefore, attenuation of the N55–P100 SEP component may be driven by activity in SII. It has been shown previously that self-generated movement resulting in tactile sensation causes a significant decrease in the BOLD signal in bilateral SII (Blakemore et al., 1999) and is decreased as the sensory input becomes less predictable (Shergill et al., 2013). This is driven by activity in the cerebellum, which is thought to represent the prediction error signal from comparing predicted and actual sensory input. This mechanism may be reflected in the attenuation of the N55–P100 SEP component. It could be argued that the N55–P100 attenuation is confounded by the greater force produced in the self-condition compared with the external condition; however, this is unlikely because this component is not modulated significantly by force level. Attenuation of this component may demonstrate a change in the state of the sensory cortex, which then modulates subsequent perception. It is harder to interpret the functional role of later components because there is more time to be modulated by other inputs and the peaks are less distinct and more difficult to quantify. Nevertheless, the dissociation between the source of the early and late SEP components and the behavioral outcomes of physiological and perceptual sensory attenuation suggests that these forms of sensory gating are not only dissociable, but also have distinct functional roles.

SEPs provide an assay with which to measure modulations in somatosensory activity, but analysis is limited to the time in which median nerve stimuli were given. To investigate modulations in somatosensory activity that may correlate with perceptual sensory attenuation throughout the entire trial, exploratory time–frequency analyses measuring oscillatory activity over sensorimotor cortex were conducted. Time–frequency analyses highlighted a significant negative correlation between gamma-band activity and the magnitude of perceptual sensory attenuation over the right sensorimotor cortex contralateral to the hand receiving the matched force. This occurred before the auditory cue to start matching rather than during the matching period, as might be expected. This signal may therefore be in a position to modulate the gain of incoming sensory information causally in preparation for receiving the matched force, which in turn may modulate subsequent perception rather than representing the perception itself. It could be argued that this result is confounded by the increased force produced in the self-condition; however, this is unlikely due to the location of the activity (ipsilateral to the hand producing the force) and the timing of this modulation (before force production).

Interestingly, this oscillatory finding supports theoretical accounts of perceptual sensory attenuation, which posit that the difference in sensory attenuation between the self- and external task conditions is due to a difference in the ability to predict the sensory consequences of our own actions but not others (Blakemore et al., 1999). When our predictions are highly accurate (as in the self-condition), prediction error is low and sensory attenuation is high and vice versa when our predictions are not accurate (external condition). Therefore, it follows that the magnitude of prediction error will correlate negatively with the magnitude of sensory attenuation. If we assume that gamma oscillations represent the forward (ascending) connections carrying prediction errors, as has been suggested previously (Arnal and Giraud, 2012; Bastos et al., 2012; Bauer et al., 2014), then these data supports the hypothesis that a changing prediction error, represented by gamma-band activity, underlies the perceptual differences measured. Trials with less perceptual sensory attenuation have higher gamma-band activity before matching the force and, consistent with the theory, have lower prediction error.

However, it is important to note that prediction errors are precision weighted. This means that an estimate of the (inverse) variance of the predicted and actual sensory input is incorporated into the prediction error signal. Consistent with the alternative hypothesis positing that sensory attenuation is caused by a reduction in sensory precision caused by a decrease in the synaptic gain of superficial pyramidal cells transmitting prediction error signals (Adams et al., 2013; Brown et al., 2013), we can see that there would also be a negative correlation between sensory precision and perceptual sensory attenuation that could explain this oscillatory finding. It has been proposed that gamma-band oscillations are responsible for altering the synaptic gain of cells transmitting prediction errors, which in turn decreases sensory precision (Friston et al., 2015). Whether the gamma-band activity represents changes in precision or prediction error or the precision-weighted prediction error, the same result

would be found. However, these exploratory analyses were *post hoc*, so specific hypothesis-driven experimental work, optimally using patient populations, is needed to elucidate the necessity and sufficiency of this neural signal for perceptual sensory attenuation.

In this study, we have demonstrated that physiological sensory attenuation of the primary and secondary SEP components in response to movement is not correlated with perceptual sensory attenuation. This is consistent with the hypothesis that these two forms of sensory attenuation are functionally distinct. The active inference framework suggests that gating of the afferent signal may be due to a reduction in sensory precision, which is a necessary step in movement initiation (Friston et al., 2011). This same mechanism has also been used to explain perceptual sensory attenuation (Brown et al., 2013). However, it is clear from this study that, at the level of the primary sensorimotor cortex, any gating of the afferent signal or theorized modulation of sensory precision does not explain behavioral attenuation in the force-matching task. That said, it may be the case that perceptual sensory attenuation occurs via the same mechanism (a reduction in sensory precision), but at a different level of the cortical hierarchy (e.g., SII). Indeed, the later SEP component, N55–P100, thought to originate in SII, was significantly modulated by perceptual sensory attenuation in the current study, supporting this hypothesis. Abnormal perceptual sensory attenuation has been highlighted in patients with schizophrenia (Shergill et al., 2005) and functional movement disorders (Pareés et al., 2014) and abnormal physiological sensory attenuation has been highlighted in patients with functional movement disorders (Macerollo et al., 2015) and Parkinson's disease (Macerollo et al., 2016). Identifying how these deficits in sensory gating interact and where they dissociate to cause particular cognitive and motor symptoms in differing patient populations will be invaluable for highlighting the key functional role(s) of sensory gating and may give novel insights into the neurobiological mechanisms of these symptoms.

References

Adams RA, Stephan KE, Brown HR, Frith CD, Friston KJ (2013) The computational anatomy of psychosis. Front Psychiatry 4:47. CrossRef Medline

Arnal LH, Giraud AL (2012) Cortical oscillations and sensory predictions. Trends Cogn Sci 16:390–398. CrossRef Medline

Bäss P, Jacobsen T, Schröger E (2008) Suppression of the auditory N1 event-related potential component with unpredictable self-initiated tones: evidence for internal forward models with dynamic stimulation. Int J Psychophysiol 70:137–143. CrossRef Medline

Bastos AM, Usrey WM, Adams RA, Mangun GR, Fries P, Friston KJ (2012) Canonical microcircuits for predictive coding. Neuron 76:695–711. CrossRef Medline

Bauer M, Stenner MP, Friston KJ, Dolan RJ (2014) Attentional modulation of alpha/beta and gamma oscillations reflect functionally distinct processes. J Neurosci 34:16117–16125. CrossRef Medline

Blakemore SJ, Wolpert DM, Frith CD (1998) Central cancellation of self-produced tickle sensation. Nat Neurosci 1:635–640. CrossRef Medline

Blakemore SJ, Wolpert D, Frith C (2000) Why can't you tickle yourself? Neuroreport 11:R11–R16. CrossRef Medline

Blakemore S, Frith CD, Wolpert DM (1999) Spatio-temporal prediction modulates the perception of self-produced stimuli. J Cogn Neurosci 11: 551–559. CrossRef Medline

Brown H, Adams RA, Parees I, Edwards M, Friston K (2013) Active inference, sensory attenuation and illusions. Cogn Process 14:411–427. CrossRef Medline

Cohen LG, Starr A (1987) Localization, timing and specificity of gating of somatosensory evoked potentials during active movement in man. Brain 110:451–467. CrossRef Medline

Friston KJ, Bastos AM, Pinotsis D, Litvak V (2015) LFP and oscillations–what do they tell us? Curr Opin Neurobiol 31:1–6. CrossRef Medline

Friston K, Mattout J, Kilner J (2011) Action understanding and active inference. Biol Cybern 104:137–160. CrossRef Medline

Hoshiyama M, Kakigi R, Koyama S, Watanabe S, Shimojo M (1997) Activity in posterior parietal cortex following somatosensory stimulation in man: magnetoencephalographic study using spatio-temporal source analysis. Brain Topogr 10:23–30. CrossRef Medline

Hughes G, Desantis A, Waszak F (2013) Attenuation of auditory N1 results from identity-specific action-effect prediction. Eur J Neurosci 37:1152–1158. CrossRef Medline

Jiang W, Chapman CE, Lamarre Y (1990) Modulation of somatosensory evoked responses in the primary somatosensory cortex produced by intracortical microstimulation of the motor cortex in the monkey. Exp Brain Res 80:333–344. Medline

Kakigi R (1986) Ipsilateral and contralateral SEP components following median nerve stimulation: effects of interfering stimuli applied to the contralateral hand. Electroencephalogr Clin Neurophysiol 64:246–259. CrossRef Medline

Kakigi R (1994) Somatosensory evoked magnetic fields following median nerve stimulation. Neurosci Res 20:165–174. CrossRef Medline

Kakigi R, Jones SJ (1985) Effects on median nerve SEPs of tactile stimulation applied to adjacent and remote areas of the body surface. Electroencephalogr Clin Neurophysiol 62:252–265. CrossRef Medline

Kakigi R, Jones SJ (1986) Influence of concurrent tactile stimulation on somatosensory evoked potentials following posterior tibial nerve stimulation in man. Electroencephalogr Clin Neurophysiol 65:118–129. CrossRef Medline

Kilner JM (2013) Bias in a common EEG and MEG statistical analysis and how to avoid it. Clin Neurophysiol 124:2062–2063. CrossRef Medline

Krubitzer LA, Kaas JH (1990) The organization and connections of somatosensory cortex in marmosets. J Neurosci 10:952–974. Medline

Macerollo A, Chen JC, Pareés I, Kassavetis P, Kilner JM, Edwards MJ (2015) Sensory attenuation assessed by sensory evoked potentials in functional movement disorders. PLoS One 10:e0129507. CrossRef Medline

Macerollo A, Chen JC, Korlipara P, Foltynie T, Rothwell J, Edwards MJ, Kilner JM (2016) Dopaminergic treatment modulates sensory attenuation at the onset of the movement in Parkinson's disease: a test of a new framework for bradykinesia. Mov Disord 31:143–146. CrossRef Medline

Pareés I, Brown H, Nuruki A, Adams RA, Davare M, Bhatia KP, Friston K, Edwards MJ (2014) Loss of sensory attenuation in patients with functional (psychogenic) movement disorders. Brain 137:2916–2921. CrossRef Medline

Roussel C, Hughes G, Waszak F (2014) Action prediction modulates both neurophysiological and psychophysical indices of sensory attenuation. Front Hum Neurosci 8:115. CrossRef Medline

Rushton DN, Rothwell JC, Craggs MD (1981) Gating of somatosensory evoked potentials during different kinds of movement in man. Brain 104:465–491. CrossRef Medline

Seki K, Fetz EE (2012) Gating of sensory input at spinal and cortical levels during preparation and execution of voluntary movement. J Neurosci 32:890–902. CrossRef Medline

Shergill SS, Bays PM, Frith CD, Wolpert DM (2003) Two eyes for an eye: the neuroscience of force escalation. Science 301:187. CrossRef Medline

Shergill SS, Samson G, Bays PM, Frith CD, Wolpert DM (2005) Evidence for sensory prediction deficits in schizophrenia. Am J Psychiatry 162:2384–2386. CrossRef Medline

Shergill SS, White TP, Joyce DW, Bays PM, Wolpert DM, Frith CD (2013) Modulation of somatosensory processing by action. Neuroimage 70:356–362. CrossRef Medline

Starr A, Cohen LG (1985) "Gating" of somatosensory evoked potentials begins before the onset of voluntary movement in man. Brain Res 348:183–186. CrossRef Medline

Teufel C, Kingdon A, Ingram JN, Wolpert DM, Fletcher PC (2010) Deficits in sensory prediction are related to delusional ideation in healthy individuals. Neuropsychologia 48:4169–4172. CrossRef Medline

Walsh LD, Taylor JL, Gandevia SC (2011) Overestimation of force during matching of externally generated forces. J Physiol 589:547–557. CrossRef Medline

Wasaka T, Kida T, Kakigi R (2012) Modulation of somatosensory evoked potentials during force generation and relaxation. Exp Brain Res 219:227–233. CrossRef Medline

Wolpert DM, Miall RC (1996) Forward models for physiological motor control. Neural Netw 9:1265–1279. CrossRef Medline

Wolpert DM, Ghahramani Z, Jordan MI (1995) An internal model for sensorimotor integration. Science 269:1880–1882. CrossRef Medline

Crucially, the effect of nostalgia on creativity was transmitted via openness.

Nostalgia Kindles Prosocial Behavior

Given its inherent sociality, nostalgia ought to manifest its motivational potency in the social domain as well. It does. Following nostalgia induction, we assessed, in separate experiments, four indices of prosocial behavior: physical proximity, helping, donations to charity, and willingness for intergroup contact. First, nostalgia decreases proximity between oneself and another person. Participants were led to believe that they would interact with a person waiting in an adjacent room. In preparation, they were instructed to place two chairs (one for themselves, one for the other person) in that room. Nostalgic (relative to control) participants placed the chairs in closer proximity to each other [5]. Second, nostalgia facilitated helping. A confederate walked into the experimental room while participants were in wait and clumsily dropped pencils on the floor. Nostalgic participants helped more (i.e., picked up a higher number of pencils) than controls [5]. Third, nostalgia increases donations to charity. Nostalgic participants evinced stronger donation intentions toward a children's charity and donated more money to it compared with controls [10]. Finally, nostalgia facilitates intergroup contact. Participants reflected either nostalgically or not on an encounter with an outgroup member – in this case, an overweight person. Nostalgic (vs control) participants expressed more trust toward the outgroup member and reported less intergroup anxiety (e.g., if they had to interact with an outgroup person, they would feel less 'self-conscious', 'awkward', or 'defensive'). Critically, nostalgic participants reported stronger willingness for intergroup contact with an outgroup member (e.g., 'talk to them', 'find out more about them'). Further, the effect of nostalgia on willingness for intergroup contact was transmitted via increased outgroup trust and reduced intergroup anxiety. These findings were conceptually replicated when the outgroup member was a person with mental illness [11,12]. Taken together, nostalgia for an encounter with an outgroup member breeds trust for, and curtails anxiety about, the entire outgroup, culminating in stronger willingness for contact with the outgroup.

Concluding Remarks

Burgeoning experimental evidence indicates that nostalgia does not deserve its gloomy reputation. Far from being a feeble escape from the present, nostalgia is a source of strength, enabling the individual to face the future. Notably, like experimentally induced nostalgia, dispositional nostalgia proneness is positively associated with approach motivation [5], optimism [7], inspiration [8], and creativity [9]. Nostalgia, then, is a deposit in the bank of memory to be retrieved for future use. This was indeed Homer's original view of nostalgia in his portrayal of history's most famous itinerant. Finally, nostalgia has managed to come full circle.

[1]Center for Research on Self and Identity, University of Southampton, Southampton, UK

*Correspondence: cs2@soton.ac.uk (C. Sedikides) and R.T.Wildschut@soton.ac.uk (T. Wildschut).

http://dx.doi.org/10.1016/j.tics.2016.01.008

References

1. Sedikides, C. *et al.* (2015) To nostalgize: mixing memory with affect and desire. *Adv. Exp. Soc. Psychol.* 51, 189–273
2. Hepper, E.G. *et al.* (2014) Pancultural nostalgia: prototypical conceptions across cultures. *Emotion* 14, 733–747
3. Wildschut, T. *et al.* (2006) Nostalgia: content, triggers, functions. *J. Person. Soc. Psychol.* 91, 975–993
4. Morewedge, C.K. (2013) It was a most unusual time: how memory bias engenders nostalgic preferences. *J. Behav. Decis. Making* 26, 319–326
5. Stephan, E. *et al.* (2014) The mnemonic mover: nostalgia regulates avoidance and approach motivation. *Emotion* 14, 545–561
6. Baldwin, M. and Landau, M.J. (2014) Exploring nostalgia's influence on psychological growth. *Self Identity* 13, 162–177
7. Cheung, W.Y. *et al.* (2013) Back to the future: nostalgia increases optimism. *Person. Soc. Psychol. Bull.* 39, 1484–1496
8. Stephan, E. *et al.* (2015) Nostalgia-evoked inspiration: mediating mechanisms and motivational implications. *Person. Soc. Psychol. Bull.* 41, 1395–1410
9. Van Tilburg, W.A.P. *et al.* (2015) The mnemonic muse: nostalgia fosters creativity through openness to experience. *J. Exp. Soc. Psychol.* 59, 1–7
10. Zhou, X. *et al.* (2012) Nostalgia: the gift that keeps on giving. *J. Cons. Res.* 39, 39–50
11. Turner, R.N. *et al.* (2012) Dropping the weight stigma: nostalgia improves attitudes toward persons who are overweight. *J. Exp. Soc. Psychol.* 48, 130–137
12. Turner, R.N. *et al.* (2013) Combating the mental health stigma with nostalgia. *Eur. J. Soc. Psychol.* 43, 413–422

Spotlight

A New Framework to Explain Sensorimotor Beta Oscillations

Clare Palmer,[1] Laura Zapparoli,[2] and James M. Kilner[1,*]

Oscillatory activity in the beta frequency range from sensorimotor cortices is modulated by movement; however, the functional role of this activity remains unknown. In a recent study, Tan *et al.* tested a novel hypothesis that beta power reflects estimates of uncertainty in parameters of motor forward models.

It is well established that oscillatory activity originating from sensorimotor cortices in the beta frequency range (~15–30 Hz) is modulated by movement. Beta power decreases when we move and is transiently increased once the movement has stopped (postmovement beta synchronization, PMBS) [1]. However, despite extensive research into these neuronal oscillations, their functional role is not known [2]. In a recent study, Tan *et al.* [3] tested a novel theory of the functional role of sensorimotor PMBS that provides an important link between theoretical models of motor control and neurophysiological measures of sensorimotor activity.

Every movement we make stimulates peripheral sensory receptors that provide sensory feedback of the motor act. It is thought that, when we move, we predict

the sensory consequences of that movement (through forward models) and compare this prediction to the actual sensory input [4,5]. Any difference between the predicted and actual sensory input will result in a prediction error, which is used to update the forward model for more accurate future predictions. To determine the relevance of any prediction errors, the model requires estimations of both the uncertainty in the motor prediction and the uncertainty of the actual sensory input [6]. This can be likened to a two-sample *t*-test: a measure of the variance (uncertainty) of each sample is essential to determine whether any difference between the sample means is significant. Tan *et al.* [3] manipulated task uncertainty to modulate the uncertainty in parameters of the model and tested the hypothesis that PMBS was correlated with these parameters.

The authors measured cortical activity with EEG from 17 healthy participants while they performed a visuomotor adaptation task. Participants were instructed to move a joystick to direct a cursor from the centre of a circle to a target located at one of eight points on the circumference of the circle. Participants completed 80 trials of either: (i) a random prime, in which a random angular error varying from trial to trial was added between the actual movement of the joystick and the visual feedback of the cursor (–60° to 60°); or (ii) a stable prime in which the perturbation (0°) remained stable across trials. Afterwards, all participants performed 150 trials of a constant 60° perturbation, followed by another 80 trials of no perturbation, for each condition. The authors predicted that, during the random priming block, participants' uncertainty in parameters of the forward model (estimation uncertainty) would be high due to their inability to correctly predict future movements, whereas when the perturbation was stable, this uncertainty would be low. They predicted that PMBS would correlate with this uncertainty rather than with the movement error. A Bayesian learning model, which uses the mean and variance of the movement error across trials to estimate this uncertainty, was applied to the behavioural data. The authors then

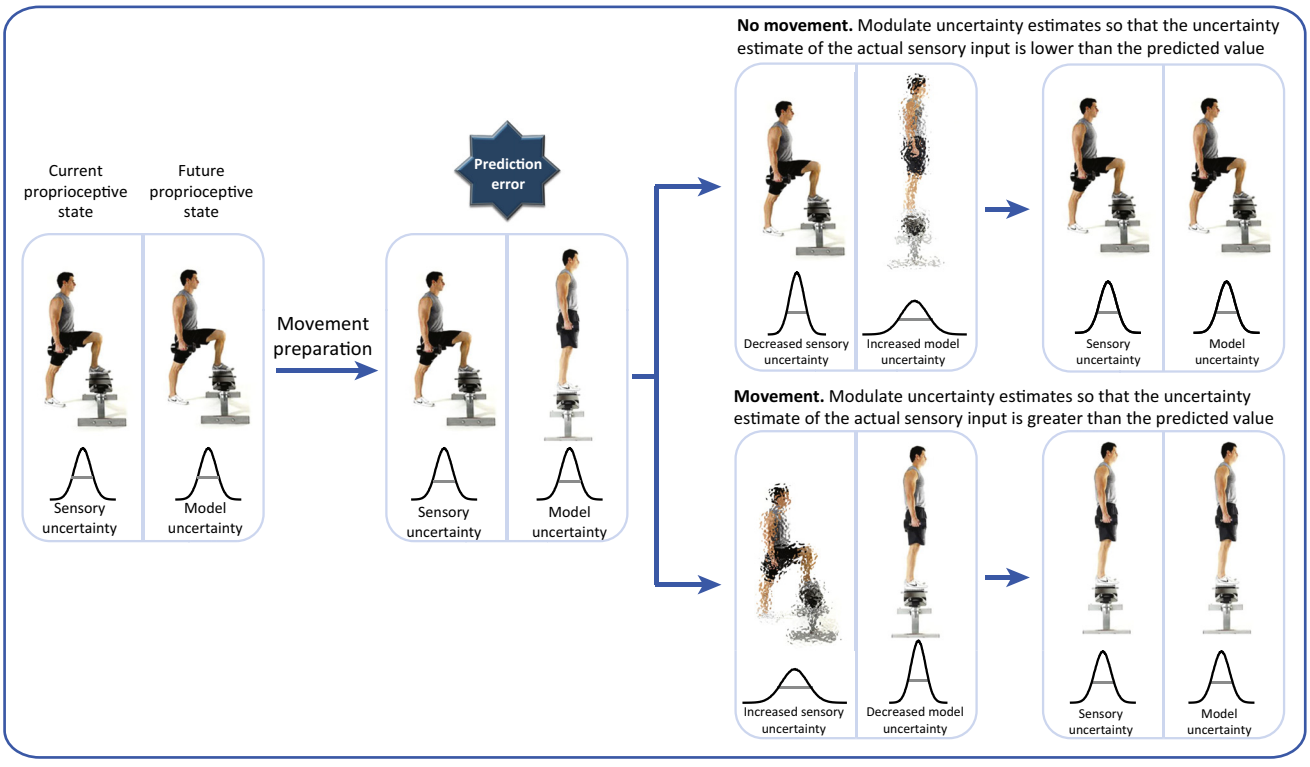

Figure 1. Schematic Illustrating Movement Initiation within the Active Inference Framework. In the schematic, each panel depicts both the actual and the predicted sensory inputs. The character shows the action that is currently being performed (left) alongside the predicted action (right). The width of the distributions below and the clarity of the figure illustrate the uncertainty in these values. Before we start to plan a new movement, our prediction of our sensory input and the actual sensory input are equivalent (left panel). According to the active inference framework, when we start to prepare a movement, we generate a prediction of what the sensory input of this movement will be and this creates a prediction error between the current and the predicted sensory states (second panel). To minimize this error, an individual can: (i) stay still and update their prior beliefs (within the forward model) so that the predicted sensory input matches the actual sensory input (top row); or (ii) move, so that the actual sensory input matches the predicted sensory input (bottom row). Modulating the relative uncertainty in these sensory states will determine which option is selected. For example, to initiate movement [option (ii)], the uncertainty in the current sensory state is increased such that the individual will shift to the predicted sensory state with the lowest uncertainty.

correlated the magnitude of the PMBS in each condition with the estimated values of uncertainty. They reported that the amplitude of the PMBS over sensorimotor cortex was negatively correlated with this uncertainty variable. This result is consistent with a novel functional role of PMBS, which suggests that beta oscillations are related to the uncertainty of the parameters of generative models that underlie motor control.

Although this paper introduces a new functional account for PMBS, this account does not generalize easily to explain all known modulations in sensorimotor beta oscillations. For example, it is known that beta power decreases during movements. If the new account is applied to this desynchronisation, then the conclusion would be that we have the highest uncertainty in our model while we move. This would seem unlikely. However, uncertainty is not only estimated for parameters of the forward model. According to motor control theory, an estimate of uncertainty in the actual sensory input is also required. The importance of the estimate of uncertainty at both of these levels was highlighted in a recent theoretical account of motor control and movement initiation: active inference [7]. Within this framework, it has been proposed that an increase in the estimate of the uncertainty of the actual sensory input is an essential step for being able to move (Figure 1). However, the neurophysiological correlates of this change in uncertainty are unknown. The study by Tan *et al.* [3] makes it possible to hypothesise that sensorimotor beta oscillatory power might be either the neurophysiological correlate of the estimate of uncertainty or causally modulating the uncertainty. Indeed, *prima facie* there is compelling evidence to predict that sensorimotor beta power and estimates of sensory uncertainty might be negatively correlated. For example, sensorimotor beta oscillations are known to be attenuated during motor preparation and execution [8], when active inference would predict an increase in sensory uncertainty. Similarly, increases in sensorimotor beta power are associated with the inhibition of executed actions [9], when active inference would require a decrease in somatosensory uncertainty to inhibit an action. Finally, sensorimotor beta power is augmented in patients with Parkinson's disease compared with healthy controls [10], when active inference would predict a lower level of sensory uncertainty in patients with Parkinson's disease compared with healthy controls.

Tan *et al.* [3] have provided the first demonstration of a link between a key parameter in theoretical models of motor control, uncertainty, and modulations in sensorimotor beta power. Future work will be required to investigate whether the modulations in beta power are best accounted for by modulations in the uncertainty of the actual sensory input, the uncertainty of the model space, or the relative uncertainties of the two.

Acknowledgments

C.P. was funded by the Wellcome Trust. J.M.K. was funded by the MRC (MR/M006603/1).

[1]Sobell Department of Motor Neuroscience and Movement Disorders, UCL Institute of Neurology, London, WC1N 3BG, UK
[2]fMRI Unit, IRCCS Galeazzi, 20161, Milan, Italy

*Correspondence: j.kilner@ucl.ac.uk (J.M. Kilner).

http://dx.doi.org/10.1016/j.tics.2016.03.007

References

1. Pfurtscheller, G. and Lopes da Silva, F.H. (1999) Event-related EEG/MEG synchronization and desynchronization: basic principles. *Clin. Neurophysiol.* 110, 1842–1857
2. Engel, A.K. and Fries, P. (2010) Beta-band oscillations: signalling the status quo? *Curr. Opin. Neurobiol.* 20, 156–165
3. Tan, H. *et al.* (2016) Post-movement beta activity in sensorimotor cortex indexes confidence in the estimations from internal models. *J. Neurosci.* 36, 1516–1528
4. Wolpert, D.M. and Ghahramani, Z. (2000) Computational principles of movement neuroscience. *Nat. Neurosci.* 3, 1212–1217
5. Adams, R.A. *et al.* (2013) Predictions not commands: active inference in the motor system. *Brain Struct. Funct.* 218, 611–643
6. Körding, K.P. and Wolpert, D.M. (2004) Bayesian integration in sensorimotor learning. *Nature* 427, 244–247
7. Friston, K. *et al.* (2011) Action understanding and active inference. *Biol. Cybern.* 104, 137–160
8. Tzagarakis, C. *et al.* (2010) Beta-band activity during motor planning reflects response uncertainty. *J. Neurosci.* 30, 11270–11277
9. Swann, N. *et al.* (2009) Intracranial EEG reveals a time- and frequency-specific role for the right inferior frontal gyrus and primary motor cortex in stopping initiated responses. *J. Neurosci.* 29, 12675–12685
10. Litvak, V. *et al.* (2011) Resting oscillatory cortico-subthalamic connectivity in patients with Parkinson's disease. *Brain* 134, 359–374